PHEROMONE SIGNALING, MATING AND BIOFILM FORMATION IN *CANDIDA* SPECIES.

By Stephen Knox Jones, Jr.

B.S. Florida Institute of Technology, 2009

Thesis

Submitted in partial fulfillment of the requirements for the Degree of Doctorate of Philosophy in the Department of Molecular Microbiology and Immunology at Brown University.

PROVIDENCE, RHODE ISLAND

MAY 2015

Dedication

This thesis is dedicated to my aunt Sandra Vadeboncoeur and my friend Steven Debonis, two people who died too early, but not without leaving a lasting impact on my life.

This dissertation by Stephen Knox Jones Jr is accepted in its present form by the Molecular Biology, Cell Biology, and Biochemistry Program in the Molecular Microbiology and Immunology department as satisfying the dissertation requirement for the Degree of Doctor of Philosophy.

Date _____ _____

Richard J. Bennett, Advisor

Recommended to the Graduate Council

Date _____ _____

Gary Wessel, Reader

Date _____ _____

Erica Larschan, Reader

Date _____ _____

Rebecca Page, Reader

Date _____ _____

Deborah Hogan, Reader

Approved by the Graduate Council

Date _____ _____

Peter M. Weber, Dean of the Graduate School

CURRICULUM VITAE

Stephen Knox Jones Jr.

Molecular Microbiology and Immunology Department

Brown University

Box G-6

171 Meeting St.

Providence, RI 02912

Phone: (401) 863-6342

80 Greeley St.

Providence, RI 02904

Phone: (603) 858-4993

Email: Stephen_Jones@Brown.edu

Born October 23rd, 1986 in Manchester, New Hampshire.

EDUCATION

2009 → 2015 Brown University, Providence, RI.

- Ph.D. candidate in Molecular Biology, Cellular Biology and Biochemistry, Systems Biology track.
- Thesis Adviser: Dr. Richard J. Bennett.
- Thesis Topic: Biofilm formation and pheromone signaling in *Candida* species.

2005 → 2009 Florida Institute of Technology, Melbourne, FL.

- B.S. in Molecular Biology, *Summa cum laude.*
- Research Mentor: Dr. David J. Carroll.
- Research Topic: Fertilization signaling pathways in *Echinoderms*.

RESEARCH EXPERIENCE

2009 → 2015 Doctoral Research: Department of Molecular Microbiology and Immunology, Brown University. Research adviser: Dr. Richard J. Bennett.

- Identified sexual biofilms and described their structure and mechanisms in the fungal pathogen, *Candida tropicalis.*

- Established the presence of a parasexual cycle in *C. tropicalis*.
- Characterized the specificity and activities of *Candida* pheromones and the aspartyl protease Bar1, which degrades sexual pheromones of *Candida albicans* and closely related species.
- Techniques included genetic engineering, protein expression and purification, western blotting, mass spectrometry, qPCR, microarray, ChIP-Seq, FRET, flow cytometry, peptide and antibody design, phenotypic analysis, SEM and confocal laser scanning microscopy, microvesicle isolation, tissue culture and biofilm quantification methods.

2005 → 2009 Undergraduate Research: Department of Biological Sciences and Department of Mathematical Sciences, Florida Institute of Technology. Research advisors: Dr. David Carroll, Dr. Semen Köksal.

- Identified similarities between calcium signal pathways in starfish oocytes and human T-cells.
- Built a preliminary neural network model to describe signaling pathways in starfish oocytes at fertilization.
- Techniques included immunoprecipitation, microinjection, MATLAB programming, 1 and 2-D gel electrophoresis and western blotting.

PUBLICATIONS

In preparation "Inter-species pheromone signaling and characterization of Bar1 protease in *C. albicans*." **Jones SK Jr**, Bennett RJ.

2014 "Sexual Biofilm Formation in *Candida tropicalis* Opaque Cells." **Jones SK Jr,** Hirakawa MP, Bennett RJ. *Mol Microbiol.* 2014 Apr; 92(2):383-98. F1000 recommended article.

2013 "Parasexuality and Ploidy Change in *Candida Tropicalis.*" Seervai RN*, **Jones SK Jr***, Hirakawa MP, Porman AM, Bennett RJ. *Eukaryot Cell.* 2013 Oct 11.

2013 "MTL-independent phenotypic switching in *Candida tropicalis* and a dual role for Wor1 in regulating switching and filamentation." Porman AM, Hirakawa MP*, **Jones SK***, Wang N, Bennett RJ. *PLoS Genet*. 2013 Mar;9(3):e1003369.

2011 *"*Fungal mating pheromones: Choreographing the dating game." **Jones SK Jr**, Bennett RJ. *Fungal Genet Biol*. 2011 Jul;48(7):668-76

2010 *"*Identification of a Cell Death Pathway in *Candida albicans* during the Response to Pheromone." Alby K, Schaefer D, Sherwood RK, **Jones SK Jr**, Bennett RJ. *Eukaryotic Cell.* 2010 Nov;9(11):1690-701

* indicates equal contribution

FUNDING

2012 → 2015 NIH-NIDCR. NRSA for Individual Predoctoral Fellows: **F31 DE022701**

- "Phenotypic Plasticity and Inter-Species Communication in *Candida albicans.*"

2010 - 2012 NIH. NRSA Institutional Research Training Grant: **T32 GM007601**

2008 - 2009 NSF-DUE. UBM-Group: Research and Education Program in Biomath. **Grant: 0734251**

- "Signal transduction during oocyte maturation and fertilization."

PRESENTATIONS AT MEETINGS

2014 "Sexual Biofilms of *Candida tropicalis*, and a Role for a Sexual Agglutinin." **Selected Speaker.** 12th ASM Conference on *Candida* and Candidiasis. March 26th-30th, 2014. New Orleans, LA.

2013 "The Perfect Couple: Sexual Interactions Drive Biofilm Formation in *Candida tropicalis."* **Selected Speaker.** CSHL Meeting: Microbial Pathogenesis and Host Response. September 17-21, 2013. Cold Spring Harbor, NY.

2012 "Love Thy Neighbor as Thyself: Pheromone Signaling Between Species in the *Candida* Clade." Poster. 11th ASM Conference on *Candida* and *Candidiasis*. March 29 - April 2, 2012. San Francisco, CA.

HONORS

2014 **ASM Travel Award.** Awarded to select speakers at the 12th ASM Conference on *Candida* and Candidiasis.

2012 Student Service Award. Graduate Program in Molecular Biology, Cellular Biology and Biochemistry. Brown University.

2011 **Honorable Mention.** National Science Foundation Graduate Research Fellowship Program

2009 → High Honors at Brown University

2009 Florida Tech Faculty Award for **perfect graduating GPA**

2009 Best of Student Showcase: 2009 Northrop Grumman Engineering & Science Student Design Showcase, Florida Institute of Technology

2007 - 2009 Distinguished Student Scholar

2008 Outstanding Senior in Molecular Biology

EXTRAMURAL ACTIVITIES AND TEACHING

2014 Brown Executive Scholars Training (BEST) Program

- Semester-long seminar and workshop series and mentoring in university administration. Certification received.

2013 IMSD Training Module: Professional and Career Development – Preparing for the Postdoc Experience.

2013 Teaching Certification 1, Sheridan Center for Teaching, Brown University

- Year-long seminar and workshop series on reflective teaching technique, teaching and assessment strategies, and communication in the learning environment. Certification received.

2011 - 2013 Rhode Island Science and Engineering Fair (RISEF) Judge

2011 - 2012 MCB Graduate Student Liaison

2010, 2012 MCB Graduate Program Retreat Committee, Student Representative

2011 Microbiology Teaching Assistant, Brown University. Course instructed by Dr. Richard Bennett.

- Lead laboratory sessions and performed grading for approximately 100 students.

2011 MCB Graduate Program Recruitment Committee, Student Representative

- Reviewed, interviewed and selected students for matriculation. Coordinated and lead three interview weekend initiatives.

2006 - 2009 K-College Tutor and Administrative Assistant. *Smart Teacher, Smart Kid Tutoring, Inc.* Melbourne, FL.

- Tutored individuals and groups in test prep and topics ranging from reading and arithmetic to developmental biology and calculus.
- Scheduled tutoring sessions, managed client accounts, interviewed job applicants

2006 → Certified Music Together Instructor. *Music Together LLC.* Princeton, NJ.

2005 - 2006 K-12 Music Teacher and Tutor. *Club Esteem*. Melbourne, FL.

WORKSHOPS AND COURSES

2014	Center for Cell Circuits Computational Genomics Workshop – Broad Institute
2014	Analyses of Microbial Community Composition and Metagenomics Using QIIME
2013	Scientific Computing and Problem Solving
2010	Quantitative Models of Biological Systems
2010	Origins of Multicellularity
2010	Scientific Communication
2009 → 2010	Methods of Applied Mathematics I + II
2009	Foundations for Advanced Study in Life Science

MEMBERSHIPS

2012 →	American Society for Microbiology (ASM)
2010 →	American Association for the Advancement of Science (AAAS)
2009 →	Phi Kappa Phi Honor Society
2008 →	Beta Beta Beta Biological Honors Society
2005 →	Phi Eta Sigma Honor Society

PREFACE

I have executed all of the experiments included in this dissertation in the laboratory of Richard Bennett at Brown University except where authorship denotes otherwise below:

Chapter 1: Parts of this chapter were published as:

Jones SK Jr, Bennett RJ. Fungal mating pheromones: choreographing the dating game. Fungal Genet Biol. 2011 Jul;48(7):668-76. doi: 10.1016/j.fgb.2011.04.001. Epub 2011 Apr 8. Review. PubMed PMID: 21496492; PubMed Central PMCID: PMC3100450.

I wrote the manuscript and crafted the figures. Dr. Richard Bennett provided editorial feedback.

Chapter 2: This chapter is in preparation for publication as:

Jones SK Jr, Clarke SC, Craik CS, Bennet RJ. Biochemical and genetic dissection of the Role of *Candida albicans* Bar1 in pheromone signaling.

I wrote the manuscript, performed all experiments, and crafted all figures with the exception of figure 2-4 A and B, where Starlynn Clarke performed the related experiments and created the figures. Dr. Charles Craik provided experimental feedback. Dr. Richard Bennett provided experimental and editorial feedback.

Chapter 3: This chapter was published as:

Jones SK Jr, Hirakawa MP, Bennett RJ. Sexual biofilm formation in *Candida tropicalis* opaque cells. Mol Microbiol. 2014 Apr;92(2):383-98. doi: 10.1111/mmi.12565. Epub 2014 Mar 19. PubMed PMID: 24612417; PubMed Central PMCID: PMC4005700.

I wrote the manuscript, performed all experiments, and crafted all figures with the exception of the scanning electron microscopy, which was performed Matthew Hirakawa. Matthew Hirakawa also provided editorial feedback. Dr. Richard Bennett provided experimental and editorial feedback.

Chapter 4: This chapter contains two subsections. The contents of the first subsection are entirely my own work with experimental assistance from Denis Huang and experimental and editorial feedback from Richard Bennett. The second subsection is an adapted excerpt published in:

Porman AM, Hirakawa MP *, Jones SK *, Wang N, Bennett RJ. MTL-independent phenotypic switching in *Candida tropicalis* and a dual role for Wor1 in regulating switching and filamentation. PLoS Genet. 2013 Mar;9(3):e1003369. doi: 10.1371/journal.pgen.1003369. Epub 2013 Mar 21. PubMed PMID: 23555286; PubMed Central PMCID: PMC3605238.

I wrote and edited portions of the manuscript, performed experiments and crafted figures related to the data contained in figure 2, which has been included in this chapter subsection. Dr. Allison Porman performed the vast majority of the work contained in the complete publication. Matthew Hirakawa wrote and edited portions of the manuscript, performed experiments and

crafted figures related to the data contained in the final figure. Na Wang assisted Dr. Porman in her experimentation. Dr. Richard Bennett provided experimental and editorial feedback.

Appendix 1: This appendix was published as:

Seervai RN *, Jones SK Jr *, Hirakawa MP, Porman AM, Bennett RJ. Parasexuality and ploidy change in *Candida tropicalis*. Eukaryot Cell. 2013 Dec;12(12):1629-40. doi: 10.1128/EC.00128-13. Epub 2013 Oct 11. PubMed PMID: 24123269; PubMed Central PMCID: PMC3889571.

Riyad Seervai wrote the manuscript, and he and I performed the majority of the experiments contained within. I provided extensive assistance in experimentation, data analysis, editing and figure design. Matthew Hirakawa performed all *in vivo* mouse experiments and crafted figure 6 C and D. Dr. Allison Porman and Dr. Richard Bennett provided experimental and editorial feedback.

Appendix 2: This appendix was published as:

Alby K, Schaefer D, Sherwood RK, Jones SK Jr, Bennett RJ. Identification of a cell death pathway in Candida albicans during the response to pheromone. Eukaryot Cell. 2010 Nov;9(11):1690-701. doi: 10.1128/EC.00155-10. Epub 2010 Sep 24. PubMed PMID: 20870881; PubMed Central PMCID: PMC2976293.

I contributed data and analysis for figure 7, as well as editorial feedback. All other contributions were made by the remaining authors.

ACKNOWLEDGEMENTS

I would like to acknowledge several groups of people that have helped me earn my doctorate: my mentors, family, friends and home.

To my mentors, thank you for all of your guidance in achieving academic excellence. Richard Bennett, for all your help in transitioning me from a graduate student to a bonafide research scientist. You have helped me reach goals I could not have on my own. David Carroll, for showing me how research differs from the textbook. My commitee members, Gary Wessel, Erica Larschan, Jeff Laney, and Rebecca Page for providing me with the assistance I needed to complete my doctorate the right way.

To my family, thank you for providing the context in which my scientific career could flourish. Your support has always been critical. You all have always thought of me as smarter than I am, and that reassurance facilitated my academic success. A special thank you to my mother and father, whose genetic material and alternative parenting approaches made me the man I am.

To my friends, thank you for being a respite when I needed it and a willing ear when I did not. Listening to science is not always easy or entertaining. Playing music, enjoying the outdoors, fixing cars – whatever it is, you all were up for it. It certainly makes life better when you've got the right people to enjoy it with.

Finally, thank you to my home. Brittany, you have been more supportive to my progress than I could have ever asked for. You have taught me lessons I never thought I needed to know. You have made things right when they were wrong, and have been a teammate, helping me become

a better person than I would be otherwise. My two nuggets: Mercedes, thank you for entertaining me and reminding me that just because you can eat something, does not mean you should. Ramesses, thank you for being prepared for anything – you are my eternal wingless wingman.

TABLE OF CONTENTS

LIST OF TABLES

LIST OF FIGURES

ABSTRACT

Candida species are a group of opportunistic fungal pathogens that cause life-threatening illness in the immunocompromised, but typically inhabit the human gastrointestinal tract as a normal component of its microbiome. An essential component to their success as both a commensal and pathogen is their ability to sense and respond to environmental signals. Signaling molecules, such as pheromones, allow *Candida* species to communicate between one another and to orchestrate complex multicellular responses, including mating and biofilm formation. This thesis addresses several aspects of pheromone signaling and responses in two prevalent *Candida* species, *Candida albicans* and *Candida tropicalis*. I began with an investigation of Bar1, a secreted protease secreted that degrades α-pheromone to modulate the signaling response in *C. albicans*. I characterized the biochemical features of Bar1-mediated pheromone degradation and identified that Bar1 acts on a variety of *Candida* species pheromones, altering the sensitivity and response of *C. albicans* to these pheromones. Several pheromone responses in *Candida* species are regulated by the white-opaque phenotypic switch, a two-state system that regulates mating competence. I showed that in addition to mating, *C. tropicalis* responds to pheromone stimulation by forming biofilms. Surprisingly, this response was limited to cells in the mating-competent opaque state, rather than the white state, as is seen in *C. albicans.* My research also indicated that the master regulator of the white-opaque switch, Wor1, can also induce filamentation and biofilm formation in *C. tropicalis*. Finally, I examine pheromone-dependent biofilm formation in *C. albicans,* showing that it varies across the species and that opaque cells make a greater contribution to biofilm formation than

previously appreciated. These results are discussed in relation to how they impact inter-species relationships among *Candida* species and with the human host.

CHAPTER 1: INTRODUCTION AND SPECIFIC AIMS

One of the basic necessities of any living organism is its ability to interact with its environment, whether to gather food, avoid predators or find a mate. Communication is integral to meeting this necessity, allowing organisms to both sense and produce important signaling cues. Pheromone-signaling systems are perhaps one of the most ancient modes of communication, where organisms produce cues specifically intended for detection by another. My focus lays in understanding how pheromones are received and interpreted by human fungal pathogens. *Candida* species, the most prominent fungal pathogens, are of particular interest and my studies explore how pheromone signaling is integrated into their lifestyle and virulence. The main areas of interest in this thesis are the biofilm response to pheromone signaling, and the role of the Bar1 protease, a regulator of pheromone signaling in *Candida*.

In order to understand the dynamics of pheromone signaling within *Candida* species, it is worthwhile considering systems in related ascomycetous species. Historically, the hemiascomycete yeast *Saccharomyces cerevisiae* has provided an excellent model system for exploring mechanisms of pheromone signaling. An overview of signaling will first be provided using *S. cerevisiae* as a foundation. Then, aspects of *Candida* biology that are integrated into pheromone signaling will be highlighted, including phenotypic switching, and how signals are interpreted through both mating and biofilm formation.

PROGRESSION OF A PHEROMONE SIGNAL

Pheromones are diffusible molecules that may be used for a variety of purposes including quorum sensing, predator detection, and mating regulation. At their most basic level, pheromones are secreted molecules that convey information from one cell to another, resulting in induction of a corresponding response. In *S. cerevisiae*, pheromones are used to coordinate mating between two cell types, **a** and α, in a manner that is tightly regulated by secreted pheromones. The **a** and α cell types secrete **a** and α pheromones (**a** and α factors), respectively, that are recognized by sex-specific receptors on the surface of the opposite cell type. This section will review how they are produced and secreted, and then received and interpreted in other cells.

Production of pheromones

Mating in *S. cerevisiae* and other ascomycetes is regulated by transcription factors encoded at the mating (*MAT*) locus. Haploid cells that contain the *MATa* locus are classified as **a** cells, and these can mate with haploid α cells that express the *MATα* locus (Heitman, 2007; Lee *et al.*, 2010). *S. cerevisiae* α cells secrete α factor, a mature peptide of thirteen amino acid residues, WHWLGLKPGQPMY, that is the processed product of the *MFα1* and *MFα2* genes. The α factor is initially translated as a prepro-protein of 165 amino acids composed of three regions: a 19 amino acid signal sequence, a 64 amino acid proregion containing several glycosylation sites, and a region containing four (*MFα1*) or two (*MFα2*) repeats of the mature α factor separated by short linker sequences (see Fig. 1A). The prepro form is translocated into the endoplasmic reticulum where the signal peptide is cleaved off and extensive glycosylation of the proregion occurs (Kurjan and Herskowitz, 1982; Singh *et al.*, 1983; Waters *et al.*, 1988). Upon transitioning to the Golgi apparatus, these recently added carbohydrate groups are modified

and three cleavage reactions occur. First, the Kex2 protease separates the α factor repeats by cleavage after conserved lysine-arginine residues. Second, Kex1 removes these two amino acids via carboxypeptidase activity. Finally, the diamino peptidase Ste13 completes the maturation process by removing excess residues at the N-terminus of the peptide (Fig. 1A) (Julius *et al.*, 1984; Dmochowska *et al.*, 1987; Wagner and Wolf, 1987; Caplan *et al.*, 1991). Mature α factor then exits the cell via the classical secretary pathway.

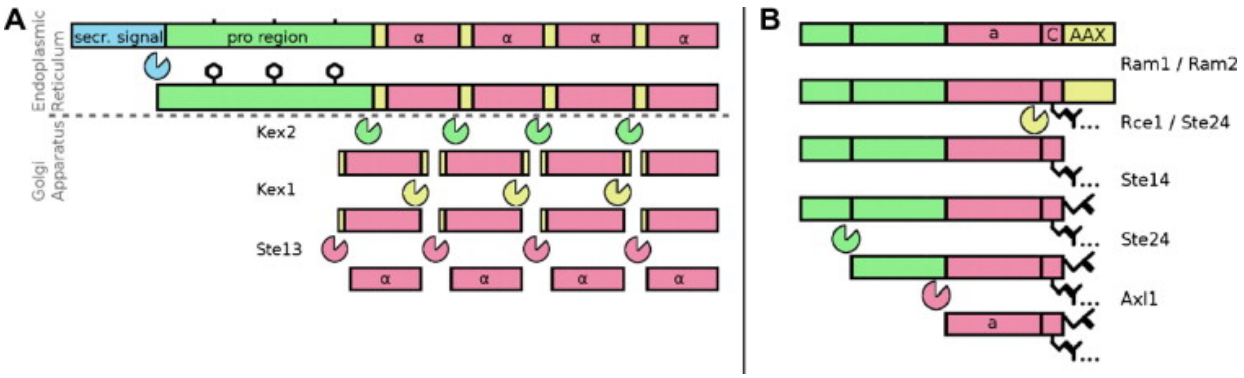

Figure 1-1: Processing of *S. cerevisiae* **a** and α mating pheromones.

(A) Processing of α factor: the secretion signal (blue) is cleaved to produce the α propheromone, which is glycosylated in the endoplasmic reticulum. Upon transport to the golgi apparatus, three proteolytic steps remove the proregion (green) and connecting regions (yellow) that separate copies of mature α factor (pink).

(B) Processing of a factor: in the cytosol, a propheromone is farnesylated at a conserved cysteine in the c-terminal CAAX motif (C = cysteine, A = aliphatic, X = any). The amino acids (yellow) preceding the cysteine are then removed and replaced with a carboxymethyl group. Finally, two proteolytic events remove N-terminus amino acids (green) to produce the mature **a** factor (pink).

Processed α factor is recognized by the Ste2 receptor on the surface of **a** cells, which initiates mating signaling. Despite its short length, different regions of α factor have specific roles in Ste2 activation. Thus, the C-terminus of α factor is important for the physical interaction with Ste2, while the N-terminus is more closely associated with downstream signaling events (Naider and Becker, 2004). The central region of the peptide (proline-8 and glycine-9) is thought to adopt a β-turn, which may orient the N-terminal 'signaling' and C-terminal 'binding' domains during the interaction with Ste2 (Shenbagamurthi *et al.*, 1983; Naider and Becker, 2004). While there is tolerance for sequence changes in these regions, specific modifications can either enhance or inhibit signaling (Raths *et al.*, 1993; Zhang *et al.*, 1997; Zhang *et al.*, 1998). In either case, the affinity of α factor for its receptor does not correlate with the ability to activate downstream signaling events (Naider and Becker, 2004). In fact, modified pheromones that bind very strongly to Ste2 often perform poorly in signal transduction. These experiments illustrate

two important points in pheromone function: (1) Even in short peptide sequences specialized functions are associated with different regions of the peptide. (2) The strength of the receptor-ligand interaction does not predict the strength of the induced biological signal.

The use of unmodified peptides as mating pheromones is characteristic of the ascomycetes, including *Saccharomyces* and *Candida* species, and they are typically produced similarly to *S. cerevisiae* α factor. In contrast, pheromones consisting of both peptide and lipid components are found throughout the ascomycetes and basidiomycetes (Olesnicky *et al.*, 1999; Davidson *et al.*, 2000; Fowler *et al.*, 2004; Coppin *et al.*, 2005; Kothe, 2008). *S. cerevisiae* **a** factor is representative of this class and undergoes secretion and processing that differs from that of α factor. *MF*a*1*/*MF*a*2* genes encode a propheromone of 36 or 38 amino acids, respectively (Fuller *et al.*, 1985; Michaelis and Herskowitz, 1988). Processing of the propheromone occurs in the cytosol, beginning with modification of a cysteine residue in the conserved C-terminal motif CAAX (Anderegg *et al.*, 1988). The cysteine residue is first farnesylated by Ram1 and Ram2 proteins that introduce a lipid moiety, followed by proteolysis of the three most C-terminal residues by Rce1 or Ste24 (Powers *et al.*, 1986; He *et al.*, 1991; Boyartchuk *et al.*, 1997; Chen *et al.*, 1997; Tam *et al.*, 1998; Boyartchuk and Rine, 1998). Further post-translational modifications are performed by Ste14, which appends a carboxymethyl group to the cysteine residue (Hrycyna *et al.*, 1991; Sapperstein *et al.*, 1994). Subsequently, a two-step proteolysis of the N-terminus occurs: Ste24 cleaves off the first seven residues, then Axl1 cleaves off fourteen additional residues, although Ste24 activity does not appear to be essential (Fujimura-Kamada *et al.*, 1997; Tam *et al.*, 2001; Huyer *et al.*, 2006:200). The final product is mature a factor, a twelve amino acid phospholipid exported by the Ste6 transporter (Fig. 1B). The vast majority of the machinery necessary to process both **a** and α pheromones is well-conserved across ascomycetes, including

Candida albicans (Tzung *et al.*, 2001; Magee *et al.*, 2002; Panwar *et al.*, 2003; Zhao *et al.*, 2005:2).

Sex-specific pheromone expression occurs in *C. albicans* and *Candida tropicalis*, in the distantly related ascomycete *Schizosaccharomyces pombe,* and in multiple filamentous ascomycetes including *Neurospora crassa, Podospora anserina, Magnaporthe grisea* and *Aspergillus nidulans* (see Fig. 2) (Zhang *et al.*, 1998; Shen *et al.*, 1999; Bobrowicz *et al.*, 2002; Coppin *et al.*, 2005; Paoletti *et al.*, 2007; Porman *et al.*, 2013). Some ascomycete species, however, show significant variations from *S. cerevisiae* pheromone processing. For example, in the filamentous ascomycete *Hypocrea jecorina*, an unusual precursor form of **a** pheromone has been uncovered. The **a** propheromone exhibits features of both *S. cerevisiae* **a** and α pheromone precursors. In particular, the C-terminal CAAX motif that is associated with farnesylsation and carboxymethylation of **a** factor is present, but so are two putative cleavage sites for the α factor protease, Kex2 (Schmoll *et al.*, 2010). The gene encoding this pheromone was demonstrated to be essential for male fertility, but Kex2 processing was apparently dispensable since deletion of putative processing sites did not block mating. The authors found similar pheromones in several *Fusarium* species, leading them to classify these pheromones as h (hybrid)-type pheromones (Schmoll *et al.*, 2010). H-type pheromones show that although **a** and α factors are the prototypical mating pheromones in ascomycetes, sequence, structure, and post-translational processing can vary significantly between species.

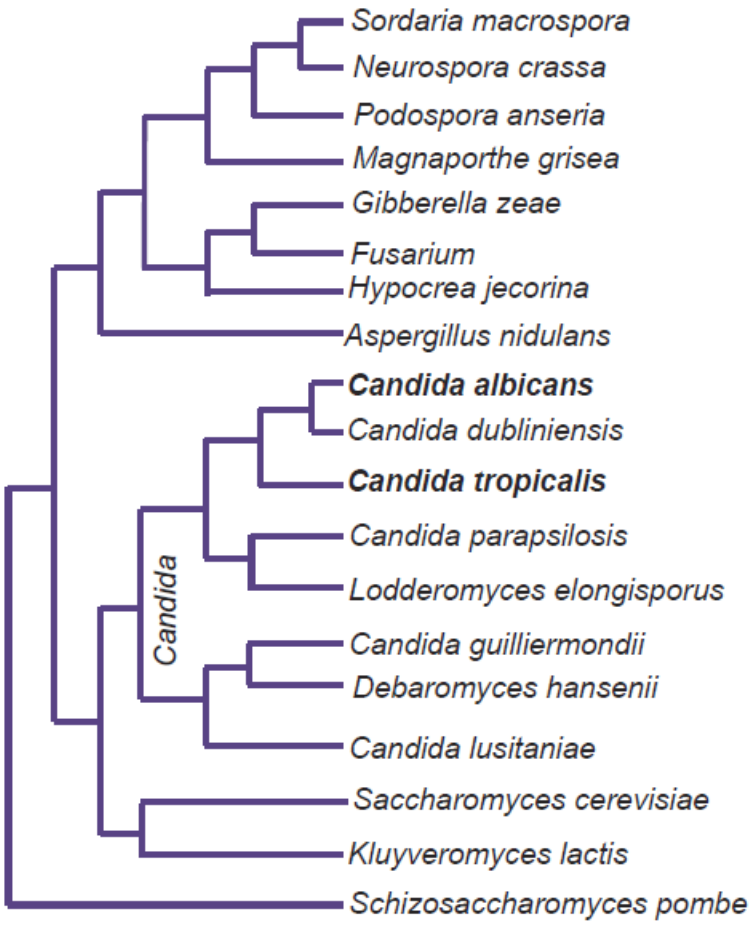

Figure 1-2: Ascomycota phylogenetic tree.

The species discussed in the text are included here for reference. Tree is not drawn to scale.

Transducing the pheromone signal

Pheromones are recognized by G protein-coupled receptors (GPCRs), which reside on the surface of recipient cells (Xue *et al.*, 2008). GPCRs represent the largest family of receptors and are currently one of the most targeted proteins in pharmacological design (Filmore, 2004). The N-terminus of these receptors is extracellular and is followed by seven membrane-spanning regions, while the C-terminus is intracellular and plays a role in downstream signaling (Dosil *et al.*, 2000). GPCRs typically interact with large ligands via their extracellular domains whereas small molecules target GPCR transmembrane domains (Eglen and Reisine, 2009). Both modes of

binding are important for peptide ligands, resulting in conformational changes that propagate the signal to cytoplasmic G proteins (Naider and Becker, 2004; Umanah *et al.*, 2010).

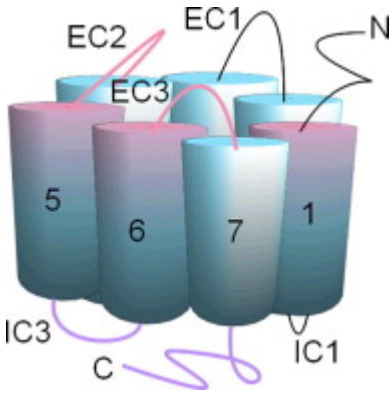

Figure 1-3: the *S. cerevisiae* Ste2 pheromone receptor.

In *S. cerevisiae*, the G-protein-coupled receptor Ste2 recognizes α factor via extracellular (EC) loops 2 and 3 and transmembrane domains 1, 5 and 6. Ste2 associates with G-proteins and activates downstream signaling primarily via the C-terminal tail and intracellular (IC) loop 3. The IC2 region is not shown. Pink colored regions are those implicated in pheromone binding.

The best-studied fungal GPCR is Ste2, the *S. cerevisiae* receptor for α factor (Eilers *et al.*, 2005). The N-terminus of α factor contacts multiple regions of Ste2, including transmembrane (TM) domains 5 and 6, and extracellular (EC) domains 2 and 3 (see Fig. 3) (Lee *et al.*, 2001; Lin *et al.*, 2003; Naider and Becker, 2004). The interaction of α factor with TM5 and TM6 is particularly interesting, since these TMs flank the third intracellular loop (IC3) critical for G protein activation (Stefan and Blumer, 1994; Schandel and Jenness, 1994). In addition, the C-terminus of α factor (Gln^{10} and Tyr^{13}) interacts with residues in TM1 (Lee *et al.*, 2001; Son *et al.*, 2004). Although a high-resolution structure of the ligand-receptor interaction is not available, proposed models reflect the flexibility of the β-turn in the central region of α pheromone (Lin *et al.*, 2003; Umanah *et al.*, 2010). There is also support for oligomerization of Ste2, with recent work showing that oligomer interfaces include TM1, TM4, and TM7, potentially allowing for large complexes to form (Wang and Konopka, 2009; Kim *et al.*, 2009).

Pheromone activation of the GPCR initiates a mitogen-activated protein kinase (MAPK) pathway (see Fig. 4) (Bardwell, 2004; Hoffman, 2005; Chen and Thorner, 2007). In *S. cerevisiae*, activation of Ste2 or Ste3 receptors targets a G protein complex composed of three subunits, α

(Gpa1), β (Ste4), and γ (Ste18). During signaling, the α subunit exchanges GDP for GTP, and dissociates from the βγ complex. The βγ dimer subsequently interacts with three proteins important for the response to pheromone: Ste20, a p21-activated protein kinase, Ste5, a scaffold protein that coordinates the MAPK pathway, and Far1, an additional scaffold protein that is involved in cell cycle control (Peter and Herskowitz, 1994). Signal transduction requires Ste20-mediated phosphorylation and activation of Ste11, the first kinase in the MAPK pathway, which then drives a cascade of phosphorylation reactions involving Ste7 and Fus3 (Zhou *et al.*, 1993; Choi *et al.*, 1994). At the culmination of the pathway, phosphorylated Fus3 accumulates in the nucleus and activates Ste12, the transcription factor required for mating gene expression. Fus3 also phosphorylates (and inactivates) Dig1 and Dig2, two negative regulators of Ste12 activity (Elion *et al.*, 1993; Tedford *et al.*, 1997; Breitkreutz *et al.*, 2001). While the role of the Gβγ subunits in transducing the pheromone signal is well established, the Gα subunit may also promote signaling via the RNA binding protein Scp160, although the mechanism is unknown (Guo *et al.*, 2003).

In comparison, studies in *K. lactis* show that the Gα and Gβ subunits function in a coordinated manner, since both subunits are important for activation of the mating program (Coria *et al.*, 2006). In *C. albicans*, Gα and Gβ also act coordinately, and intriguingly, ectopic expression of either Gα or Gβ can rescue the sterile phenotype of Gγ mutants (Dignard *et al.*, 2008; Lu *et al.*, 2014). Conversely, the response to pheromone in *S. pombe* does not involve Gβγ subunits, and the Gα subunit is solely responsible for signal transduction (Obara *et al.*, 1991; Ladds and Davey, 2000). Thus, even between this subset of ascomycetes, distinct G protein-coupled mechanisms have evolved to transmit the pheromone signal.

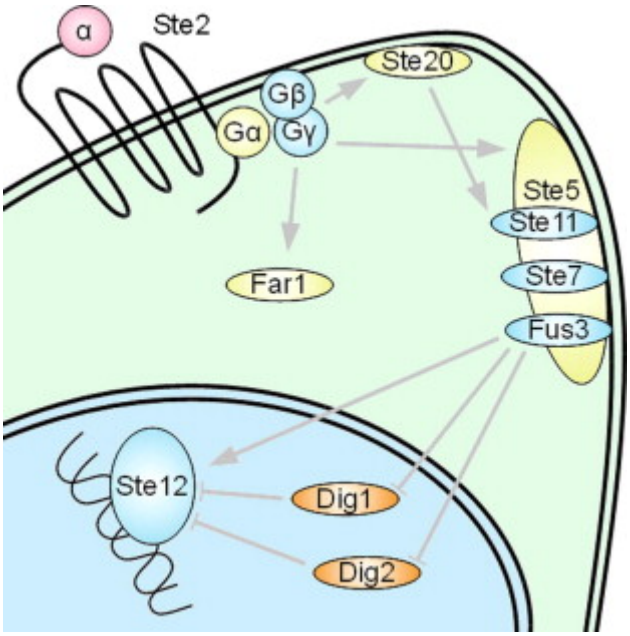

Figure 1-4: The mating MAPK signaling cascade.

Following activation of the pheromone receptor in *S. cerevisiae*, the associated G-protein α subunit exchanges GDP for GTP, releasing β and γ subunits. The βγ complex then interacts with both the Ste5 scaffold and Ste20, which causes sequential activation of kinases Ste11, Ste7 and Fus3. Finally, Fus3 enters the nucleus where it regulates the transcription factor Ste12 to regulate expression of genes important for mating. The Kss1 kinase is primarily involved in filamentation signaling but can also substitute for Fus3 in mating signaling.

Pheromone signaling outputs

The final output of pheromone signaling in *S. cerevisiae* involves three steps: (1) Ste12-mediated transcription of genes involved in mating, (2) formation of polarized mating projections (or shmoos) that promote growth towards the prospective mating partner, and (3) G1 cell cycle arrest that allows fusion of unreplicated nuclei during karyogamy. The latter two processes require Far1; activation of Far1 by Fus3-mediated phosphorylation leads to cell cycle arrest due to Far1 inhibition of Cln2-Cdc28 kinase activity (Chang and Herskowitz, 1990; Peter *et al.*, 1993; Peter and Herskowitz, 1994). During mating projection formation, a Far1-Cdc24 complex also shuttles from the nucleus to the cytoplasm in response to pheromone and promotes interaction of Gβγ with a Cdc24/Cdc42/Bem1 protein complex (Butty *et al.*, 1998; Shimada *et al.*, 2000; Wiget *et al.*, 2004). This complex catalyses actin assembly, resulting in polarized growth towards the highest concentration of pheromone. In *C. albicans, FAR1* plays an even more central role in the pheromone response than it does in *S. cerevisiae. C. albicans far1*

mutants are defective in all three aspects of the pheromone response; thus, they lack the transcriptional response to pheromone, as well as the morphological response and cell cycle arrest phenotypes (Côte and Whiteway, 2008). A *STE5* homolog, *CST5*, exists in *C. albicans*, and loss of this gene prevents signaling in response to pheromone, similar to *S. cerevisiae* (Côte *et al.*, 2011; Yi, Sahni, Daniels, Lu, Huang, Garnaas, *et al.*, 2011). Mating in *S. pombe* utilizes a related MAPK pathway, except mating is also controlled via a nutrient-sensing, cAMP-regulated protein kinase A (PKA) pathway (Mochizuki and Yamamoto, 1992; Lengeler *et al.*, 2000; Hoffman, 2005).

OUTPUTS OF PHEROMONE SIGNALING IN *CANDIDA* SPECIES

With a thorough understanding of the signaling progression of pheromones among ascomycetes, it is prudent to consider how pheromone signaling is integrated into the biology of the *Candida* clade of fungal pathogens. While initially identified by its shared morphological characteristics (Heitman, 2007), the *Candida* clade of can be differentiated from most other fungal species by its alternative genetic code. Rather than encoding CUG as leucine, members of the *Candida* clade encode CUG as serine (Sugita and Nakase, 1999). Perhaps more importantly, however, the majority of fungi that infect the human host are members of this phylogenetic clade (Butler *et al.*, 2009; Butler, 2010). In fact, *Candida* species are the most common cause of human fungal infection (Pfaller and Diekema, 2007) and the fourth-greatest cause of nosocomial bloodstream infections in America (~10%) (Wisplinghoff *et al.*, 2004). The main causal species is *C. albicans*; in conjunction with *C. tropicalis, Candida parapsilosis* and *Candida glabrata*, it is responsible for 85% of invasive *Candida* infections (Pfaller and Diekema, 2007). Despite their pathogenesis, *Candida* species are also commensal to humans. Approximately 70% of healthy individuals carry *C. albicans* in their GI tract (Ruhnke and Maschmeyer, 2002).

The white-opaque switch

Candida species diverged from *S. cerevisiae* approximately 840 million years ago (Hedges, 2002). Throughout this evolutionary span, a multitude of changes have occurred to *Candida*, including those that alter initiation of pheromone signaling and mating. The white-opaque switch is one of the most prominent changes, and occurs in a few of the most pathogenic *Candida* species, including *C. albicans* and *C. tropicalis* (Slutsky *et al.*, 1987; Porman *et al.*, 2011; Xie *et al.*, 2012). In *C. albicans,* the white-opaque switch is a heritable epigenetic transition between two morphologically distinct phenotypes: cells in the white state are smooth and round, producing domed bright colonies, while cells in the opaque state are pimpled and elongated, producing flat, dull colonies (Slutsky *et al.*, 1987; Huang *et al.*, 2006; Zordan *et al.*, 2006:200). Each state has unique metabolic requirements, responds differently to environmental cues, and prefers different host niches (Lan *et al.*, 2002; Sudbery, 2011; Si *et al.*, 2013). For example, white cells are better in systemic infection models, while opaque cells are optimized for cutaneous colonization (Kvaal *et al.*, 1997; Kvaal *et al.*, 1999).

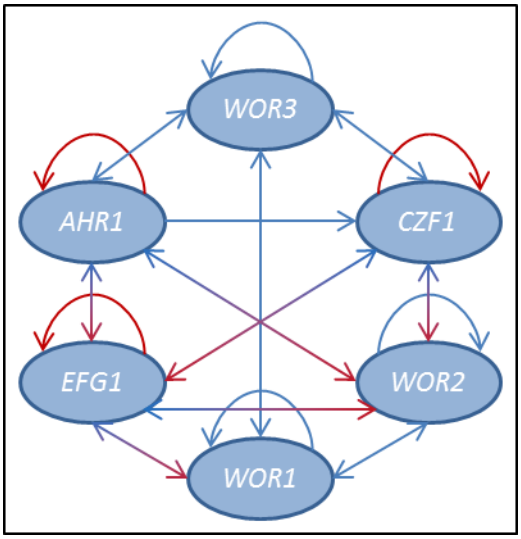

Figure 5: Core transcriptional regulation of the white-opaque switch.

Six core transcriptional factors interact with one another to regulate the white to opaque phenotypic switch. Blue arrows indicate direct binding of the transcription factor to the indicated gene in opaque cells, while red arrows indicate binding in both opaque and white cells. Adapted from Hernday *et al,* 2013.

Until recently, the white-opaque switch was thought to be controlled by just a few main feedback interactions between genes *WOR1, WOR2, EFG1*, and *CZF1*. Here, high Wor1 levels ensured cells were maintained the opaque state, and high Efg1 levels ensured cells were maintained in the white state (Zordan *et al.*, 2007). With the prodigious use of sequencing and chromatin immunoprecipitation technologies, however, our understanding of this network has expanded. Two additional components, *AHR1* and *WOR3* are now considered among the core group of transcription factors regulating the switch (Lohse *et al.*, 2013; Hernday *et al.*, 2013). Further, each of these transcription factors is regulated by itself and nearly every other component (Hernday *et al.*, 2013) as summarized in Figure 5. The number of genes controlled by this network has expanded from earlier estimates of approximately 400 (Tsong *et al.*, 2003), to more than 1,300 genes, including non-coding genes and anti-sense transcripts (Tuch *et al.*, 2010).

One of the most significant differences between cells in the white and opaque states is their differential response to sexual pheromones. In particular, opaque cells secrete mating-type specific pheromones and respond to them by mating (Miller and Johnson, 2002; Bennett and Johnson, 2005). Alternatively, white cells do not secrete high levels of pheromones and undergo mating a million times less frequently than opaque cells (Miller and Johnson, 2002). Interestingly, however, white cells are able to respond to pheromone, becoming adherent and forming biofilms in the presence of pheromones (Daniels *et al.*, 2006). These two responses are detailed below.

Mating: The opaque cell pheromone response

C. albicans is typically isolated in the white state, where expression of mating-specific genes is repressed. For this reason, *C. albicans* and nearly all other *Candida* species were once thought to be asexual. After showing that *C. albicans* contains mating-type genes (Hull and Johnson, 1999), two groups showed that mating is indeed possible in *C. albicans* (Hull *et al.*, 2000; Magee and Magee, 2000). It was subsequently discovered that switching to the opaque state allows cells to undergo mating a million times more frequently than in white cells (Miller and Johnson, 2002) and that switching (and therefore mating) is often limited to either diploid **a**/**a** or α/α cells (Lockhart *et al.*, 2002). This limitation is imposed by a heterodimer composed of **a**1 and α2, which blocks mating-type specific genes in **a**/α cells, as it does *S. cerevisiae*. However, in *C. albicans*, **a**1/α2 also blocks *WOR1* expression, thereby prohibiting cells from switching to the opaque state (Lockhart *et al.*, 2002).

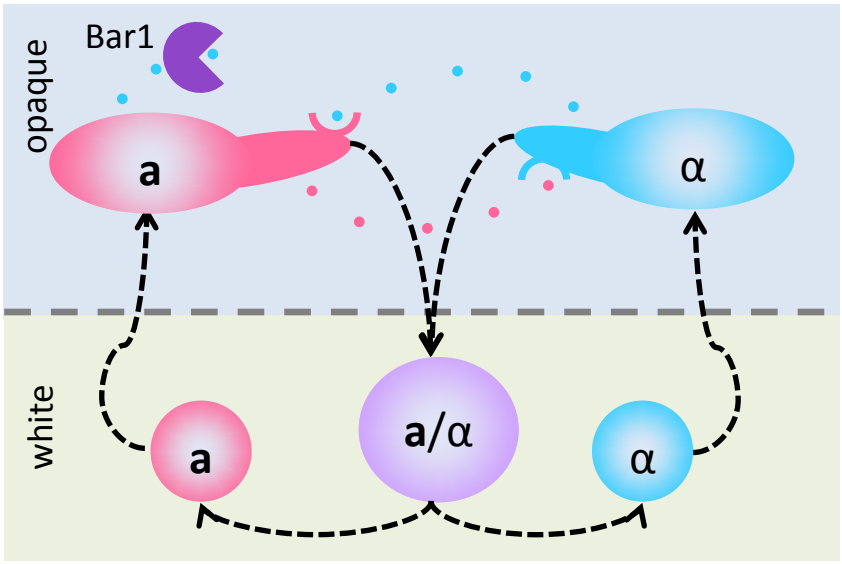

Figure 6: The *C. albicans* mating cycle.

After switching from the white to opaque phenotypic state, diploid **a** and α cells secrete mating pheromones to initiate and guide mating projection growth. Upon contact, the cells fuse to form a tetraploid zygote, which undergoes chromosome loss to return to a diploid state.

More recently, it was shown that white-opaque switching and mating also occur in *C. tropicalis* and are under the control of Wor1 (Porman *et al.*, 2011). In *C. tropicalis*, however, it was shown that **a**/α cells are able to undergo the white-opaque switch similarly to **a** and α cells (Xie *et al.*, 2012) despite producing **a**1 and α2 proteins (Porman *et al.*, 2013). This suggests that either the **a**1/α2 heterodimer does not form, or that it does not repress *WOR1* expression as in *C. albicans*. Perhaps more surprising was the finding that *C. albicans* **a**/α cells are also able to switch to opaque under conditions that mimic the host environment (Xie *et al.*, 2013). As discussed by the authors, this is likely an effect of the complex regulation of *WOR1* (Fig. 5), where competing transcription factors may bind and lead to gene expression by overcoming the typical repressive elements.

In *C. albicans,* opaque cells secrete and respond to pheromones similarly to *S. cerevisiae.* The **a** cells produce **a**-pheromone and the α cells produce α pheromone, each of which is received by receptors on the opposite mating type cell (Ste2 and Ste3) (Fig. 6). Upon reception of the signal, cells upregulate mating-specific genes (Bennett *et al.*, 2003; Dignard *et al.*, 2007), leading to formation of mating projections that ultimately fuse with one another. Karyogamy (nuclear fusion) then occurs, yielding a tetraploid zygote (Shawn R Lockhart *et al.*, 2003). Zygotes assume the white phenotype due to co-production of **a**1 and α2. *C. albicans* undergoes a parasexual cycle, relying on concerted chromosome loss to reduce tetraploid progeny back down to a diploid state, rather than meiosis as in *S. cerevisiae* (Bennett and Johnson, 2003).

Meiosis and chromosome loss are very different strategies for ploidy reduction. Some *Candida* species, such as *C. lusitaniae* undergo meiosis similarly to *S. cerevisiae* (Sherwood *et al.*, 2014). In meiosis, chromosomes are first replicated, increasing the ploidy content two-fold.

After replication is complete, chromosomes are paired and undergo cross-over, which results in greater degree of independence in the distribution of alleles across the paired chromosomes. Next, both the chromosomes and cell divide to produce two cells with ploidy content equivalent to the original cell prior to replication (Meiosis I). Then, a subsequent round of division occurs where sister chromatids are separated and cells are divided to yield four cells, each containing half the ploidy content of the original cell (Meisosis II) (Alberts *et al.*, 2002). For example, a diploid zygote produced from successful mating between two haploid cells will ultimately yield four haploid cells following successful completion of meiosis. In this respect, meiosis can be considered a series of multiplication and *division* operations. Thus, the precise pairing and alignment of chromosomes during meiotic stages results in maintenance of euploid states, and rare instances of aneuploidy are not well-tolerated (Torres *et al.*, 2007).

Chromosome loss, the ploidy reduction strategy employed by *C. albicans* and *C. tropicalis* (see Appendix II), contrasts markedly from meiosis. Here, cells undergo mitosis, cycling between their original ploidy state (G1) and one containing twice the chromosomal content (G2). However, as this cycling occurs, cells randomly discard chromosomes through an unknown mechanism (Bennett and Johnson, 2003). After the first chromosome is discarded, the process continues until cells loss approximately half their ploidy content, settling to an euploid or near-euploid state (Bennett and Johnson, 2003; Forche *et al.*, 2008). It is unknown if there is a mechanism to prevent loss of all copies of a particular chromosome, though further-reduced cells, i.e. haploids in *C. albicans*, have been occasionally isolated (Hickman *et al.*, 2013). Using *C. albicans* as an example, tetraploid zygotes produced from successful mating between diploid cells slowly decrease in ploidy by passing through many aneuploid states, until it ultimately yields diploid cells. In this way, the disorderly nature of chromosome loss can be considered a

series of *subtraction* operations, where aneuploid states are integral to the process and well-tolerated, and in some cases, are even selected for (Forche *et al.*, 2008; Hirakawa *et al.*, 2014).

As in *S. cerevisiae*, pheromone exposure induces growth arrest to facilitate mating in *C. albicans* (Panwar *et al.*, 2003). In both species, an α pheromone-degrading protease Bar1 is secreted by **a** cells in response to pheromone signaling. Degradation of pheromone by Bar1 allows cells to resume normal growth after pheromone exposure and also helps guide mating partners toward one another by sharpening pheromone gradients (Sprague Jr and Herskowitz, 1981; Chan and Otte, 1982; Barkai *et al.*, 1998; Schaefer *et al.*, 2007). Upon deletion of *BAR1*, *C. albicans* cells exhibit heightened sensitivity to α pheromone that can lead to cell death (Alby *et al.*, 2010). Studies also indicate that **a** cells can produce α pheromone (Fig. 6), which in the absence of Bar1, results in homothallic (same-sex) mating. This implicates Bar1 as a control mechanism for alternative mating strategies in this species, a topic that will be revisited in Chapter 2 (Alby et al., 2009).

Biofilms: The white cell pheromone response.

While opaque cells mate in response to pheromone signaling, it was discovered that white cells also produce a pheromone response. In 2006, Daniels *et al.* showed that white cells display pheromone receptors on their surface, and that exposure to pheromones allows white cells to become adherent and form biofilms on plastic and silicone substrates (Daniels *et al.*, 2006). In mixed white/opaque biofilms, opaque cells produce the pheromone necessary to induce biofilm formation in white cells, although adhesion and overall biofilm formation is considered specific to cells in the white state. The biofilm facilitated mating between opaque cells within the biofilm (Daniels *et al.*, 2006). Biofilm formation was consistent across several white **a** and α isolates of *C. albicans*, but has not been reported in any other *Candida* species

(see Chapter 3) (Sahni *et al.*, 2009). Further experimentation has indicated that white cells in a biofilm can also augment pheromone levels by producing pheromone themselves, suggesting that opaque cells may not generate all of the pheromone responsible for the biofilm response (see Chapter 4) (Yi, Sahni, Daniels, Lu, Huang, Srikantha, *et al.*, 2011).

The pheromone-induced biofilm response in white cells utilizes the same receptor and MAPK signaling cascade as the mating response in opaque cells (Yi *et al.*, 2008). However, other aspects of the signaling mechanism have been controversial. It was initially reported that different intracellular loops of the Ste2 receptor were responsible for the divergent pheromone response between white and opaque cells (Yi *et al.*, 2009). This result was later proven to be false, suggesting that downstream components are responsible for the differential response of the two phenotypes. This notion was supported by data showing that Tec1, a regulator of hyphal development (Schweizer *et al.*, 2000) and other biofilm types (Nobile and Mitchell, 2005; Nett *et al.*, 2011), was the terminal transcription factor in the biofilm response (Sahni *et al.*, 2010). This was also proved incorrect. Instead, Cph1, the terminal transcription factor in mating (Ste12 in *S. cerevisiae*) was shown to fulfill this role in the biofilm response (Lin *et al.*, 2013).

Alternative targets for pheromone signaling

With the exception of signaling and mating between sister-species *C. albicans* and *C. dubliniensis* (Pujol 2004), *C. albicans* cells were presumed to only detect pheromones produced by other *C. albicans* cells. However, recent experiments suggest that this may not be the case. Our group recently showed that the *C. albicans* Ste2 pheromone receptor can be activated by pheromones encoded by other *Candida* species (Alby and Bennett, 2011; Lin *et al.*, 2011). This was surprising since some of the pheromone sequences differed by up to 8 out of 13 amino acids, when compared to *C. albicans* α pheromone (see Chapter 2, Table 4). The predicted α

pheromones of *C. dubliniensis, C. tropicalis, C. parapsilosis* and *L. elongisporus* all induced biofilm formation in white cells and homothallic mating in opaque cells of *C. albicans* (Alby and Bennett, 2011). Interestingly, *C. parapsilosis* maintains genes encoding both a pheromone and receptor (Butler *et al.*, 2009), though it has never been observed to mate (Sai *et al.*, 2011). It is possible that these genes are used for an alternative purpose, such as inducing biofilm formation as is seen in *C. albicans* white cells.

These interactions are particularly intriguing given the co-incidence of *Candida* species within the human host. In a recent study by Ghannoum *et. al.*, 15% of healthy study participants had at least two *Candida* species residing within their oral cavity (Ghannoum *et al.*, 2010). While these typically included the well-studied *C. albicans*, *C. parapsilosis* and *C. tropicalis* were frequently present. In diseased individuals, both fungal loads and co-incidence rates are further exacerbated. For example, in a study of individuals with cystic fibrosis undergoing antibacterial treatment, the sputum of every individual contained multiple *Candida* species, which comprised anywhere from three-quarters to the entirety of this mycobiome (Willger *et al.*, 2014). In HIV sufferers with active candida infections such as oral thrush, co-incidence of *Candida* species reached over 70% (Herrera *et al.*, 2012), showing that while individual species may dominate a given infection, pathogenesis often involves multiple *Candida* species. It is also worth noting that while other fungi such as *Mallessezia* and Cladosporium species are often present within the mycobiomes of humans, *Candida* species almost always the main constituent (Ghannoum *et al.*, 2010; Herrera *et al.*, 2012; Willger *et al.*, 2014).

SPECIFIC AIMS

Aim 1. Examine pheromone, receptor and protease interactions in *Candida*.

In many fungal species including *S. cerevisiae*, *S. pombe*, and *C. albicans*, pheromones interact with receptors to initiate mating, and secreted proteases are used to remove pheromones from the extracellular environment. This leads to a three-way state of evolutionary flux among the pheromones, receptors and proteases. Furthermore, the diverse environments that these fungi inhabit dictate that receptors and proteases often interact with other ligands, including pheromones of related fungi. In fact, both *S. cerevisiae* and *C. albicans* receptors can be activated by pheromones from related fungal species (Hisatomi *et al.*, 1988; Alby and Bennett, 2011). We were curious if this was also true of pheromone proteases, particularly *C. albicans* Bar1 protease. To address this question, we characterized the activity and specificity of Bar1 enzymatically and genetically, showing that protease-pheromone interactions can occur and subsequently alter the response of *C. albicans* to other *Candida* pheromones. Aim 1 is explored in Chapter 2.

Aim 2. Determine the pheromone responses of *Candida* species.

Work in *Candida albicans* has shown that sexual pheromones can initiate additional cell responses beyond mating, particularly biofilm formation. Biofilms also enhance mating by facilitating chemotaxis in opaque cells (Daniels *et al.*, 2006). The related species *C. tropicalis* was recently shown to undergo mating in a pheromone-dependent manner similarly to *C. albicans.* However, no additional responses to sexual pheromones were noted. Given the close evolutionary relationship of these two species, we speculated that *C. tropicalis* might also form biofilms in response to sexual pheromones. We found this to indeed be the case, then

investigated the genetic and architectural features of the biofilms, as well as their ability to support mating. Aim 2 is primarily covered in Chapter 3.

Aim 3. Evaluate the relationship between biofilm formation and cell phenotype.

In *C. albicans* and C. *tropicalis* there is a close relationship between the ability to form biofilms and the phenotypic state (white or opaque) of the cell. In order to examine the relatedness of these phenomena, we first investigated the effects of overexpressing white-opaque regulators in *C. tropicalis*. We found that overexpression of *WOR1* modulated both filamentation and biofilm formation independently of pheromone stimulation in all mating-type backgrounds, including **a**/α. To probe the phenotype-biofilm relationship across *C. albicans*, we explored the ability of white and opaque cells from a wide range of clinical isolates to form sexual biofilms under different pheromone signaling regimes. Aim 3 is the main focus of Chapter 4 and a minor focus of Chapter 3.

CHAPTER 2: BIOCHEMICAL AND GENETIC DISSECTION OF THE ROLE OF *C. ALBICANS* BAR1 IN PHEROMONE SIGNALING

ABSTRACT

Candida albicans is one of several opportunistic *Candida* species that can co-inhabit the human host. Several species encode unique sexual pheromones that are integral to successful mating. In *C. albicans*, as in many types of yeast, mating involves the reciprocal secretion of sex-specific pheromones by **a** and α cells, leading to the formation of mating projections and subsequent cell fuse to form zygotes. This process is regulated by Bar1, a conserved aspartyl peptidase that is secreted by **a** cells and acts to degrade α pheromone. Here, we characterize the biochemical activity of purified *C. albicans* Bar1 and show that it degrades not only the canonical α pheromone but also α pheromones from related *Candida* species, including those of *C. dubliniensis* and *C. tropicalis*. Analysis of *C. albicans* Bar1 indicates that it demonstrates several unusual properties, with a near neutral pH optima, low specificity requirements at the P1 and P1' sites, and insensitivity to aspartyl peptidase inhibitors based on Pepstatin A. To address the role of Bar1 in inter-species pheromone signaling, *C. albicans bar1* mutants were evaluated and shown to exhibit increased sensitivity to pheromones secreted by *C. dubliniensis, C. tropicalis* and *C. parapsilosis*. This indicates a novel role for Bar1 in regulating inter-species signaling events in addition to its established roles in controlling intra-species signaling. We discuss these findings with respect to how pheromone signaling affects the evolution of α pheromone, Bar1 protease and the Ste2 receptor within *C. albicans* and across the *Candida* clade.

INTRODUCTION

Candida species are the most prevalent fungal pathogens affecting humans. While several *Candida* species are commensal to the human population (Glick and Siegel, 1999; Nucci and Anaissie, 2001; Ruhnke and Maschmeyer, 2002), the immunocompromised are subject to a substantial risk of candidiasis (Wisplinghoff *et al.*, 2004). Within the clinical setting, close to one in two sufferers of systemic *Candida* infection ultimately succumb to the disease (Pfaller and Diekema, 2007). Furthermore, *Candida* species affect 5% of newborns and 10% of the elderly due to oral candidiasis, the latter contributing to a 65% frequency of stomatitis in denture wearers (Glick and Siegel, 1999; Samaranayake *et al.*, 2002; Zordan *et al.*, 2006). These seemingly manageable infections can also provide a reservoir for future life-threatening infections (Nucci and Anaissie, 2001).

The human oral microbiome hosts a diverse array of microbial species, which form an interdependent environment both with each other and with host cells. Signaling between microbial species, as well as with the host, is integral to the success of these microbial communities. Notable examples of signaling include bacterial quorum sensing molecules such as acyl homoserine lactone and peptide auto inducers that coordinate biofilm formation and colony growth (Solano *et al.*, 2014), and host immune system molecules acting within the oral cavity, such as cytokines, reactive oxygen species and antimicrobial peptides (Ji and Choi, 2013). Of the thousands of microbial species thus far identified in the oral cavity (Liu *et al.*, 2012), recent work shows that a large proportion of the fungal flora is composed of several *Candida* species, which are frequently isolated together from the same host (Ghannoum *et al.*, 2010). The importance of these findings is emphasized by current figures showing that while approximately half of *Candida* infections are caused by *C. albicans,* other major causal species include *Candida tropicalis, Candida parapsilosis* and *Candida glabrata*, and that the prevalence

of non-*albicans Candida* infections is expected to continue to rise (Krcmery and Barnes, 2002). Less is known about secreted fungal effectors, although farnesol and tyrosol are well-documented regulators of quorum sensing and filamentation in *C. albicans* (Hornby *et al.*, 2001; Chen *et al.*, 2004; Mallick and Bennett, 2013).

One of the established extracellular signals utilized by *Candida* species are sexual pheromones. In *C. albicans*, pheromones are known to control both mating and sexual biofilm formation (Miller and Johnson, 2002; Daniels *et al.*, 2006; Yi *et al.*, 2008), and these two alternative responses are governed by a heritable, epigenetic switch between 'white' and 'opaque' states. Originally named for their colony appearance on solid media (Slutsky *et al.*, 1987), these two states show marked differences in morphology, metabolism, and signaling, including distinct responses to many environmental cues, including pheromones (Geiger *et al.*, 2004; Sudbery, 2011; Si *et al.*, 2013). *C. albicans* opaque cells secrete and respond to pheromones in a mating type-specific manner similar to that in the model yeast, *Saccharomyces cerevisiae*. In both species, **a** cells produce **a** pheromone, which activates Ste3 receptors on α cells, while α cells produce α pheromone, which activates Ste2 receptors on **a** cells (Lockhart *et al.*, 2003; Bennett *et al.*, 2003; Panwar *et al.*, 2003). Pheromone signaling results in mating responses, where conjugation tubes are extended and fusion between diploid **a** and α cells generates **a**/α zygotes (Shawn Lockhart *et al.*, 2003; Bennett *et al.*, 2005). Cells responding to pheromone experience cell cycle arrest until either mating is complete, or pheromones have been depleted from the environment. *C. albicans* white **a** and α cells also respond to pheromones, but rather than undergoing conjugation, they are induced to form sexual biofilms (Daniels *et al.*, 2006; Yi *et al.*, 2008). Given that biofilms are important mediators of colonization and infection in the host (Harriott and Noverr, 2011), understanding these mechanisms can contribute to the prevention of disease.

An additional layer of complexity in fungal pheromone signaling derives from proteolytic activities that act to degrade mating pheromones and thus regulate sexual behavior. In *S. cerevisiae*, it has long been recognized that **a** cells secrete an aspartyl protease, Bar1, that degrades α pheromone and thus acts as a partial barrier to pheromone signaling from α cells (Sprague Jr and Herskowitz, 1981; Chan and Otte, 1982). The role of this protease was originally thought to be the removal of excess α pheromone, thereby allowing unmated **a** cells to resume the cell cycle following pheromone-induced cell cycle arrest. *S. cerevisiae* cells lacking Bar1 also mated less efficiently than wildtype cells (Sprague Jr and Herskowitz, 1981), and Barkai *et. al.* subsequently showed that Bar1-mediated pheromone destruction leads to sharpening of the α pheromone gradient and greater success in mate detection (Barkai *et al.*, 1998).

Studies in *C. albicans* revealed that this species produces an equivalent aspartyl protease, also named Bar1, that is similarly produced by **a** cells and degrades α pheromone (Schaefer *et al.*, 2007). Loss of Bar1 resulted in a marked defect in mating between *C. albicans* **a** and α cells that was due, at least in part, to overstimulation of pheromone signaling in responding **a** cells (Schaefer *et al.*, 2007). Interestingly, *C. albicans* **a** cells were found to secrete low levels of α pheromone (in addition to the conventional **a** pheromone), and thus loss of Bar1 resulted in autoactivation of the pheromone response, and even same-sex **a**-**a** mating (Alby *et al.*, 2009). The presence of Bar1 is therefore necessary to prevent autocrine signaling by α pheromone in **a** cells, whereas α pheromone produced by α cells is sufficient to override Bar1 activity (Schaefer *et al.*, 2007; Alby *et al.*, 2009).

Structurally, *S.cerevisiae* Bar1 and *C.albicans* Bar1 proteins share greater than 36% sequence similarity both to one another and to the well-characterized aspartyl proteases, pepsin and renin (MacKay *et al.*, 1988). *S.cerevisiae* Bar1 is a highly-glycosylated, heat-stable aspartyl protease, with a pH optima of 6.5 (Manney, 1983; MacKay *et al.*, 1991). It acts

specifically on *S.cerevisiae* α pheromone, cleaving between residues 6 and 7 of the 13 amino acid peptide, WHWLGL$^{\downarrow}$KPGQPMY. Furthermore, *S.cerevisiae* Bar1 is an unusual aspartyl protease in that it is not inhibited by Pepstatin A, a standard inhibitor for many aspartyl proteases (MacKay *et al.*, 1991; Nath, 1993). In contrast to *S.cerevisiae*, *C. albicans* Bar1 has not been biochemically characterized.

In this work, we address the role that Bar1 plays in regulating *C. albicans* pheromone signaling through biochemical characterization of the peptidase and elucidation of the effects of the loss of Bar1 on intra- and inter-species signaling. *C. albicans* Bar1 was overexpressed and purified, and its specificity determined, including cleavage activity on pheromones from related *Candida* species. Genetic experiments reveal that Bar1 and endogenous α pheromone modulate the response of *C. albicans* white and opaque cells to pheromones from *C. dubliniensis*, *C. tropicalis* and *C. parapsilosis*. These results have important implications for interspecies signaling events, particularly when considering host niches where multiple *Candida* species are present in a single microbial community.

MATERIALS AND METHODS

Media

All media was prepared using previously described methods (Lee *et al.*, 1975; Guthrie and Fink, 1991). Spider media contained 1% nutrient broth, 0.4% potassium phosphate, and 2% mannitol (pH 7.2). Solid media were made with 1.35% agar.

Strain and plasmid construction

Strains used here are listed in Table 1. To overexpress *C. albicans* Bar1 protein, polymerare chain reaction (PCR) was used to generate a DNA product containing the entire open reading frame (ORF) of *BAR1* from genomic DNA. The primers used added a 6x His tag to the end of the ORF and restriction endonuclease cut sites. The PCR product was then cloned into the pPinkα-HC plasmid under the *AOX1* promoter (Life Technologies) to yield plasmid pBar1-His. Site-directed mutagenesis via the QuikChange II kit (Agilent Technologies) was used to mutate position +695 from adenine to cytosine to yield plasmid pBar1(D232A)-His, which contains amino acid substitution D232A in the predicted active site of the Bar1 protein. Both plasmids were transformed into *PichiaPink* strains to generate strains CAY793-796 and CAY800-802.

To construct *C. albicans* deletion strains of *MFα* and *BAR1*, plasmids pRB13 and pRB35, respectively, were used with the previously-described SAT1-flipper method (Reuss *et al.*, 2004; Noble and Johnson, 2005). Briefly, regions flanking the ORF of the gene of interest were PCR amplified together with oligonucleotides containing ApaI/XhoI (5' flank) and SacII/SacI (3'flank) restriction sites. The products were cloned into plasmid pSFS2a (Reuss *et al.*, 2004). The resulting plasmids were digested with ApaI and SacI and transformed into *C. albicans*. Correct integration was confirmed by PCR and the *SAT1* marker was excised by growth on maltose medium to induce the FLP recombinase (Reuss *et al.*, 2004). Transformations were then

repeated to replace the second copy of the gene of interest. To overexpress *WOR1*, strains were transformed with plasmid pRB99 (p*ACT1*-*WOR1*) (Alby *et al.*, 2010).

Bar1 production

P. pastoris strains CAY794 and CAY800 were grown in BMGY media (1% yeast extract, 2% peptone, 100 mM potassium phosphate, pH 6.0, 1.34% YNB, 0.00004% biotin, 1% glycerol) for two days, then cells were concentrated and switched to BMMY media (1% yeast extract, 2% peptone, 100 mM potassium phosphate, pH 6.0, 1.34% YNB, 0.00004% biotin, 0.5% methanol) to induce expression of *C. albicans* Bar1 for two days. Methanol concentration was maintained by further addition of methanol after 24 h. Cells were centrifuged and the supernatant was collected, followed by 40-fold concentration using an Amicon cell (EMD Millipore, Darmstadt, Germany). The cell was also used to perform buffer exchange into Ni-NTA binding buffer (300 mM NaCl, 50 mM NaH_2PO_4, 10 mM imidazole, pH 8.0). The resulting solution was batch-bound to HisPur Ni-NTA resin (Thermo Fisher Scientific, Waltham, MA), then washed twice (300 mM NaCl, 50 mM NaH_2PO_4, 20 mM imidazole, pH 8.0), and the product eluted (300 mM NaCl, 50 mM NaH_2PO_4, 500 mM imidazole, pH 8.0). The product was dialyzed into storage buffer (PBS, 20% glycerol). Protein concentration was determined using a Bradford protein assay (Thermo Scientific).

Analysis of peptide cleavage by liquid chromatography – mass spectrometry

Lyophilized peptides (Lifetein LLC) were dissolved in 10% DMSO, mixed with 127 nM of either Bar1-His or Bar1(D232A)-His protein in 50 µM potassium phosphate solution (pH 6.5) for one hour at 37°C, then passed through a centrifugal filtration unit to separate peptide fragments from the peptidase. Samples were analyzed using a Shimadzu HPLC and Thermo LCQ Deca XP Max ion trap mass spectrometer system.

Multiplex Substrate Profiling by Mass Spectrometry (MSP-MS).

MSP-MS assays were carried out as described previously (O'Donoghue *et al.*, 2012). Briefly, ~60 nM active Bar1-His, Bar1(D232A)-His and matched no-enzyme control were assayed against a diverse library of 228 tetradecapeptides pooled at 500 nM in 10mM KH_2PO_4 (pH 6.5) and incubated at 37°C. After 60, 240 and 1200 minutes, 30 µL of assay mixture was removed, quenched with 7.5 µL 2% formic acid, and frozen. Prior to mass spectrometry acquisition, peptide samples were desalted using Millipore C_{18} ZipTips and rehydrated in 0.2% formic acid. LC-MS/MS data were acquired using a Thermo Scientific LTQ-Orbitrap mass spectrometer, which was equipped with a Thermo Scientific EASY-Spray Ion Source, EASY-Spray PepMap C_{18} Column (3 µM, 100 Å), and Waters nanoACQUITY UPLC System. Mass spectrometry peak lists were generated using PAVA, and data were searched against the 228-member peptide library using Protein Prospector software v.5.12.4 (UCSF). Protein Prospector score thresholds were selected with a minimum protein score of 15 and minimum peptide score of 10. Maximum expectation values of 0.01 and 0.05 were used for protein and peptide matches, respectively. Peptides corresponding to cleavage products were imported into iceLogo (Colaert *et al.*, 2009) to generate substrate specificity profiles as described (O'Donoghue *et al.*, 2012). Octapeptides corresponding to either P4-P4' or P1'-P8' were used as the positive dataset, and octapeptides corresponding to all possible cleavages in the MSP-MS library (N = 2,964) were used as the negative data set.

Protein Characterization

To determine Bar1 levels in culture, *C. albicans* strains were grown at room temperature overnight in synthetic complete dextrose (SCD) medium (Guthrie and Fink, 1991) and cells washed. Next, 20*10^7 cells were grown for 5 hours in 10 mls SCD medium with or without 0.3

μM synthetic α pheromone. The supernatant and cells were separated by centrifugation, and 40 μl of each was prepared for SDS-PAGE in Laemmli sample buffer. Samples were analyzed by SDS-PAGE and Western blotting. For anti-His blots, a 1:5000 dilution of Sigma's HRP-conjugated monoclonal anti-poly Histidine antibody (A7058) was used according to manufacturer's directions. For anti-Bar1 blots, a 1:1000 dilution of sera containing a poly-clonal anti-Bar1 antibody designed by New England Peptides (Project 2095, raised against epitopes Ac-YFINETIRSNDWKC-amide and Ac-CSDDKITSVTSNPQ-amide) was used, followed by a 1:10,000 dilution of GAR-HRP (Jackson Immuno Research). Proteins were visualized using a chemiluminescent substrate (Pierce) and a Chemidoc XRS+ system (Bio-Rad).

For assessing glycosylation of Bar1, a protein deglycosylation assay was performed on the purified Bar1 protein according to the manufacturer's directions (New England Biolabs P6039S), and followed by SDS-PAGE and western blotting as described above. Assessment of the signal peptide sequence of Bar1 was completed using SignalP-4.1 prediction (http://www.cbs.dtu.dk/services/SignalP/).

Internally Quenched (IQ) Peptide Assays

The IQ peptide was produced by LifeTein, LLC (Hillsborough, New Jersey) with the following sequence and fluorophores: DABCYL-GFRLTNFGYEPG-E-EDANS. Unless otherwise noted, all experiments were done at 37°C in 50 μM potassium phosphate buffer, pH 6.5, with a substrate concentration of 50 μM and 60 nM recombinant Bar1 protease. The protease and substrate were combined in a 96-well plate immediately before beginning the experiment, and then fluorescence emission was measured over 90 minutes using a BioTek Synergy HT plate reader (Winooski, Vermont).

Pheromone-Induced Cell Death and Halo Asays

C. albicans opaque cells were grown in SCD overnight at room temperature in a rotating drum. Cultures were washed with water, then resuspended in Spider media at 2X10^7 cells/ml, and α pheromone was added at the indicated concentration. After 5 hours incubation at room temperature in a rotating drum, 500 µl of culture was removed and washed with water. Then, the cells were resuspended in SCD media containing 1 µg/ml propidium iodide for 15 minutes. Cells were washed again, resuspended in SCD media and analyzed by flow cytometry on FACSCalibur cell sorter. At least 10,000 events were analyzed for fluorescence in channel FL3. For halo assays, 10^5 opaque cells were plated onto Spider solid media. Twenty µg of α-pheromone was spotted onto the center of the plate. The plates were incubated at room temperature for three days, after which images were acquired.

Biofilm Adherence

C. albicans white cells were grown overnight in Spider media at room temperature on a rotating drum. Cells were washed with water, then administered to each well of a 12-well plate containing 1 ml of Lee's + Glucose media at a concentration of 4*10^7 cells/ml. Pheromones were added at the indicated concentration, then plates were incubated at room temperature for 2 days with no shaking. Each well was then washed gently 3 times with water to remove non-adherent cells. Adherent cells were then scraped and resuspended in 1 ml of water, then the optical density of each sample was determined at 600nm on a Nanodrop 2000c (Thermo Scientific).

Table 2-1: Strains used in this study.

Strain number	Name	Genotype	MAT
Pichia production			
CAY 5091	PP2	ade2/ade2 pep4/pep4	
CAY 794	PP2-Bar1-His	ade2/ade2 pep4/pep4 AOX1/BAR1HIS	diploid
CAY 801	PP3-Bar1*-His	ade2/ade2 pep4/pep4 AOX1/BAR1(D232A)HIS	diploid
Westerns			
CAY 851	Ca Bar1 Histag	bar1/bar1::BAR1HIS	a/a
CAY 852	Ca Bar1 Histag	bar1/bar1::BAR1HIS	a/a
CAY 1049	Bar1.His.Wor1(A)	bar1/bar1::BAR1HIS pACT1/pACT1-WOR1::SAT1	a/a
CAY 1050	Bar1.His.Wor1(B)	bar1/bar1::BAR1HIS pACT1/pACT1-WOR1::SAT1	a/a
Bar1 testing			
PID			
DSY89	AM2003-0191		a/a
CAY 1010	AM2003.Wor1	pACT1/pACT1-WOR1::SAT1	a/a
CAY 1078	AM2003.deltaBar1	bar1/bar1	a/a
CAY 1230	AM2003.dBar1-Wor1	bar1/bar1 pACT1/pACT1-WOR1::SAT1	a/a
Halo			
RBY1177	opaque of 1173		a/a
RBY1220			
CAY 846	Ca Bar1 Mutant Histag	bar1/bar1::BAR1(D232A)HIS	a/a
CAY 847	Ca Bar1 Mutant Histag	bar1/bar1::BAR1(D232A)HIS	a/a
CAY 851			
CAY 852			
Biofilms			
DSY89			
CAY 1467	AM2003 dBar1 (2)	bar1/bar1	a/a
CAY 1468	AM2003 dBar1 (3)	bar1/bar1	a/a
CAY 1078			
CAY 3949	AM2003 dMFalpha	mfα/mfα	a/a
CAY 3950	AM2003 dMFalpha	mfα/mfα	a/a
CAY 1607	AM2003 dBar1 (9x) SAT-	bar1/bar1	a/a
CAY 1545	AM2003 dBar1 dMFalpha (a2)	bar1/bar1 mfα/mfα	a/a
CAY 716	P37005		a/a
CAY 1148	P37005 Bar1 -/-	bar1/bar1	a/a
CAY 1149	P37005 Bar1 -/-	bar1/bar1	a/a
CAY 2208	716 dBar1 dMfalpha	bar1/bar1 mfα/mfα	
CAY 2209	716 dBar1 dMfalpha	bar1/bar1 mfα/mfα	
PID			
CAY 1010			
CAY 1230			
CAY 2096	AM2003 dBar1 -Wor1	bar1/bar1 pACT1/pACT1-WOR1::SAT1	
CAY 3980	AM2003 dMFalpha	mfα/mfα	a/a
CAY 3981	AM2003 dMFalpha	mfα/mfα	a/a
CAY 4051	AM2003 dMFalpha	mfα/mfα	a/a
CAY 4052	AM2003 dMFalpha	mfα/mfα	a/a
CAY 1997	AM2003 dBar1 dMFalpha -Wor1stim	bar1/bar1 mfα/mfα pACT1/pACT1-WOR1::SAT1	
CAY 1606	AM2003 dBar1 dMFalpha (a2) SAT-	bar1/bar1 mfα/mfα	a/a
Interspecies			
RBY1177			
RBY1178			
RBY1179			
RBY1180			
CAY 3985	1179 dMFalpha		a/a
CAY 3986	1179 dMFalpha		a/a
CAY 3713	1179 dMFalpha		a/a
CAY 3714	1179 dMFalpha		a/a
CAY 3654	1174dMFalpha		alpha/alpha
CAY 3885	1174dMFalpha		alpha/alpha
CAY 2322	320(dBar1)dMfalpha		a/a
CAY 2325	320(dBar1)dMfalpha		a/a
CAY 4696	1174 dMFalpha dBar1		alpha/alpha
CAY 4707	1174 dMFalpha dBar1opaque		alpha/alpha
CAY 3680	dMFalpha MFparap		alpha/alpha
CAY 3681	dMFalpha MFparap		alpha/alpha
CAY 4002	dMFalpha MFparap		alpha/alpha
CAY 3676	dMFalpha MFtropic		alpha/alpha
CAY 3855	dMFalpha MFtropic		alpha/alpha
CAY 320	bar1 KO		a/a
CAY 321	bar1 KO		a/a
CAY 2053	Ct a ARG4 KO opaque		a/a
CAY 4247	CAY1502 opaque b		a/a
CAY 2055	Ct alpha HIS1 KO opaque		alpha/alpha
CAY 2056	Ct alpha ARG4 KO opaque		alpha/alpha

Table 2-2: Oligonucleotides used in this study.

number	oligo name	sequence
Making pPINK plasmid		
441	Bar 1 (StuI) for	5' GGA GCG AGG CCT TTG TTT AGA ATT CTT AGT TTA C 3'
521	3' END CaBAR1 (NEW)	GGCCGCGTTAACCTCGACATAATGGTGATGATGGTGATGGCCACAATACTGTGGGTTAGAGG
And the mutant via SDM:		
516	BAR1 (DA) MUTANT	AACCAGAAAACCTTGTACCAAATTGCTAGTGGCACCAACGGATT
517	BAR1 (MUTANT) REV	ACAGTGGTTTCACTTTCAGC
Bar1 deletion		
	YPS3 5' ORF	GATCTACAACTTCTCGGCTT
	YPS3 3' ORF	TGGTACAAATCCGTTGGTGC
588	BAR1 FOR (-1000)	AGGTCTATTAGAATCTCTTTTGTCC
	YPS3 3' check	GGCGAAAATGACAAGTACTGG
567	pSFS LEFT	CTCAACCATAGCAATCATGG
1483	pSFSright	gcgaaaaagtgggcactaag
Mfα deletion		
	Mfα 5' ORF	GCCACTATTGTTGCTGCTGC
	Mfα 3' ORF	GTCTAAAACGGGCTTGAGCA
	Mfα 5' check	CGCAGTTCATTTATGCACGTC
	Mfα 3' check	GCTTATGGTACGTGAATGAG

Table 2-3: Plasmids used in this study.

Number	Name	Purpose
RB13	pSFS2a MFα KO	Delete MFα in C. albicans
RB35	pSFS2a BAR1 KO	Delete BAR1 in C. albicans
RB99	pSFS2a pACT1-WOR1	Over-express WOR1 in C.albicans, locking cells in opaque state

RESULTS

Purification and characterization of *C. albicans* Bar1 protease

To study the biochemical activity of *C. albicans* Bar1, a recombinant form of the protein was overexpressed and purified from *Pichia pastoris*. The *BAR1* gene was engineered to include a hexahistidine tag at the C-terminus and overexpressed in *P. pastoris* using the PichiaPink expression system (see Methods). This system involves expression of the target gene under the control of the regulated alcohol oxidase gene (*AOX1*) promoter and secretion of the target protein into the supernatant using the endogenous α pheromone signal peptide sequence. The secreted *C. albicans* Bar1 protein was concentrated and purified by nickel affinity chromatography (Fig. 1A, Supp. Fig. 1) with a final yield of 6 mg per liter of cells. The purified Bar1 protein migrated as a broad range of high molecular weight bands in western blots, which was likely due to extensive glycosylation. Indeed, *in vitro* treatment of the Bar1 protein with purified glycosylases reduced the molecular weight in SDS-PAGE gels (Fig 1B). Both wildtype and mutant Bar1 proteins were generated; the mutant form consisted of an amino acid substitution in the predicted active site aspartyl residue (D232A).

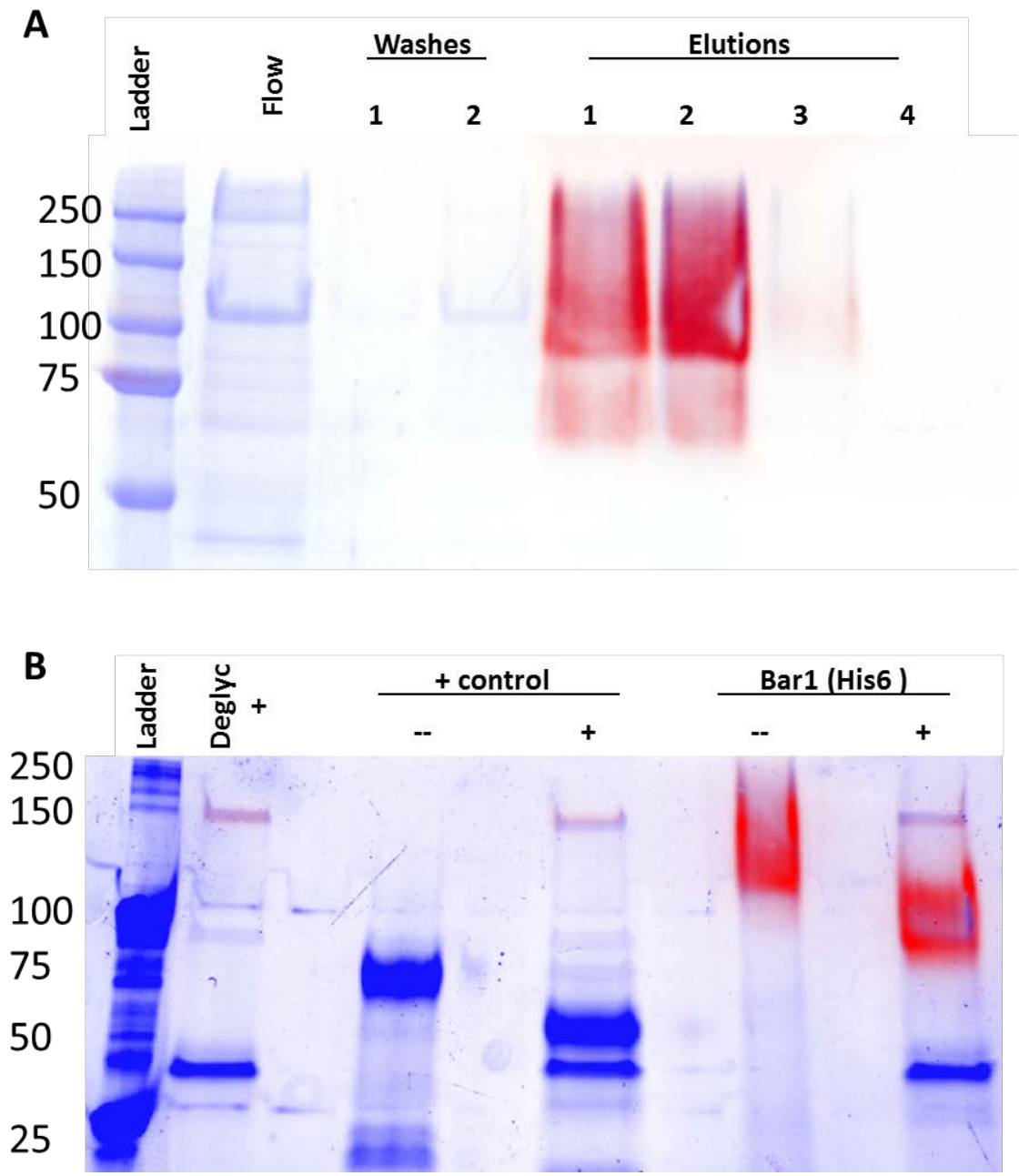

Figure 2-1: Purification and glycosylation of recombinant Bar1 protease.

(A) Following secretion of recombinant Bar1 from *Pichia pastoris*, the protein was concentrated then purified using nickel affinity chromatography. Flow: 10mM imidazole. Wash: 20mM imidazole. Elution: 500mM imidazole.

(B) Recombinant Bar1 protease and a positive control protein (fetuin) were treated (+/-) with a deglycosylation cocktail according to the manufacturer's directions (NEB P6039). Deglyc + is deglycosylase enzymes alone.

Blue indicates total protein via coomassie stain (A) or Biorad Stainfree © indicator (B). Red indicates Bar1 protein via anti-His6 antibody (see Materials and Methods for procedure).

To test activity of recombinant Bar1, the purified protein was used in reconstitution experiments with *C. albicans* strains lacking the *BAR1* gene. A quantitative readout of the pheromone response in *C. albicans* is pheromone-induced cell death (PID); *C. albicans* opaque **a** cells responding to synthetic α pheromone undergo cell death in a significant proportion of the population (Alby *et al.*, 2010). This response is sensitive to pheromone levels, so that **a** cells lacking the Bar1 protease undergo PID at lower pheromone concentrations than wildtype cells (Alby *et al.*, 2010). Wildtype opaque **a** cells exposed to 10 µM α pheromone showed low levels (<10%) cell death, while *bar1Δ/bar1Δ* mutants exposed to pheromone showed ~70% cell death (Fig. 2A). Addition of recombinant Bar1 protein (12.7 nM) to *bar1Δ/bar1Δ* mutants restricted cell death to <10% of the population, indicating that the purified protein reduced pheromone concentrations in the absence of endogenous Bar1 activity. In contrast, addition of the Bar1 D232A mutant failed to restore wildtype levels of PID, consistent with this mutant being catalytically inactive (Fig. 2A). A similar result was obtained using a halo assay to monitor pheromone activity. In this assay, pheromone is spotted onto a lawn of cells and cells then allowed to grow to confluence; growth is inhibited in cells that respond robustly to the spotted pheromone indicative of the strength of the pheromone response. As shown in Figure 2B, wildtype opaque **a** cells typically generate a weak halo in response to α pheromone. However, *bar1/bar1* mutants showed a much larger and more distinct halo in response to pheromone. Addition of the wildtype Bar1 protein reduced halo formation in the *bar1Δ/bar1Δ* mutant to that of the wildtype control (Fig. 2B), whereas the mutant Bar1 did not, further establishing that the recombinant protein was functional.

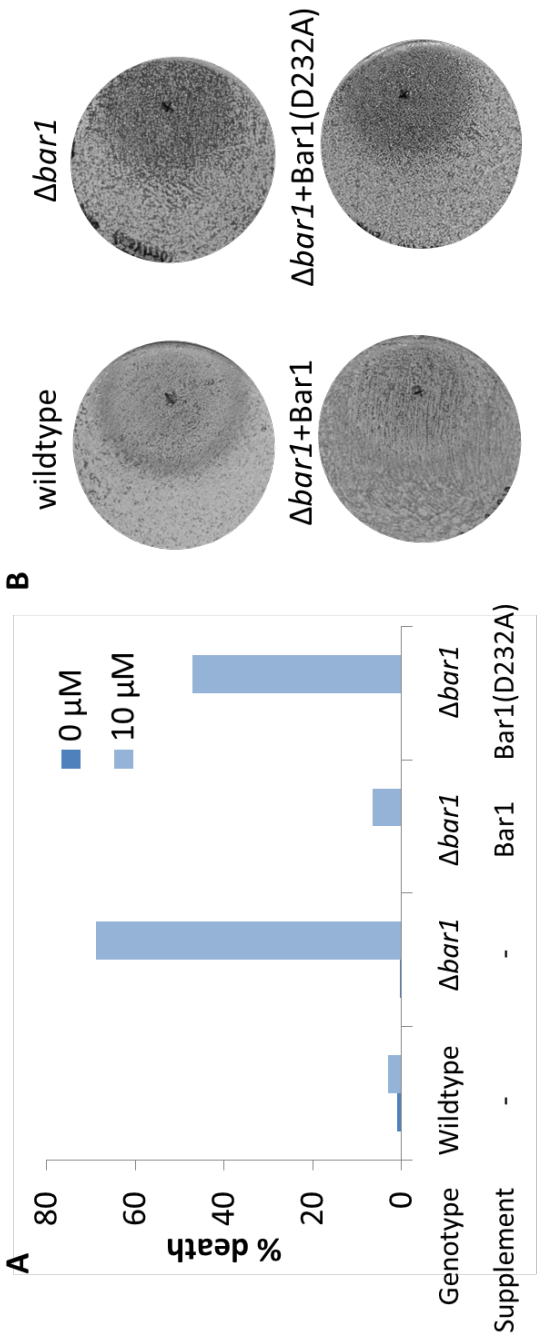

Figure 2-2: Effect of Bar1 and the D232A mutant on pheromone response in *C. albicans*.

Wildtype, and *Δbar1* opaque **a** strains were treated with α pheromone and either recombinant Bar1 or the Bar1* mutant. (A) The indicated strain was treated with or without 10µM α-pheromone for 5 hours in liquid culture. In indicated cases, either recombinant Bar1 or the D232A mutant were also included in the 5 hour incubation at 12.7 nM. Percent death was analyzed by staining with propidium iodide and flow cytometry. (B) Cell cycle arrest was analyzed by plating a lawn of cells on solid media, spotting with pheromone and protease, then imaging after 2 days growth.

Cleavage of α pheromone by *C. albicans* Bar1

To determine the position of Bar1 cleavage on α pheromone, the purified peptidase was used to digest *C. albicans* α pheromone, GFRLTNFGYEPG, and the digested product analyzed by HPLC and mass-spectroscopy (see Methods). Two degradation products were formed, indicating a single cleavage event and positioning the scissile bond between threonine 5 and asparagine 6 (Fig. 3). This specificity differs from many aspartyl peptidases, which typically prefer hydrophobic amino acids at the scissile bond (Dunn, 2001). Peptidases, including aspartyl peptidases, often exhibit specificity for residues neighboring the scissile bond, as well as substrate length requirements (Dunn, 2001). To examine the specificity of *C. albicans* Bar1 a series of alternative pheromone-like peptides were tested, including those containing di-alanine substitutions (Table 5). Most alanine-substituted peptides were still suitable substrates for degradation by Bar1, although substitution of C-terminal residues (residues 10-13) resulted in inhibition of cleavage (Table 5). Peptides of different lengths were also evaluated and Bar1 did not degrade peptides that lacked P1-P3 residues, whereas peptides of extended length were still actively processed (Table 5).

C. albicans Bar1 was also tested for its ability to cleave α pheromone peptides secreted by other *Candida* clade species (Table 4). Using LC-MS, Bar1 was found to degrade *C. dubliniensis* and *C. tropicalis* α pheromones. As with *C. albicans* α pheromone, cleavage was between residues 5 and 6. No cleavage products were found with any of the other *Candida* pheromones. These results indicate that Bar1 has a relatively relaxed cleavage specificity that allows it to cleave peptides beside the conventional *C. albicans* α pheromone target.

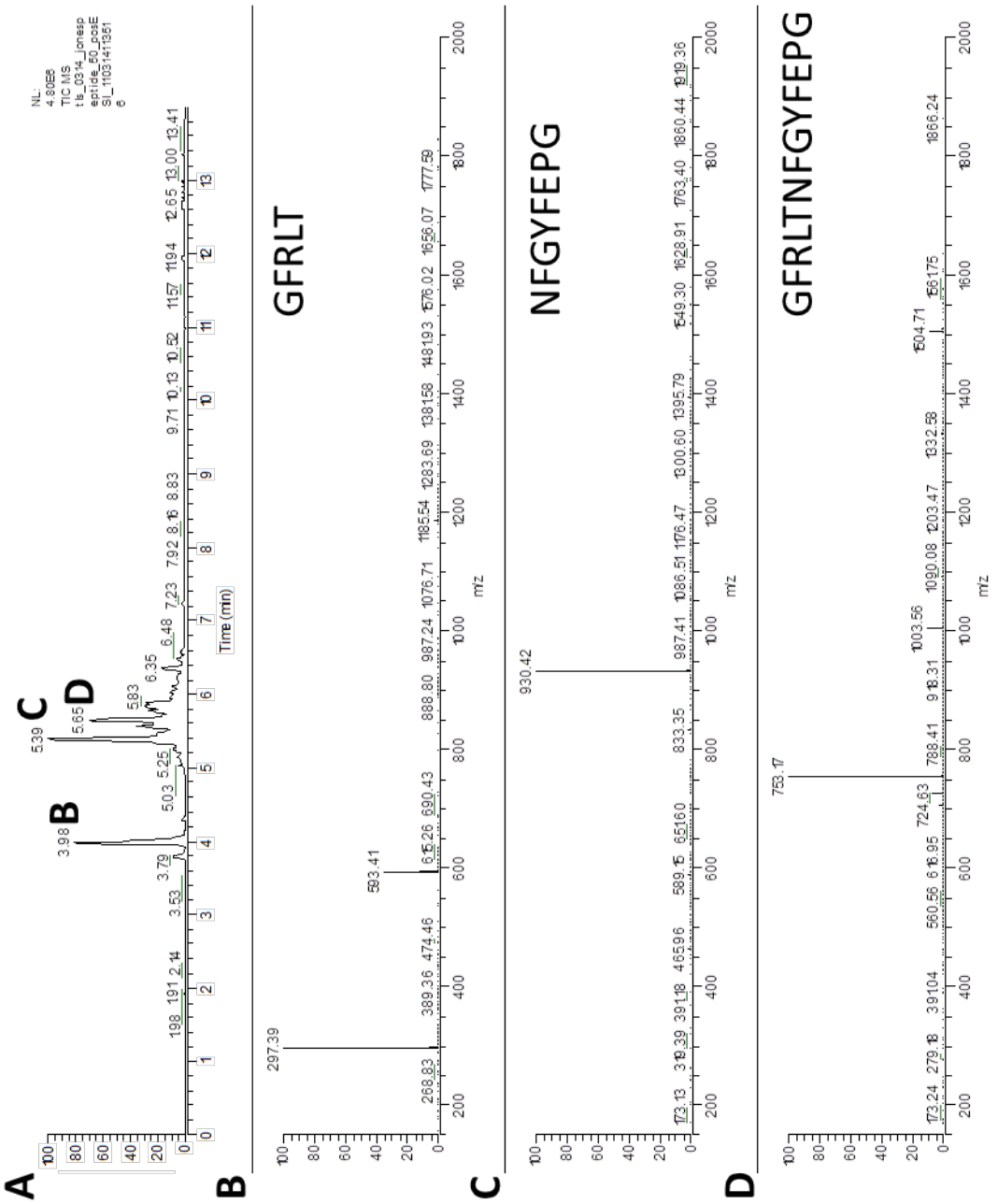

Figure 2-3: α pheromone degradation by Bar1 protease

C. albicans α pheromone was degraded for one hour by Bar1 protease, then products were determined by LC-MS. HPLC elution of degradation products (A). Mass spectrometry identified two major products GFRLT (B) and NFGYFEPG (C), as well as the uncleaved α pheromone (D).

Table 2-4: Bar1 activity on α pheromone sequences of five closely-related *Candida* species.

The α pheromone sequences of five *Candida* species as predicted by conserved processing sites across fungal species (Alby and Bennett, 2011). Underlined residues indicate deviation from the *C. albicans* pheromone sequence. *Candida* α pheromones were incubated with Bar1 protease, and then products were detected using LC-MS. Pluses indicate a cleavage product was detected within one hour, while +/- indicates overnight incubation was required.

Candida species	Pheromone sequence	Cut
C. albicans	GFRLTNFGYFEPG	+
C. dubliniensis	KFKLTNFGYFEPG	+
C. tropicalis	KFRLTRYGWFSPN	+/-
C. parapsilosis	KPHWTTYGYYEPQ	-
L. elongisporus	GWMWTRYGRFSPV	-

Table 2-5: Bar1 activity on α pheromone analogs

C. albicans α pheromone and related sequences were degraded for one hour by Bar1 protease, and then products were detected using LC-MS. Underlined residues indicate deviation from the *C. albicans* α pheromone sequence. Pluses indicate a cleavage product was detected.

Peptide		Native	Cut
α pheromone		GFRLTNFGYFEPG	+
		Substitutions	
	1	AARLTNFGYFEPG	+
	2	GAALTNFGYFEPG	+
	3	GFAATNFGYFEPG	+
	4	GFRAANFGYFEPG	+
	5	GFRLAAFGYFEPG	+
	6	GFRLTAAGYFEPG	+
	7	GFRLTNAAYFEPG	+
	8	GFRLTNFAAFEPG	+
	9	GFRLTNFGAAEPG	-
	10	GFRLTNFGYAAPG	-
	11	GFRLTNFGYEAAG	-
	12	GFRLTNFGYFEAA	-
		Truncations, Additions	
N – 3		___LTNFGYFEPG	-
N – 2		__RLTNFGYFEPG	-
N – 1		_FRLTNFGYFEPG	+
C – 1		GFRLTNFGYFEP_	+
N + 2		AAGFRLTNFGYFEPG	+
C + 2		GFRLTNFGYFEPGKA	+
N +2, C + 2		AAGFRLTNFGYFEPGKA	+

To address global peptidase specificity from an unbiased perspective, Bar1 activity was tested on a physiochemically diverse library of 228 tetradecapeptides and products analyzed by mass spectrometry (O'Donoghue *et al.*, 2012). A consensus motif was generated using iceLogo (Colaert *et al.*, 2009) that centered about the scissile bond (Fig. 4A). Interestingly, this motif did not show any obvious similarity to the sequence of *C. albicans* α pheromone. Given that substitution of C-terminal residues blocked α -pheromone cleavage (Table 5), a second Bar1

consensus motif was generated that centered on cleavage sites detected C-terminal to the scissile bond (Fig. 4B). The second motif showed a closer resemblance to the *C. albicans* α pheromone sequence. However, the overall cleavage specificity of Bar1 appeared to be less reliant on amino acids close to the scissile bond than that of other characterized aspartyl proteases (Dunn and Hung, 2000; Dunn, 2001).

To measure the kinetics of Bar1 cleavage on α pheromone, an assay was employed harnessing a Dabcyl/EDANS-glutamine internally quenched (IQ) peptide. Quenching of the EDANS fluorophore occurs by distance-dependent resonance energy transfer to the dabcyl quencher. Upon cleavage by an endoprotease, the fluorophore is released and fluorescence can be measured (see Methods). Under defined conditions, Bar1 was found to process α pheromone with a K_{cat}/K_m of ~$7.7*10^6$ $M^{-1}s^{-1}$ (Fig. 5A). This rate is comparable to that of secreted aspartyl proteases of several *Candida* species (Fusek *et al.*, 1994). The mutant Bar1 protein (D232A) did not show detectable cleavage activity on the IQ substrate, indicating that fluorescence was due to specific proteolytic activity of the Bar1 protein.

Using the IQ peptide assay, Bar1 was shown to exhibit maximal activity at pH 6.5 and at 37°C. Activity was inhibited by increasing osmolarity, with maximal activity occurring in low molarity solutions (Fig. 5). Furthermore, addition of either α pheromone cleavage product to the reaction had no effect on reaction rates (data not shown). Given that Bar1 is an aspartyl protease, analogs of a powerful inhibitor of this protease class, Pepstatin A, were tested for their ability to block α pheromone cleavage. None showed inhibition of *C. albicans* Bar1 (Fig. 4C). It is noted there are several aspartyl proteases that are resistant to Pepstatin A (Ghosh, 2011), including the *S. cerevisiae* Bar1 protein (Nath, 1993).

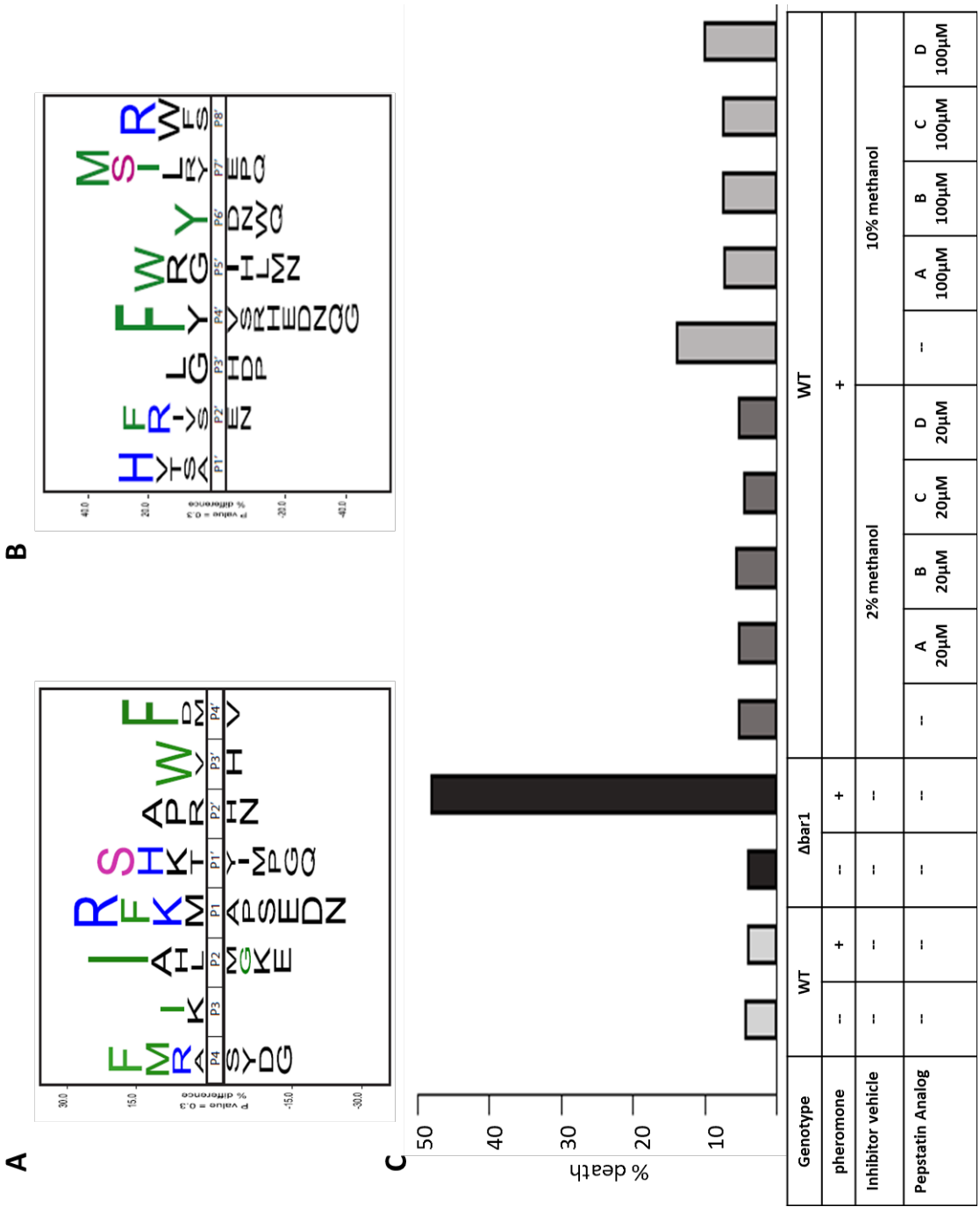

Figure 2-4: Bar1 substrate cleavage motifs and inhibition

iceLogo generated from amino acids that are enriched or de-enriched in the P4 through P4' (A) or P1' through P8' (B) positions of Bar1 cleavage sites after incubation for 60 min. Percent difference is the difference of amino acid frequency surrounding the Bar1 cleavage sites relative to the frequency of amino acids surrounding all peptide bonds in the library (*n* = 2,964).
(C) Cells were exposed to four pepstatin analogs and 0.3 μM α pheromone within a pheromone-induced cell death assay as indicated. A: P2'(Lys)-pepstatin, B: P2'(Arg)-pepstatin, C: P3(Phe)-pepstatin, D: P3(Tyr)-pepstatin.

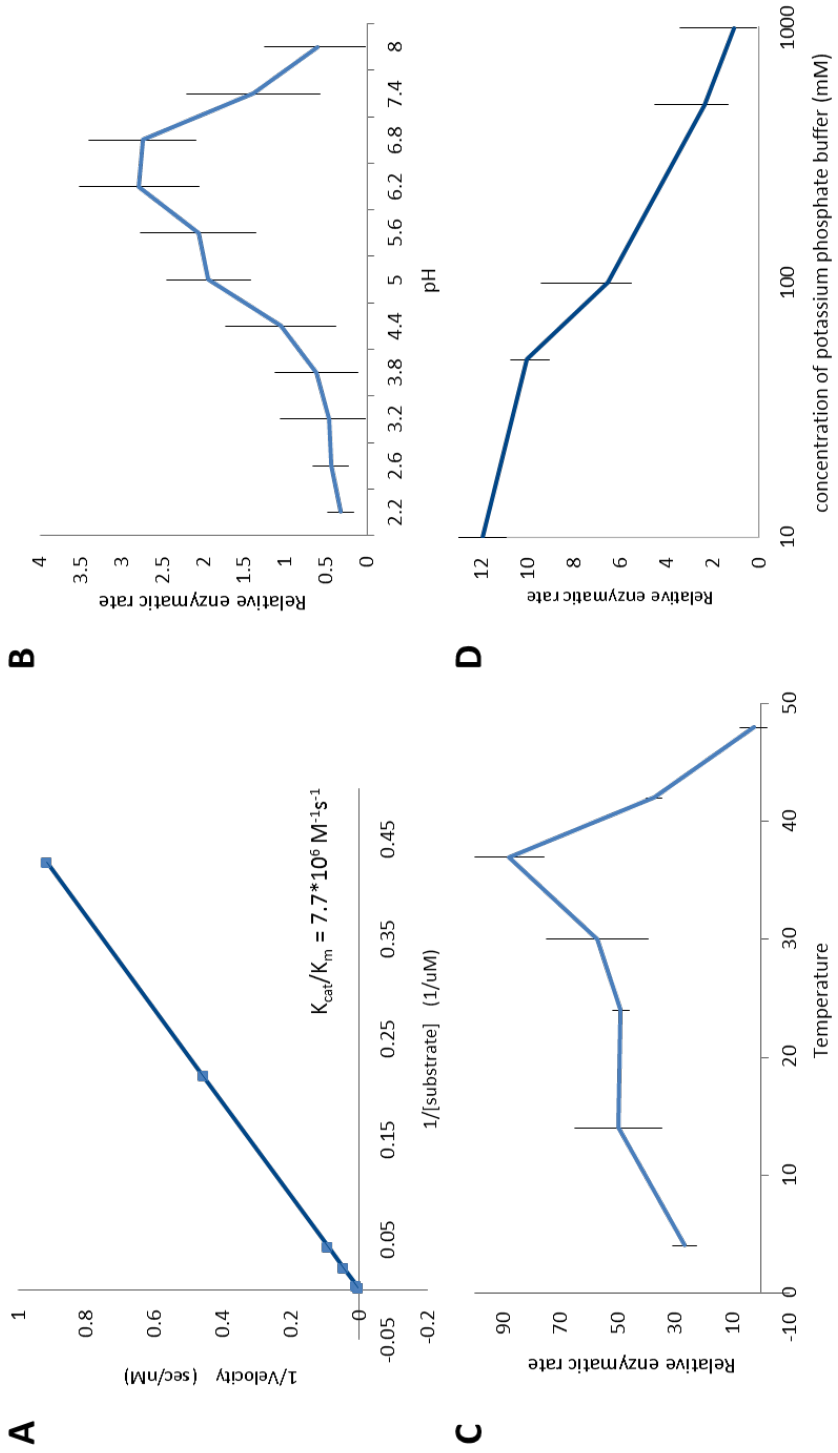

Figure 2-5: Enzymatic properties of Bar1 protease.

Bar1 activity on an α pheromone FRET peptide was used to generate a Lineweaver-Burk plot of enzyme kinetics (A), and determine the pH (B), temperature (C), and osmolar (D) dependencies of the cleavage reaction *in vitro*. Relative enzymatic rate is the amount of fluorescence per unit time due to cleavage of the fluorophore-conjugated peptide. Mean±SD.

Contributions of Bar1 and α pheromone to pheromone signaling in *MTL*a cells

The pheromone response in *C. albicans MTL***a** cells is dependent on α pheromone to activate MAPK signaling. This response is often induced by exogenous α pheromone (e.g. from α cells), but can also be mediated by autocrine pheromone signaling. Autocrine signaling involves secretion of α pheromone by **a** cells, which binds to the Ste2 receptor on the cell surface initiating activation of the pheromone response via a positive feedback loop (Alby *et al.*, 2009). Bar1 restricts this autocrine loop by degradation of α pheromone, thereby limiting self-activation (Alby *et al.*, 2009). To determine the relative contributions of Bar1 and α pheromone to exogenous and autocrine signaling, we constructed *bar1Δ/bar1Δ, mfαΔ/mfαΔ* and *bar1Δ/bar1Δ mfαΔ/mfαΔ* mutants in an *MTL***a** background. For opaque cells, pheromone responses were determined using the pheromone-induced death (PID) assay described earlier. Pheromone responses in white strains were analyzed by challenging cells with synthetic α pheromone and monitoring pheromone-induced biofilm formation (Daniels *et al.*, 2006; Yi *et al.*, 2008).

In the PID assay, deletion of the *BAR1* gene resulted in heightened sensitivity of opaque cells to exogenous α pheromone, in agreement with previous studies (Alby *et al.*, 2010). Thus, the majority of *bar1Δ/bar1Δ* cells underwent cell death at pheromone concentrations as low as 30 nM, while wild type cells required > 1 μM to elicit a similar level of cell death (Fig. 6A). Deletion of the *MFα* gene effectively short-circuits the autocrine signaling loop, and yet *bar1Δ/bar1Δ mfαΔ/mfαΔ* performed similarly to the *bar1Δ/bar1Δ* single mutant (Fig. 6A), indicating the *MFα* gene (and autocrine signaling) has a negligible effect in these assays.

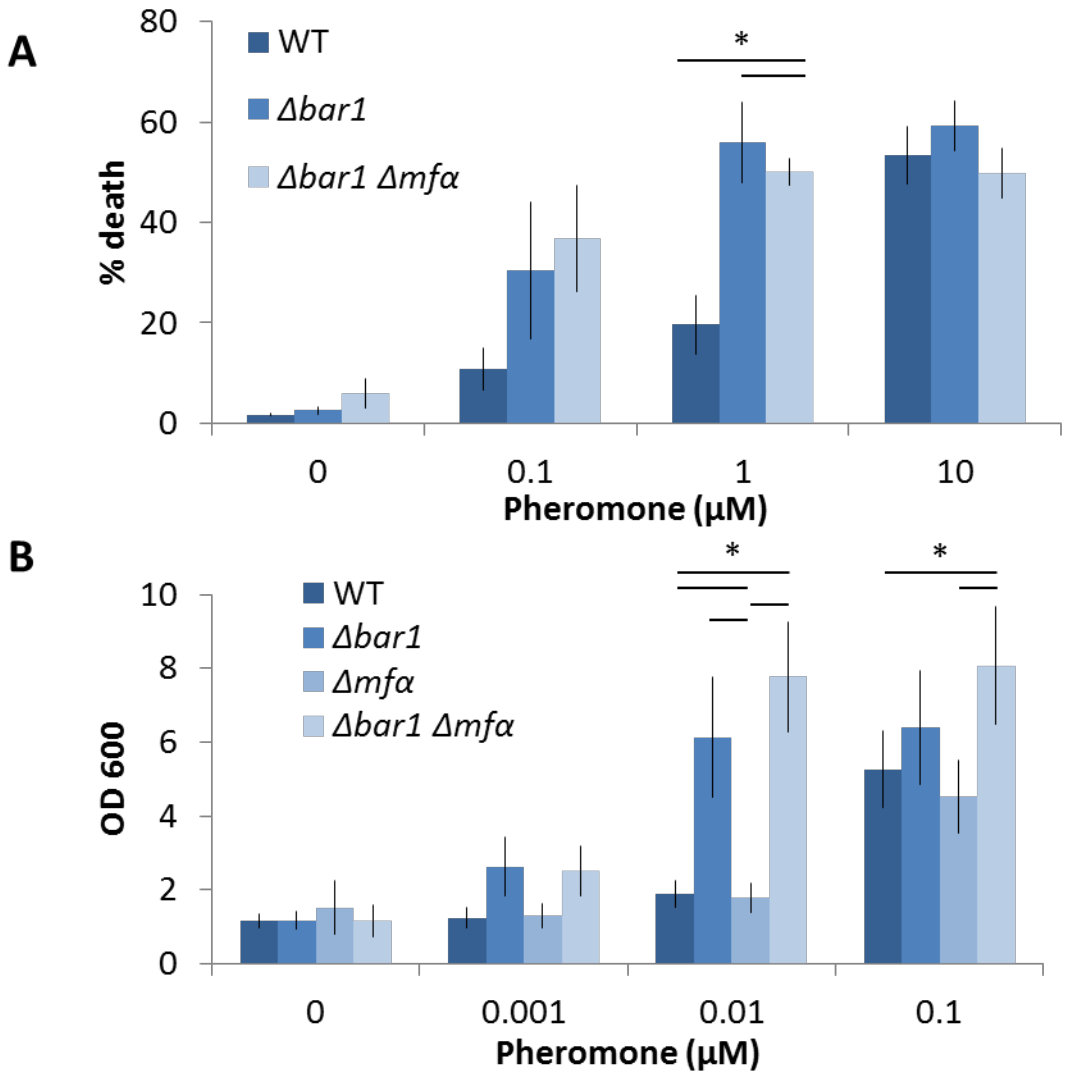

Figure 2-6: *BAR1* and *MFα* effect rates of pheromone response in white and opaque cells.

Wildtype, *Δbar1*, and *Δbar1 Δmfα* a strains were titrated with α pheromone.

(A) A pheromone-induced death assay was used to assess the response of opaque strains to α-pheromone. After a five-hour incubation with the indicated amount of pheromone, cells were stained with propidium iodide and percent death was determined using flow cytometry. Mean±SE.

(B) A biofilm assay was used to assess the response of white strains to α-pheromone. After two days incubation with the indicated amount of pheromone, adherent cells were resuspended in media and quantified using spectrometry at 600nm. Mean±SD. * = $p<0.05$ by T-test.

Similar results to those with opaque cells were found in pheromone-induced biofilm assays performed on white cells. Loss of *BAR1* increased the sensitivity of white cells to exogenous α pheromone, with robust biofilms forming at lower pheromone concentrations (Fig 6B). Deletion of the *MFα* gene, either singly or in combination with *BAR1*, did not show a significant effect on pheromone-induced biofilm formation (Fig. 6B).

Expression levels of *BAR1* were also compared between white and opaque cells. Analysis of published RNA-Seq data (Tuch *et al.*, 2010) revealed that *BAR1* expression was similar between white and opaque cells prior to pheromone exposure, and separate studies showed that this gene was one of the most highly induced genes upon pheromone exposure in both cell types (Bennett *et al.*, 2003; Lin *et al.*, 2013). An antibody was developed against Bar1 (see Methods) and used to measure Bar1 protein secretion levels by white and opaque cells in liquid culture. Bar1 was detected in opaque cell supernatant, it was not detected in white cells, unstimulated opaque cells, or *bar1Δ/bar1Δ* controls (Fig 7).

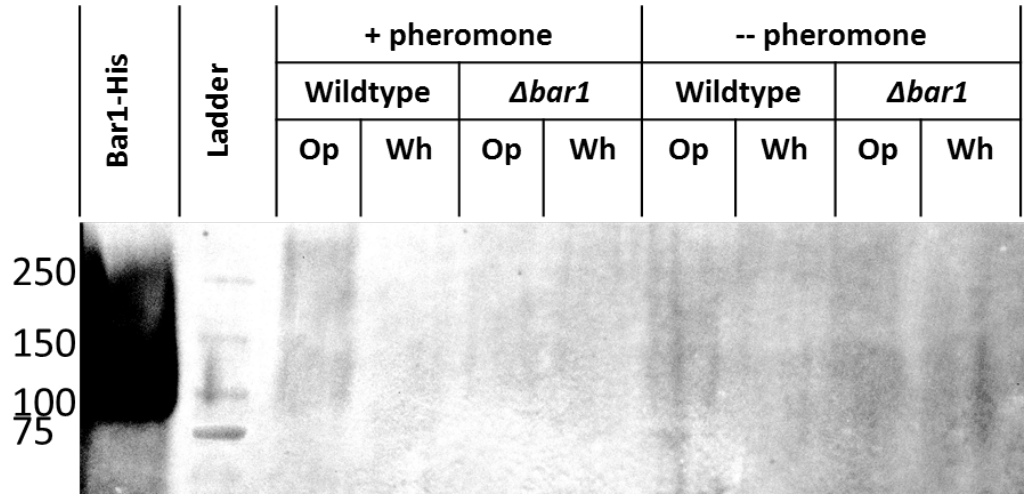

Figure2-7: Bar1 protein levels in white and opaque cells upon pheromone exposure.

Wildtype and *Δbar1* cells in white and opaque phenotypic states were exposed to 0.3 μM α pheromone for 5 hours, then Bar1 protein was detected from the supernatant via western blot using an anti-Bar1 antibody. Bar1-His is the recombinant Bar1 protein, and used as a positive control.

Does Bar1 Regulate Inter-Species Signaling in *C. albicans*?

There is significant conservation among α pheromone sequences within the *Candida* clade (Alby and Bennett, 2011; Lin *et al.*, 2011), with 39% to 92% conservation seen with *C. albicans* α pheromone at the amino acid level (Table 4). When challenged with synthetic α pheromones from related *Candida* species, *C. albicans* was shown to undergo same-sex mating (in opaque **a** cells) or sexual biofilm formation (in white **a** cells) (Alby *et al.*, 2009; Alby and Bennett, 2011). These results led us to pose the following questions: First, does secretion of endogenous α pheromone from **a** cells contribute to the response to inter-species pheromones by activating autocrine signaling? Second, does *C. albicans* Bar1 also contribute to the regulation of inter-species pheromone signaling? That is, does Bar1 recognize and cleave pheromones from other *Candida* clade species, or does it act to modulate autocrine signaling? Finally, does inter-species signaling occur at pheromone levels that are physiologically relevant? To address these questions, we performed a series of genetic experiments that address the role of the *BAR1* and *MF*α genes in inter-species pheromone signaling.

Having established the specificity of Bar1 for *Candida* α pheromone sequences earlier, cell-based assays were performed to determine if either Bar1 activity or autocrine pheromone signaling alter *C. albicans*' response to pheromones from different *Candida* species. The effects of *BAR1* and/or *MFα* gene deletions on the response to pheromone were determined for both white cells (by measuring biofilm production) and opaque cells (by measuring PID) (Figs. 8 and 9). We considered three main hypotheses for how pheromone signaling could be influenced by *BAR1* and *MFα* genes in **a** cells: (1) Signaling between species is unaffected by Bar1 or endogenous α pheromone produced by *C. albicans* **a** cells. (2) Bar1 degrades non-*albicans* pheromones thereby restricting inter-species pheromone signaling. (3) Bar1 does not influence

inter-species signaling directly but rather restricts inter-species signaling by degrading endogenous α pheromone produced by **a** cells (Fig. 9A).

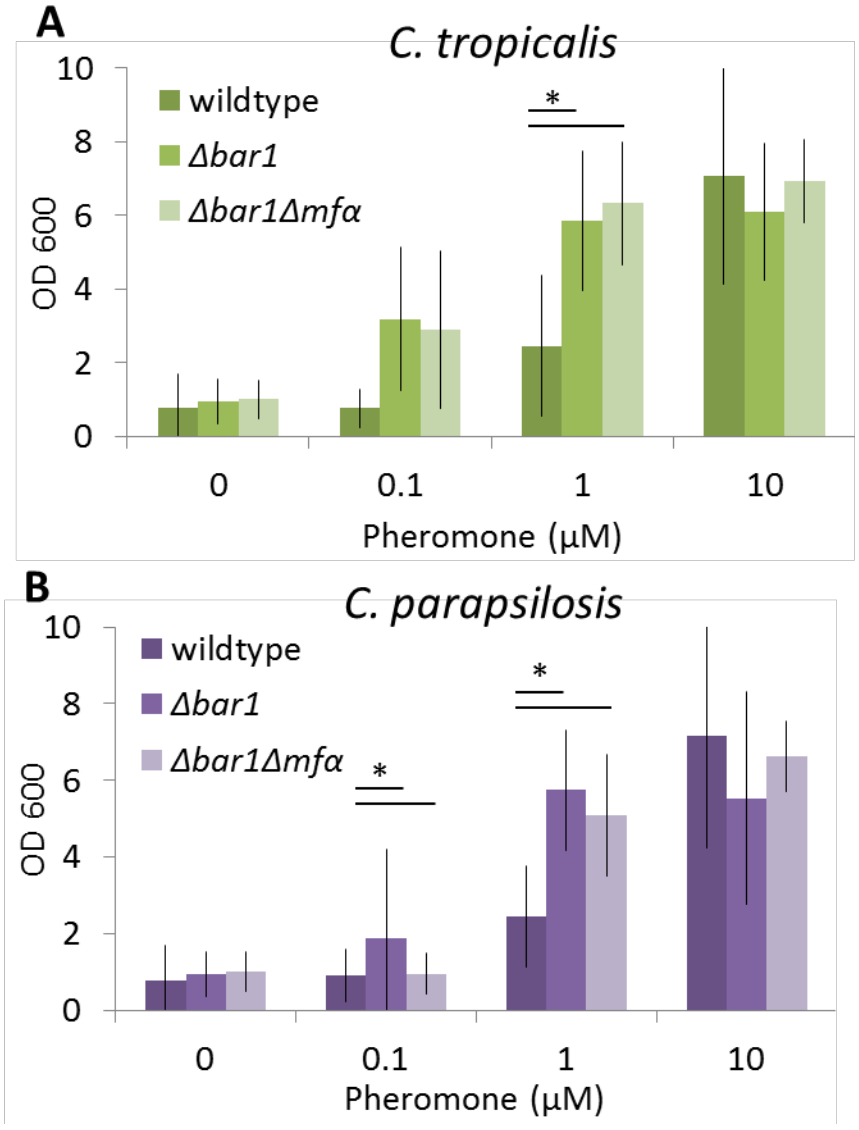

Figure 2-8: *BAR1* affects *C. albicans* white cells' response to *Candida* pheromones.

Wildtype, *Δbar1*, and *Δbar1Δmfα C. albicans* white cells were incubated with increasing levels of *C. tropicalis* (A), and *C. parapsilosis* (B) α pheromones in a biofilm assay. After two days, adherent cells were resuspended in media and quantified using spectrometry at 600nm. Mean ±SD. * = $p<0.05$ by T-test.

Deletion of the *BAR1* gene in *C. albicans* white **a** cells led to a heightened response to *C. dubliniensis* α pheromone (Supp. Fig. S2A), which was expected given that *C. dubliniensis* α pheromone is almost identical to that of *C. albicans*. In contrast, deletion of the *MF*α gene did not affect the response to *C. dubliniensis* pheromone (Supp. Fig. S2A). This indicates that Bar1 directly affects the response to the *C. dubliniensis* pheromone and that autocrine pheromone signaling does not influence the response, similar to results with exogenous *C. albicans* α pheromone.

The loss of *BAR1* also increased the response of *C. albicans* white **a** cells to *C. tropicalis* and *C. parapsilosis* α pheromones (Fig. 8). Thus, pheromone-induced biofilm formation was significantly increased in *bar1Δ/bar1Δ* mutants in response to these pheromones relative to the wildtype control. Deletion of *MF*α did not change the response to pheromone, again suggesting that autocrine signaling does not contribute to the increased pheromone response observed in *bar1Δ* mutants (Fig. 8).

Analogous experiments were performed using *C. albicans* opaque **a** cells to determine the contributions of Bar1 and α pheromone to inter-species signaling (Fig. 9B, Supp. Fig. 2B). *C. dubliniensis* α pheromone produced a similar response to the native *C. albicans* α pheromone in opaque cells, and like white cells, the deletion of *MFα* did not affect the outcome (Supp. Fig. 2B). Interestingly, however, deletion of *MFα* depressed the response of *C. albicans* to *C. parapsilosis* pheromone, indicating a possible role for autocrine signaling in this response (Fig. 9B).

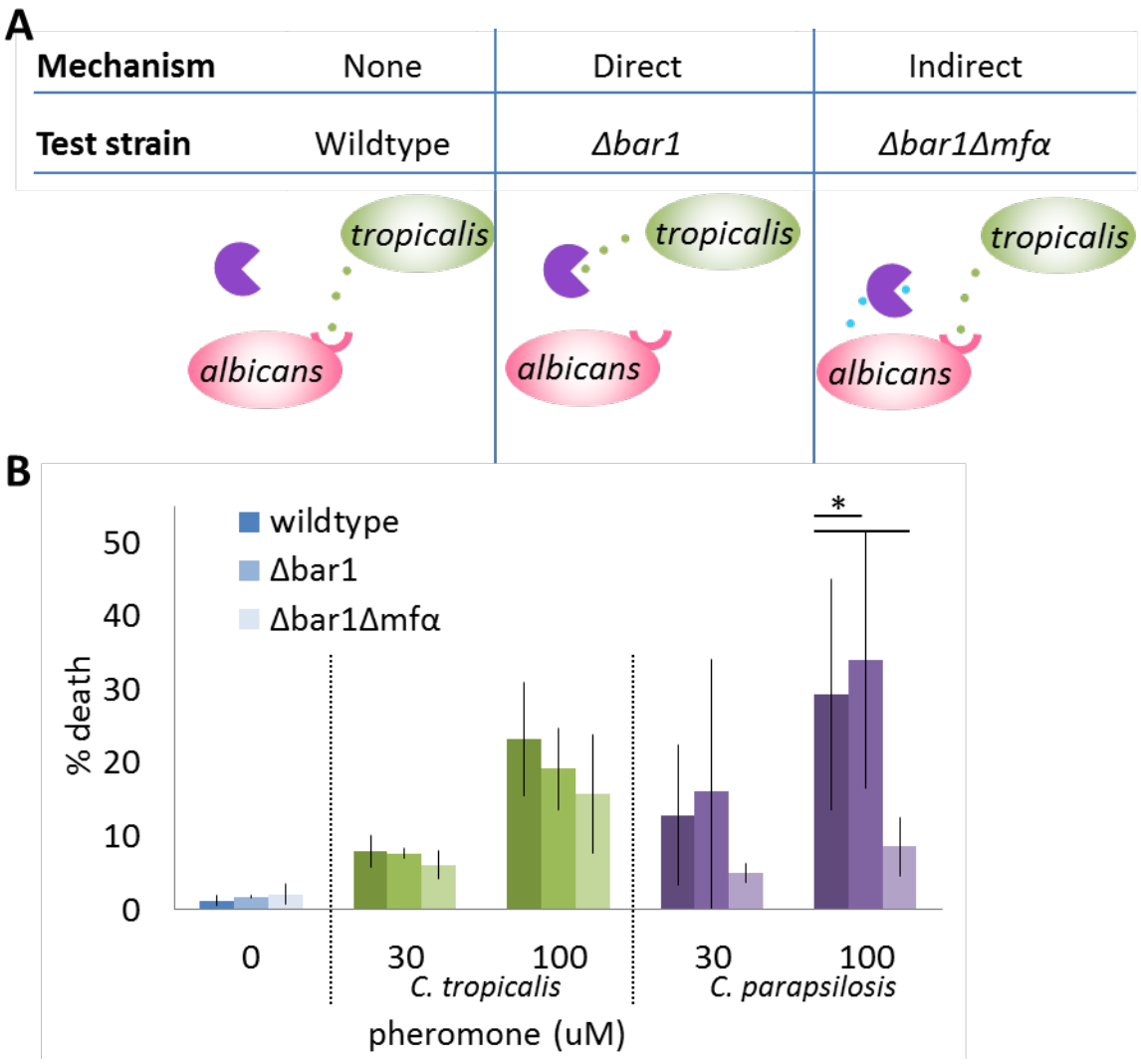

Figure 2-9: *BAR1* and *MFα* effects on interspecies signaling.

(A) Three alternative models for how Bar1 may affect pheromone signaling between *Candida* species. Bar1 may have no effect on interspecies signaling events, may affect signaling through direct degradation of foreign pheromones, or may affect signaling indirectly through degradation of *C. albicans* α pheromone produced following receptor activivation with a foreign pheromone.

(B) Wildtype, *Δbar1*, and *Δbar1Δmfα C. albicans* opaque cells were titrated with increasing levels of *C. tropicalis* and *C. parapsilosis* α pheromones. Percent death was analyzed by PI staining and flow cytometry following 5 hours of pheromone exposure. Mean±SD. * = $p<0.05$.

DISCUSSION

In this work, we first addressed the biochemical properties of *C. albicans* Bar1, a conserved aspartyl protease that is secreted by several hemiascomycete species. Similar to its *S. cerevisiae* counterpart, *C. albicans* Bar1 is produced by *MTL***a** cells where it acts to degrade α pheromone in the extracellular environment (Hicks and Herskowitz, 1976; Manney, 1983; MacKay *et al.*, 1988; Schaefer *et al.*, 2007). In conventional mating, the loss of Bar1 in **a** cells results in a hypersensitive response to α pheromone from α cells, and a resultant >100-fold decrease in mating efficiency (Schaefer *et al.*, 2007). Significantly, α pheromone is also produced by **a** cells where it is normally degraded by Bar1, but in the absence of Bar1 the build-up of α pheromone results in auto-activation of mating responses and same-sex conjugation (Alby *et al.*, 2009). The fission yeast *Schizosaccharomyces pombe* utilizes a similar pheromone signaling mechanism for mating, yet in this species a serine carboxypeptidase, Sxa2, degrades the P-factor pheromone (Ladds and Davey, 1996; Ladds and Davey, 2000; Ladds *et al.*, 2005). This suggests that independent evolutionary events have led to similar proteolytic mechanisms for pheromone regulation, and that pheromone-degrading proteases therefore play key roles in regulating sexual behavior.

Biochemical characterization of *C. albicans* Bar1 peptidase

We identified similarities between *C. albicans* and *S. cerevisiae* Bar1 activities, despite limited sequence homology (36% similarity, 23% identity). Both proteins are secreted, heavily glycosylated, are heat tolerant, contain the conserved aspartyl protease motif Asp-Thr/Ser-Gly, and show maximal activity at a near-neutral pH (Manney, 1983; MacKay *et al.*, 1988; MacKay *et al.*, 1991). Their preference for neutral pH differs from many aspartyl proteases, which typically show increased activity in acidic environments, and has likely evolved to match the environment

where the protease is active (Ghosh, 2011). Such an optimization requires that the pK_a of aspartic acid residues in the active site be increased to yield the partial protonation necessary for catalysis, similar to observations in the well-characterized HIV protease (Hyland *et al.*, 1991; Ido *et al.*, 1991; Northrop, 2001). *C. albicans* Bar1 was found to cleave *C. albicans* α pheromone specifically between threonine-5 and asparagine-6 residues, thereby inactivating it. Similarly, *S. cerevisiae* Bar1 cleaves its α pheromone between residues 6 and 7, near the center of the peptide. Bar1 cleavage activity was not inhibited by pepstatin A analogs; pepstatin A is a standard aspartyl protease inhibitor (Ghosh, 2011). Similar results were previously observed using conditioned medium from *C. albicans* opaque **a** cells to degrade synthetic α pheromone (Janiak *et al.*, 2005).

C. albicans Bar1 required at least four residues N-terminal to the scissile bond for activity, which is similar to *S. cerevisiae* Bar1, but different from the three residue minimum seen among many aspartyl proteases (Manney, 1983; Dunn, 2001). Curiously, residues immediately flanking the scissile bond did not appear to have a strong effect on cleavage activity; dialanine substitutions at positions 5 and 6 in *C. albicans* α pheromone did not block activity, whereas substitutions at the extreme C-terminus of α pheromone did inhibit Bar1 cleavage. For example, substitutions between positions 9-13 of *C. albicans* α pheromone inhibited Bar1 cleavage. Interestingly, this parallels what was previously seen for Ste2 activation, where mutation of the most C-terminal residues of α pheromone resulted in the biggest reduction in signaling through the receptor (Alby and Bennett, 2011). To our knowledge, this result is unique for a characterized peptidase, as it indicates that amino acid residues distal to the scissile bond have the strongest effect on cleavage specificity. This conclusion was supported by a global proteolytic analysis of Bar1 activity, which showed limited overlap between an optimal consensus sequence and the α pheromone sequence.

One possibility for the unusual cleavage specificity of Bar1 is that a particular structure, rather than a primary amino acid sequence, is recognized by the peptidase, as is seen in the aspartyl-type HIV peptidase (Prabu-Jeyabalan *et al.*, 2002). Despite the short length of α pheromone peptides, a β-turn in the *S. cerevisiae* α pheromone is integral to activation of its receptor, Ste2, supporting a role for secondary structure in some α pheromone peptides (Lin *et al.*, 2003; Umanah *et al.*, 2010). Similarly, it is thought that many aspartyl proteases prefer β-turns in their substrates, as it leaves the scissile bond most exposed for catalysis (Dunn and Hung, 2000).

Comparative analysis of *C. albicans* Bar1 cleavage of different *Candida* pheromones revealed preferential activity for *C. albicans* α pheromone, as well as that of the closely related *C. dubliniensis* pheromone. Extended co-incubation of *C. albicans* Bar1 with *C. tropicalis* α pheromone also revealed this peptide to be a substrate, albeit with lower efficiency than the native pheromone. Cleavage of *C. parapsilosis* and *L .elongisporus* pheromones by *C. albicans* Bar1 was not detected. Previous studies on *S. cerevisiae* Bar1 also indicated a species-specific function, as *S. cerevisiae* cells were unable to cleave *C. albicans* α pheromone (Janiak *et al.*, 2005). Together, these studies reveal that changes in Bar1 specificity have co-evolved with changes in the α pheromone sequence. These changes also required accompanying changes in the Ste2 receptor, indicating that co-evolution of all three components, Bar1, α pheromone, and Ste2 must be coordinated for correct pheromone regulation.

Defining the biological roles for Bar1 and α pheromone in *C. albicans*

To complement the biochemical analysis of Bar1, genetic experiments were performed to determine the role of Bar1 in regulating pheromone signaling in *C. albicans* white and opaque cells. In general, loss of the *BAR1* gene sensitized both white and opaque **a** cells to respond to lower concentrations of exogenously added *C. albicans* α pheromone, consistent with previous

observations (Alby *et al.*, 2010). In contrast, loss of the *MFα* gene (encoding α pheromone) had minimal effects in these assays, indicating that the autocrine pheromone loop does not significantly contribute to the response to exogenous *C. albicans* α pheromone under these conditions.

We were particularly interested in addressing the role of the Bar1 peptidase in inter-species pheromone signaling. Previous studies demonstrated that *C. albicans* **a** cells can response to synthetic α pheromones from other *Candida* clade species; opaque cells are induced to form mating projections and undergo same-sex **a**-**a** mating, whereas white cells are induced to form sexual biofilms (Alby and Bennett, 2011). As indicated above, *C. albicans* Bar1 was able to cleave α pheromone peptides from non-native species including *C. dubliniensis* and *C. tropicalis*, and it was therefore reasonable to assume that Bar1 could restrict responses to these pheromones. Furthermore, *C. albicans* is frequently associated with multiple *Candida* species in the oral cavity (Ghannoum *et al.*, 2010), where inter-species signaling could be common.

Deletion of *BAR1* sensitized *C. albicans* white **a** cells to α pheromones from *C. dubliniensis*, *C. tropicalis* and *C. parapsilosis.* This data reveals that Bar1 acts as an effective inhibitor of inter-species communication. In contrast, deletion of *MF*α did not significantly affect the response to other species' pheromones, indicating that autocrine signaling does not play a substantial role in enhancing the response to these pheromones. Future experiments will expand on these results by co-culturing *C. albicans* with *C. tropicalis*, which was recently shown to undergo mating and sexual biofilm formation, and accordingly secretes pheromones (Porman *et al.*, 2011; Jones *et al.*, 2014). This will allow us to answer questions related to the compatibility of these species for mating and biofilm formation.

In summary, we have shown the specific activity of *C. albicans* Bar1 protease on its endogenous substrate, α pheromone, as well as other potentially relevant peptide sequences. Bar1 is shown to be an unusual aspartyl protease, being resistant to standard aspartyl protease inhibitors and recognizing amino acids distal to the scissile bond. This study also extends the biological role of Bar1 in pheromone signaling to include regulation of inter-species signaling events between *C. albicans* and its closest relatives. Future work will further determine if such events coordinate mating and biofilm formation among *Candida* species in shared host communities.

ACKNOWLEDGEMENTS

We would like to thank members of the Bennett and Craik labs for their support and thoughtful input. MSP-MS data were acquired in the National Bio-Organic, Biomedical Mass Spectrometry Resource Center (UCSF), which is supported by a grant from the National Institutes of Health (P41GM103481).

SUPPLEMENTAL FIGURES

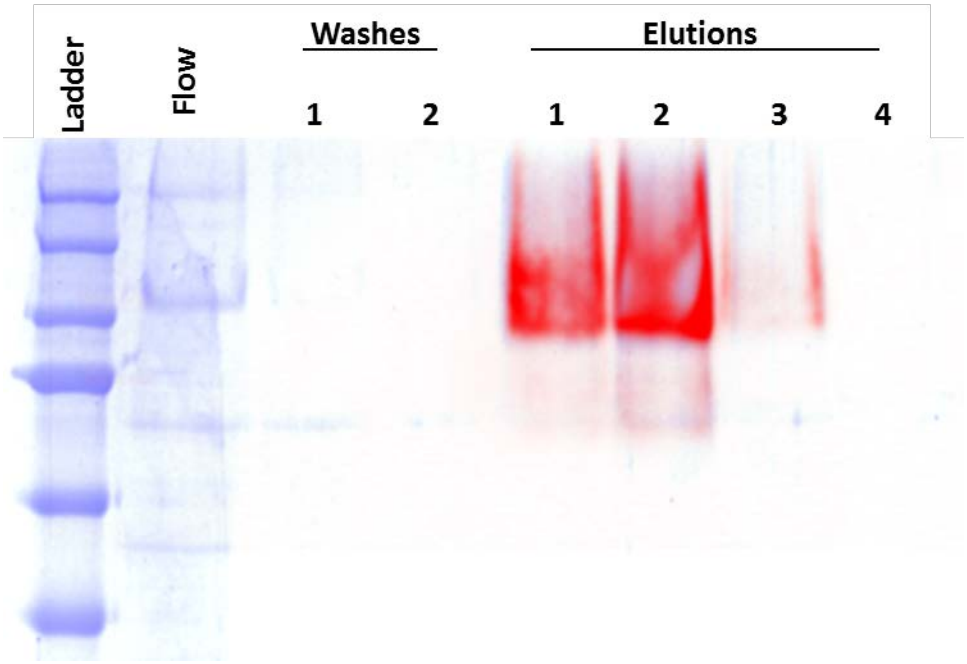

Supplemental Figure 2-1: **Purification of recombinant mutant Bar1 protease.**

Following secretion of the mutant recombinant (D232A) Bar1 from *Pichia pastoris*, the protein was concentrated then purified using nickel affinity chromatography. Flow: 10mM imidazole. Wash: 20mM imidazole. Elution: 500mM imidazole.

Blue indicates total protein via Coomassie stain and red indicates Bar1 protein via Western blot with anti-His6 antibody.

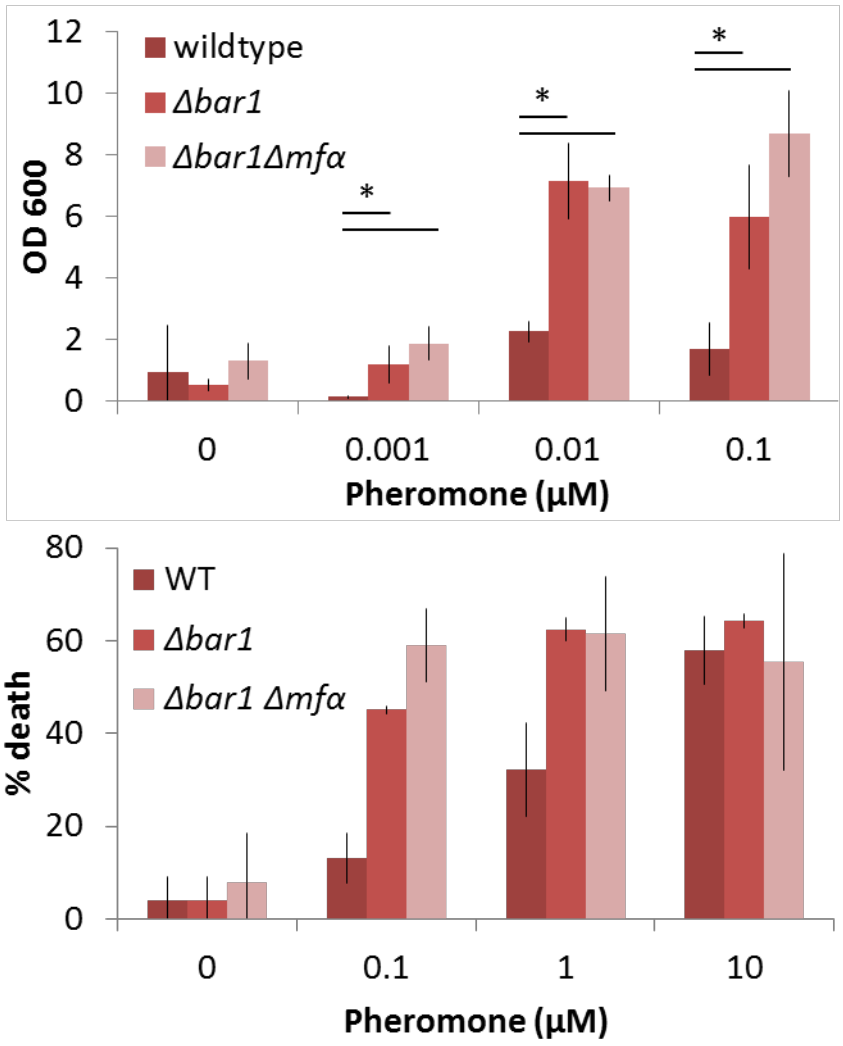

Supplemental Figure 2-2: *BAR1* affects *C. albicans* white cells' response to *C. dubliniensis* α pheromone.

(A) A pheromone-induced death assay was used to assess the response of opaque strains to *C. dubliniensis* α-pheromone. After a five-hour incubation with the indicated amount of pheromone, cells were stained with propidium iodide and percent death was determined using flow cytometry. Mean±SE.

(B) A biofilm assay was used to assess the response of white strains to *C. dubliniensis* α-pheromone. After two days incubation with the indicated amount of pheromone, adherent cells were resuspended in media and quantified using spectrometry at 600nm. Mean±SD. * = $p<0.05$ by T-test.

CHAPTER 3: SEXUAL BIOFILM FORMATION IN *CANDIDA TROPICALIS* OPAQUE CELLS

ABSTRACT

Candida albicans and *Candida tropicalis* are opportunistic fungal pathogens that can transition between white and opaque phenotypic states. White and opaque cells differ both morphologically and in their responses to environmental signals. In *C. albicans*, opaque cells respond to sexual pheromones by undergoing conjugation, while white cells are induced by pheromones to form sexual biofilms. Here, we show that sexual biofilm formation also occurs in *C. tropicalis* but, unlike *C. albicans*, biofilms are formed exclusively by opaque cells. *C. tropicalis* biofilm formation was dependent on the pheromone receptors Ste2 and Ste3, confirming the role of pheromone signaling in sexual biofilm development. Structural analysis of *C. tropicalis* sexual biofilms revealed stratified communities consisting of a basal layer of yeast cells and an upper layer of filamentous cells, together with an extracellular matrix. Transcriptional profiling showed that genes involved in pheromone signaling and conjugation were upregulated in sexual biofilms. Furthermore, *FGR23*, which encodes an agglutinin-like protein, was found to enhance both mating and sexual biofilm formation. Together, these studies reveal that *C. tropicalis* opaque cells form sexual biofilms with a complex architecture, and suggest a conserved role for sexual agglutinins in mediating mating, cell cohesion and biofilm formation.

INTRODUCTION

Candida species are the fourth most common cause of bloodstream infections in hospital patients (Wisplinghoff *et al.*, 2004). While *Candida albicans* accounts for the majority of such infections, *C. tropicalis* is also commonly encountered in the clinic, particularly in individuals with hematologic malignancies (Sipsas *et al.*, 2009; Papon *et al.*, 2013). Multiple factors contribute to the ability of *Candida* species to infect the human host, including the capacity to form biofilms (Hasan *et al.*, 2009). Biofilms are complex structures involving both cell-cell and cell-substrate interactions. *C. albicans* biofilm organization typically consists of a basal layer of yeast cells upon which a mesh-like layer of hyphal and pseudohyphal cells develops together with an extracellular matrix (Chandra *et al.*, 2001; Bonhomme and d' Enfert, 2013). Biofilms are a growing concern in the medical community; they can be difficult to remove, can impede antifungal drug penetration, and can seed subsequent systemic infections (Donlan and Costerton, 2002; Blankenship and Mitchell, 2006; Finkel and Mitchell, 2011).

Candida species have the ability to colonize multiple clinical devices, including venous and urinary catheters and prosthetics (Febré *et al.*, 1999; Crump and Collignon, 2000; Mohammadi *et al.*, 2013). Similarly, the majority of cases of denture-associated stomatitis, which affects approximately 65% of denture wearers, are caused by *Candida* species forming biofilms on these devices (Davenport, 1970; Gendreau and Loewy, 2011). *Candida* species have been observed to colonize other abiotic surfaces important for dental health such as stainless steel and porcelain (Ratnasari *et al.*, 2008; Li *et al.*, 2010). Thus, the factors allowing *Candida* species to form biofilms on synthetic surfaces are of direct relevance for preventing both mucosal and systemic infections by these pathogens.

C. albicans biofilm formation is strongly influenced by the phenotypic state of the cell. While *C. albicans* can undergo multiple forms of phenotypic switching, the best-characterized switch is the 'white-opaque' transition, which has also been observed in the related species *Candida dubliniensis* and *Candida tropicalis* (Slutsky *et al.*, 1987; Pujol *et al.*, 2004; Porman *et al.*, 2011; Xie *et al.*, 2012). The white-opaque switch is an epigenetic, heritable transition, in which cells reversibly switch between the white state, where cells appear round and smooth, and the opaque state, where cells are elongated and pimpled (Slutsky *et al.*, 1987). In *C. albicans*, the two phenotypes are specialized for growth in different *in vivo* niches and respond differently to environmental stimuli. For example, while white cells are more adept at systemic infection, opaque cells are better suited for colonization of the skin (Kvaal *et al.*, 1997; Kvaal *et al.*, 1999; Xie *et al.*, 2013). In addition, white cells undergo filamentation in response to a variety of environmental cues, including high temperature and elevated CO_2 levels, while opaque cells undergo filamentation in response to distinct nutritional cues (Sudbery, 2011; Si *et al.*, 2013). Finally, the two cell types exhibit very different behaviors when challenged with sexual pheromones. While pheromones initiate a mating response in *C. albicans* opaque cells (Miller and Johnson, 2002), white cells respond to pheromones by becoming cohesive and adherent, forming a 'sexual' biofilm (Daniels *et al.*, 2006; Yi *et al.*, 2008; Lin *et al.*, 2013).

The regulation of sexual biofilm formation in *C. albicans* involves a pheromone-induced MAPK cascade (Daniels *et al.*, 2006; Yi *et al.*, 2008). Pheromones secreted by opaque cells interact with the G-protein coupled receptors Ste2 and Ste3 expressed on a and α cells, respectively. The pheromone signal is transduced via a heterotrimeric G protein complex and conserved MAPK cascade, culminating in activation of the transcription factor Cph1, an ortholog of *Saccharomyces cerevisiae* Ste12 (Bennett *et al.*, 2003; Yi *et al.*, 2008; Jones Jr. and Bennett, 2011; Lin *et al.*, 2013). *Candida* mating types are defined by transcription factors encoded at the

mating-type-like (*MTL*) locus (Hull and Johnson, 1999; Butler *et al.*, 2009). Cells containing the *MTL*a locus mate with cells containing the *MTL*α locus, while *MTL*a/α cells are unable to mate (Hull *et al.*, 2000; Magee and Magee, 2000; Tsong *et al.*, 2003). Sexual biofilms in *C. albicans* are most efficient when formed by a or α white cells responding to pheromones secreted by opaque cells of the opposite mating type. These biofilms contrast with conventional (or asexual) biofilms that are pheromone-independent and formed preferentially by white a/α cells (Baillie and Douglas, 1999; Yi *et al.*, 2011; Bonhomme and d' Enfert, 2013). Studies comparing the genetic networks involved with sexual and asexual biofilm formation have found both shared and unique transcription factors regulating the two biofilm models. For example, Cph1 and MAPK signaling are essential only for sexual biofilm formation, while a core set of transcription factors (including Bcr1, Brg1, Rob1 and Tec1) are required for both sexual and asexual biofilm formation (Sahni *et al.*, 2010; Nobile *et al.*, 2012; Lin *et al.*, 2013).

Why has the white-opaque switch evolved to regulate mating in a subset of *Candida* species? One proposal is that sexual biofilms formed by white cells are used to promote mating between rare opaque cells (Soll, 2009). Consistent with this model, experiments have established that sexual biofilms provide an optimal environment for mating to occur. Pheromone gradients accumulate to high concentrations within the sexual biofilm and aid chemotropic growth between opaque cells of opposite mating types (Daniels *et al.*, 2006; Park *et al.*, 2013). Thus, the *raison d'etre* for the white-opaque switch could be that sexual biofilms formed by white cells provide an appropriate environment for rare opaque cells to undergo successful conjugation *in vivo*.

Recently, a white-opaque phenotypic switch was discovered in *C. tropicalis* that shows similarities to that in *C. albicans* (Porman *et al.*, 2011; Xie *et al.*, 2012; Porman *et al.*, 2013). The

master regulator of the white-opaque switch in both *Candida* species is the transcription factor Wor1 (Huang *et al.*, 2006; Zordan *et al.*, 2006; Srikantha *et al.*, 2006; Porman *et al.*, 2011; Xie *et al.*, 2012). In *C. albicans,* Wor1 acts as part of a transcriptional network to promote formation of the opaque state (Zordan *et al.*, 2007; Hernday *et al.*, 2013). In *C. tropicalis*, overexpression of *WOR1* was shown to drive switching to the opaque state as well as increase filamentation and biofilm formation (Porman *et al.*, 2013). These results indicate that significant crosstalk exists between the programs regulating the white-opaque switch and biofilm formation.

In this work, we address if mating pheromones can induce sexual biofilm formation in *C. tropicalis*. Similar to the case in *C. albicans*, we demonstrate that pheromone signaling in *C. tropicalis* drives the formation of sexual biofilms on synthetic surfaces. Surprisingly, however, *C. tropicalis* sexual biofilms are formed exclusively by opaque cells, and pheromone signaling is necessary but not sufficient for biofilm formation. This is in marked contrast to *C. albicans*, where activation of pheromone signaling in white cells was sufficient for induction of sexual biofilm formation. We also show that *C. tropicalis* sexual biofilms exhibit a stratified structure composed of a base layer of yeast-like cells, while the upper stratum is composed of highly filamentous cells. This structure contrasts with asexual biofilms induced by *WOR1* overexpression in *C. tropicalis*, which have a homogeneous makeup of filamentous cells surrounded by a more extensive extracellular matrix. Furthermore, our studies led to the identification of Fgr23, an ortholog of *S. cerevisiae* a-agglutinin, as a mediator of sexual mating and biofilm formation in *C. tropicalis*. These results are discussed with respect to the role of the white-opaque switch and agglutinin-like proteins in regulating biofilm formation in *Candida* species.

RESULTS

C. tropicalis opaque cells form sexual biofilms

White-opaque phenotypic switching was recently discovered in *C. tropicalis*, where cells in the opaque phenotypic state were shown to mate a hundred times more efficiently than cells in the white state (Porman *et al.*, 2011; Xie *et al.*, 2012). To determine if *C. tropicalis* exhibits the same capacity as *C. albicans* to form sexual biofilms, mixtures of a and α cells from both phenotypic states were tested in a modified biofilm assay. *C. tropicalis* cells were incubated in Lee's + Glucose medium on a polystyrene surface at 25°C for 48 hours, then non-adherent cells were removed by washing and the remaining adherent cells were quantified. Mixtures of opaque a and α cells formed a robust biofilm under these conditions, while mixtures of white a and α cells did not (Fig. 1A). Analysis of the opaque biofilms revealed the presence of highly filamentous cells (49±1%). In contrast, cells of a single mating type produced very few filamentous cells on the polystyrene surface (Fig. 2D, 4±1%, p = 9.3E-6, Student's T-test), and no filamentous cells were produced in mixtures of white a and α cells (Fig. 1A).

In *C. albicans*, opaque cells secrete pheromones that can stimulate biofilm formation in responding populations of white cells. In particular, the presence of 2-10% opaque cells mixed with 90-98% white cells was reported to result in optimal sexual biofilm formation (Daniels *et al.*, 2006; Yi *et al.*, 2008). To test if a similar phenomenon occurs in *C. tropicalis*, white and opaque cells were coincubated at different ratios and the resulting biofilm formation was quantified. As shown by cell density measurements (Fig. 1B) and crystal violet staining (Fig. 1C), *C. tropicalis* biofilms did not form from mixtures of white a and α cells, whereas robust biofilms formed from mixtures of opaque a and α cells. Overall, the efficiency of biofilm formation increased as white cells were substituted with opaque cells in these assays (Fig. 1B and C).

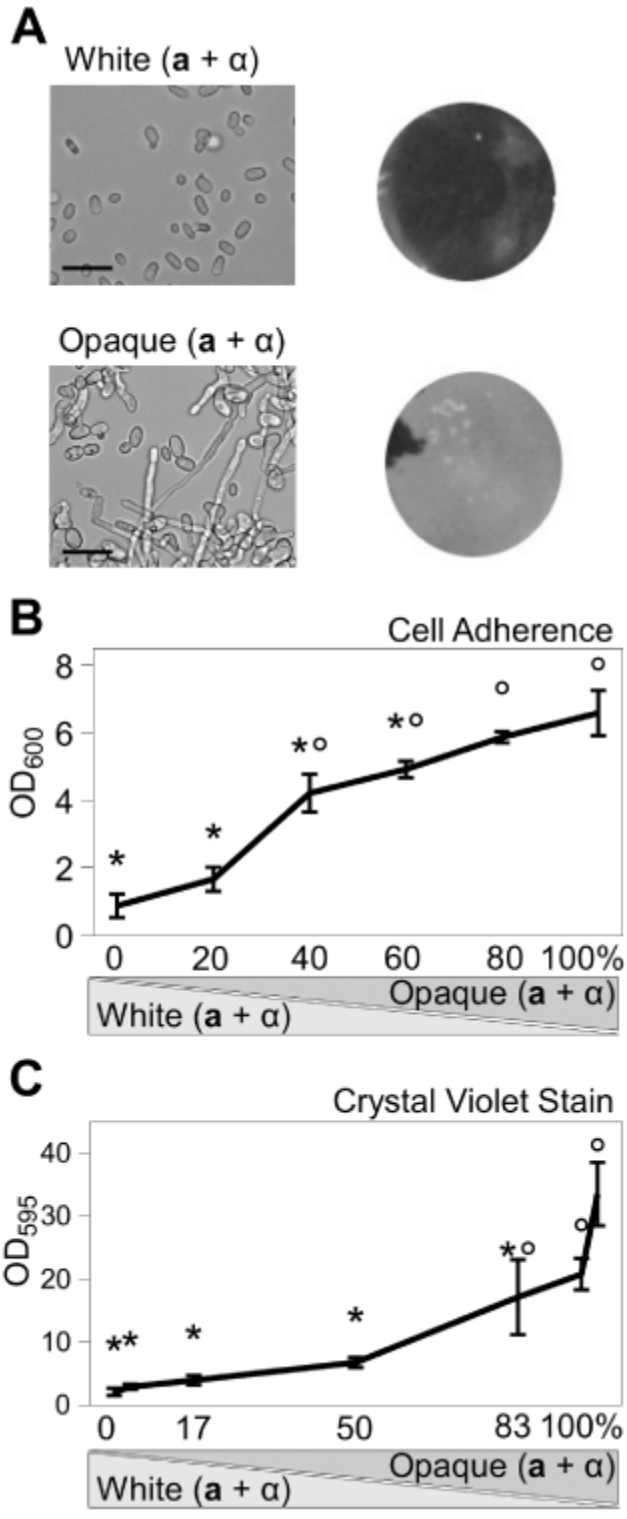

Figure 3-1: *C. tropicalis* opaque cells form sexual biofilms.

Mixtures of white and opaque a and α cells were compared for their ability to form biofilms. (A) A 50:50 mix of a and α cells were grown on polystyrene plates for 48 h and non-adherent cells removed by washing. Mixtures of white a and α cells showed little adherence to the plastic while a mixture of opaque a and α cells formed an adherent layer on the plastic. Left side, DIC microscopy of cells scraped from biofilm-inducing conditions, scale bar = 15 µm; right side, images of biofilms following washing of the plate. Black areas indicate unbound polystyrene while lighter-colored areas show adherent Candida cells. (B and C) White and opaque cell populations were mixed together at the indicated ratios. A 50:50 ratio of a and α cells was used for these experiments. Adherent cells were resuspended and quantified by absorbance at 600nm (B) or by crystal violet staining then absorbance at 595nm (C). Mean ± standard deviation (N≥4). * $p<0.005$ compared to 100% opaque cells. ° $p<0.005$ compared to 100% white cells (Tukey's test).

Similar sexual biofilms were formed when opaque cultures were grown at 30 or 37°C (Supp. Fig. 1). The latter result presumably reflects the stability of *C. tropicalis* opaque cells at 37°C (Porman *et al.*, 2011), whereas *C. albicans* opaque cells are unstable at this temperature and rapidly revert to the white state (Rikkerink *et al.*, 1988; Lohse and Johnson, 2010).

Next, to determine the role of mating type in *C. tropicalis* biofilm formation, assays were performed using populations of opaque cells with varying proportions of the two mating types. Both cell adherence (Fig. 2A and C) and crystal violet staining (Fig. 2B) were maximal when both a and α cells were present, whereas biofilms did not form when pure populations of either a or α cells were used. The requirement for both mating types is seen in the efficiency of overall biofilm formation and also at a cell morphology level; experiments involving only a single mating type yielded cells with a predominantly yeast morphology, whereas filamentous cells were prevalent in experiments containing mixtures of both mating types (Fig. 2D).

Given these results, we reasoned that pheromone signaling between opaque a and α cells could be important for *C. tropicalis* sexual biofilm formation. Pheromone signaling was previously shown to be essential for the formation of sexual biofilms in *C. albicans* (Daniels *et al.*, 2006; Yi *et al.*, 2008). We therefore tested *C. tropicalis* strains containing deletions in the pheromone receptor genes *STE2* and *STE3* in a and α cells, respectively. *STE2* encodes the α pheromone receptor expressed on a cells, while *STE3* encodes the a pheromone receptor expressed on α cells, and loss of either receptor is sufficient to block mating (Porman *et al.*, 2011). Deletion of either *STE2* in a cells or *STE3* in α cells effectively abolished sexual biofilm formation in *C. tropicalis* (Fig. 3A). This result establishes that pheromone signaling is essential for sexual biofilm formation in *C. tropicalis*.

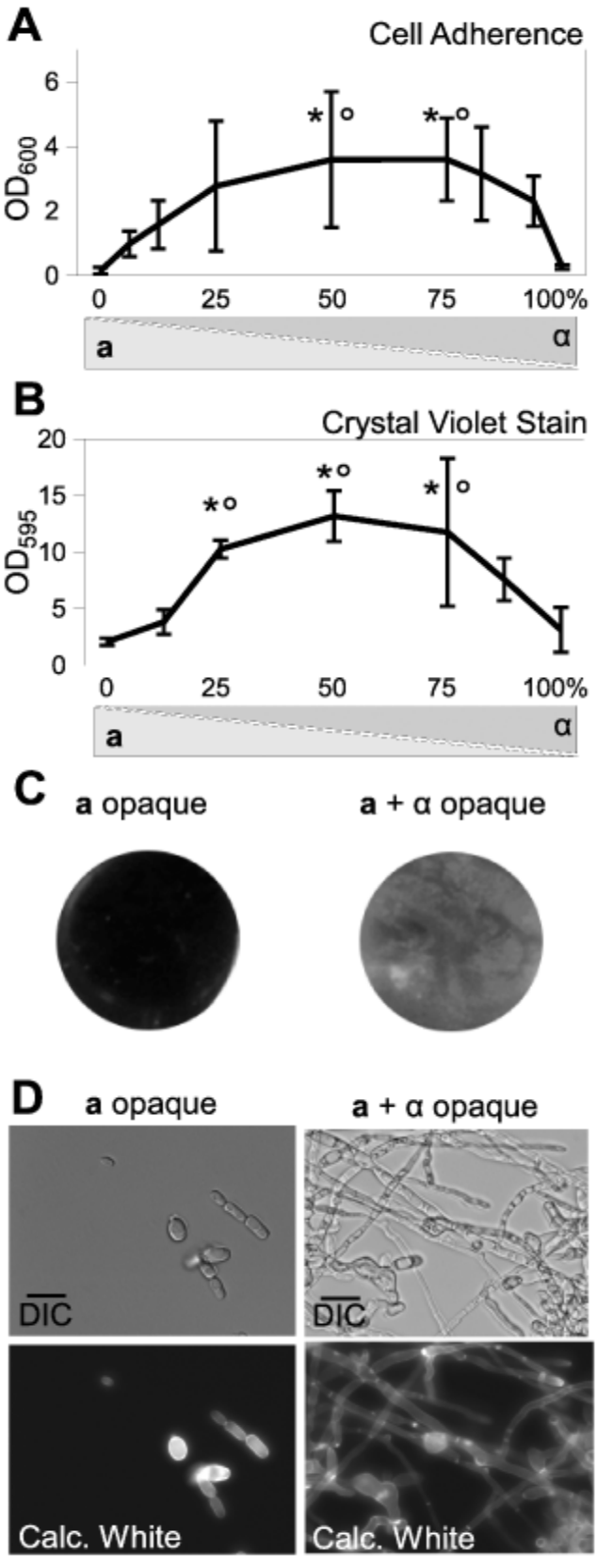

Figure 3-2: Equal proportions of **a** and α cells yield maximum sexual biofilm formation.

After growth of opaque cells for 48 h in polystyrene plates, the plates were washed to remove non-adherent cells then (A) adherent cells were resuspended and quantified by absorbance at 600nm, or (B) adherent cells were stained with crystal violet and quantified by absorbance at 595nm. Mean ± standard deviation (N≥3). * $p<0.05$ compared to 100% **a** cells. ° $p<0.05$ compared to 100% α cells. Tukey's test. (C) Images of biofilms following washing of the plate. Black areas indicate unbound polystyrene while lighter-colored areas show adherent *Candida* cells. (D) Microscopy of cells scraped from biofilm-inducing conditions. Top panels are DIC images and bottom panels are corresponding calcofluor white-stained cells. Scale bars = 15 µm.

We next tested whether the addition of synthetic *C. tropicalis* pheromone was sufficient to drive biofilm formation in responding opaque cells. Several synthetic versions of *C. tropicalis* α pheromone were utilized including 13-mer, 15-mer and 16-mer (A-KF-KFRLTRYGWFSPN) peptides. Each of these peptides activated the *C. tropicalis* Ste2 receptor when heterologously expressed in *C. albicans* (Lin *et al.*, 2011). Synthetic pheromones were added to opaque a cells at concentrations up to 100 μg/ml but did not induce efficient biofilm formation (Fig. 3B). This is despite the fact that *C. tropicalis* a cells effectively formed mating projections in response to synthetic α pheromone (Supp. Fig. 2). We also tested whether biofilm formation was more efficient when cells were responding to natural pheromones secreted by both a and α cells. For this purpose, a transwell system was employed in which a semipermeable membrane separated a mixture of opaque a and α 'source' cells from a population of opaque a 'sink' cells contacting the polystyrene surface (Fig. 3D). Using this system, biofilms were not formed by 'sink' cells, although the induction of mating projections was not as strong as in response to synthetic pheromones or to co-cultures of a and α cells (Fig. 3C and data not shown). Together, these results suggest that pheromone signaling is necessary, but not sufficient, to induce efficient biofilm formation in *C. tropicalis* opaque cells.

Our results establish that *C. tropicalis* forms sexual biofilms between opaque a and α cells in a pheromone-dependent manner. However, direct cell-to-cell contact between a and α cells also appears to be necessary for efficient biofilm production. In contrast, pheromone alone is sufficient to stimulate cohesion and biofilm formation amongst responding white cells in *C. albicans* (Daniels *et al.*, 2006; Lin *et al.*, 2013). It therefore appears that the mechanisms regulating sexual biofilm formation exhibit significant differences between *C. tropicalis* and *C. albicans*.

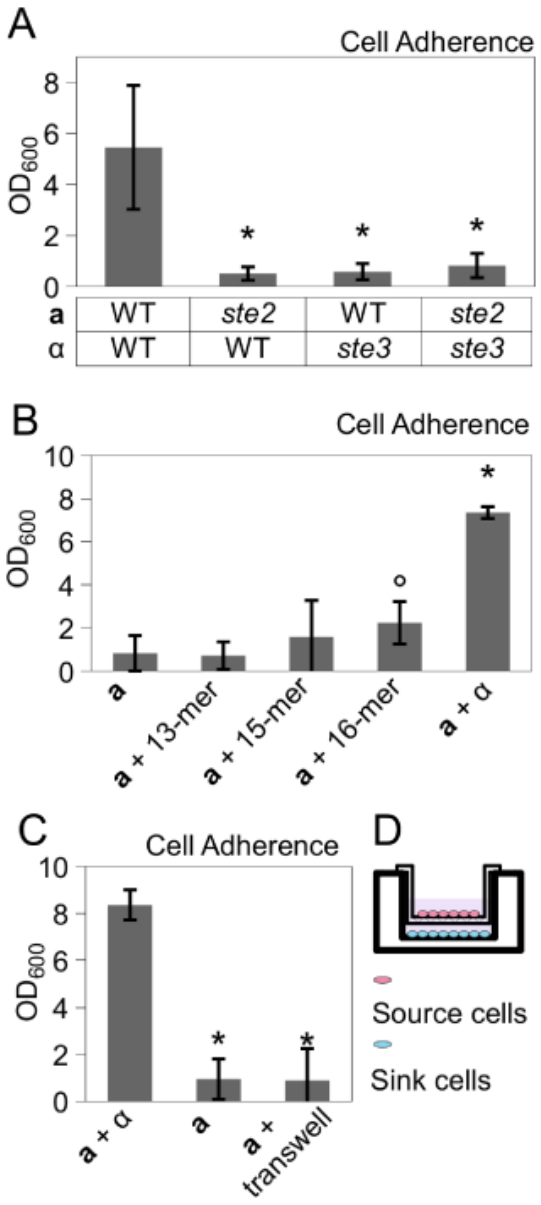

Figure 3-3: Pheromone signaling is necessary, but not sufficient, for sexual biofilm formation by *C. tropicalis* opaque cells.

(A) Quantification of biofilm formation by *C. tropicalis* strains lacking pheromone receptors for α pheromone (Ste2) or for a pheromone (Ste3). * $p<0.001$. Mann-Whitney test. (B) Biofilm formation by *C. tropicalis* a cells supplemented with synthetic α pheromone at 100 µg/ml (13-mer, 15-mer or 16-mer) or α cells. ° $p<0.05$ compared to a cells alone. * $p<0.01$ compared to a cells alone. Mann-Whitney test. (C) Biofilm formation of a cells (sink cells) exposed to pheromones produced by a mixed culture of opaque a and α cells (source cells), that were separated from sink cells by a semi-permeable transwell. * $p<0.001$, Tukey's test. (D) Schematic diagram of transwell setup. Biofilm measurements show mean ± standard deviation (N≥4).

C. tropicalis sexual biofilms exhibit a complex structure

In *C. albicans*, the hallmarks of a mature biofilm include yeast and hyphal cell layers, as well as the presence of an extracellular matrix (Chandra *et al.*, 2001; Andes *et al.*, 2004; Finkel and Mitchell, 2011). To analyze the structure of *C. tropicalis* biofilms, scanning electron microscopy (SEM) and confocal laser scanning microscopy (CLSM) were employed. *C. tropicalis*

sexual biofilms examined after co-culture of opaque a and α cells showed a bilayer structure; the cells closest to the polystyrene surface consisted mainly of chains of yeast cells and pseudohyphae, while the upper stratum consisted of much longer filamentous cells (Fig. 4A, Supp. Fig. 3). Given that sexual biofilms are dependent on pheromone signaling, filamentous cells could include conjugation tubes, true hyphae, or pseudohyphae. Many of the long filaments contained septa with no obvious constrictions between cells, consistent with being true hyphae. However, other elongated cells did not exhibit septation and showed morphologies more consistent with mating projections (Fig. 2D and 4A). We therefore suggest that a combination of filamentous forms contributes to biofilm structure.

To examine the frequency of mating within the sexual biofilm, auxotrophic opaque a and α strains were mixed and grown as a biofilm for 48 hours. Mating frequencies were determined by recovering cells and plating onto selective media (see Experimental Procedures). We observed that productive mating occurred within the sexual biofilm, with a mating frequency of 3.1% (±3.0%). While this indicates relatively efficient mating, a mating frequency of 23.2% (±11.5%) was observed when cells were co-incubated on Lee's + glucose agar plates under non-biofilm conditions ($p= 0.031$, Student's T-test). Thus, under the conditions tested, mating within a biofilm was less efficient than between opaque cells mixed under standard *in vitro* conditions.

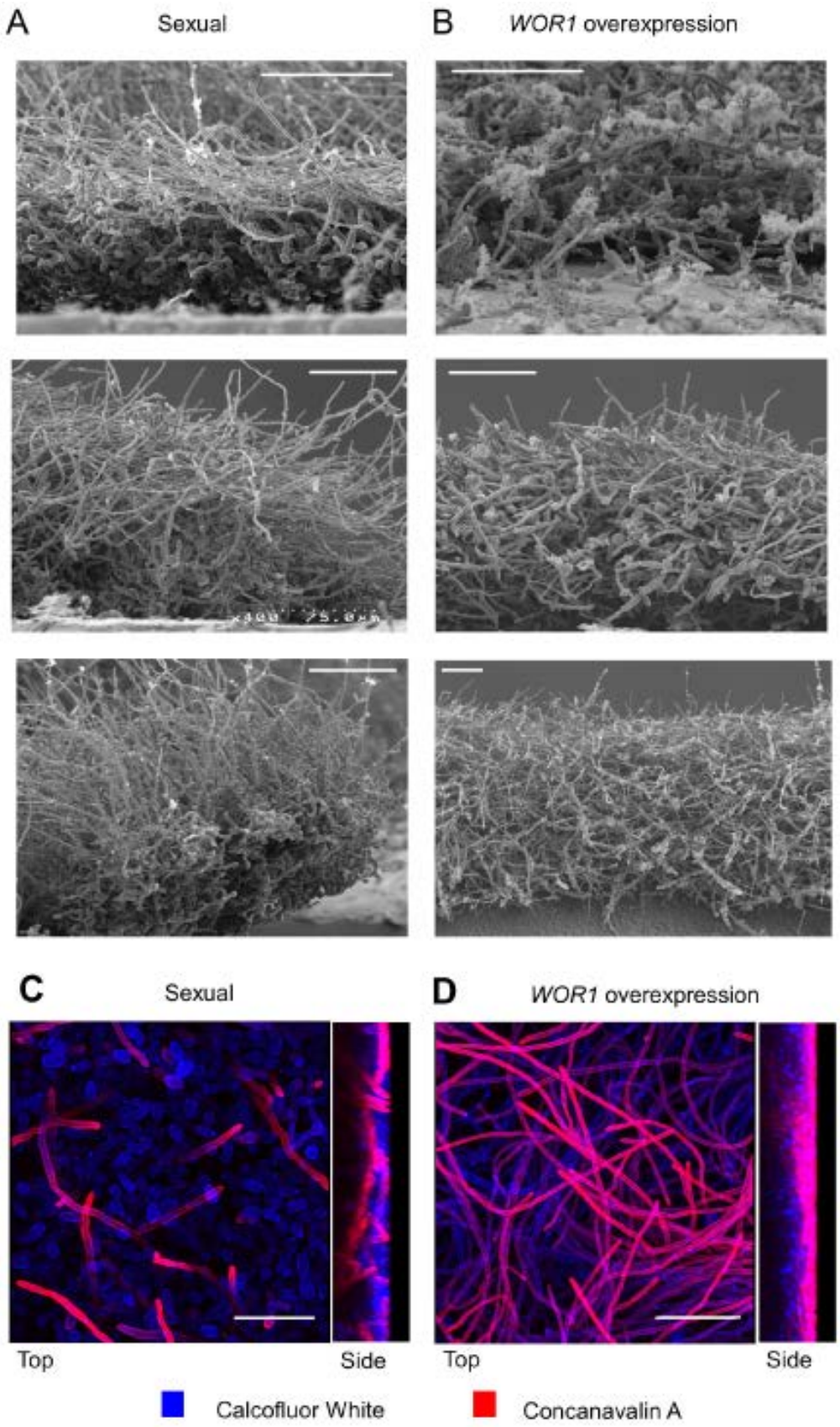
A
Sexual
B
WOR1 overexpression
C
Sexual
D
WOR1 overexpression
Top
Side
Top
Side
Calcofluor White
Concanavalin A

Figure 3-4: Microscopic analysis of *C. tropicalis* sexual and *WOR1* overexpression biofilms.

Scanning electron micrographs showing side views of biofilms formed after 48 hours of development. (A) *C. tropicalis* **a** and α opaque cells (sexual biofilm). (B) *WOR1* overexpression biofilm. 600X (top image), 400X (middle and bottom left images) or 200X magnification (bottom right). Scale bar = 60 µm (valid only in foreground). Confocal imaging of (C) sexual and (D) *WOR1* overexpression biofilms. Left, top views projected from outer biofilm surface inward. Right, side views of biofilms. Images were taken with the same settings to allow for direct comparison. Scale bar = 36 µm. Blue = Calcoflour White. Red = Rhodamine conjugated Concanavalin A.

In order to gain a better understanding for how the sexual biofilm structure develops, SEM was performed on biofilms at different stages of development. At early time points (4 h), a layer of yeast cells was deposited onto the polystyrene surface (Fig. 5A, Supp. Fig. 4A). Adhesion occurred in a subset of cells, as the majority of the cells were washed away post-inoculation. The initial cell distribution was sparse, but by 12 hours of growth the base layer had spread to occupy the majority of the polystyrene surface. In several regions, filamentous cells had also begun to appear. Filamentous growth was extensive by 24 hours, by which time a meshwork of filamentous cells and extracellular matrix (ECM) had grown over the base layer of yeast cells, and by 48 hours the biofilm was completely covered by filamentous cells. Distinct cell morphologies were observed between the two layers of the biofilm; the upper layer was composed of mainly filamentous cells, while the lower layer was composed mainly of yeast cells (Fig 4A and 5A). Biofilm thickness ranged from 30 µm to 100 µm. In addition to extensive filamentous growth, the upper stratum contained a considerable amount of ECM material, as evidenced by clusters of fibrous material throughout this layer (Fig. 5A, Supp. Fig. 4A).

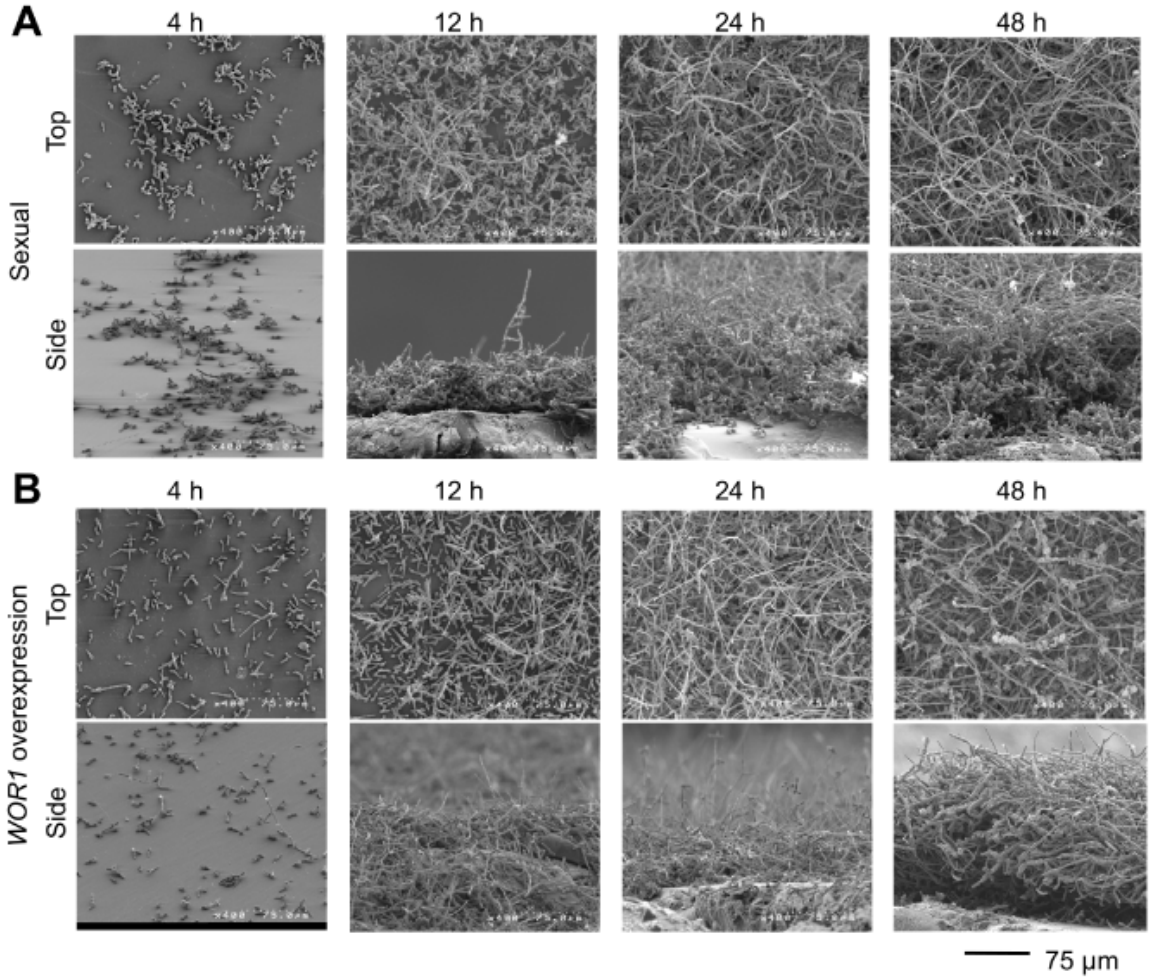

Figure 3-5: Time course of *C. tropicalis* biofilm development.

(A) Representative SEM images of sexual biofilms consisting of a 50:50 mixture of opaque a and α cells. (B) Representative SEM images of biofilms from opaque cells overexpressing WOR1. Cells were grown on a polystyrene substrate and then samples were analyzed by scanning electron microscopy at 4, 12, 24, and 48 h following inoculation. Magnification = 400X. Scale bars = 75 µm.

To further determine the distribution pattern of the ECM, cells were stained with the lectin Concanavalin A (ConA). ConA binds mannan and glucan polysaccharides that compose the majority of the cell wall and extracellular matrix (Mandal *et al.*, 1994; Chandra *et al.*, 2001; Gow and Hube, 2012). It appeared that ECM was primarily associated with filamentous cells of the outer layer, although matrix was also evident at appreciable levels throughout the biofilm (Fig.

4C). Matrix production was variable, with some filamentous cells brightly stained for ECM while others were not. An alternative possibility was that differential staining of filamentous cells was due to variable stain penetration, as previously observed in *C. albicans* (Yi *et al.*, 2011). To address this concern, confocal microscopy was performed on biofilms that were dispersed prior to fixation and staining (Supp. Fig. 5). ConA staining again localized to distinct subsets of cells, suggesting that some cells produce high quantities of ECM material or that ECM is preferentially bound to these cells.

Confocal microscopy was also performed on pure populations of opaque a cells that do not form a sexual biofilm. Although adhesion of some cells to the substrate was seen (Supp. Fig. 5D), dense growth did not occur, and there was a lack of ECM material. Furthermore, filamentous growth was rare in these single-sex experiments, despite the fact that the distribution of adherent cells was similar to that of early biofilms containing both mating types. We conclude that ECM production and filamentous growth occurs during maturation of sexual biofilms, which is dependent on pheromone signaling between the two mating types.

WOR1 Overexpression Biofilms Exhibit Distinct Structures from Sexual Biofilms

In *C. tropicalis*, overexpression of *WOR1,* the master transcriptional regulator of the white-opaque switch, was recently shown to induce filamentation on solid media and biofilm formation in cells grown on a polystyrene substrate (Porman *et al.*, 2013). These biofilms involved opaque cells expressing *WOR1* under the control of the strong constitutive promoter, *TDH3,* and were characterized by extensive filamentation, demonstrating links between the white-opaque switch, filamentation, and biofilm formation. In contrast to sexual biofilms, however, *WOR1* overexpression biofilms were formed in cultures of a single mating type

(opaque a, α, or a/α cells) (Porman *et al*., 2013). To determine if these biofilms were dependent on pheromone signaling, *WOR1* was also overexpressed in cells lacking the Ste2 receptor. Despite the absence of the pheromone receptor, these cells produced biofilms that were indistinguishable from wildtype cells overexpressing *WOR1* (data not shown). Thus, in contrast to the sexual biofilms formed by mixed cultures of opaque a and α cells, the biofilms formed by *WOR1* overexpression are asexual biofilms.

We directly compared the structures of sexual biofilms with *WOR1* overexpression biofilms using SEM and CLSM. Several notable differences were evident between the two models. First, whereas in sexual biofilms filamentous growth was restricted to the upper stratum of the biofilm, in *WOR1* overexpression biofilms filamentation occurred throughout the biofilm structure (compare Fig. 4A with B, and Fig. 4C with D). Second, extensive filamentous growth occurred at earlier time points in the *WOR1* overexpression biofilm (see 12 h time points in Fig. 5 and Supp. Fig. 4), consistent with high *WOR1* expression enhancing filamentation (Porman *et al.*, 2013). Third, ECM was consistently distributed in the *WOR1* overexpression biofilms, whereas ECM production was more variable in the sexual biofilms (Fig. 4A and B). Quantification of ECM content by a Glucatell assay confirmed that both biofilm types contained more ECM than wildtype opaque a cells alone ($p<0.01$, Tukey's test), and that *WOR1* overexpression biofilms contained 36% more ECM than sexual biofilms, although this difference was not significant (Supp. Fig. 6). Despite these structural differences, overall biofilm thicknesses were similar in the two models as determined by SEM (Fig. 4). Together, these results demonstrate that *C. tropicalis* can form biofilms with different structural features, as exemplified by sexual and *WOR1* overexpression biofilms.

Transcriptional Profiling of *C. tropicalis* Biofilm Formation

Cells within biofilms often exhibit distinct properties compared to cells grown under planktonic conditions. Transcriptional profiling was therefore used to compare non-biofilm populations (white *wor1Δ* a cells or opaque a cells), sexual biofilm populations (mixtures of opaque a and α cells), and *WOR1* overexpression biofilms (opaque a cells overexpressing the *WOR1* transcription factor). RNA was recovered from cells grown under each of these conditions, and the resulting cDNA was hybridized to custom *C. tropicalis* microarrays (see Experimental Procedures).

Most informative were the profiles of sexual and *WOR1* overexpression biofilms compared to that of planktonic opaque a cells that do not form biofilms under the assay conditions (Fig. 6A). In this comparison, sexual biofilms upregulated 68 genes and downregulated 11 genes (>2 fold change), while *WOR1* overexpression biofilms upregulated 21 genes and downregulated 37 genes (Fig. 6C, Supp. Table 3). Significant overlap was found between sets of biofilm-regulated genes with five genes exhibiting similar expression changes in the two biofilm populations (p= 6.9E-4, hypergeometric distribution, Supp. Table 4). Shared upregulated genes included *EFH1*, whose ortholog regulates filamentation in *C. albicans*, and *CTRG_04837*, whose ortholog (orf19.2457) is upregulated in conventional *C. albicans* biofilms (Doedt *et al.*, 2004; Nobile *et al.*, 2012). In addition, *CTRG_03464* was downregulated in both *C. tropicalis* biofilm types, although its *C. albicans* ortholog (orf19.5282) is upregulated in rat biofilm models in *C. albicans* (Nett *et al.*, 2009).

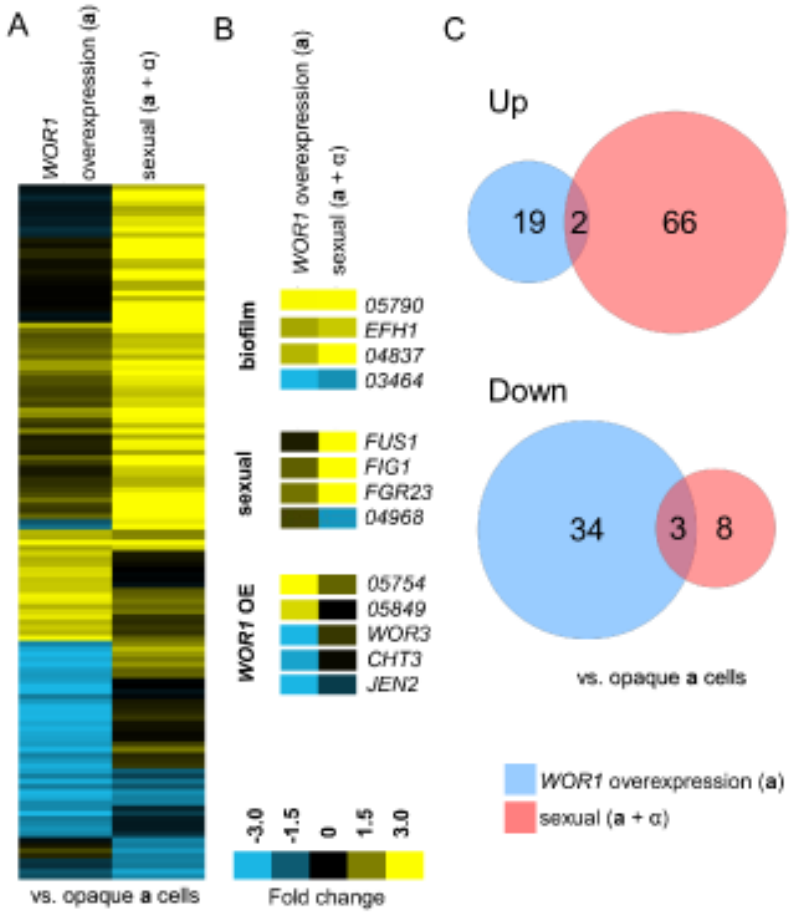

Figure 3-6: Transcriptional profiling of *C. tropicalis* sexual and *WOR1* overexpression biofilms.

(A) Gene expression profiles comparing a *WOR1* overexpression biofilm (p*TDH3-WOR1* in opaque **a** cells) and a sexual biofilm (consisting of a 50:50 mixture of opaque **a** and α cells) to that of opaque **a** cells. Genes were filtered for greater than 2-fold expression change and clustered via average linkage (see Experimental Procedures). Upregulated genes are yellow and downregulated genes are blue. (B) Examples of genes regulated by both biofilm conditions, sexual biofilm conditions only, or *WOR1* overexpression biofilm conditions only. (C) Venn diagrams illustrate biofilm genes with a 2-fold or more change in expression relative to wild type opaque **a** cells. Overlaps between transcriptional profiles were significant as determined by the hypergeometric distribution (Supp. Table. 4).

We also directly compared the transcriptional profile of *C. tropicalis* sexual biofilms to those formed by *C. albicans* (Supp. Table 5). We found that 13% of the genes upregulated in *C. tropicalis* sexual biofilms were also induced in *C. albicans* sexual biofilms (Lin *et al.*, 2013), a significant overlap (p=3.3E-5, hypergeometric distribution, Supp. Table 4 and 5). This is in spite of the fact that sexual biofilm formation in *C. albicans* occurred in white cells whereas *C.*

tropicalis sexual biofilms occurred in opaque cells. In contrast, a comparison of upregulated genes between *C. tropicalis* sexual biofilms and conventional *C. albicans* biofilms (Nobile *et al.*, 2012) revealed no significant overlap (p=0.17, Supp. Table 4 and 5).

GO-Term analysis was performed on *C. tropicalis* sexual biofilm genes when compared either to the white control strain (Supp. Table 6) or the opaque control strain (Supp. Table 7). In these analyses, significant gene expression changes included those associated with multi-organism processes, pheromone response, conjugation, and biofilm formation. These results indicate that *C. tropicalis* biofilms undergo significant transcriptional changes in genes involved in specialized growth and communication in order to establish the new community structure. Sexual *C. tropicalis* biofilms showed specific induction of many genes associated with mating, including *FIG1, FUS1,* and *KAR4*. These sex-related genes accounted for 20 of the 55 genes with known orthologs that were upregulated greater than 2-fold in the sexual biofilm assays (Supp. Table 7), and establish a strong connection between the mating response and sexual biofilm formation in *C. tropicalis* (Fig. 6B).

WOR1 overexpression biofilms also included gene expression changes that were not observed in sexual biofilms. For example, *WOR3, CHT3*, *JEN2*, *CTRG_05754*, and *CTRG_05849* were all regulated only in the *WOR1*-mediated biofilms (Fig. 6B). The transcriptional regulator *WOR3* is known to be highly upregulated in both *C. albicans* opaque cells compared to white cells and in cells grown within biofilms (Nobile *et al.*, 2012; Lohse *et al.*, 2013). This was not the case in *C. tropicalis*, however, since planktonic opaque cells showed decreased expression of *WOR3* relative to white cells (Porman *et al.*, 2013), and *WOR3* expression was further decreased in *WOR1*-overexpressing biofilms compared to control opaque cells (Fig. 6B).

Analysis of the Role of FGR23 and EFH1 in C. tropicalis Biofilm Formation

Cell adhesion and cell fusion are critical steps in the mating process, and it is possible that the physical interactions that facilitate these processes promote biofilm formation. We noted that *C. tropicalis FGR23* (*CTRG_02409*) is strongly induced in sexual biofilms (5.5-fold) as well as weakly induced in *WOR1* overexpression biofilms (1.4-fold). The *FGR23* gene is an ortholog of *S. cerevisiae AGA1*, which encodes the anchorage subunit for the a-agglutinin heterodimer (Roy *et al.*, 1991). *AGA1* is expressed in both a and α cell types of *S. cerevisiae* and is also highly induced in response to pheromone (Roberts *et al.*, 2000; Guo *et al.*, 2000; Dranginis *et al.*, 2007). Aga1 is a glycophosphatidylinositol-linked protein that anchors Aga2 to the cell surface of a cells, where it interacts with the complementary α-agglutinin expressed on the surface of α cells. Contacts between agglutinins facilitate the interaction of *S. cerevisiae* mating partners, and thus loss of Aga1 results in a reduction of mating efficiency in liquid medium (Roy *et al.*, 1991; de Nobel *et al.*, 1995). Deletion of Aga1 also disrupts mating on solid medium if combined with deletion of the related adhesin, Fig2 (Guo *et al.*, 2000).

To determine if Fgr23 facilitates mating or biofilm formation in *C. tropicalis*, we generated *fgr23*Δ and *FGR23* over-expression (*pTDH3-FGR23*) strains. Deletion of *FGR23* resulted in a decrease in sexual biofilm production, as co-culture of a and α *fgr23*Δ strains generated biofilms that were significantly reduced compared to those formed by wild type strains (Fig. 7, p= 1.2E-4, Student's T-test). Interestingly, deletion of *FGR23* from either a or α cells alone also resulted in a defect in biofilm formation (data not shown). Reintegration of *pTDH3-FGR23* into the deletion strain background significantly increased biofilm formation by 43% compared to deletion strains (p=0.049, Student's T-test), partially restoring the wildtype

phenotype. In contrast, integration of the *pTDH3-FGR23* construct into the wildtype background did not significantly alter biofilm formation compared to wildtype (data not shown).

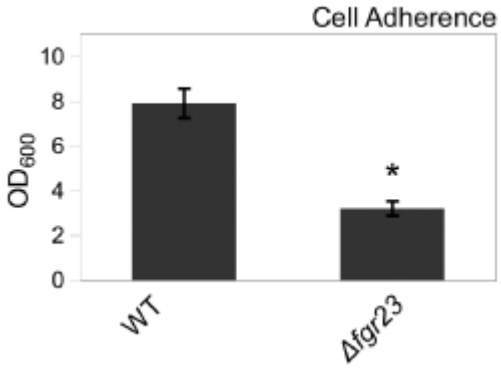

Figure 3-7: The sexual agglutinin-related protein Fgr23 promotes sexual biofilm development.

Deletion of *FGR23* decreases biofilm formation. Mean ± standard deviation (N≥4). * $p<0.05$. Mann-Whitney.

The role of *FGR23* in mediating mating in *C. tropicalis* was also addressed. Wildtype cells and *fgr23*Δ mutants were compared for mating efficiency when a and α cells were co-incubated on Spider medium. Mutants lacking *FGR23* were still able to fuse and mate, although mating efficiency was reduced by an order of magnitude between *fgr23*Δ cells under standard conditions (Supp. Fig. 7). This indicates that Fgr23 plays an important role in promoting both biofilm formation and conjugation in *C. tropicalis*.

Filamentation is an integral part of biofilm formation in *Candida* species, and many mutants defective in filamentation are unable to form biofilms or mount successful infections (Lo *et al.*, 1997; Ramage *et al.*, 2002; Nobile *et al.*, 2006; Laforet *et al.*, 2011). In *C. albicans, EFH1* is a regulator of filamentous growth and works in concert with the related APSES transcription factor *EFG1* (Doedt *et al.*, 2004). Given that *EFH1* was upregulated approximately 2-fold in both sexual and *WOR1*-overexpression biofilms, the *EFH1* gene was deleted to determine its role in biofilm formation. However, deletion of *EFH1* had no significant effect on sexual biofilm formation (Supp. Fig. 8). This could be due to functional redundancy with a yet-to-be identified transcription factor, or could simply indicate that *EFH1* does not contribute to biofilm efficiency.

DISCUSSION

Here, we report that *C. tropicalis* forms a sexual biofilm as a result of pheromone signaling between a and α cells. Biofilm formation required that cells be in the opaque phenotypic state, and cells in the white state did not contribute to overall biofilm formation. Structural analysis of the biofilms revealed them to be highly stratified, with the lower layer of the biofilm consisting mostly of yeast cells, while the upper stratum contained primarily filamentous cells. The latter included a mixture of both hyphae and conjugation tubes, and extracellular matrix was associated with sub-populations of filamentous cells. Overall, the structure of *C. tropicalis* sexual biofilms showed physical similarities to both sexual and asexual biofilms formed by *C. albicans*. These, too, consist of a basal layer of yeast cells upon which a meshwork of filamentous cells develops together with associated ECM material (Chandra *et al.*, 2001; Daniels *et al.*, 2006; Bonhomme and d' Enfert, 2013; Daniels *et al.*, 2013).

Previously, it was shown that *C. albicans* also forms a sexual biofilm (Daniels *et al.*, 2006). In this species, biofilms result from white a or α cells responding to sexual pheromones produced by opaque cells of the opposite sex (Daniels *et al.*, 2006; Park *et al.*, 2013). Thus, the most efficient biofilms are generated by cultures containing a majority of white a and α cells mixed with a minority of opaque cells as a source of pheromone (Daniels *et al.*, 2006). In both white and opaque cells, pheromone signaling occurs via a conserved MAPK cascade that culminates in activation of the Cph1/Ste12 transcription factor (Yi *et al.*, 2008; Sahni *et al.*, 2010; Lin *et al.*, 2013). Additional factors regulating *C. albicans* sexual biofilm formation include the transcription factors Bcr1, Brg1, Rob1 and Tec1, downstream effectors such as the G1 cyclin-related protein Hgc1, as well as cell surface proteins Eap1, Csh1, and Pgc10 (Nobile *et al.*, 2006; Sahni *et al.*, 2010; Lin *et al.*, 2013).

The current studies establish that while both *C. albicans* and *C. tropicalis* form sexual biofilms, the regulation of biofilm formation has diverged since these species last shared a common ancestor. In *C. albicans*, pheromones induce white cells to produce robust biofilms, whereas opaque cells form weak, unstable biofilms (Daniels *et al.*, 2006; Lin *et al.*, 2013). The formation of sexual biofilms was shown to promote *C. albicans* mating *in vitro* (Park *et al.*, 2013), as biofilms stabilized pheromone gradients between opaque cells, thereby promoting chemotropism between potential mating partners (Daniels *et al.*, 2006). Given the low frequency of *C. albicans* mating in natural populations, it was suggested that the white-opaque switch has been retained in this species as a mechanism for promoting biofilm formation rather than for directing rare mating events (Soll, 2009).

In contrast to *C. albicans*, we demonstrate that sexual biofilms in *C. tropicalis* are formed exclusively by cells in the opaque state. In addition, whereas substrate adhesion in *C. albicans* cells can be induced by pheromone alone (Daniels *et al.*, 2006), biofilm formation in *C. tropicalis* was most efficient when there was physical contact between a and α cells. Taken together, our studies establish that opaque cells of *C. tropicalis* are both the mating-competent form *and* the form most capable of generating a sexual biofilm. Furthermore, the thermostability of the opaque state in *C. tropicalis* allows sexual biofilms to form equally well at both 25°C and 37°C, potentially making sexual biofilm formation relevant for infections in the clinic.

Sexual biofilms in *C. tropicalis* were also compared to asexual biofilms formed due to overexpression of Wor1, the master regulator of the white-opaque switch. Wor1 forms part of a network of interacting transcriptional feedback loops that promotes stable and heritable formation of the opaque state (Huang *et al.*, 2006; Zordan *et al.*, 2006; Srikantha *et al.*, 2006;

Zordan *et al.*, 2007; Hernday *et al.*, 2013). While *C. tropicalis* white cells and single-sex cultures of opaque cells formed insubstantial biofilms, overexpression of Wor1 in a, α, or a/α cell types induced filamentation and resulted in biofilms that were comparable in size to sexual biofilms. Interestingly, the structures of Wor1-mediated and sexual biofilms were distinct. Whereas sexual biofilms showed clear stratification and variable ECM density, Wor1-mediated biofilms exhibited more homogeneous filamentation throughout the biofilm structure.

Expression profiling of *C. tropicalis* cells grown in the two biofilm models revealed both similarities and significant differences between these models. For example, only sexual biofilms were associated with the induction of mating genes, including pheromone and pheromone receptor genes, consistent with the key role of mating signaling in generating these biofilms. *WOR1* overexpression and sexual biofilms also upregulated a shared set of genes, which included *FGR23, EFH1, XOG1* and several uncharacterized genes. *XOG1* encodes a glucanase that may potentially affect adhesion of cells to the substrate surface (González *et al.*, 1997), although this possibility was not tested here.

The potential roles of *FGR23* and *EFH1* in sexual biofilm formation were further assessed by genetic analysis of these two genes. *EFH1* is a transcription factor regulating filamentous growth in *C. albicans* (Doedt *et al.*, 2004), yet deletion of this gene in *C. tropicalis* did not lead to an obvious colony or cellular phenotype and did not alter sexual biofilm formation. In contrast, deletion of the *C. tropicalis FGR23* gene resulted in a significant decrease in sexual biofilm formation. *FGR23* is an ortholog of *AGA1* in *S. cerevisiae*, which encodes a component of the mating-type a-agglutinin. *S. cerevisiae* agglutinins consist of a-agglutinin, formed by a complex of Aga1 and Aga2, and the α-agglutinin, Sag1. These cell surface factors bind one another irreversibly during mating to promote conjugation (Lipke and Kurjan, 1992; Cappellaro *et al.*,

1994; Dranginis *et al.*, 2007). Significantly, the *C. albicans* Agglutinin-Like Sequence (ALS) gene family shows homology to *S. cerevisiae* α-agglutinin and this family plays a prominent role in *C. albicans* biofilm formation (García-Sánchez *et al.*, 2004; Silverman *et al.*, 2010).

We demonstrate that the a-agglutinin-related protein, Fgr23, is necessary for efficient formation of sexual biofilms by *C. tropicalis* opaque cells. *C. tropicalis fgr23Δ* mutants also showed a reduced mating efficiency compared to wildtype cells, indicating that the function of *FGR23* may be conserved with that of *S. cerevisiae AGA1*. In *S. cerevisiae*, *aga1* mutants show mating defects that are highly exacerbated by additional loss of the related *FIG2* gene (Guo *et al.*, 2000). In fact, *S. cerevisiae* proteins with adhesive properties are often interchangeable, even if they exhibit considerable differences at the amino acid sequence level. Thus, adhesins that function in flocculation can substitute for adhesins that promote mating and vice versa, if expressed at a high enough level and localized appropriately (Guo *et al.*, 2000). It is therefore apparent that adhesins can play diverse roles in mating, flocculation, and filamentation, and that these functions depend more on their expression pattern than their primary sequence. In the case of *C. tropicalis*, the function of Fgr23 further supports these conclusions, as this protein promotes both mating and sexual biofilm formation. Additional experiments will be required to address the specific role of Fgr23, and whether this factor acts to promote cell-cell or cell-substrate interactions to enhance biofilm formation by this pathogen.

EXPERIMENTAL PROCEDURES

Media

Preparation of YPD and SCD followed established protocols (Guthrie and Fink, 1991; Liu *et al.*, 1994). Nourseothricin resistant strains (*SAT*^{R}) were selected on yeast extract peptone dextrose (YPD) plates containing 200 µg/ml nourseothricin. Spider medium contained 1% nutrient broth (v/v), 0.4% potassium phosphate (w/v), 2% mannitol (pH 7.2) (w/v), and 1.35% agar (w/v). Lee's medium was formulated as previously described (Lee *et al.*, 1975) with leucine, arginine and histidine added at 0.13%, 0.01% and 0.01%, respectively.

Strain and Plasmid Construction

Strains used in the current experiments are listed in Supplemental Table 1. *WOR1* over-expression and deletion strains were constructed as described (Porman *et al.*, 2013). Opaque strains were obtained by plating white strains on Lee's + N-acetyl glucosamine medium for 2-7 days, then re-plating on Spider medium for 2-7 days and selecting opaque colonies following visual and microscopic examination of phenotype.

Deletion of *FGR23* and *EFH1* was performed using a previously described method (Noble and Johnson, 2005). 5' and 3' regions flanking the ORF (open reading frame) were PCR amplified (Supp. Table 2). *HIS1* and *ARG1* auxotrophic markers were PCR amplified from plasmids pSN64 (*ARG4*) and pSN52 (*HIS1*). ORF flanks were then combined with the auxotrophic markers using a fusion PCR protocol (Noble and Johnson, 2005). The resulting PCR product was used to transform auxotrophic strains. Correct integration was determined by PCR across the junctions of the integrating construct. The process was repeated to delete the second copy of the ORF, and then ORF PCR was performed to confirm deletion of the gene.

FGR23 complementation strains were constructed by PCR amplification of the *FGR23* ORF and the *TDH3* promoter, which were subsequently joined in a fusion PCR step. The PCR product was cloned into pSFS2a (Reuss *et al.*, 2004) using *Kpn*I and *Xho*I restriction sites. The resulting plasmid was used to transform wild type and *fgr23* deletion strains. Integration was confirmed by PCR.

Biofilm Adherence Assay and Biofilm Staining

Strains were grown overnight at 25ºC in Spider medium. Cells were centrifuged and resuspended in Lee's + Glucose medium. One ml of Lee's + Glucose medium was added per well of a 12-well plate. Either a single mating type or combinations of each mating type were added to each well for a total of 4×10^7 cells per well. Plates were incubated at room temperature for two days unless otherwise stated. Each well was then gently washed thrice with 1 ml of Phosphate-Buffered Solution (PBS) to remove non-adherent cells. Biofilms were imaged using a Bio-Rad Chemi-Doc imager. Optical density of biofilms was determined by scraping off adherent cells and resuspending them in PBS, diluting appropriately, and measuring absorbance at 600 nm on a Thermo-Scientific Nanodrop 2000c spectrophotometer.

Crystal violet staining was performed by decanting the wells and drying the adherent cells for 45 minutes. Cells were stained for 45 minutes with 385 µl of 0.4% aqueous crystal violet per well, followed by three 1 ml washes with water and destaining with 700 µl of 95% ethanol. The destain solution was diluted 10-fold into a 96-well plate, and absorbance at 595 nm was read using a BioTek Synergy HT plate reader.

Transwell Assay

Strains were grown overnight at 25ºC in Spider medium. Cells were then centrifuged and resuspended in Lee's + Glucose medium. One ml of Lee's + Glucose medium was added to the lower region of each well of a transwell plate (Costar Transwell, 0.4 µm polycarbonate membrane,12-well), along with 2 x 10^7 cells of a single mating type. Then, 0.5 ml of Lee's + glucose medium was added to the inner chamber, along with 2 x 10^7 cells of the opposite mating type, or a mix of the two mating types. Plates were incubated at room temperature for two days unless otherwise stated. The transwell chambers were removed, and the wells were washed and treated similarly to the previously described adherence assay.

Mating Assay

Auxotrophic strains were grown overnight at 25ºC in Spider medium. Cultures were centrifuged and resuspended in either Lee's + glucose medium or Spider medium as indicated. Approximately 2*10^7 cells of each mating type were spotted onto a filter (Millipore Cat. # AAWG01300) on a Lee's + glucose agar plate, a Spider agar plate (if Spider liquid was used), or cultured in the above-described sexual biofilm assay. After two days, cells were scraped from the filters or biofilms and resuspended in 1 ml of water. Cells were diluted appropriately and plated on selective media to select for parental strains or progeny. CFUs were counted after two days, and mating success was calculated by dividing the number of progeny by the limiting parent.

Zygote staining

Cultures were grown overnight at 25ºC in Spider medium, then centrifuged and resuspended in water. FITC-Concanavalin A (a strains) or Rhodamine-Concanavalin A (α strains) was added to each culture at a concentration of 25 µg/ml, and cells stained for one hour at 25ºC. Cells were washed and 10^7 of each mating type were combined and plated onto a filter on

Spider medium for one day at 25ºC. Cells were recovered from the filters, resuspended in water, and analyzed via fluorescence microscopy using a Zeiss Axio Observer Z1.

Microscopy and Imaging

For scanning electron microscopy, biofilms were prepared similarly to the adherence assay except a 1 cm^2 polystyrene square cut from a tissue-culture lid was added to each well prior to the addition of cells so that the majority of the biofilm formed on the square. Each biofilm square was fixed with 2.5% (w/v) glutaraldehyde in buffer (0.1 M Na-cacodylate, pH 7.4) overnight at 4°C. Squares were washed with the buffer, then subjected to 1% aqueous osmium tetroxide in buffer at 25°C for 90 minutes, then washed again. Squares were dehydrated using a 15% gradient ethanol series, dried in a critical point dryer, and finally coated with 20 nm 60:40 gold:palladium in an Emitech K550 sputter coater. Imaging was performed using a Hitachi S-2700 and Quartz PCI software.

For confocal microscopy, biofilms were also prepared on polystyrene squares, however they were fixed overnight in 4% formaldehyde at 4ºC. Squares were then washed with water, followed by staining in 1 ml of 25 µg/ml Rhodamine-conjugated Concanavalin A for one hour in the dark at 25ºC. Next, they were stained with 50 µg/ml Calcoflour White for one minute and washed with 1 ml water. Squares were then inverted onto coverslips and microscopy was performed on a Zeiss LSM 510 META microscope. Microscope settings were static across samples so that direct comparisons of staining intensities could be made when possible.

To image individual cells, biofilms were prepared similarly to the adherence assay, however, any staining was performed on the wells following washing, and then cells were scraped from the wells and suspended in approximately 10 µl water on a glass slide. Differential

Interference Contrast (DIC) and fluorescence images were collected using a Zeiss Axio Observer Z1.

RNA Purification and Microarray Analysis

Biofilms were prepared similarly to the adherence assay, except after the two-day incubation period biofilms were not washed. Rather, adherent cells were resuspended in the medium with non-adherent cells. RNA was extracted from cells using the RiboPure-Yeast Kit (Ambion). DNA was removed using DNAseI (Ambion) followed by phenol/chloroform extraction. Aminoallyl-labeled cDNA was generated from the purified RNA, and then hybridized to a custom *C. tropicalis* Agilent microarray, as previously described (Porman *et al.*, 2011). The microarrays were read and quantified using a Genepix 4000 scanner with GENEPIX PRO v3.0 (Axon Instruments) software. Data was then normalized using Goulphar web-based software (http://transcriptome.ens.fr/goulphar) with the following conditions: Foreground – Median, Background – Median background subtraction, Normalization – Print-tip group lowess (200), Flags – filter all, Saturating spots – remove if intensity is >50k in a single channel. Data was organized, averaged (two replicates each) and labeled in Microsoft Excel using known *C. albicans* or *S. cerevisiae* gene ortholog names for unannotated genes (candidagenome.org, yeastgenome.org, cgob3.ucd.ie, or www.broadinstitute.org/regev/orthogroups). Data was analyzed using Cluster v2.11 and visualized using TreeView v1.60 (http://rana.lbl.gov/EisenSoftware.htm). Cluster was also used for filtering results, where differentially regulated genes were selected by applying a >2-fold change cutoff. Array data is available from GEO (GSE52634 and GSE43267). Gene ontologies were determined using the CGD Gene Ontology Mapper (www.candidagenome.org/cgi-bin/GO/goTermMapper), and p-values for GO terms were calculated using a hypergeometric distribution with Multiple

Hypothesis Correction. The p-value for comparing overlap between the sexual and *WOR1* overexpression biofilms was generated using a hypergeometric distribution in Microsoft Excel.

Extracellular Matrix Quantification

Extracellular matrix was quantified similarly to previously described methods (Taff *et al.*, 2012) using the Glucatell © assay (Associates of Cape Cod, Inc. Falmouth, MA). Briefly, biofilms formed in the biofilm adherence assay were scraped and resuspended in the supernatant. Next, samples were sonicated for 10 minutes to disassociate cells and matrix material, and then centrifuged three times at 4,500x*g* for 20 minutes to remove cells. Glucan concentration of the recovered supernatants was then determined per the manufacturer's supplied protocol.

Statistical Analysis

Statistical analysis was performed using the PAST software package (folk.uio.no/ohammer/past/). All datasets were tested for normality using the Anderson-Darling method, and then the appropriate tests were performed. Tests across sample sets, such as one-way ANOVA or Kruskal-Wallis, were performed first, followed by between-sample tests, including Student's T-test, Tukey's test or Mann-Whitney test, as indicated in figure legends.

ACKNOWLEDGEMENTS

We would like to thank Allison Porman and Na Wang for generating several strains used in this study and members of the Bennett lab for comments on the manuscript. S.K.J. is supported by pre-doctoral fellowship F31DE022701 and M.P.H. is supported by a training grant for Graduate Assistance in Areas of National Need (P200A100100). R.J.B. is supported by NIAID (AI081704) and a PATH Award from the Burroughs Wellcome Fund.

SUPPLEMENTAL FIGURES

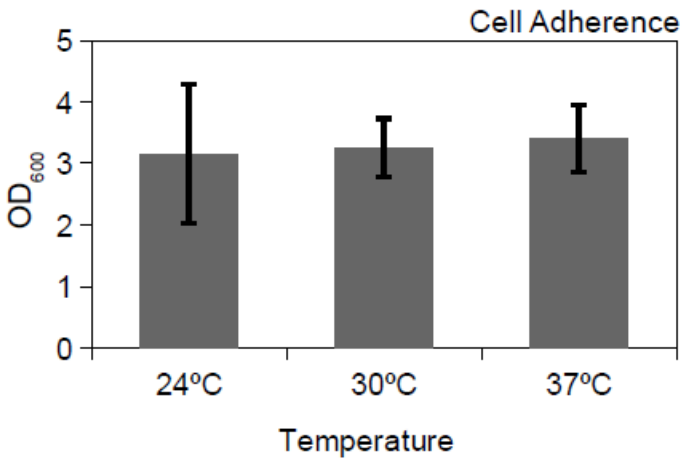

Figure S3-1: Temperature sensitivity of *C. tropicalis* sexual biofilms.

Sexual biofilms were developed at the indicated temperature for 48 h. Mean ± standard deviation (N=3). One-way ANOVA.

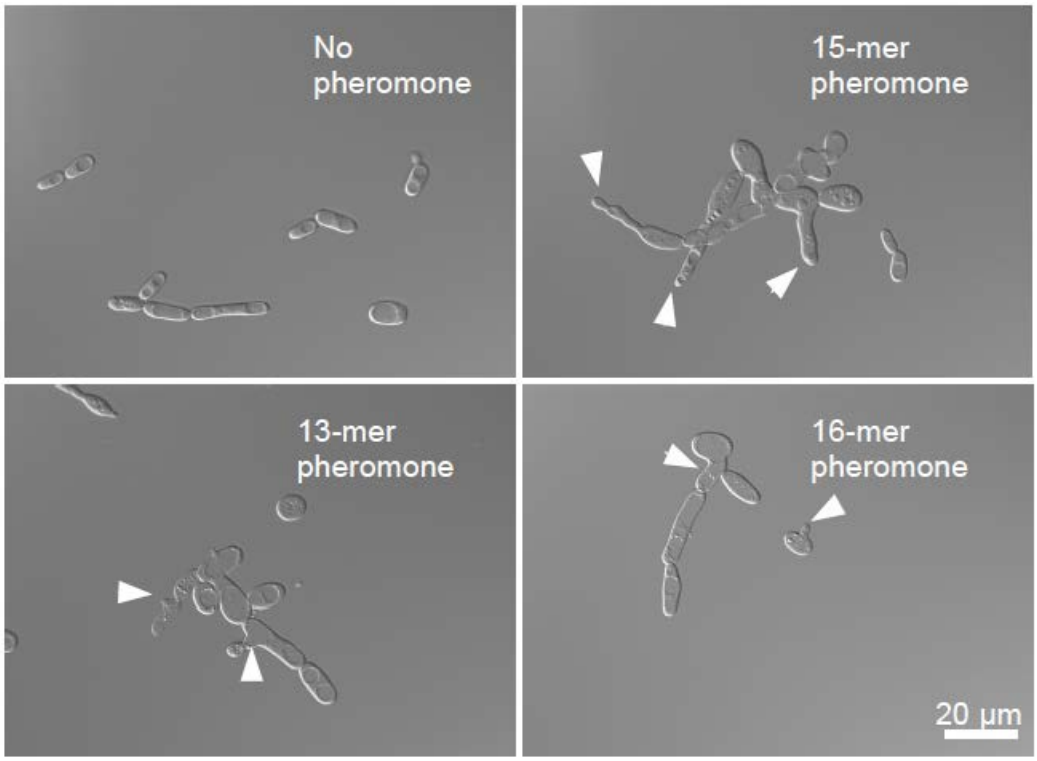

Figure S3-2: Opaque **a** cells respond to synthetic pheromones by forming mating projections.

Images of cells from biofilm assay in Fig. 3B. 100 µg/ml of *C. tropicalis* synthetic pheromone (a 13-mer, 15-mer or 16-mer version) was added to each well containing opaque **a** cells and incubated at 25°C for two days. Arrows indicate mating projections. Scale bars = 20 µm.

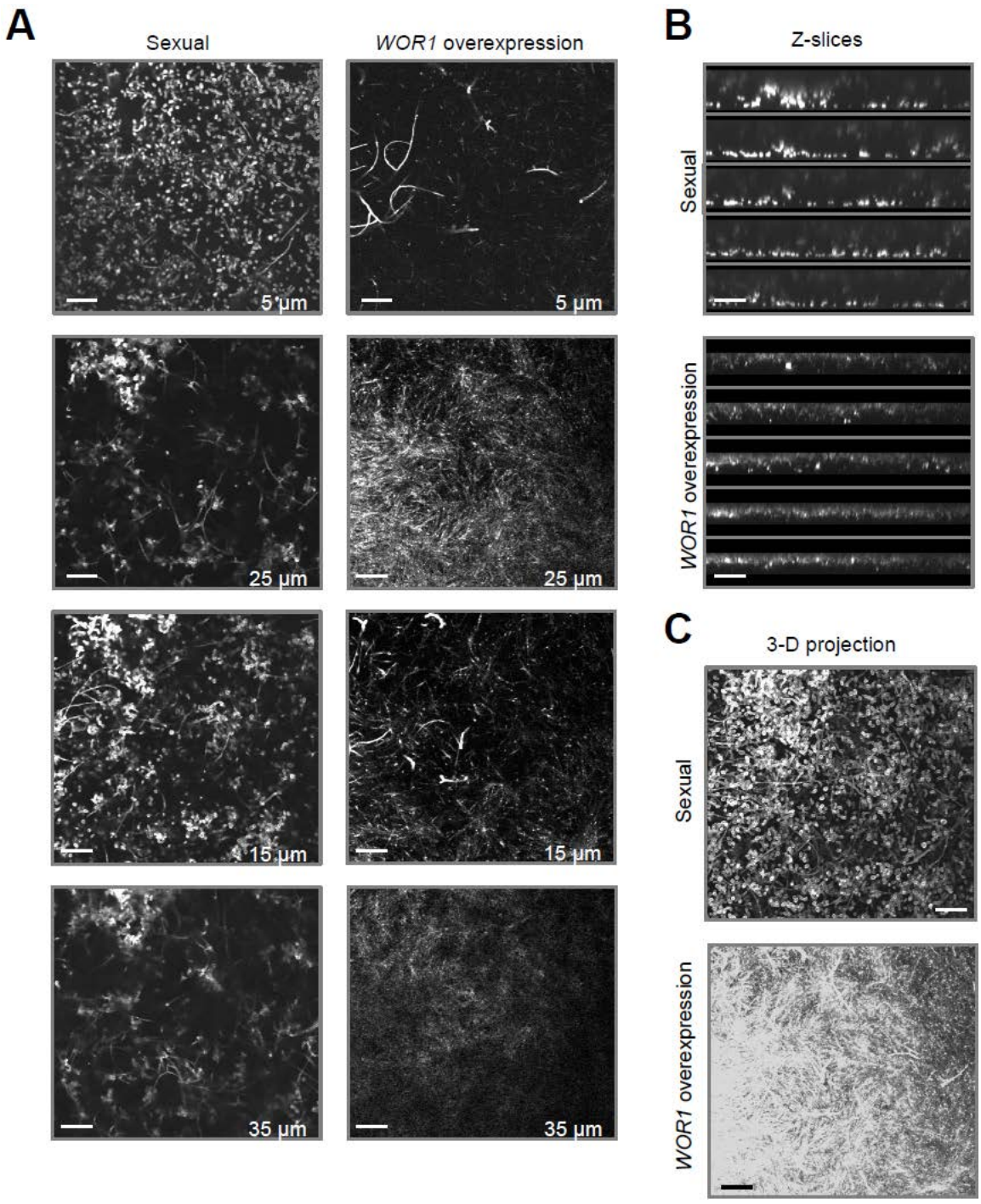

Figure S3-2: Confocal imaging of 48-hour sexual and WOR1 overexpression biofilms stained with Calcofluor White.

(A) Horizontal slices through the biofilm structures at indicated heights above the polystyrene substrate. (B) Vertical slices through five equally spaced sections of the biofilms. (C) 3-D projections of biofilm structures from outer biofilm surface inward. Scale bar = 50 µm.

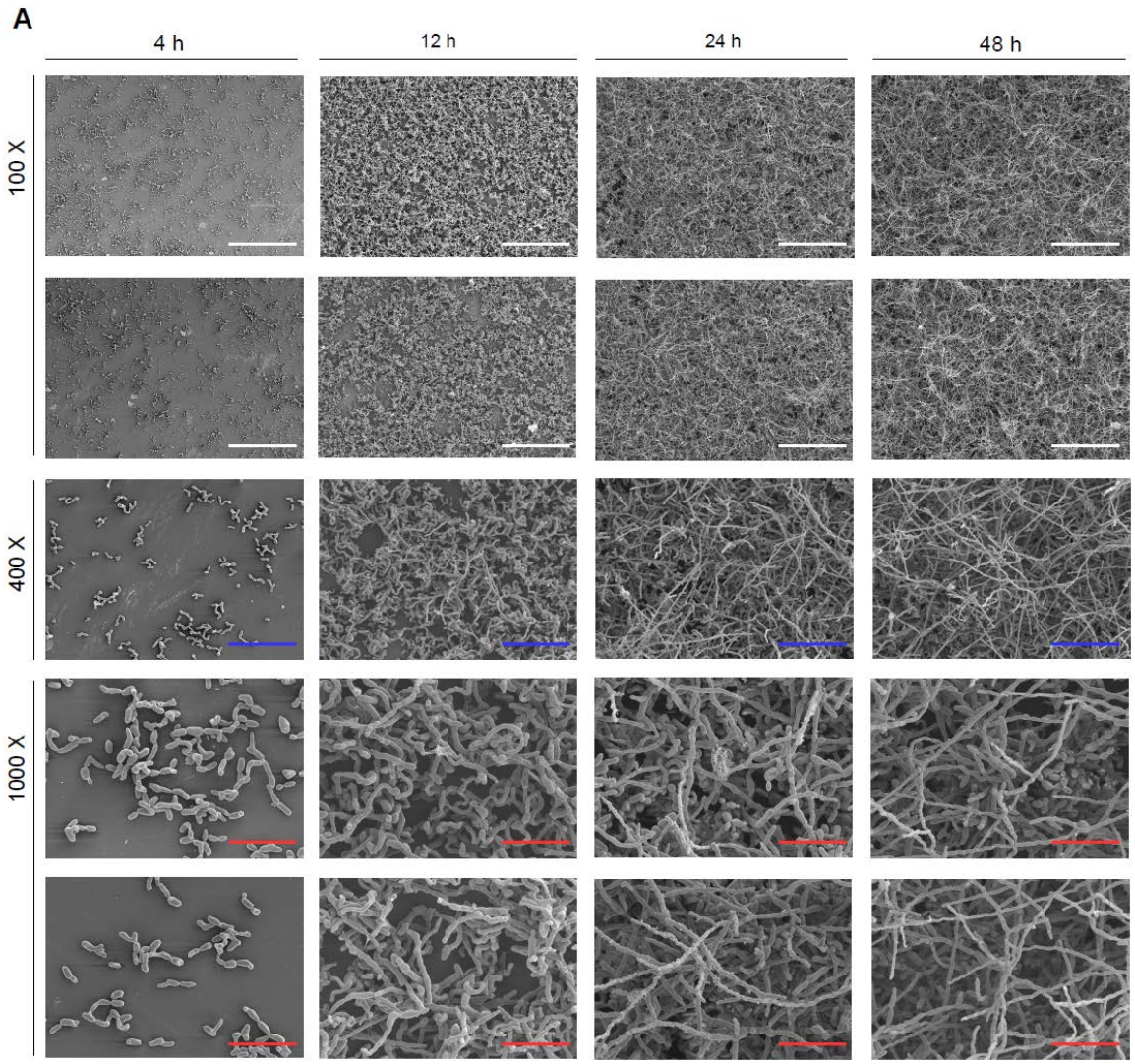

Figure S3-3: Additional time course images of *C. tropicalis* biofilm development.

(A) Representative SEM time course of sexual biofilms consisting of a 50:50 mixture of opaque **a** and α cells. (B; next page) Biofilms due to overexpression of the Wor1 transcription factor in opaque **a** cells. Cells were grown on a polystyrene substrate and samples analyzed by scanning electron microscopy at 4, 12, 24, and 48 h following inoculation. Magnification as indicated. Scale bars = (white) 300 µm, (blue) 75 µm, (red) 30 µm.

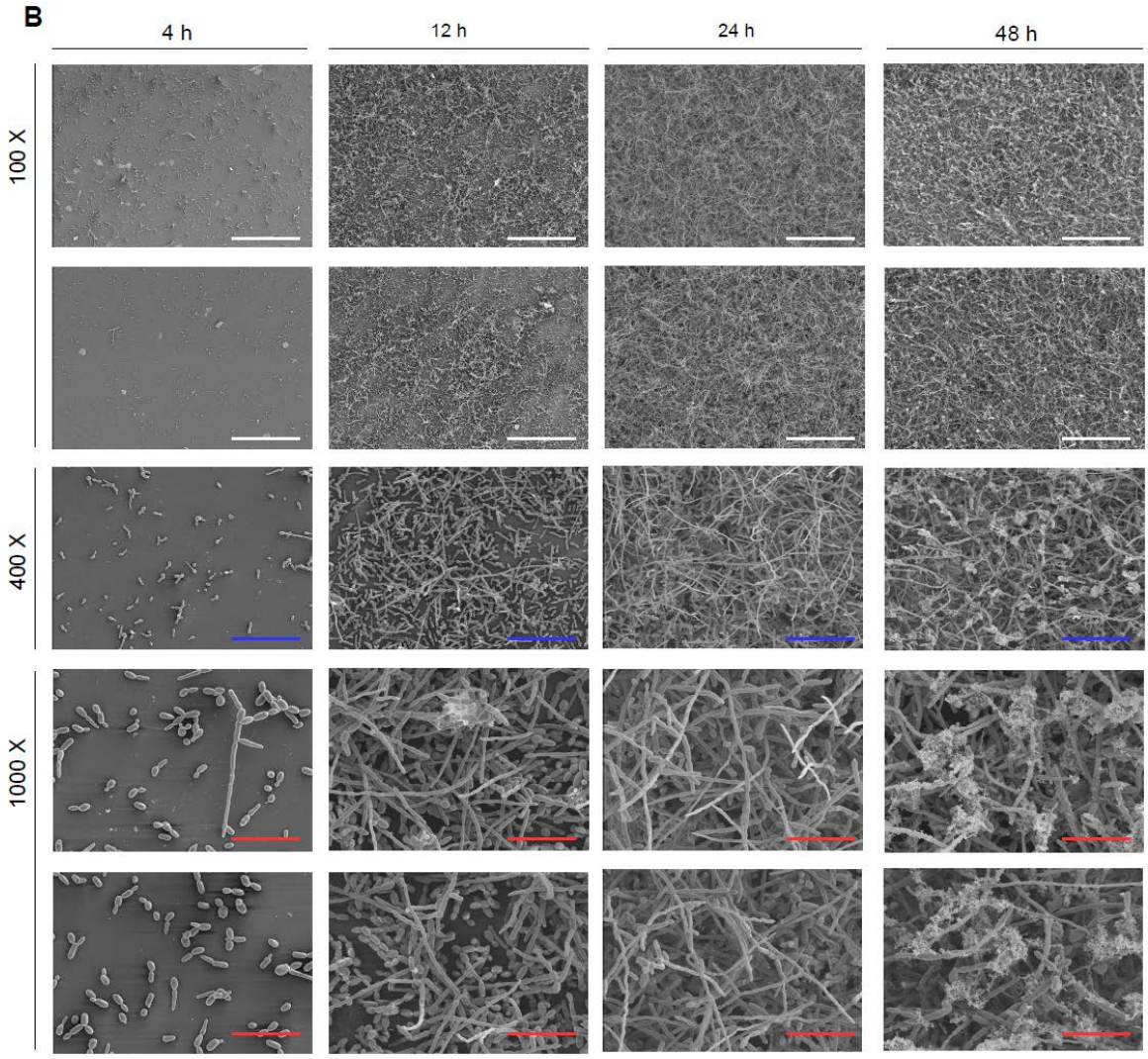
B
4 h
12 h
24 h
48 h
100 X
400 X
1000 X

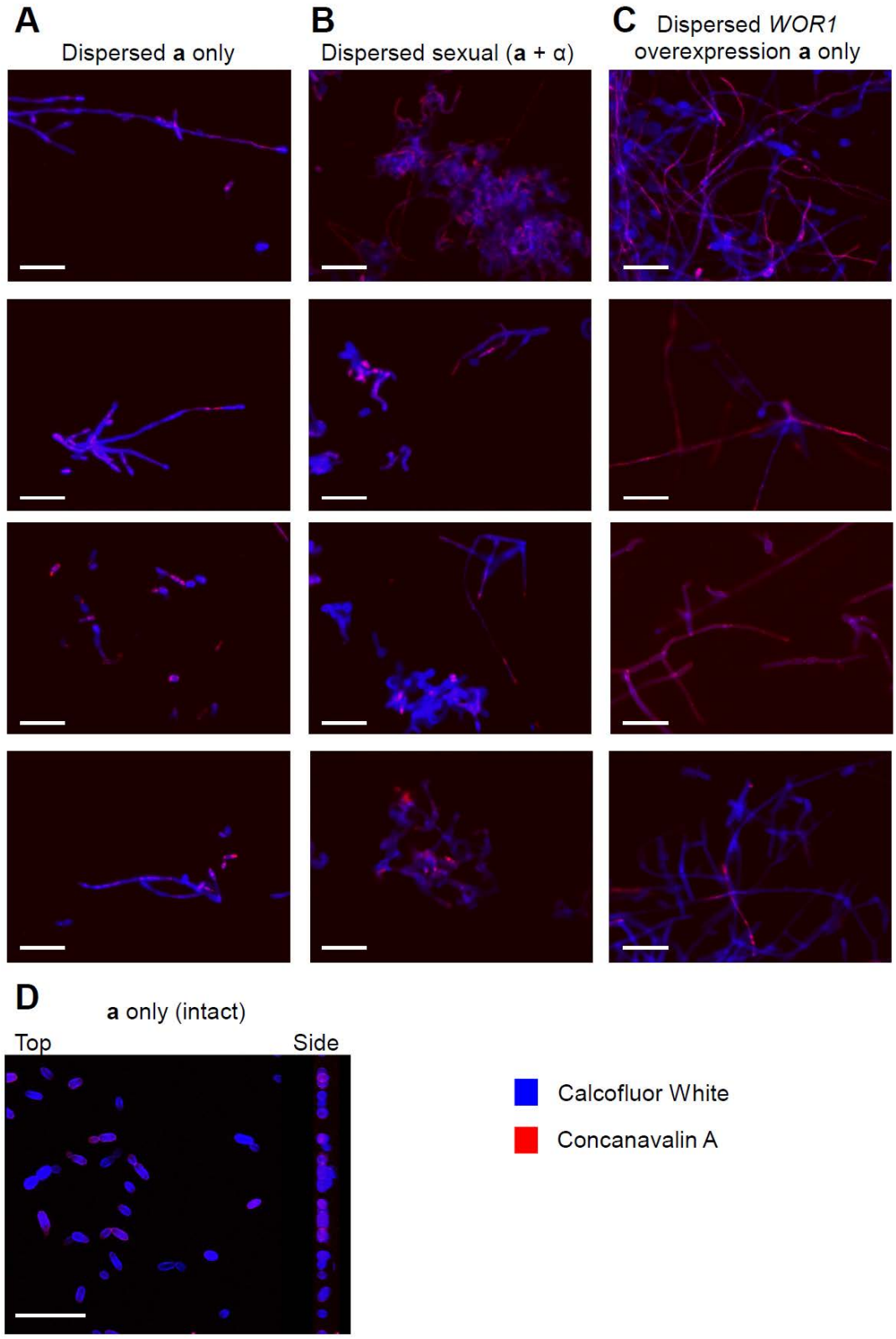

Figure S3-4: Confocal imaging of dispersed cells from C. tropicalis 48-hour biofilms.

Dispersed cells from (A) opaque a cells, (B) sexual biofilms, or (C) WOR1 overexpression biofilms. (D) Top view (left) and side view (right) projections of opaque a cells grown on the polystyrene substrate. Left, top view projected from outer biofilm surface inward. Right, side view. For D, images were taken with the same settings as Figures 4C and 4D. Scale bars = 36 µm. Blue = Calcoflour White. Red = Rhodamine-conjugated Concanavalin A.

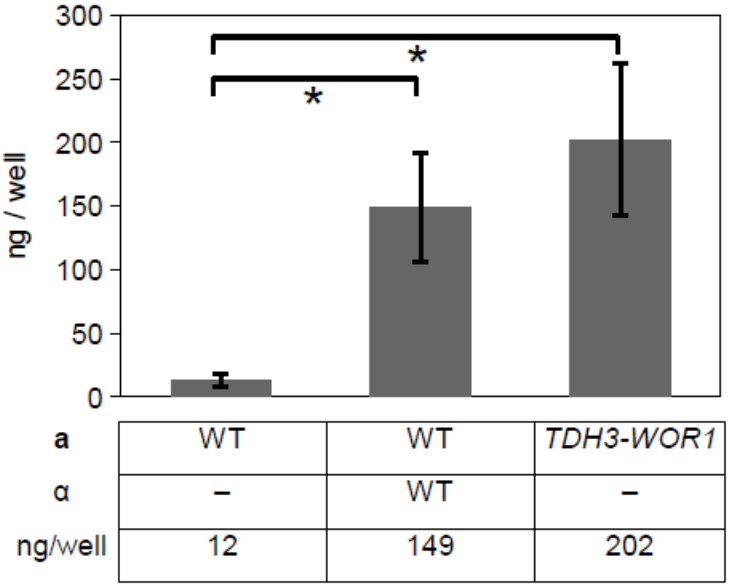

a	WT	WT	*TDH3-WOR1*
α	–	WT	–
ng/well	12	149	202

Figure S3-5: Extracellular matrix content of sexual and WOR1 overexpression biofilms.

Glucan content quantified using the Glucatell © assay. Mean ± standard deviation (N=3). * $p<0.01$. Tukey's test.

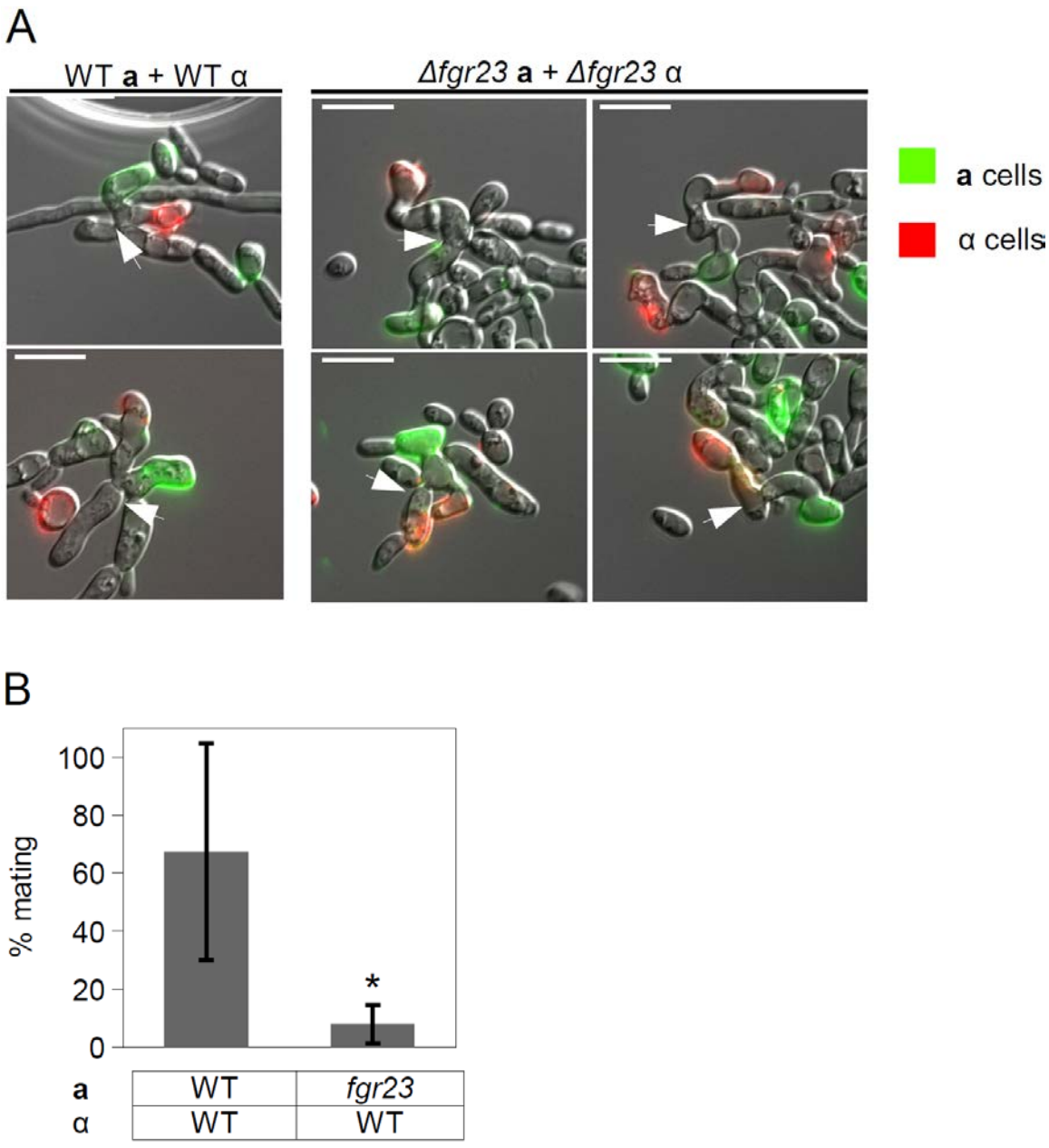

Figure S3-6: Analysis of the role of *FGR23* in mating.

(A) Zygote formation is not abolished by deletion of *FGR23*. Opaque **a** and α WT and *fgr23Δ* cells were stained and mated on Spider medium for 24 h. **a** cells stained with FITC-conjugated Concanavalin A. α cells stained with Rhodamine-conjugated Concanavalin A. Arrows indicate zygotes. Scale bar = 15 µm. (B) *FGR23* deletion significantly decreases mating frequency. **a** and α cells were mixed then mated on Spider medium for 48 h (see Experimental Procedures). Mean ± standard error (N=4). * $p<0.05$. Student's T-test (log-transform).

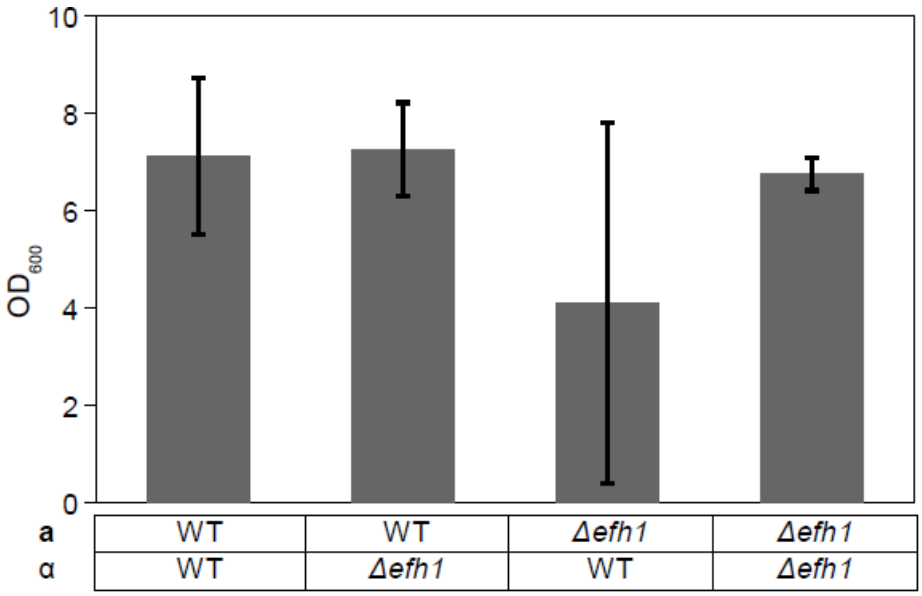

Figure S3-7: Deletion of EFH1 does not significantly affect sexual biofilm formation.

Mean ± standard deviation (N=4). One-way ANOVA.

SUPPLEMENTAL TABLES

Table 3-1: C. tropicalis strains used in this study.

Strain	**Genotype**	***Type***	***MTL***
CAY1503	*arg4/arg4::SAT1* (white)	Arginine auxotroph	**a/a**
CAY1504	*arg4/arg4::SAT1* (white)	Arginine auxotroph	**a/a**
CAY1505	*his1/his1::SAT1* (white)	Histidine auxotroph	α/α
CAY1506	*his1/his1::SAT1* (white)	Histidine auxotroph	α/α
CAY3378	*arg4/arg4::SAT1* (opaque)	Arginine auxotroph	**a/a**
CAY3386	*arg4/arg4::SAT1* (opaque)	Arginine auxotroph	**a/a**
CAY3392	*his1/his1::SAT1* (opaque)	Histidine auxotroph	α/α
CAY3398	*his1/his1::SAT1* (opaque)	Histidine auxotroph	α/α
CAY2438	*arg4/arg4 ste2/ste2* (opaque)	*ste2* deleted mutant	**a/a**
CAY2284	*arg4/arg4 ste3/ste3* (opaque)	*ste3* deleted mutant	α/α
CAY2285	*arg4/arg4 ste3/ste3* (opaque)	*ste3* deleted mutant	α/α
CAY3578	*arg4/arg4 ste3/ste3* (opaque)	*ste3* deleted mutant	α/α
CAY3853	*arg4/arg4 pTDH3/pTDH3-WOR1::SAT1* (opaque)	*WOR1* overexpressor	**a/a**
CAY3854	*arg4/arg4 pTDH3/pTDH3-WOR1::SAT1* (opaque)	*WOR1* overexpressor	**a/a**
CAY3975	*his1/his1 pTDH3/pTDH3-WOR1::SAT1* (opaque)	*WOR1* overexpressor	α/α
CAY3976	*his1/his1 pTDH3/pTDH3-WOR1::SAT1* (opaque)	*WOR1* overexpressor	α/α
CAY2206	*arg4/arg4 wor1/wor1::SAT1* (opaque)	*wor1* deleted mutant	**a/a**
CAY5435	*his1/his1 ste2/ste2 pTDH3/pTDH3-WOR1::SAT1*	*ste2* deleted *WOR1* overexpressor	**a/a**
CAY5437	*arg4/arg4 ste2/ste2 pTDH3/pTDH3-WOR1::SAT1*	*ste2* deleted *WOR1* overexpressor	**a/a**
CAY5439	*arg4/arg4 ste2/ste2 pTDH3/pTDH3-WOR1::SAT1*	*ste2* deleted *WOR1* overexpressor	**a/a**
CAY4791	*arg4/arg4 his1/his1::SAT1 fgr23::HIS1/fgr23::ARG4* (opaque)	*fgr23* deleted mutant	**a/a**
CAY4792	*his1/his1 arg4/arg4::SAT1 fgr23::HIS1/fgr23::ARG4* (opaque)	*fgr23* deleted mutant	α/α
CAY4793	*his1/his1 arg4/arg4::SAT1 fgr23::HIS1/fgr23::ARG4* (opaque)	*fgr23* deleted mutant	α/α
CAY5017	*arg4/arg4 his1/his1 fgr23::HIS1/fgr23::ARG4* (opaque)	*fgr23* deleted mutant	**a/a**
CAY5252	*arg4/arg4 his1/his1 fgr23::HIS1/fgr23::ARG4* (opaque)	*fgr23* deleted mutant	**a/a**

CAY4940	*arg4/arg4 his1/his1 fgr23::HIS1/fgr23::ARG4 pTDH3/pTDH3-FGR23::SAT1* (opaque)	*FGR23* over-expression addback	α/α
CAY4941	*arg4/arg4 his1/his1 fgr23::HIS1/fgr23::ARG4 pTDH3/pTDH3-FGR23::SAT1* (opaque)	*FGR23* over-expression addback	α/α
CAY4942	*arg4/arg4 his1/his1 fgr23::HIS1/fgr23::ARG4 pTDH3/pTDH3-FGR23::SAT1* (opaque)	*FGR23* over-expression addback	α/α
CAY5071	*arg4/arg4 his1/his1 fgr23::HIS1/fgr23::ARG4 pTDH3/pTDH3-FGR23::SAT1* (opaque)	*FGR23* over-expression addback	**a/a**
CAY5103	*arg4/arg4 his1/his1 fgr23::HIS1/fgr23::ARG4 pTDH3/pTDH3-FGR23::SAT1* (opaque)	*FGR23* over-expression addback	**a/a**
CAY5104	*arg4/arg4 his1/his1 fgr23::HIS1/fgr23::ARG4 pTDH3/pTDH3-FGR23::SAT1* (opaque)	*FGR23* over-expression addback	**a/a**
CAY3715	*arg4/arg4 his1/his1:SAT1 efh1::HIS1/efh1::ARG4* (opaque)	*efh1* deleted mutant	**a/a**
CAY3720	*arg4/arg4 his1/his1:SAT1 efh1::HIS1/efh1::ARG4* (opaque)	*efh1* deleted mutant	α/α
CAY3722	*arg4/arg4 his1/his1:SAT1 efh1::HIS1/efh1::ARG4* (opaque)	*efh1* deleted mutant	α/α
CAY3726	*arg4/arg4 his1/his1:SAT1 efh1::HIS1/efh1::ARG4* (opaque)	*efh1* deleted mutant	**a/a**

Table 3-2: Oligonucleotides used in this study.

Lowercase letters denote adapter and restriction site sequences.

Oligo	Name	Sequence
1	*WOR1* (ApaI) -900	ggagcggggcccCTACTACATTAGTTGTTCCCTG
2	*WOR1* (XhoI) 0	gccggcctcgagATAATCTAGACGCCGACATG
3	*WOR1* (SacII) +2100	ggagcgccgcggGGTAACTACAGGTGACGAATC
4	*WOR1* (SacI) +3000	ggccgcgagctcTTACCCACAAGTGTGTCTAG
5	*WOR1* 5’ check -950	GAATCTAAGGCAACAAACGATTTC
6	*WOR1* 3’ check +3100	GGTGATTAAAATCACATTCTCGG
7	*WOR1* 5’ ORF +200	GACTGATGGAATTTCTTGGTC
8	*WOR1* 3’ ORF +550	GCAGCTGTCCATAAACATGG
9	*HIS1* (ApaI) -900	ggagcggggcccACCTCAAGAGATGAATGACA
10	*HIS1* (XhoI) 0	gccggcctcgagACTCTAAACTATGATTGTATTC
11	*HIS1* (SacII) +900	ggagcgccgcggAGTTCATCTGTATAATAGTACA
12	*HIS1* (SacI) +1800	ggccgcgagctcTCCACACATTCATAAATGTTCA
13	*HIS1* 5’ check -950	CCAAGGACAACACTCGTGCAGT
14	*HIS1* 3’ check +1900	CAAATTGATCACTTCTCTAGTCGA
15	*HIS1* 5’ ORF +200	AGGGTAATTGTGATTTGGGTA
16	*HIS1* 3’ORF +600	CTTGGAAGAAACCAAGTGAG
17	*ARG4* (ApaI) -900	ggagcggggcccTGAATGTGTTGGTGGTGATG
18	*ARG4* (XhoI) 0	gccggcctcgagGACATTGTTGTTAGAATAAGTT
19	*ARG4* (NotI) +1400	ggagcggcggccgcACATTCATTCTCCTTCCCTCTC
20	*ARG4* (SacII) +2300	ggccgcccgcggGAATATTGATTGTTGATTGTTG
21	*ARG4* 5’ check -950	GACGTTGTTTACCCTTGGTATC
22	*ARG4* 3’ check +2400	TTGTGGAATGTAATTTGCACAC
23	*ARG4* 5’ ORF +200	TCAGGATTAGAAGAAATTCGTG
24	*ARG4* 3’ ORF +600	TGGACTTTGATTAACTCTGGT

25	*TDH3* (ApaI) -950	ggagcggggcccGTTAGTCGTTATGGAGGACA
26	*TDH3* 0	TGTTAAAATTTAATTTGTAAGTGATTTGATTT
27	*WOR1* 0	AAATCAAATCACTTACAAATTAAATTTTAACATCCATGTCGGCGTCTA GATTATCATC
28	*WOR1* (XhoI) +2500	gccggcctcgagGTCATATACCCAACACCGAAC
29	*STE2* (ApaI) -950	ggcgccgggcccGTCTAGAGTTGCTCTTCTCT
30	*STE2* (XhoI) 0	gccggcctcgagCACCAGAAGACTGAATAGTATTG
31	*STE2* (SacII) +1200	ggagcgccgcggCTGAAGTCACTTACAAGAAGG
32	*STE2* (SacI) +2100	ggccgcgagctcGGGAATGGCACAATTGGAGTC
33	*STE2* 5’ check -970	CGAGCATTAGTGTAACTAGTC
34	*STE2* 3’ check +2150	CAATAGGACCAACTGGGAAATG
35	*STE2* 5’ ORF +150	GCTTAGTCATGGGTGTGATG
36	*STE2* 3’ ORF +650	GACATAAGATTGACACTAACGG
37	*STE3* (ApaI) -900	ggcgccgggcccGATCTTGAAACACGAACAAGC
38	*STE3* (XhoI) 0	gccggcctcgagCCAGCAGCTGCAGCAATCAT
39	*STE3* (SacII) +1200	ggagcgccgcggCGCCTAGCGAACATTTCTCA
40	*STE3* (SacI) +2100	ggccgcgagctcgTCGAGATCAAGAATTTGGG
41	*STE3* 5’ check -970	CGTTGATGATGAAGAAGCTC
42	*STE3* 3’ check +2150	CATTTGGATATTTGTACCGGAG
43	*STE3* 5’ ORF +100	GCATGGCATATTAAGTGTGC
44	*STE3* 3’ ORF +650	CAGAAGTAAAGAGACAATGGC
45	*STE2* (XhoI) +1500	gccggcctcgagAACTGGATCTGCAACCATGG
46	*STE3* (XhoI) +1500	gccggcctcgagGCAATTGGCAGTGAAAGAAATC
47	02409 primer 3.2 +43	CACGGCGCGCCTAGCAGCGGAGTGGGGTAGTAACAAGTCT
48	02409 new primer 1 -647	GGCTTATGAAGATGGGGATG
49	02409 new 5’ check -823	GTGGATTGGTTTGTCTACTATTG
50	02409 primer 4.2 +2033	gtcagcggccgcatccctgcTGAACAACAAGTACCAACCA
51	02409 primer 6 +2923	TGCAGCAACTCACTCCACAT
52	02409 3’ check +2977	CCAGGGGGTAAAGAATGAA
53	02409 OE for 0	aatcaaatcacttacaaattaaattttaacaATGAGGGTGAACCATTCATT
54	02409 OE rev +2774	ggccggctcgagGAACTAAGCAAAACGCCTTA
55	02409 AB For Apa1 -917	ggccgcgggcccGTGGATGGTTTGTCTACTATTG
56	02409 qPCR forward	CACCAGTGAAGAAACCACCA
57	02409 qPCR reverse	AGTGGATGGACCAGCAAGAG
58	Ct EFH1 5’ fwd -550	GCTATTGACTTACCAGTTTCCT
59	Ct EFH1 5’ rev 0	cacggcgcgcctagcagcggTTATAAATCGAGCAATGTATTTC
60	Ct EFH1 3’ fwd +3000	gtcagcggccgcatccctgcACTTTGGATCTTTACTTTTTATATG
61	Ct EFH1 3’ rev +2550	GAGGTCCAGGAATTCAACATAT
62	Ct EFH1 5’ check -600	ATCTATATTCGGTTTATGAGTTCTT
63	Ct EFH1 3’ check +2600	ATGCCAATAAATGAACCAGTTAAA

For supplemental tables 4-7, please follow the links provided in the following reference:

(Jones *et al.*, 2014).

CHAPTER 4: THE RELATIONSHIP BETWEEN BIOFILM FORMATION AND CELL PHENOTYPE.

Please note: This chapter is separated into two sections, A and B.

CHAPTER 4A: THE ROLE OF THE WHITE-OPAQUE SWITCH IN *C. ALBICANS* SEXUAL BIOFILMS

ABSTRACT

Candida albicans is both a commensal and pathogenic fungus that switches between phenotypic states to alter its interaction with the human host. The yeast-hyphae and white-opaque switches are two of the most well studied state transitions in this species and contribute to its ability to form biofilms. In *C. albicans*, cells in the opaque state typically respond to sex pheromones by inducing the mating program, while white cells alternatively form sexual biofilms. Here, we examine the prevalence of sexual biofilm formation across clinically isolated *C. albicans* strains in both the white and opaque states when induced by three different pheromone sources: either exogenous α pheromone, **a** and α opaque cells, or a mating partner in the same phenotypic state. We show that α pheromone induces robust biofilms in white cell populations, but not in opaque cell populations. Unlike previous publications, we find that **a** and α opaque cells do not consistently induce biofilm formation in white cells. Co-culture of cells with a reciprocal mating partner yield biofilms in a strain-dependent manner, suggesting that compatibility factors influence the ability of *C.albicans* to undergo biofilm formation. Using phenotype-locked strains, a near equal mixture of white and opaque cells undergo maximal biofilm formation, proposing a more substantial role for opaque cells in sexual biofilms.

INTRODUCTION

Candida albicans is the most prominent fungal pathogen in humans. While a prevalent opportunistic pathogen, *C. albicans* is also a common component of the gastrointestinal microbiota in approximately 70% of healthy individuals (Ruhnke and Maschmeyer, 2002). Additional sites of colonization and infection include the skin, mouth, and urogenital tract. To be able to grow and infect such a wide array of host niches, *C. albicans* can undergo several phenotypic transitions, including the yeast-to-hyphal switch and the white-to-opaque switch. The former is crucial to the virulence of the species, where studies show that blocking this transition prevents *C. albicans* from mounting a successful infection (Sudbery, 2011). Furthermore, both yeast and hyphal cells contribute important roles to fungal community structures, such as biofilms.

The white-to-opaque switch regulates multiple important aspects of *C. albicans* biology. The default state of *C. albicans* is the white form where cells are round and smooth, and yield bright, glossy colonies on solid media. Alternatively, opaque cells are rod-shaped with a variable surface texture, and yield darker, flatter colonies (Slutsky *et al.*, 1987). White and opaque cells preferentially inhabit different host niches; for example, white cells are more adept at systemic infection (Kvaal *et al.*, 1997), whereas opaque cells are better at colonization of the skin (Kvaal *et al.*, 1999). Environmental cues influence switching between states, with N-acetyl glucosamine, carbon dioxide, anaerobiasis, and elevated temperatures representing established signals that can induce switching between states *en masse* (Anderson and Soll, 1987; Dumitru *et al.*, 2007; Huang *et al.*, 2009; Huang *et al.*, 2010). There are also marked differences between white and opaque cells regarding their metabolic profiles, their ability to filament, and their responses to immune cells (Lan *et al.*, 2002; Lohse and Johnson, 2008; Sudbery, 2011; Sasse *et al.*, 2013; Si *et al.*, 2013).

One of the most significant differences between white and opaque cells is their differential response to sexual pheromones. In particular, opaque cells secrete mating-type specific pheromones and respond to them by forming mating projections and ultimately undergoing conjugation (Miller and Johnson, 2002; Bennett and Johnson, 2005). Alternatively, white cells do not secrete high levels of pheromones and undergo mating a million times less frequently than opaque cells (Miller and Johnson, 2002). Interestingly, however, white cells are able to respond to pheromone, becoming more adherent and forming sexual biofilms in the presence of pheromones. Biofilms formed by white cells have been shown to facilitate mating events between opaque cells by forming a structure that maintains pheromone gradients (Daniels *et al.*, 2006). In this model, opaque cells generate the pheromone necessary to induce biofilm formation in white cells, although adhesion and overall biofilm formation is specific to cells in the white state. Further experimentation has indicated that white cells in a biofilm can also augment pheromone levels by producing it themselves (Yi, Sahni, Daniels, Lu, Huang, Srikantha, *et al.*, 2011; Tao *et al.*, 2014).

Mating in *Candida* species, as in many ascomycetes, is regulated by conserved transcription factors encoded at the mating-type-like (*MTL*) locus. Conventional mating occurs between *MTL***a** and *MTL*α cells, and is driven by sex-specific pheromones secreted by these cell types. *MTL***a** cells secrete **a** pheromone and *MTLα* cells secrete α pheromone; each activates pheromone MAPK signaling in cells of the opposite mating type (Soll, 2014). In *C. albicans*, the same MAPK pathway regulates the pheromone response in both white and opaque cells, indicating that other cell-type specific components must be responsible for the differing responses of the two cell types (Yi *et al.*, 2008). It is also apparent that *C. albicans MTL***a** opaque cells secrete low levels of α pheromone in addition to the canonical **a** pheromone; normally this α pheromone is degraded by the Bar1 protease, but in the absence of Bar1 the accumulation of

α pheromone induces mating projections in **a** cells and even same-sex (**a**-**a)** mating (Alby *et al.*, 2009). The *MTL* locus also regulates the ability of cells to undergo white-opaque switching. *MTL***a**/*MTLα* cells, such as the direct progeny of heterothallic mating, are unable to switch to the opaque state because **a**1 (an *MTL**a*** product) and α2 (an *MTLα* product) form a heterodimeric transcription factor that inhibits transcription of *WOR1*, which encodes the master regulator of the opaque state (Miller and Johnson, 2002).

More recently, it has been shown that *Candida tropicalis*, a close relative of *C. albicans*, also undergoes sexual mating, and that mating is similarly regulated by a white-opaque switch (Porman *et al.*, 2011; Xie *et al.*, 2012). Thus, *C. tropicalis* opaque cells were the most efficient at mating, whereas white cells mated very inefficiently. However, in marked contrast to *C. albicans*, it was found that *C. tropicalis* opaque cells were induced to form pheromone-induced biofilms, whereas *C. tropicalis* white cells were not (Porman *et al.*, 2011; Jones *et al.*, 2014). This suggests that the regulation of sexual biofilm formation may have diverged since *C. albicans* and *C. tropicalis* last shared a common ancestor.

In this work, we examine in more detail the ability of *C. albicans* to form sexual biofilms, with an expanded analysis of multiple clinical isolates from both white and opaque states, and by induction through three different methods. We establish that, in general, α pheromone is potent inducer of biofilm formation in *C. albicans* white cells, but not in opaque cells, and that biofilm formation is greater in white **a** cells than in α cells when challenged with pheromones produced by a mixture of opaque **a** and α cells. We also show that both white and opaque cells are capable of sexual biofilm formation in co-culture, but that strain-dependent factors contribute to significant differences in this response.

MATERIALS AND METHODS

Media and Strain Construction

Media was prepared according to previously described methods (Lee *et al.*, 1975; Guthrie and Fink, 1991). Spider media contained 1% nutrient broth, 0.4% potassium phosphate, and 2% mannitol (pH 7.2). Solid media were made with 1.35% agar. Deletion strains of *WOR1* and *MTLα,* and *WOR1* overexpression strains were constructed as previously described (Alby and Bennett, 2009; Alby *et al.*, 2010). Confirmation of all engineered strains was completed by PCR using oligonucleotides in Table 1.

Table 4-1: Oligonucleotides used in this study.

Oligonucleotide Name	Sequence	Purpose
pSFS2a left	CTCAACCATAGCAATCATGG	Check for single deletions
pSFS2a right	GCGAAAAAGTGGGCACTAAG	Check for single deletions
WOR1 5' check	CATCGAAGTCAACTTTTTCGGCG	Check for single wor1 deletion
WOR1 3' check	CTTAAACTAGCCAATTCGTTCAG	Check for single wor1 deletion
WOR1 5' ORF	GACTACAGAACGAGTCTAGG	Check for complete wor1 deletion
WOR1 3' ORF	GCCATAACCTCCATTGGATATTG	Check for complete wor1 deletion
*MTL*α 5' check	GACAGAATTACAATGTCTTACAGTC	Check for single mtlα deletion
*MTL*α 3' check	CATGTTGGTGAACCTAAAGTAC	Check for single mtlα deletion
PAPα ORF-5'	CTGGCATTCGATGAAGTCTA	Used to determine mating type and check for full mtlα deletion.
PAPα ORF-3'	CATGTCCGATTCAATGGCCC	Used to determine mating type and check for full mtlα deletion.
PAPα (410)	CGGGTAAAATATGGTCGC	Used to determine mating type.
PAPα (1650)	TACTTTCCACCATCCCACT	Used to determine mating type.

Table 4-2: Plasmids used in this study.

Plasmid number	Name	Purpose
RB98	pSFS2a *wor1* KO	Delete *WOR1* in *C. albicans* to lock cells in white state.
RB99	pSFS2a *pACT1-WOR1*	Overexpress *WOR1* in *C. albicans* to lock cells in opaque state.
RB102	pSFS2a *mtlα* KO	Delete *MTLα* in *C. albicans* to make them a mating-type.

Table 4-3**: Strains used in this study.**

Strain number	Name	Mating type	Genotype	Description
RBY1173	SC5314	a/a	*leu2/leu2*	SN87 derivative. Sorbose selected for MTLloss.
RBY1174	SC5314	α/α	*leu2/leu2*	SN87 derivative. Sorbose selected for MTLloss.
RBY1176	SC5314	α/α	*arg4/arg4*	SN87 derivative. Sorbose selected for MTLloss.
RBY1177	SC5314	a/a	*leu2/leu2*	RBY1173 switched to opaque.
RBY1178	SC5314	α/α	*leu2/leu2*	RBY1177 switched to opaque.
RBY1180	SC5314	α/α	*arg4/arg4*	RBY1177 switched to opaque.
CAY700	P76067	a/α		Clinical Isolate
CAY701	P37037	a/α		Clinical Isolate
CAY702	P57055	a/α		Clinical Isolate
CAY703	19F	α/α		Clinical Isolate
CAY704	P60002	a/a		Clinical Isolate
CAY705	P78042	a/α		Clinical Isolate
CAY706	P75016	a/α		Clinical Isolate
CAY707	P37039	a/α		Clinical Isolate
CAY708	P75010	a/α		Clinical Isolate
CAY709	GC75	α/α		Clinical Isolate
CAY710	P94015	a/a		Clinical Isolate
CAY711	P75063	a/α		Clinical Isolate
CAY712	P76055	a/α		Clinical Isolate
CAY713	12C	a/a		Clinical Isolate
CAY714	P57072	α/α		Clinical Isolate
CAY715	L26	a/a		Clinical Isolate
CAY716	P37005	a/a		Clinical Isolate
CAY717	P87	a/a		Clinical Isolate
CAY718	P78048	α/α		Clinical Isolate
CAY4921	P75063 a/-	a/-	*MTLa/mtlα:SAT1*	Clinical strain transformed with RB102 to delete MTLα.
CAY4925	P37039 a/-	a/-	*MTLa/mtlα:SAT1*	Clinical strain transformed with RB102 to delete MTLα.
CAY4921	P75063 a/-	a/-	*MTLa/mtlα:SAT1*	Clinical strain transformed with RB102 to delete MTLα.
CAY4925	P37039 a/-	a/-	*MTLa/mtlα:SAT1*	Clinical strain transformed with RB102 to delete MTLα.
CAY5245	P37037 a/-	a/-	*MTLa/mtlα:SAT1*	Clinical strain transformed with RB102 to delete MTLα.
CAY5410	P78042 *MTLa*	a/a		Subcultured from CAY705
CAY2763	L26 opaque	a/a		Clinical isolate switched to opaque using N-Acetylglucosamine.
CAY6138	GC75 opaque	α/α		Clinical isolate switched to opaque using N-Acetylglucosamine.
CAY2765	P57072 opaque	α/α		Clinical isolate switched to opaque using N-Acetylglucosamine.
CAY2766	P37005 opaque	a/a		Clinical isolate switched to opaque using N-Acetylglucosamine.
CAY2767	12C opaque	a/a		Clinical isolate switched to opaque using N-Acetylglucosamine.
CAY2768	19F opaque	α/α		Clinical isolate switched to opaque using N-Acetylglucosamine.
CAY5253	P94015 opaque	a/a		Isolated from colony sector.
MMY284	WO-1 opaque	α/α		Clinical isolate
CAY4156	SC5314 a *wor1* KO	a/a	*wor1/wor1::SAT1 arg4/arg4 leu2/leu2 his1/his1*	SN87 derivative. Sorbose selected for *MTL* loss. Transformed twice with RB98 to delete *WOR1*.
CAY2022	SC5314 α *wor1* KO	α/α	*wor1/wor1 arg4/arg4*	SN87 derivative. Sorbose selected for *MTL* loss. Transformed twice with RB98 to delete *WOR1*.
CAY2903	SC5314 a *WOR1* overexpressor	a/a	*pACT1-WOR1:SAT1*	Transformed with RB99 to overexpress *WOR1* at *ACT1* promoter.
CAY2904	SC5314 a *WOR1* overexpressor	a/a	*pACT1-WOR1:SAT1*	Transformed with RB99 to overexpress *WOR1* at *ACT1* promoter.
DSY1040	SC5314 α *WOR1* overexpressor	α/α	*pACT1-WOR1:SAT1 arg4/arg4*	Transformed with RB99 to overexpress *WOR1* at *ACT1* promoter.
DSY1041	SC5314 α *WOR1* overexpressor	α/α	*pACT1-WOR1:SAT1 arg4/arg4*	Transformed with RB99 to overexpress *WOR1* at *ACT1* promoter.
DSY4820	SC5314 α *WOR1* overexpressor	α/α	*pACT1-WOR1:SAT1 leu2/leu2*	Transformed with RB99 to overexpress *WOR1* at *ACT1* promoter.
CAY1237	P37005 *wor1* KO	a/a	*wor1/wor1*	Transformed twice with RB98 to delete *WOR1*.
CAY1247	P37005 *wor1* KO	a/a	*wor1/wor1::SAT1*	Transformed twice with RB98 to delete *WOR1*.
CAY1352	P37005 *WOR1* overexpressor	a/a	*pACT1-WOR1:SAT1*	Transformed with RB99 to overexpress *WOR1* at *ACT1* promoter.
CAY1353	P37005 *WOR1* overexpressor	a/a	*pACT1-WOR1:SAT1*	Transformed with RB99 to overexpress *WOR1* at *ACT1* promoter.

Biofilm Adherence

Liquid cultures were prepared in Spider media, and incubated overnight at room temperature on a rotating drum. Cultures were washed with water, and then the optical density (OD) of each was determined. Into each well of a 12-well plate containing 1 ml of Lee's media, $4*10^7$ cells (2 ODs) were added. When indicated, 10 μg/ml of pheromone or $4*10^6$ SC5314**a**/SC5314α opaque cells (0.2 ODs) were also added to the well. Plates were incubated at room temperature for 1-2 days, and then washed with water three times to remove non-adherent cells. The plates were imaged using the Bio-Rad Chemidoc XRS, and then adherent cells from each well were scraped and resuspended in 1 ml of water. The OD of these cells was measured using a Nanodrop 2000c (Thermo Scientific).

Microscopy

Imaging of individual cells was performed on a Zeiss Axio Observer Z1 using differential interference contrast microscopy. Adherent cells from biofilms were obtained after resuspension in water following washing. Ten μl of cell suspension were placed on a glass slide for examination.

Statistical analysis

Statistics were performed using Past v3.04 (Hammer *et al.*, 2001). When possible, Tukey boxplots were used to provide a comprehensive summary of the data, with outliers represented as points. The Jarque-Bera method was employed for all normality tests. For comparison of two normally-distributed data sets, a T-test was used; otherwise, a Mann-Whitney test was used. For normally-distributed data sets greater than two, ANOVA was performed with post-hoc Tukey

pairwise comparisons; otherwise, a Kolmogrov-Smirnov test was followed by Mann-Whitney tests.

RESULTS

Biofilm formation in *C. albicans* white cells

Many traits of *C. albicans*, including virulence, have proven to vary greatly across different clinical isolates (Wu *et al.*, 2007). Accordingly, we wanted to determine whether the biofilm response to pheromone exposure is generally applicable to all *C. albicans* white *MTL*-homozygous strains, or if the strength of the response varies between different isolates. *C. albicans* strains sort into several clades that have been isolated from a variety of host niches and geographical locations (Soll and Pujol, 2003). Some virulence traits appear to be clade specific (Pujol, Pfaller, *et al.*, 2004), so it was prudent to test biofilm formation across clade boundaries. For a subset of clinical **a**/α strains, these strains were converted to the **a** mating type by gene deletion of the *MTLα* locus. Initially, ten strains were tested for sexual biofilm formation upon exposure to 10 μg/ml α pheromone according to previously described methods (Daniels *et al.*, 2006) (Fig. 1). Unless otherwise stated, assays were performed in Lee's + Glucose medium at 25 °C for 48 h. Nine of the strains showed strong biofilm formation in the presence of pheromone, similarly to previously published results (Sahni *et al.*, 2009). The exception was the clade III isolate P78042. While P78042 clearly responded to pheromone exposure, the resulting biofilm was extremely brittle and easily disrupted by washing. This does not appear to be a general trait of clade III strains as other strains from this clade successfully produced adherent sexual biofilms (Sahni *et al.*, 2009). These results indicate that sexual biofilm formation is a common response in *C. albicans* white **a** cells responding to exogenous α pheromone.

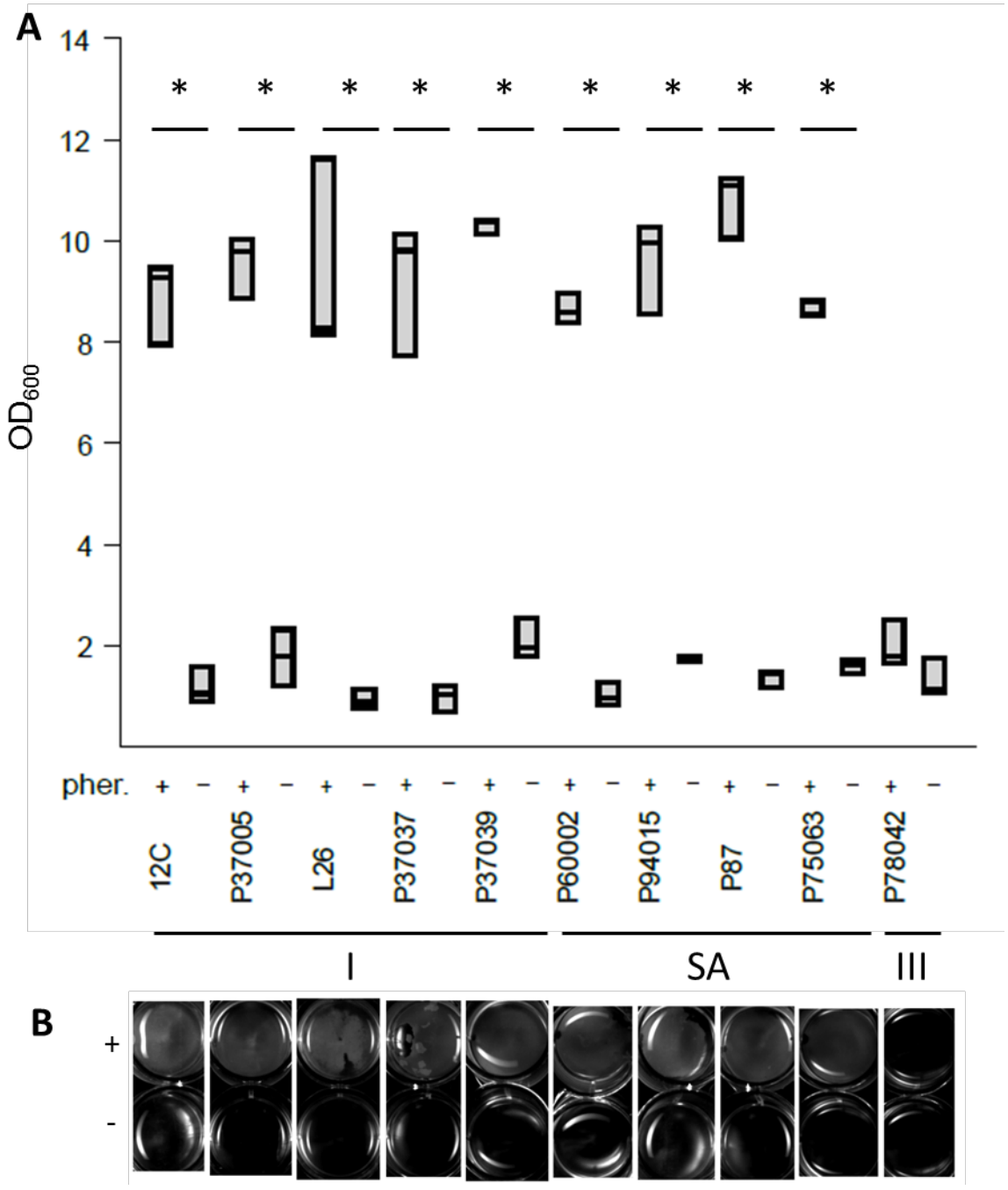

Figure 4-1: **White cell adhesion across three *C. albicans* clades in response to α pheromone exposure.**

(A) *MTL**a*** cells were exposed to 10 µg/ml α pheromone in a biofilm adherence assay. Tukey boxplot. * = $p<0.05$ by T-test. N=3.

(B) Images of wells containing biofilms as indicated above. +/ – denote pheromone presence.

Recent studies of sexual biofilm formation in *C. tropicalis* revealed that direct cell-to-cell contact was important for a robust biofilm development (Jones *et al.*, 2014). To assess if cell-cell contact enhances biofilm formation in *C. albicans*, and if natural pheromone levels produced by opaque cells can induce efficient biofilm formation similar to that of exogenous pheromone, we performed two sets of co-culture experiments. First, a collection of clinically-isolated white **a** and α cells were mixed with a minority (10% of total cells) of opaque **a** and α cells (50:50 mix) (Fig. 2). The biofilm response among responding white **a** strains was generally more variable than when exogenous α pheromone was used (Figs. 1 and 2). For example, whereas P37005**a** produced biofilms in response to opaque cells that ranged in optical density from ~2 to ~10 (Fig. 2), the same cells produced biofilms with an optical density of ~9 to ~10 in response to exogenous α pheromone (Fig. 1). In contrast, α strains were inconsistent with **a** strains – despite the pheromone produced by the opaque cells, α strains did not form biofilms as consistently (Fig 2).

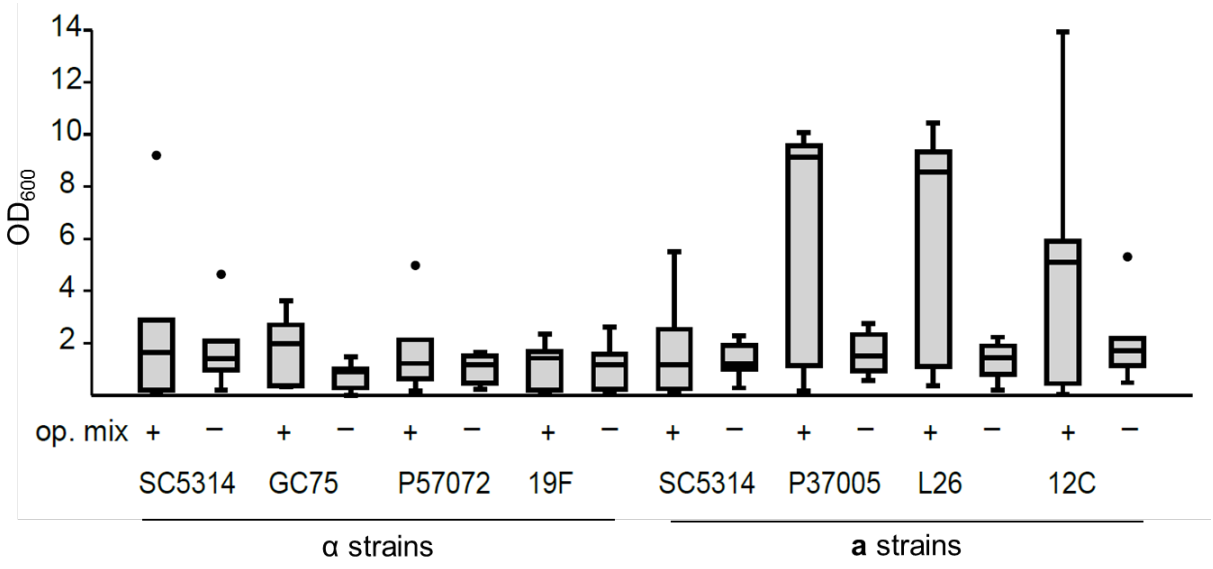

Figure 4-2: **White cell adhesion upon exposure to opaque cells.**

The indicated white strains were incubated with opaque **a** and α cells comprising 10% of the population in a biofilm adherence assay. Tukey boxplot. ● = outliers. N=6.

In a second set of co-culture experiments, white **a** strains were co-cultured with white α strains (in the absence of exogenous pheromone or pheromone-secreting opaque cells). Although it was originally thought that white cells cannot secrete pheromone, white cells have been shown to produce pheromone within the context of a biofilm (Yi, Sahni, Daniels, Lu, Huang, Srikantha, *et al.*, 2011). We therefore posited that reciprocal signaling between certain white **a** and α strains might be sufficient for biofilm formation. For the majority of paired strains, biofilms were not observed using exclusively white cells (Figure 3A). However, the P37005**a** x SC5314α pairing produced significant biofilms. Microscopic analysis found no evidence for opaque cells being present within the biofilm (Fig. 3B). This argued that successful pheromone signaling could occur in white communities, or that some other compatibility trait between mixed white strain populations contributes to biofilm formation.

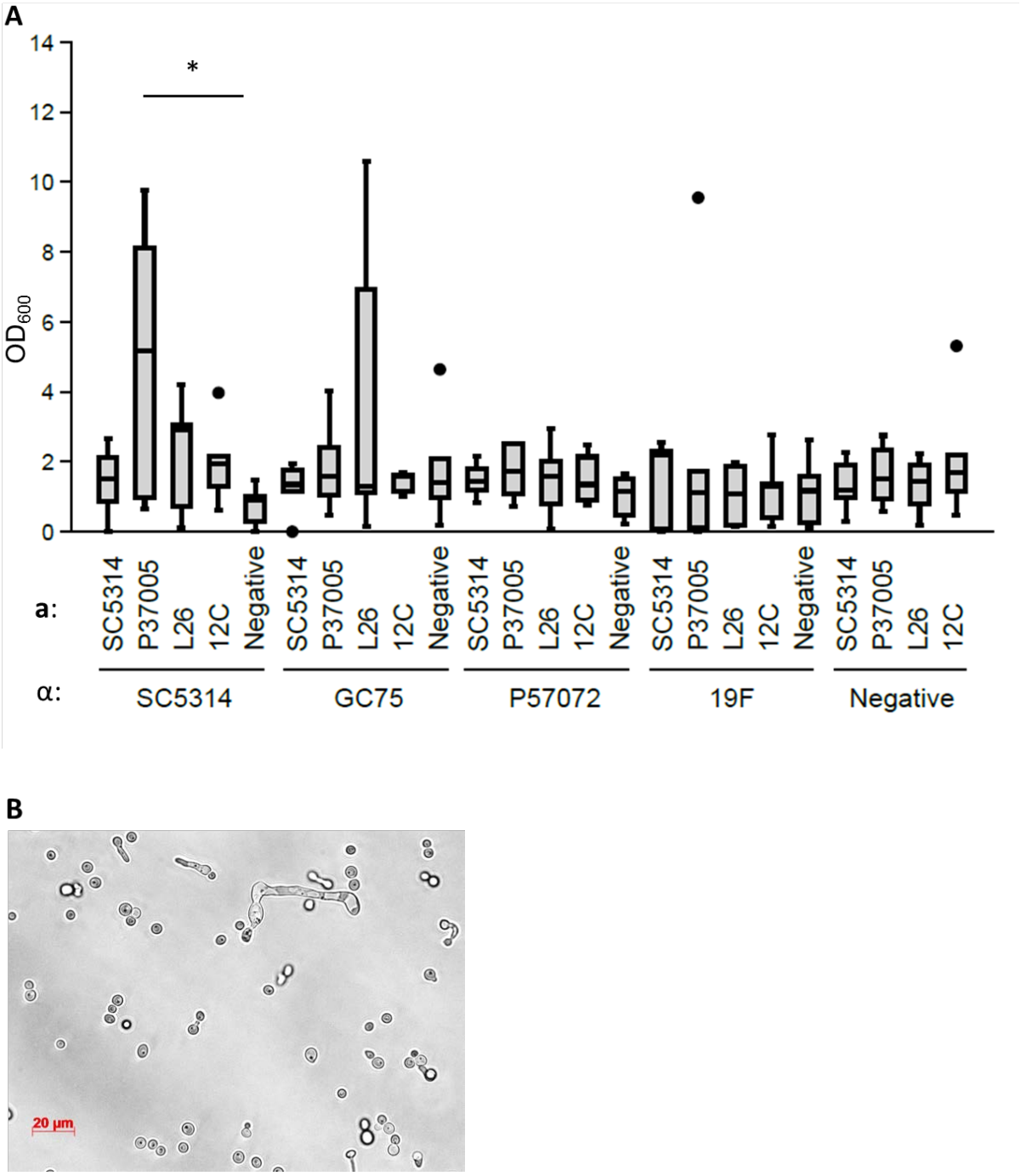

Figure 4-3: **White cell adhesion upon co-culture of a strains with α strains.**

(A) The indicated white strains were mixed with one another in a biofilm adherence assay. Tukey boxplot. ● = outliers. * = $p<0.05$ by Tukey pairwise comparison. N≥6.

(B) 40X DIC image of cells from the P37005**a** x SC5314α pairing in a biofilm adherence assay.

Biofilm formation in *C. albicans* opaque cells

We next tested whether opaque cells could form biofilms in the absence of white cells. To test this, the collection of clinical strains was first switched to the opaque state via growth on N-acetyl glucosamine-containing medium (Huang *et al.*, 2010). Opaque **a** strains were challenged by exposure to 10 μg/ml α pheromone, and then biofilm formation was evaluated. Of the six strains analyzed, only P37005**a** opaque cells formed a substantial biofilm, although P94015**a** cells also showed weak response (Figure 4A). A previous study indicated that P37005**a** opaque cells do not form biofilms (Daniels *et al.*, 2006), and it was therefore possible that cells switching from opaque to white could be responsible for the observed phenotype in our assays. Indeed, microscopy indicated that, at least in some replicates, white cells were present by the end of the assay. (Figure 4B).

To test whether opaque-to-white switching contributed to the biofilms produced by 'opaque' P37005**a** cells, we generated *WOR1* deletion and overexpression mutants in P37005**a**, locking cells into either the white state (*Δwor1/Δwor1*) or opaque state (*pACT1-WOR1*). Interestingly, in contrast to natural P37005**a** opaque cells, locked opaque cells were unable to form biofilms upon incubation with α pheromone (Fig. 5). Alternatively, the P37005**a** cells that were deleted for *wor1,* and thus locked in the white state, showed no biofilm defect (Fig .5).

We also performed co-incubation biofilm experiments with opaque cells, where the majority of cells in the population were a single opaque strain, to which a minority (10%) of **a** and α (50:50 mix) opaque cells were added to act as a source of pheromones. Here, opaque strains only occasionally formed detectable biofilms (Fig. 5). This contrasts with white cells, where white **a** strains (but not α strains) produced biofilms in the analogous co-incubation experiments (Fig. 2). Similarly, when the state-locked P37005**a** strains were co-incubated with

the **a** and α opaque cell mix, the white *wor1* strain formed a biofilm while the *WOR1* overexpression strain did not.

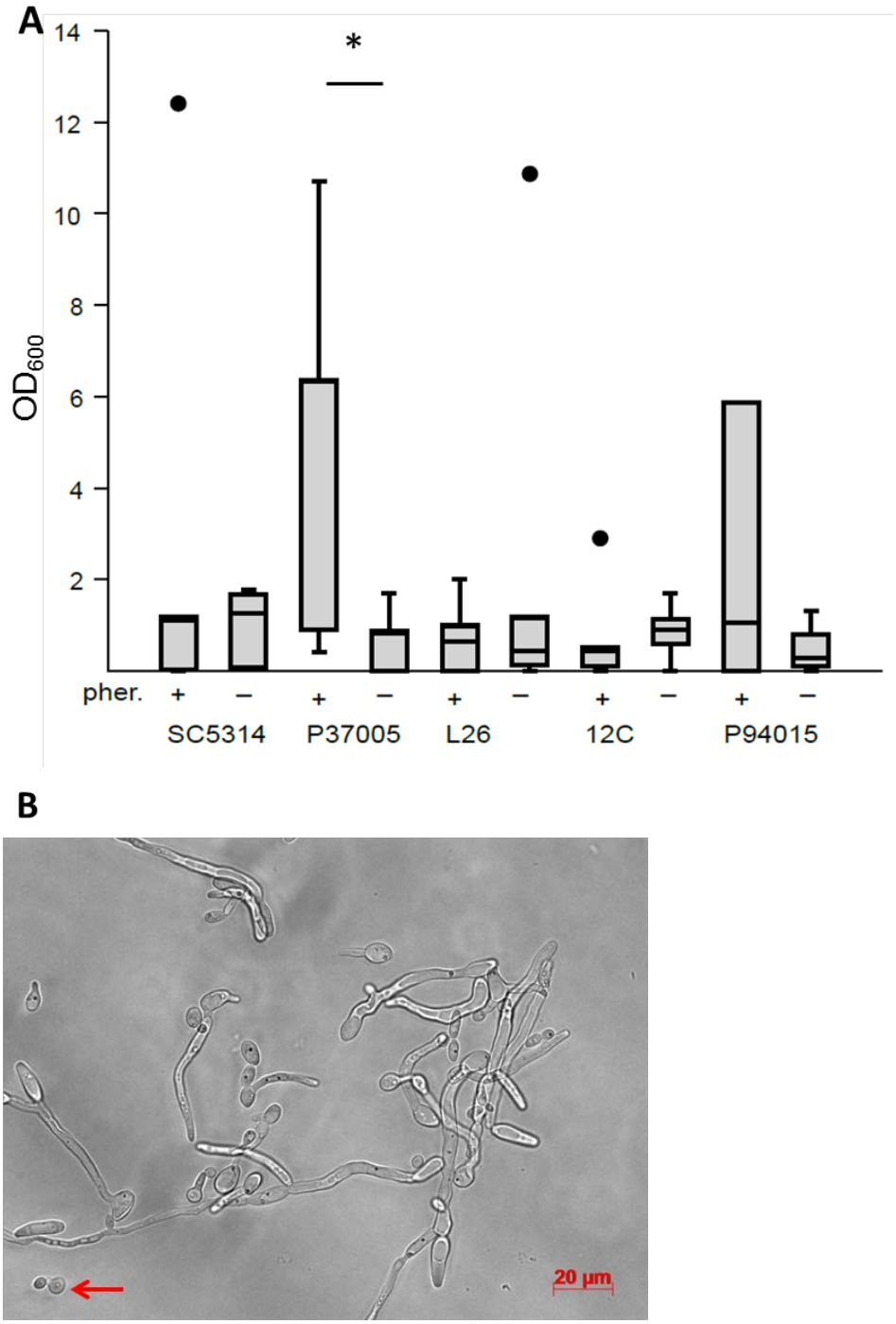

Figure 4-4: Opaque cell adhesion in response to α pheromone exposure

(A) Cells were exposed to 10 µg/ml α pheromone in a biofilm adherence assay. Tukey boxplot. ● = outliers. * = $p<0.05$ by T-test. $N \geq 4$.

(B) 40X DIC image of cells from P37005**a** exposed to 10 µg/ml α pheromone in a biofilm adherence assay. Arrow identifies a pair of white cells.

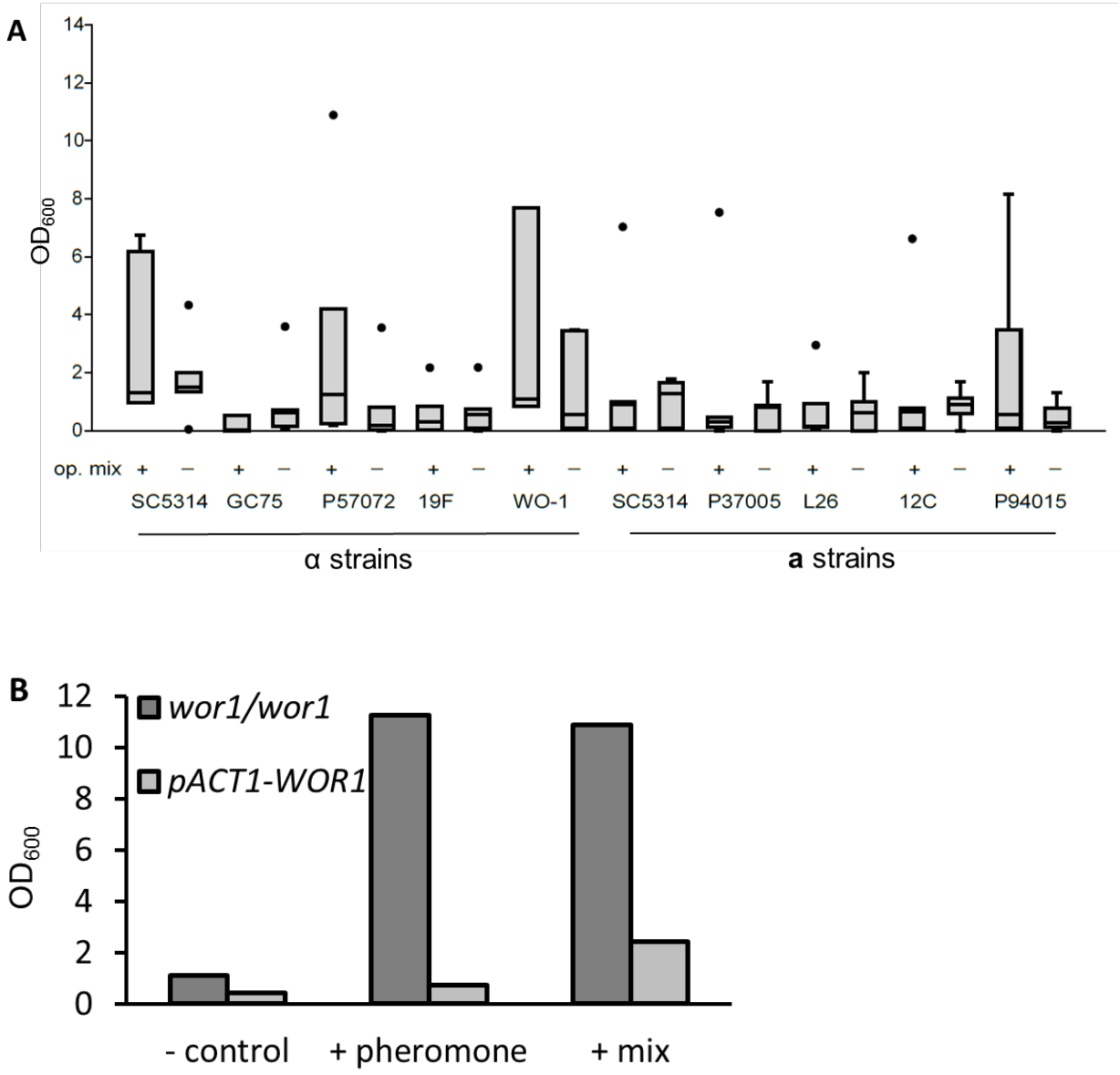

Figure 4-5: **Cell** adhesion upon exposure to opaque cells **or pheromone**.

(A) The indicated opaque strain was incubated with opaque a and α cells comprising 10% of the population in a biofilm adherence assay. Tukey boxplot. ● = outliers. N≥4.

(B) White-locked (*wor1/wor1*) and opaque-locked (*pACT1-WOR1*) P37005**a** strains were exposed to 10 µg/ml α pheromone or incubated with opaque a and α cells comprising 10% of the population in a biofilm adherence assay.

As stated earlier, it is also possible that cell-cell interactions between responding **a** and α partners contribute to overall biofilm success. Accordingly, we performed a series of co-incubation experiments pairing equal amounts of clinical opaque **a** with α strains. Unlike equivalent experiments with white cells (Fig. 3A), several combinations of opaque **a** and α strains yielded significant biofilms (Figure 7). Nearly all successful combinations included either the SC5314**a** or SC5314α strain. In fact, maximum biofilm formation was observed in experiments containing mixtures of these two strains. Several other combinations of opaque strains (including those that did not involve SC5314) also formed substantial biofilms, indicating that this was a common occurrence under the tested conditions. Finally, when the ratio of SC5314**a** to SC5314α cells was varied in the same co-culture experiment, as long as each mating type made up at least 10% of the population, a robust biofilm was formed (Fig. 7B).

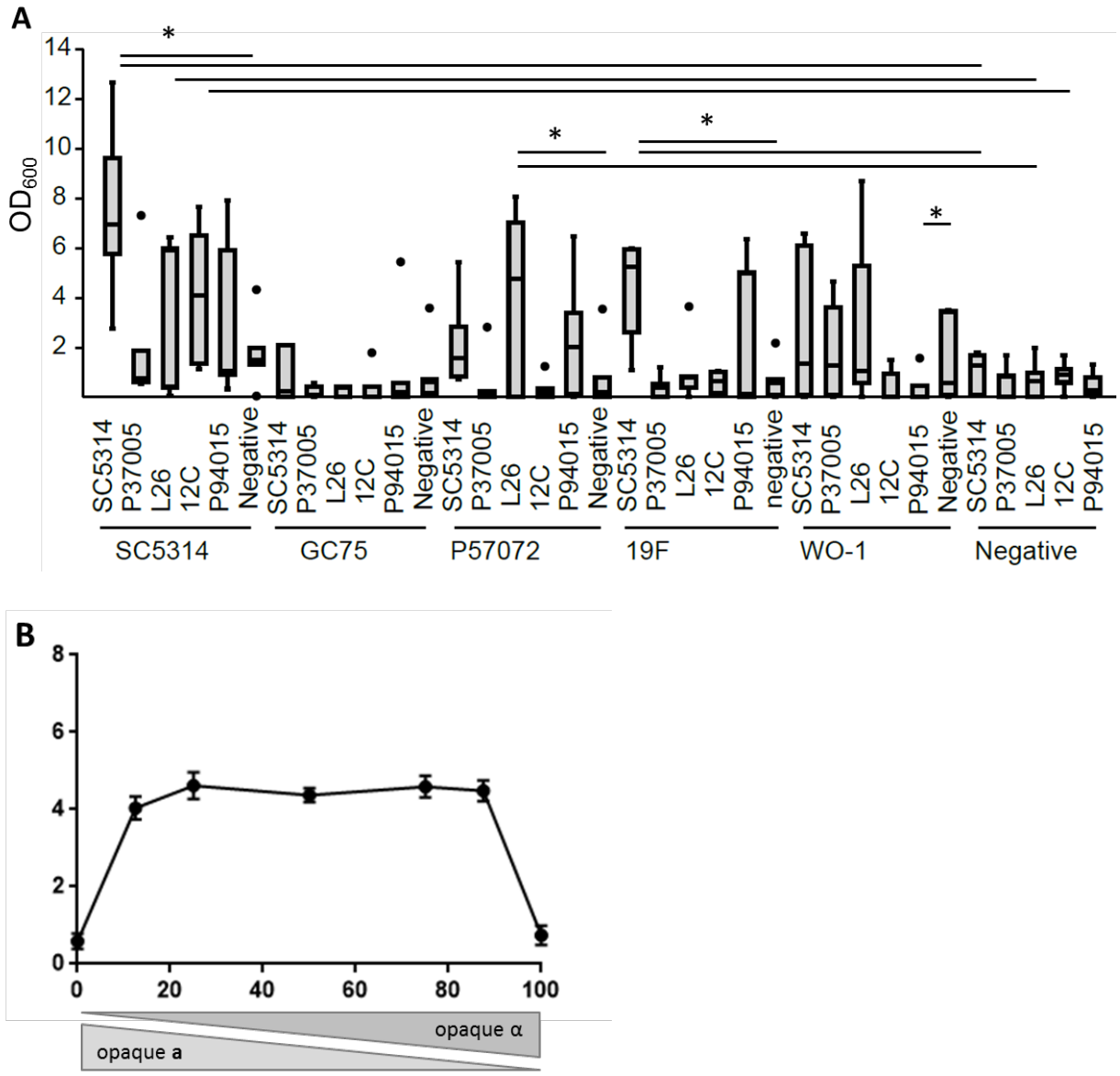

Figure 4-6: Opaque cell adhesion upon co-culture of a strains with α strains.

(A) The indicated opaque strains were mixed equally with one another in a biofilm adherence assay. * = $p<0.05$ by Tukey's pairwise comparison. Tukey boxplot. ● = outliers. N≥4.

(B) Opaque SC5314**a** and SC5314α cells were mixed together at the indicated ratio in a biofilm adherence assay. Mean ± SD. N≥3.

Cooperative white and opaque cell biofilm formation

To determine if switching contributed to biofilms formed in the co-culture experiments, additional state-locked strains were constructed in SC5314α and SC5314**a** strains. The state-locked *WOR1* deletion and overexpression mutants in P37005**a** and SC5314α were then used together to determine the proportion of white to opaque cells (1:1 **a**:α) that allowed the maximum amount of biofilm to form. In this white to opaque 'titration', a 40% mixture of white to opaque cells (2:2:3:3, *wor1* P37005**a** : *wor1* SC5314α : *pACT1-WOR1* P37005**a** : *pACT1-WOR1* SC5314α) produced the greatest amount of adherent biofilm, which was significantly more than biofilms produced by all white or all opaque cultures. This titration was then repeated using SC314**a** and SC5314α locked strains, and was directly compared to unlocked, wildtype strains. The locked strain pairing (SC5314**a** x SC5314α) showed a slightly higher peak ratio (60%) of white to opaque cells, and the unlocked pairing's ratio was even higher (80%). Comparing these two numbers suggests that unlocked opaque cells switch to white state during the course of the biofilm assay.

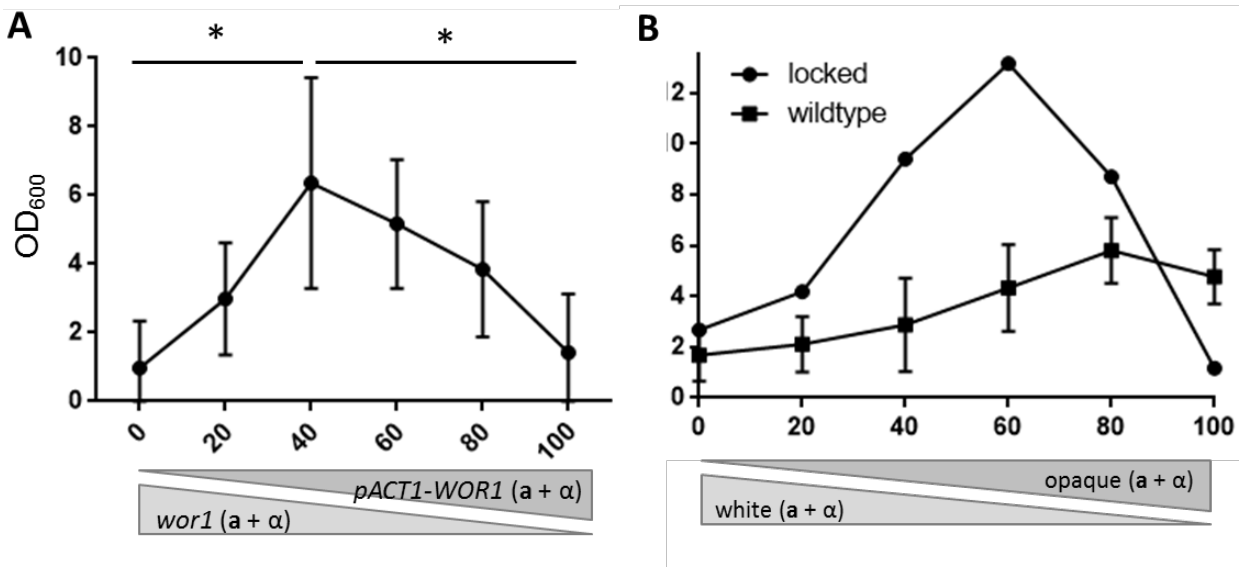

Figure 4-7: **Titration of white and opaque cells** from natural and locked strains **in a biofilm assay.**

(A) White-locked cells (*wor1/wor1* P37005**a** and *wor1/wor1* SC5314α) were titrated with opaque-locked cells (*pACT1-WOR1* P37005**a** and *pACT1-WOR1* SC5314α) at the indicated ratios in a biofilm adherence assay. * = $p<0.05$ by Tukey's pairwise comparison. Mean ± SD. N≥3.

(B) Overlay of two biofilm adherence assays:

- White-locked cells (*wor1/wor1* SC5314**a** and *wor1/wor1* SC5314α) titrated with opaque-locked cells (*pACT1-WOR1* SC5314**a** and *pACT1-WOR1* SC5314α) at the indicated ratios. N=2.
- Wildtype white cells titrated with opaque cells (SC5314**a** and SC5314α) at the indicated ratios. Mean ± SD. N≥3.

DISCUSSION

This work further addresses the phenomenon of sexual (pheromone-induced) biofilm formation in *C. albicans*. Previous studies indicated that sexual biofilm formation was a general property of *C. albicans* white cells from multiple clinical isolates (Sahni *et al.*, 2009), and occurred with similar efficiency under a variety of media conditions (Sahni *et al.*, 2009). There, biofilm formation was maximal when majority white **a** or α cells were mixed with minority populations of opaque **a** and α cells; pheromones secreted by the mating opaque cells induced adherence and biofilm formation by the responding white cells (Daniels *et al.*, 2006). However, recent experiments in the related fungal pathogen, *C. tropicalis*, showed that opaque cells, and not white cells, exclusively formed sexual biofilms in this species (Jones *et al.*, 2014). We therefore returned to *C. albicans* to more closely evaluate the ability of white and opaque cells from this species to respond to pheromone and undergo biofilm generation. This included an analysis of biofilm formation by a range of clinical isolates to three alternate pheromone sources, and experimentation using strains that were genetically locked into either the white or opaque phenotypic state.

Sexual biofilms involve cooperation between whites and opaques

The white-opaque phenotypic switch is one of the most studied phenomena in *C. albicans* biology. The switch regulates almost every aspect of *C. albicans* biology, from host specificity and virulence to mating and sexual competency. Sexual (pheromone-induced) biofilm formation has been extensively studied in this species, and it was generally thought that induction of adherence and biofilm formation was unique to cells in white state. Furthermore, it has been shown that biofilm formation by white cells can support and promote mating by rare

opaque cells. In this model, pheromones secreted by opposite-sex opaque cells leads to biofilm formation by responding white cells; this structure can maintain pheromone gradients between potential opaque cell partners, leading to more efficient chemotropism and opaque cell conjugation (Daniels *et al.*, 2006; Daniels *et al.*, 2013). More recently, it was also shown that *C. albicans* white cells can secrete sexual pheromones when stimulated by opaque cells of the opposite mating type, and that these pheromone levels can stimulate either biofilm formation in white cells or mating between opaque cells (Yi, Sahni, Daniels, Lu, Huang, Srikantha, *et al.*, 2011; Tao *et al.*, 2014).

Here, we focused on comparing the ability of *C. albicans* white and opaque cells to form sexual biofilms. We show that white cells from multiple clinical isolates are able to form pheromone-induced biofilms when challenged with exogenous pheromone. However, the response was not consistent once a mixture of opaque **a** and α cells was used as a pheromone source. This presumably reflects differences in pheromone concentrations between the two experiments, with exogenous pheromone concentrations being sufficient to more robustly stimulate biofilm production. Interestingly, isolate P37005**a** was consistently one of the best sexual biofilm forming strains, and perhaps explains why this strain has been extensively used for biofilm assays (Daniels *et al.*, 2006; Yi *et al.*, 2008; Alby and Bennett, 2011; Lin *et al.*, 2013). Overall, we conclude that the strain background can have a very significant effect on the efficiency of sexual biofilm formation, a result that is a common thread discussed here.

We further showed that some co-cultured white strains were able to form cooperative biofilms (*e.g*. P37005**a** x SC5314α). This result was surprising, as white cells do not generally secrete pheromone in the absence of opaque stimulatory cells. To probe this question with greater depth, we used strains that were either deleted for *WOR1*, or over-expressed it (white and opaque locked, respectively) (Alby and Bennett, 2009; Alby *et al.*, 2010). When P37005**a**

and SC5314α were forced into an exclusively white state (*wor1Δ/wor1Δ)*, they were unable to form biofilms.

Like white cells, some combinations of opaque **a** and α strains generated biofilms. The strongest example was SC5314**a** x SC5314α, and almost all significant biofilms included either SC5314**a** or SC5314α. Similar to the most successful white pairing (P37005**a** x SC5314α), however, the use of state-locked strains showed that robust biofilm formation between the two SC5314 strains occurred when both white and opaque cells were present. It was reasonable to hypothesize that few opaque cells would be necessary for sexual biofilm formation, but the ideal ratio of white to opaque cells was nearly one to one. This differs from previous estimates that suggest 1-10% opaque cells yield the maximal biofilm. This also illuminates an important aspect of *C. albicans'* biology: when beginning as a complete white population or opaque population, switching events allow sexual biofilm formation to proceed. It would be worthwhile to determine how the phenotypic frequency of cells changes during biofilm development, as it may be informative at to what, if any, contributions opaque cells make to biofilms beyond pheromone. Taken together, our experiments indicate that sexual (pheromone-induced) biofilms are not exclusive to white cells, but that *C. albicans* opaque cells are a frequent and needed component.

Intra-Species Differences Affect Biofilm Formation

Multiple *C. albicans* traits vary between strains, including adherence and invasion (Bernhardt *et al.*, 2001), the ability to cause systemic infections (Wu *et al.*, 2007), and genetic karyotype (Magee and Magee, 1987). Some traits, such as fluconazole resistance, are known to correlate with sub-species clades (Pujol, Pfaller, *et al.*, 2004). To see if this was also true of the pheromone-induced biofilm response in *C. albicans*, here we tested a collection of clinically-

isolated strains. Response to exogenous pheromone addition was almost entirely consistent across isolates in the white phase, but when the pheromone source changed, our results became extremely variable. For example, when a minority of **a** and α opaque cells were included as a source of natural pheromone, **a** strains responded much more consistently than α strains did. This discrepancy suggests an imbalance between the **a** and α pheromone signaling systems. From a biochemical perspective, the two pheromones differ in that α pheromone is an unmodified peptide, whereas **a** pheromone is prenylated (Bennett *et al.*, 2003; Dignard *et al.*, 2007). The added hydrophobicity introduced with prenylation is thought to limit the diffusion of **a**-pheromone (Dignard *et al.*, 2007). This may result in the imbalance between mating types that we noted. Further cell-based experiments comparing the distance of signal partners to signal responses could address this hypothesis.

Inter-strain compatibility

The ability of particular strain combinations to form biofilms in co-culture suggests that compatibility factors contribute to this cellular response. For example, the white P37005A X SC5314 and pairing succeeded, while the pairing of either of these strains with other strains did not. The simplest explanation may be that the amount of pheromone signaling components varies across *C. albicans* strains, as it does between white and opaque cells (Tuch *et al.*, 2010), which could be tested by adding pheromone exogenously. For example, if baseline pheromone expression is too low, reciprocal pheromone exchange never begins and biofilms never develop. Alternatively, even if one strain produces sufficient pheromone, a signal transduction bottleneck may still occur in the other, preventing reciprocal signaling and thereby extinguishing the necessary signal amplification. A different hypothesis is that compatible cell surface receptors must be expressed appropriately by co-cultured cells in order for proper cohesion to occur. This

is evidenced in *C. tropicalis*, where the proposed sexual agglutinin Fgr23 is necessary for maximal biofilm formation and mating (Jones *et al.*, 2014). In *S. cerevisiae*, expression of genes encoding sexual agglutinins is mating-type dependent, and the resulting agglutinins pair reciprocally and irreversibly to facilitate mating (Zhao *et al.*, 2001). This explanation could indicate why some strains inherently form biofilms more frequently than others, such as P37005**a**, and why mixes between white and opaque cells elicit the strongest biofilm responses.

In total, we showed that the white response to pheromone alone is well-established across *C. albicans* strains. This was not true when cells were stimulated by signaling opaque cells, or when **a** and α strains were co-cultured. In these cases, biofilm formation was found to occur in white and opaque cells, although in a strain-dependent manner. This work shows that opaque cells play a more prominent role in sexual biofilms than previously appreciated. Additional experimentation will elucidate the mechanisms that determine compatibility between populations in the *C. albicans* species and uncover how they relate to cellular phenotype.

CHAPTER 4B: A ROLE FOR WOR1 IN REGULATING FILAMENTATION AND BIOFILM FORMATION IN *C. TROPICALIS*

ABSTRACT

Phenotypic switching allows for rapid transitions between alternative cell states, and is important in pathogenic fungi for colonization and infection of different host niches. In several *Candida* species, the white-opaque phenotypic switch plays a central role in regulating the program of sexual mating as well as interactions with the mammalian host. In both *C. albicans* and *C. tropicalis*, mating is relegated to cells in the opaque state. The transcription factor Wor1 is the master regulator of the white-opaque switch, where its expression is required for cells to reach and maintain the opaque state. Wor1 is conserved amongst fungal ascomycetes, and alternatively acts as a master regulator of the yeast-to-filament transition in these species. Here, we show an expanded role for *WOR1* in *C. tropicalis*, where its overexpression promotes filamentous growth and biofilm formation in *C. tropicalis,* independent of the white-opaque switch. These results demonstrate *C. tropicalis* Wor1 has an expanded biological role, encompassing both the ancestral role of Wor1 as a transcriptional regulator of the transition between yeast form and filamentous growth, and its more recently evolved role as regulator of the white-opaque switch.

INTRODUCTION

The incidence of opportunistic fungal infections has increased in recent years as a result of immunosuppressive diseases such as AIDS, as well as the use of immunosuppressive drugs in modern medical practices(Brown *et al.*, 2012). *Candida* species are typically harmless commensals of humans but are also important fungal pathogens, responsible for both systemic and mucosal opportunistic infections (Pfaller and Diekema, 2007). Most clinically relevant species belong to the *Candida* clade of hemiascomycete yeasts, which diverged from the model yeast *Saccharomyces cerevisiae* 300-600 million years ago (Pesole *et al.*, 1995; Hedges, 2002). Three *Candida* clade pathogens, *Candida albicans, Candida dubliniensis,* and *Candida tropicalis,* have been shown to undergo an epigenetic switch between distinct 'white' and 'opaque' states (Slutsky *et al.*, 1987; Pujol, Daniels, *et al.*, 2004; Porman *et al.*, 2011; Xie *et al.*, 2012), and this phenotypic switch plays a crucial role in modulating behavior. The white-opaque switch has been extensively studied in *C. albicans*, where the two states differ in metabolic preferences (Lan *et al.*, 2002), environmental responses (Kolotila and Diamond, 1990; Ramírez-Zavala *et al.*, 2008; Huang *et al.*, 2009; Alby and Bennett, 2009; Huang *et al.*, 2010), interactions with host immune cells (Geiger *et al.*, 2004; Lohse and Johnson, 2008), and the ability to undergo sexual reproduction (Miller and Johnson, 2002; Lockhart *et al.*, 2002).

C. albicans and *C. dubliniensis* are closely related species that can undergo productive mating with one another (Pujol, Daniels, *et al.*, 2004). While *C. albicans* represents the most commonly isolated *Candida* species in the clinic, *C. dubliniensis* is rarely found in infections, which may reflect the more limited ability of this species to undergo filamentation (Pfaller and Diekema, 2007; Stokes *et al.*, 2007). *C. tropicalis* is also a prevalent human pathogen, particularly in individuals with neutropenia or hematologic malignancies (Pfaller and Diekema,

2007), and shows a similar overall genome structure to that of *C. albicans*, including synteny at the mating-type-like (*MTL*) locus (Butler *et al.*, 2009). *C. albicans* and *C. tropicalis* both contain more than 6,000 protein-coding genes, and analysis of the 5,254 orthologs shared between the two species indicates an average protein sequence identity of ~70% (Butler *et al.*, 2009). However, relatively little is known about the biology of *C. tropicalis* compared to that of the model species *C. albicans*, including the factors that promote pathogenesis in the mammalian host.

In all three *Candida* species, white and opaque forms are distinguished by differences in cell shape, colony morphology, and gene expression profiles. White cells are generally round and give rise to smooth, shiny colonies, while opaque cells are elongated and produce duller, darker colonies (Slutsky *et al.*, 1987; Porman *et al.*, 2011). The transcriptional profiles of white and opaque forms are also significantly different, with one-sixth of the transcriptome regulated by the switch in *C. albicans* (Prabu-Jeyabalan *et al.*, 2002; Tsong *et al.*, 2003; Tuch *et al.*, 2010). Furthermore, white and opaque forms exhibit differences in the propensity to undergo filamentous growth; *C. albicans* white cells are induced to filament in response to multiple environmental stimuli while opaque cells do not generally undergo filamentation (Anderson *et al.*, 1989; Ernst, 2000).

The white-opaque switch plays a particularly prominent role in regulating mating, as only cells in the opaque state undergo efficient conjugation(Miller and Johnson, 2002; Porman *et al.*, 2011). Switching is regulated by *WOR1* such that loss of this gene prevents formation of the opaque state while, in *C. albicans*, *WOR1* overexpression drives cells into the opaque state(Huang *et al.*, 2006; Zordan *et al.*, 2006; Srikantha *et al.*, 2006; Porman *et al.*, 2011). Genes encoded at the *MTL* locus control white-opaque switching in *C. albicans*; only **a** or α cells switch

to the opaque state as a complex between *MTL***a**1 and *MTL*α2 proteins blocks **a**/α cell switching due to repression of *WOR1* (Miller and Johnson, 2002; Tsong *et al.*, 2003; Srikantha *et al.*, 2006). An analysis of 220 clinical isolates of *C. albicans* further demonstrated that only *MTL* homozygous (**a**/**a** or α/α) strains could form stable opaque cells at a detectable frequency [17]. *MTL* regulation ensures that opaque formation only occurs in cells that have the potential to undergo mating, which can take place between *MTL***a** and *MTL*α cells or via same-sex mating of these cell types (Miller and Johnson, 2002; Alby *et al.*, 2009).

The white-opaque switch is thought to have evolved relatively recently in the *Candida* clade, probably just prior to the divergence of *C. albicans/C. dubliniensis* and *C. tropicalis* (Porman *et al.*, 2011; Xie *et al.*, 2012:2). Although this phenotypic switch is limited to within the *Candida* clade, the master transcriptional regulator Wor1 is conserved across the ascomycete lineage (Lohse and Johnson, 2010). In *S. cerevisiae*, the Wor1 homolog Mit1 acts as part of a transcriptional network to regulate pseudohyphal formation (Cain *et al.*, 2012), while in the more distantly related ascomycete *Histoplasma capsulatum*, the Wor1 homolog Ryp1 is a master regulator of the transition between yeast and mycelial forms (Nguyen and Sil, 2008). It has therefore been proposed that the ancestral role of Wor1 was the transcriptional regulation of morphological changes, including the control of filamentous growth (Cain *et al.*, 2012).

In this study, we investigated the master regulator of the white-opaque transition in *C. tropicalis*, Wor1, and uncovered several features that further distinguish it from the analogous regulator in *C. albicans*. We show that Wor1 promotes filamentous growth in *C. tropicalis*, as elevated *WOR1* expression led to a significant increase in both filamentous growth independent of mating-type. We also find that elevated *WOR1* expression induced biofilm formation, which

was also found to be independent of mating-type. These studies provide new insights into the evolution of Wor1 homologs as regulators of switching, filamentation and biofilm formation.

RESULTS

Wor1 Regulates Filamentation and Biofilm Formation in *C. tropicalis*

In several diverse fungal species, Wor1 homologs do not mediate phenotypic switching but still act as transcriptional regulators of cellular morphogenesis. This is evident in *S. cerevisiae* and *H. capsulatum*, where Wor1 homologs regulate the transition from budding yeast forms to filamentous forms (Nguyen and Sil, 2008; Cain *et al.*, 2012). Colony morphologies of *C. tropicalis* strains were compared on several media, and it was found that *WOR1* overexpression strains were markedly more wrinkled than wild-type white or opaque cells when grown on Spider medium (Figure 8A). Spider medium is a low nutrient medium that also induces filamentation in *C. albicans* (Liu *et al.*, 1994). Examination of cells from the wrinkled colonies confirmed that Wor1 overexpression strains were significantly more filamentous than other cell types due to a higher percentage of both hyphal and pseudohyphal cells (Figure 8B). In addition, filamentation generally increased as *WOR1* gene expression levels increased. Thus, for **a**/α cells, filamentation increased from *wor1* mutants (4.4%) to white cells (10.7%) to opaque cells (23.9%) to *WOR1* overexpressing cells (32.9%, Figure 8B). These results indicate that filamentation correlates with *WOR1* expression in *C. tropicalis*, and that Wor1 regulates filamentous growth independent of its regulation of the white-opaque switch.

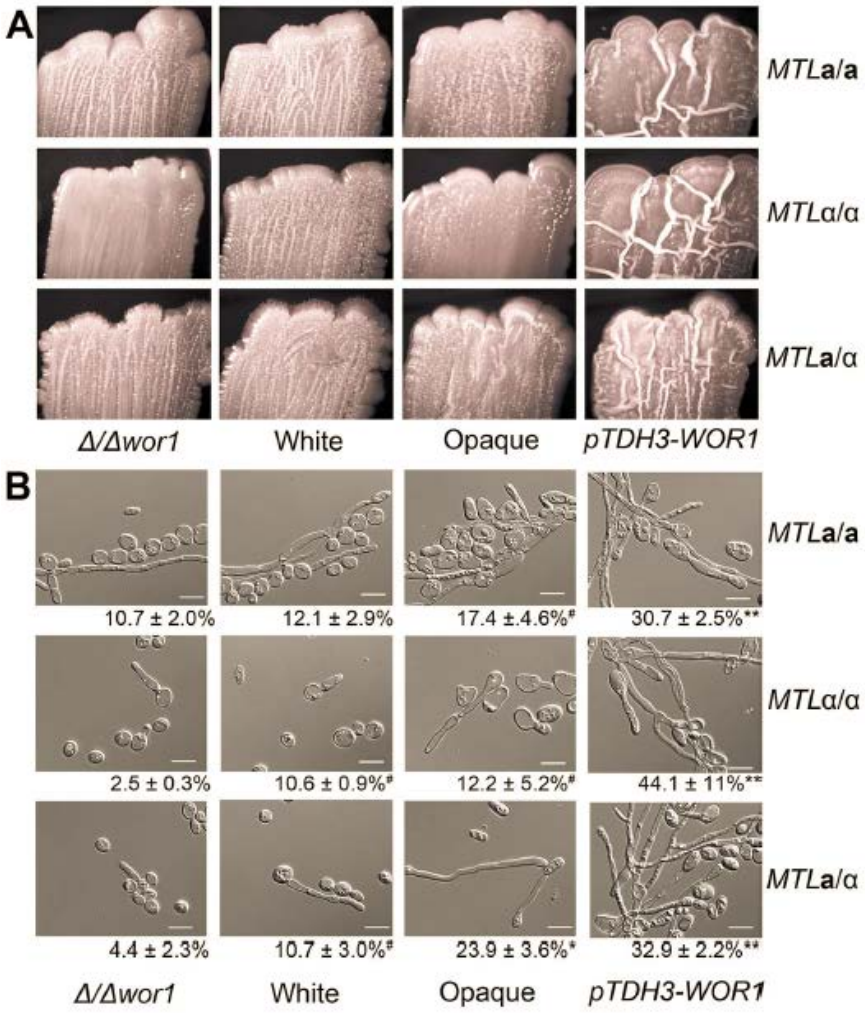

Figure 4-8: *C. tropicalis WOR1* expression regulates filamentous growth.

(A) Wild-type white, wild-type opaque, *Δwor1* mutant, and *WOR1*- overexpression (*pTDH3-WOR1*) strains were grown on Spider medium at 37°C for 7 days and photographed. (B) Cells from corresponding patches in (A). The percentage of filamentous cells is shown below each image. Scale bar = 10 mm. ** = significantly different from opaque, white, and *Δwor1 strains*, p,0.001. * = significantly different from white and *Δwor1*, p,0.001. # = significantly different from *Δwor1*, p,0.05.

Filamentous growth is directly associated with biofilm formation in *C. albicans*. Biofilms are surface-associated communities of cells and often involve both yeast and filamentous cells in stable, complex structures that form on biotic and abiotic surfaces (Nobile *et al.*, 2006; Finkel and Mitchell, 2011). Furthermore, *C. albicans* biofilms are responsible for the seeding of serious

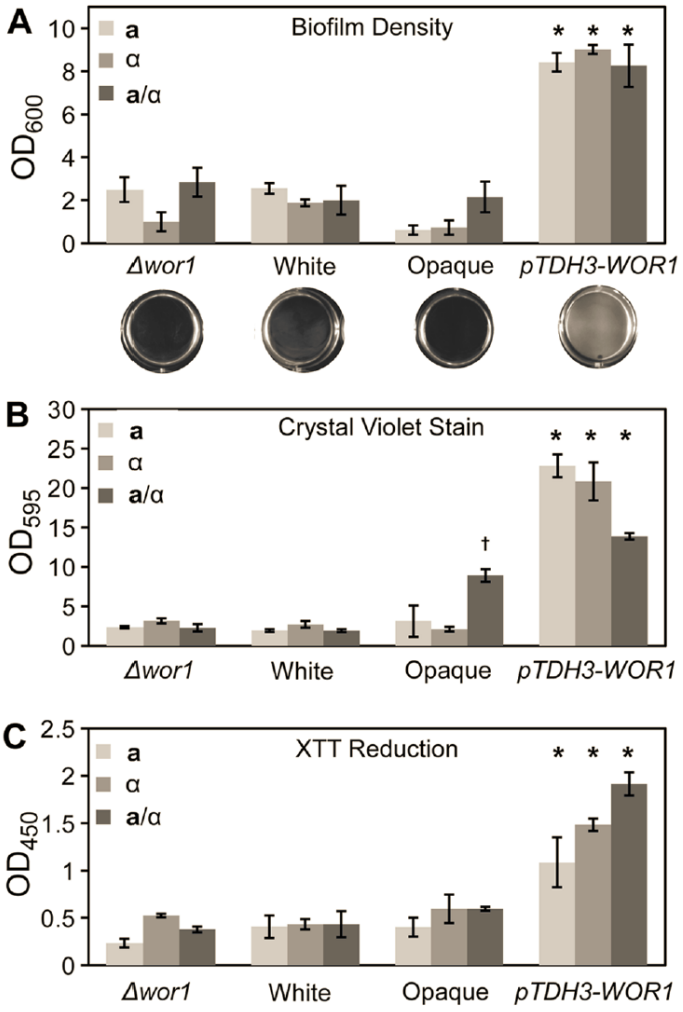

Figure 4-9: Biofilm formation is induced by WOR1 overexpression in *C. tropicalis*.

(A) Quantification of cells adhering to a 12-well polystyrene dish following a 48-hour incubation in Lee's medium. Representative images of wells appear below the corresponding strains. Data from three experimental replicates, error bars indicate SD. * = p,0.001 when compared to Dwor1, white, and opaque strains. (B, C) Quantification of biofilm production by colorometric assays. (B) Beta-glucan content was determined by crystal violet staining. (C) Cellular viability was measured by formazan formation upon XTT reduction. Each biofilm experiment includes three or more replicates, error bars indicate S.D. * = p,0.001 when compared to *Δwor1*, white, and opaque strains. † = p,0.001 when compared to *Δwor1*, white, and *pTDH3-WOR1* strains.

bloodstream infections and are associated with antifungal drug resistance (Nobile *et al.*, 2006; Finkel and Mitchell, 2011). We therefore examined whether *C. tropicalis wor1* mutant cells, white cells, opaque cells, or cells overexpressing *WOR1* displayed differences in their ability to form biofilms using an adherence to plastic assay. White cells, opaque cells, and *wor1* mutants generally performed poorly in these adherence assays, regardless of *MTL* configuration (Figure 9A). In contrast, cells overexpressing *WOR1* generated robust biofilms on the polystyrene plates, as noted by visual inspection as well as quantification of the biofilm by optical density (Figure 9A). Increased biofilm formation was also demonstrated by an elevated level of staining with crystal violet, which indicates extracellular matrix production (Figure 9B), and by increased XTT reduction, indicating that there were significantly more adherent, viable cells in the *WOR1* overexpressing biofilms (Figure 9C). Many cells within the *WOR1*-overexpressing biofilms were filamentous (22-59%), whereas comparatively few cells were filamentous in white, opaque, or *wor1* cells (0-12%, Figure 6D).

Transcriptional profiling was performed under biofilm culture conditions on *WOR1* overexpression strains and compared to gene expression in wild-type opaque strains. This revealed that 58 genes were differentially expressed (>4-fold) between these strains (Figure 10E). Gene expression changes included *CHT3,* which encodes a chitinase whose expression is repressed in *C. albicans* hyphal cells (McCreath *et al.*, 1995), and which was also repressed in the *C. tropicalis WOR1* overexpression strain. Conversely, *JEN2* was upregulated in *C. tropicalis WOR1*-mediated biofilms, and encodes a dicarboxylic acid transporter whose expression is also upregulated in *C. albicans* biofilms (Nett *et al.*, 2009). In addition, several *C. tropicalis* white-specific genes (e.g., *ADAEC* and *WH11*) were further downregulated in the *WOR1*-overexpressing cells relative to opaque cells (Figure 10E). However, no genes with defined roles

in filament regulation were obtained from these profiling studies, although many of the differentially regulated genes currently have no known function.

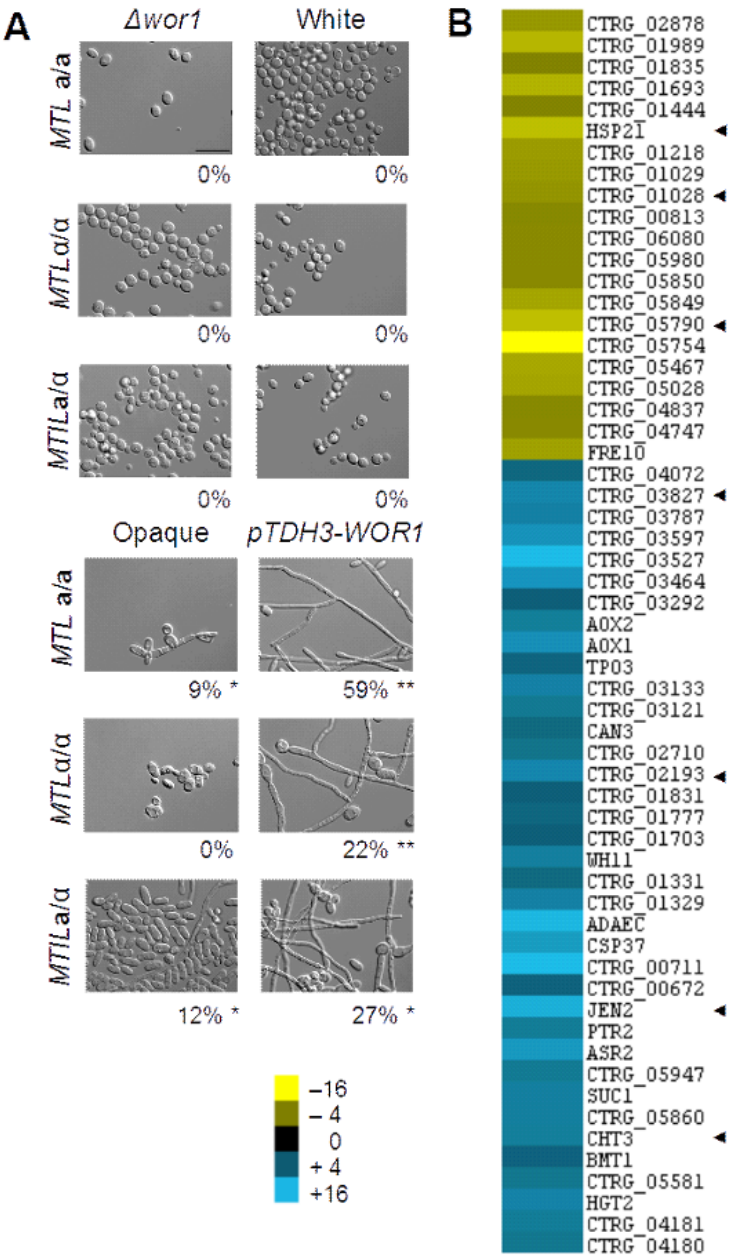

Figure 4-10: Cellular morphology and gene expression of *WOR1* overexpression biofilms.

(A) Morphology of adherent cells taken from biofilms. Percentage of filamentous cells indicated below image. Scale bars = 20 mm. Statistical significance was determined using Mann-Whitney pair-wise tests. ** = significantly different from opaque, white, and awor1 strains, p,0.001. * = significantly different from white and awor1 strains, p,0.001. (B) Genes induced in *MTLa/α WOR1* overexpressing cells under biofilm conditions. Heat map shows relative expression changes between *pTDH3-WOR1* (CAY3853) and opaque (CAY3378) strains in the adherence to plastic biofilm assay. Data set was filtered for genes with a fold-change greater than 4 and clustered by Average Linkage Clustering. Data shows average of two independent biological replicates. Arrowheads highlight *C. albicans* homologs that are biofilm regulated.

Together, these results demonstrate that Wor1 promotes filamentous growth and biofilm formation in *C. tropicalis* and these functions are independent of the white-opaque switch. The role of Wor1 in this species is therefore analogous to that of several distantly related Wor1 homologs in the fungal lineage. The increase in filamentous growth is presumably a major reason for the increased adhesion and biofilm formation in the *C. tropicalis* Wor1-overexpression strains.

DISCUSSION

During an analysis of white and opaque cells in *C. tropicalis* (Porman *et al.*, 2013:20) we noted a link between *C. tropicalis* Wor1 and filamentous growth. Here, we found that overexpression of *WOR1* in *C. tropicalis* resulted in increased filamentation relative to wild-type white or opaque cells. Like the white-opaque switch in *C. tropicalis*, this activity was independent of mating-type, which prevents the switch to the opaque phenotype in *C. albicans* (Lockhart *et al.*, 2002). *C. tropicalis* Wor1 is therefore a key regulator of filamentation, and this control can be separated from regulation of the white-opaque switch. The role of Wor1 was most clearly manifested in biofilm assays, where increased expression of *WOR1* led to enhanced biofilm formation. This is presumably a direct result of the increase in filamentous growth, as filamentation and biofilm formation are inter-related processes in multiple *Candida* species (Laffey and Butler, 2005; Nobile *et al.*, 2006; Finkel and Mitchell, 2011). Regulation of filamentation by the white-opaque switch has also been noted in *C. albicans*, although here white cells were shown to be more conducive to undergoing filamentation than opaque cells (Anderson *et al.*, 1989; Ernst, 2000).

The observation that *C. tropicalis* Wor1 induces filamentation shows interesting parallels with the role of Wor1 homologs in more distantly related ascomycete species. In *S. cerevisiae* and *H. capsulatum*, the Wor1 homologs Mit1 and Ryp1, respectively, are both master regulators of filamentation (Nguyen and Sil, 2008; Cain *et al.*, 2012). It has therefore been proposed that the ancestral function of Wor1/Mit1/Ryp1 was to control morphological transitions such as that between yeast form and filamentous form (Cain *et al.*, 2012:20). The discovery that *C. tropicalis* Wor1 promotes filamentation suggests that it has retained the ancestral function of Wor1 in this species. In contrast to filamentous growth, the white-opaque

switch evolved only recently in the ascomycete lineage, probably immediately prior to the divergence of *C. tropicalis* and *C. albicans* (Tuch *et al.*, 2008; Porman *et al.*, 2011:20; Xie *et al.*, 2012). We therefore propose that *C. tropicalis* Wor1 has retained both the ancestral role of the Wor1 family of transcription factors (regulation of filamentous growth), as well as adopting control over the more recently evolved white-opaque switch. Furthermore, Wor1's role in filamentation likely contributes to its ability to form biofilms. In *C. albicans,* Wor1 is not involved in regulation of filamentation, and similarly does not promote biofilm formation under the conditions tested here (data not shown), and can even inhibit filamentous growth (Xie *et al.*, 2012). A more complete discussion on the relationship between *WOR1* overexpression biofilms, sexual biofilms, and biofilms formed by *C. albicans* is contained in Chapter 3.

MATERIALS AND METHODS

Media

Yeast extract peptone dextrose medium (YPD), synthetic complete dextrose medium (SCD), and Spider medium were made as described previously (Guthrie and Fink, 1991; Liu *et al.*, 1994). YPD plates containing 200 µg/ml nourseothricin (NAT) were used for selection of strains that were resistant to nourseothricin (Werner Bioagents, Jena, Germany) as previously described (Reuss *et al.*, 2004). Lee's media containing 12.5 g/L N-acetylglucosamine (Alpha Acera) was used for switching assays, and Lee's media containing 1.25% glucose was used for biofilm assays (Bedell and Soll, 1979; Huang *et al.*, 2010).

Plasmids and Strains

C. tropicalis strains used in this study are listed in Tables S1 and S2. Gene deletions were constructed by using the *SAT1* flipper strategy as described (Park and Morschhäuser, 2005). Strains were transformed with 1–4 µg of DNA by using a modified electroporation protocol (Porman *et al.*, 2011). To delete *WOR1, HIS1, ARG4, MTLa2*, and *MTLα1* genes using the *SAT1*-flipper method, oligonucleotides were used to amplify ~900 bp of the 5′ and 3′ homologous flanks of each gene. The resulting PCR products were digested with restriction enzymes noted in Table S3 and cloned into the plasmid pSFS2a (Park and Morschhäuser, 2005). The resulting plasmids were digested with restriction enzymes as noted in Table S4 to liberate cassettes containing the 5′ and 3′ gene flanks as well as the *SAT1* selectable marker and used for transformation. Correct genomic integration of transformant colonies was confirmed by PCR of the 5′ and 3′ junctions (for oligonucleotides, see Table S3). The *SAT1* marker was recycled by growing transformants on maltose media at room temperature or 30°C and subsequent replica patching to both YPD and YPD+NAT plates. Alternatively, the *SAT1* marker was recycled by

growing cells in liquid YEP + 2% maltose at room temperature for ~2 days and selected by plating to YPD+ low NAT (10 μg/mL), as previously described (Park and Morschhäuser, 2005). The transformation process was repeated to delete the remaining copy of the gene, and loss of the ORF was confirmed by PCR. To overexpress *WOR1*, fusion PCRs were performed to create a *pTDH3-WOR1* construct, which was cloned into pSFS2a. The plasmid was linearized in the *TDH3* promoter with *Sma*I and transformed. Correct genomic integration was confirmed by PCR. To insert a *SAT1* marker next to the *MTL*, PCR was performed to amplify a sequence immediately upstream of the *MTL*, which was cloned into pSFS2a. The plasmid was linearized within this sequence with *Eco*RI and transformed into *C. tropicalis*. Correct genomic integration next to the *MTL***a** or *MTL*α locus was confirmed by PCR.

Microarrays

Cells were harvested after being grown to OD_{600} 1.0-1.2 in Spider medium at room temperature. Cells were collected, flash frozen, and stored at -80°C. For microarrays performed on biofilms, cells were collected after the two-day incubation detailed in the biofilm method. Total RNA was extracted from cell pellets using the RiboPure-Yeast Kit protocol (Ambion). RNA was treated with Turbo DNaseI (Ambion) to eliminate DNA contamination and re-extracted with phenol/chloroform. Aminoallyl-labeled cDNA synthesis and hybridization to custom Agilent *C. tropicalis* microarrays was previously described by Porman *et al*. (Porman *et al.*, 2011). Arrays were scanned on a GenePix 4000 scanner (Axon Instruments), data quantified using GENEPIX PRO version 3.0 and normalized using Goulphar (http://transcriptome.ens.fr/goulphar). Data analysis was performed as previously described (Porman *et al.*, 2011). GO term analysis was facilitated by CGD (http://candidagenome.org) and Princeton University's Generic GO Term Mapper (http://go.princeton.edu/cgi-bin/GOTermMapper). Array data is available from GEO

(accession numbers GSE40179, GSE42517 and GSE43267).

Microscopy

Digital images of colonies were collected using a Zeiss Stemi 2000-C microscope using an Infinity 2 digital camera and Infinity Analyzer software (Lumenera Corperation, Ottawa, Canada). Differential interference contrast (DIC) of cells were captured using a Zeiss Inverted Microscope (Axio Observer. Z1) fitted with an AxioCam HR. Images were processed with AxioVision Rel. 4.8 (Zeiss, Germany).

To quantify filamentation from colonies grown on Spider medium, cells were removed from the center of patches and counted for the fraction of filamentous cells. At least 4 fields of view and 400 cells were counted for each data point. Statistical significance was determined using a Student's T-test.

Adherence Assays

Cultures were inoculated in 3 ml of Spider medium then incubated at 25°C overnight. 2 ODs of cells were spun down and resuspended in 1 ml of Lee's + Glucose medium and transferred to the well of a 12-well polystyrene plate. Plates were incubated at 25°C for 1-2 days without shaking, then decanted. Each well was washed 3 times with 1 ml of water to remove non-adherent cells. Plates were imaged using a Chemidoc XRS+ with Image Lab software (Bio-Rad). Adherent cells were scraped off the plastic surface and resuspended in 1 ml of water and optical density determined. For significant differences between data sets, each was tested for normal distribution. A one-way ANOVA was performed on OD_{600} results. Nine representative microscope fields were counted for each condition to determine the fraction of

filamentous cells. Statistical significance was determined using a Mann-Whitney pair-wise test due to non-parametric datasets.

Crystal Violet Staining

Samples were prepared similarly to the adherence assays. Following the 3 washes of the biofilm, 12-well plates were decanted and left to dry for 45 minutes, and subsequently stained with 385 µL of 0.4% aqueous crystal violet per well for 45 minutes. Each well was washed 3 times with 1 mL of water, then destained with 700 µL of 95% ethanol. Finally, 100 µL of each destain solution was transferred to a 96-well plate and diluted 10-fold. Optical density was read at 595 nm using a BioTek Synergy HT plate reader and statistics performed similar to the adherence assays.

XTT Reduction Assay

Samples were prepared similarly to the adherence assays. Following the 3 washes of the biofilm the plates were decanted, then 315 µL of 1 mg/mL XTT (2,3-bis-(2-methoxy-4-nitro-5-sulfophenyl)-2H-tetrazolium-5-carboxanilide) and 35 µL of 360 µg/mL phenazine methosulfate were added to each well. The plates were incubated at room temperature for 20 minutes, then 100 µL of solution from each well was transferred to a 96-well plate. Optical density was read at 450 nm using a BioTek Synergy HT plate reader and statistics performed as for the adherence assays.

Acknowledgements: We would like to thank Donna MacCallum of the Aberdeen Fungal Group for clinical isolates, and Brian Tuch [University of California, San Francisco (UCSF)], Sandy Johnson (UCSF), and Aaron Hernday (UCSF) for the gift of *C. tropicalis* strains.

SUPPLEMENTAL TABLES

Table S1. List of *C. tropicalis* strains used in this study.

White Strain	Opaque Strain	Genotype	*MTL*
CAY675		ATCC 34139 ST-120	**a**/α
CAY677/785	CAY784	Sorbose selected ATCC 34139	**a**/**a**
CAY679/787	CAY786	Sorbose selected ATCC 34139	α/α
CAY1117/1118		*wor1/wor1::SAT1*	**a**/**a**
CAY1502		*his1/his1::SAT1*	**a**/**a**
CAY1503/1504	CAY2053/2275	*arg4/arg4::SAT1*	**a**/**a**
CAY1505/06	CAY2054/2055	*his1/his1::SAT1*	α/α
CAY1509/1510	CAY2056/2057	*arg4/arg4::SAT1*	α/α
CAY2058		*his1/his1*	**a**/**a**
CAY2059/2060		*arg4/arg4*	**a**/**a**
CAY2061/2062		*his1/his1*	α/α
CAY2063		*arg4/arg4*	α/α
CAY2200		*his1/his1 ste2/ste2*	**a**/**a**
CAY2201/2245		*his1/his1 ste3/ste3*	α/α
CAY2202		*arg4/arg4 ste2/ste2*	**a**/**a**
CAY2203/2243		*arg4/arg4 ste3/ste3*	α/α
CAY2247		*his1/his1 ste2/ste2/STE2::SAT1*	**a**/**a**
CAY2246		*arg4/arg4 ste2/ste2/STE2::SAT1*	**a**/**a**
CAY2380		*his1/his1 ste3/ste3/STE3::SAT1*	α/α
CAY2378/2379		*arg4/arg4 ste3/ste3/STE3::SAT1*	α/α
CAY2136/2251	CAY2257/2260	*arg4/arg4 HTB/HTB-mCherry:SAT1*	**a**/**a**
CAY2134/2135	CAY2258/2259	*his1/his1 HTB/HTB-GFP:SAT1*	α/α
CAY2205/2206/2248		*arg4/arg4 wor1/wor1::SAT1*	**a**/**a**
CAY2342/2439		*his1/his1 wor1/wor1::SAT1*	α/α
CAY2347/2348/2441		*arg4/arg4 wor1/wor1/WOR1::SAT1*	**a**/**a**
CAY2440/2805		*his1/his1 wor1/wor1/WOR1::SAT1*	α/α

Table S2. Oligonucleotides used in this study. Underlined sequences denote restriction sites.

Oligo	Name	Sequence
1	*WOR1* (ApaI) -900	ggagcggggcccCTACTACATTAGTTGTTCCCTG
2	*WOR1* (XhoI) 0	gccggcctcgagATAATCTAGACGCCGACATG
3	*WOR1* (SacII) +2100	ggagcgccgcggGGTAACTACAGGTGACGAATC
4	*WOR1* (SacI) +3000	ggccgcgagctcTTACCCACAAGTGTGTCTAG
5	*WOR1* 5' check -950	GAATCTAAGGCAACAAACGATTTC
6	*WOR1* 3' check +3100	GGTGATTAAAATCACATTCTCGG
7	*WOR1* 5' ORF +200	GACTGATGGAATTTCTTGGTC
8	*WOR1* 3' ORF +550	GCAGCTGTCCATAAACATGG
9	*HIS1* (ApaI) -900	ggagcggggcccACCTCAAGAGATGAATGACA
10	*HIS1* (XhoI) 0	gccggcctcgagACTCTAAACTATGATTGTATTC
11	*HIS1* (SacII) +900	ggagcgccgcggAGTTCATCTGTATAATAGTACA
12	*HIS1* (SacI) +1800	ggccgcgagctcTCCACACATTCATAAATGTTCA
13	*HIS1* 5' check -950	CCAAGGACAACACTCGTGCAGT
14	*HIS1* 3' check +1900	CAAATTGATCACTTCTCTAGTCGA
15	*HIS1* 5' ORF +200	AGGGTAATTGTGATTTGGGTA
16	*HIS1* 3'ORF +600	CTTGGAAGAAACCAAGTGAG
17	*ARG4* (ApaI) -900	ggagcggggcccTGAATGTGTTGGTGGTGATG
18	*ARG4* (XhoI) 0	gccggcctcgagGACATTGTTGTTAGAATAAGTT
19	*ARG4* (NotI) +1400	ggagcggccggccgcACATTCATTCTCCTTCCCTCTC
20	*ARG4* (SacII) +2300	ggccgccgcggGAATATTGATTGTTGATTGTTG
21	*ARG4* 5' check -950	GACGTTGTTTACCCTTGGTATC
22	*ARG4* 3' check +2400	TTGTGGAATGTAATTTGCACAC
23	*ARG4* 5' ORF +200	TCAGGATTAGAAGAAATTCGTG
24	*ARG4* 3' ORF +600	TGGACTTTGATTAACTCTGGT
25	*STE2* (ApaI) -950	ggcgccgggcccGTCTAGAGTTGCTCTTCTCT
26	*STE2* (XhoI) 0	gccggcctcgagCACCAGAAGACTGAATAGTATTG
27	*STE2* (SacII) +1200	ggagcgccgcggCTGAAGTCACTTACAAGAAGG
28	*STE2* (SacI) +2100	ggccgcgagctcGGGAATGGCACAATTGGAGTC
29	*STE2* 5' check -970	CGAGCATTAGTGTAACTAGTC
30	*STE2* 3' check +2150	CAATAGGACCAACTGGGAAATG
31	*STE2* 5' ORF +150	GCTTAGTCATGGGTGTGATG
32	*STE2* 3' ORF +650	GACATAAGATTGACACTAACGG
33	*STE3* (ApaI) -900	ggcgccgggcccGATCTTGAAACACGAACAAGC
34	*STE3* (XhoI) 0	gccggcctcgagCCAGCAGCTGCAGCAATCAT
35	*STE3* (SacII) +1200	ggagcgccgcggCGCCTAGCGAACATTTCTCA
36	*STE3* (SacI) +2100	ggccgcgagctcgTCGAGATCAAGAATTTGGG
37	*STE3* 5' check -970	CGTTGATGATGAAGAAGCTC
38	*STE3* 3' check +2150	CATTTGGATATTTGTACCGGAG
39	*STE3* 5' ORF +100	GCATGGCATATTAAGTGTGC
40	*STE3* 3' ORF +650	CAGAAGTAAAGAGACAATGGC
42	*STE2* (XhoI) +1500	gccggcctcgagAACTGGATCTGCAACCATGG
43	*STE3* (XhoI) +1500	gccggcctcgagGCAATTGGCAGTGAAAGAAATC
44	*HTB-FP* forward	GTTAGATTGATCTTGCCAGGTGAATTGGCTAAACATGCCG TTTCTGAAGGTACTAGAGCTGTTACCAAATACTCTTCTGC

		TTCAAACcggatccccgggttaattaacgg
45	*HTB-FP* reverse	ATGGATTAGCATATTATAAATTAATAATTATGCAAAGTT GGGTACAAGTAATGAAATTGGTTCTCTTCTGTTTGAAATG GTTATggcggccgctctagaactagtggatc
46	*HTB* check	GATTGTTTCTCTCTCCTCTC
47	prBT_74 (a2)	GATTTGGTATGAAAAGAGGAACTCTAAC
48	prBT_75 (a2)	CTACTAATTTTGAAACCATTTGGAGTCT
49	prBT_70 (alpha2)	TAAAACATTAAGCATAGAGGACAAAGAA
50	prBT_71 (alpha2)	AACTTCAAATGCAAAATGTAAAACATAC
51	*ACT1* 5Q	GGTGATGGTGTTACCCACGTT
52	*ACT1* 3Q	TGTAACCACGTTCAGACAAGATCTTC
53	*ADAEC* 5Q	ATCAATGTATTCCAACCAAAACCA
54	*ADAEC* 3Q	TGAAACCAAGTACACCACCTCTTC
55	*WOR1* 5Q	CCGTCTAATGTTATACCTGCATCAA
56	*WOR1* 3Q	TTCGTCGTACTTATGGTAATTGTTTTCT
57	*FUS1* 5Q	CCTTCATCAACCACAACTAGAAGAATT
58	*FUS1* 3Q	TCCCAAAGCAATGAAAAAAATAGC
59	*WOR1* (XhoI) +2500	gccggcctcgagGTCATATACCCAACACCGAAC

Table S3. Plasmids used in this study.

Plasmid	Name	Oligos used	Enzymes used for transformation
pRB29	*WOR1* deletion plasmid	1/2, 3/4	*Apa* I/*Sac* I
pRB55	*HIS1* deletion plasmid	9/10, 11/12	*Apa* I/*Sac* I
pRB59	*ARG4* deletion plasmid	17/18, 19/20	*Apa* I/*Sac* II
pRB94	*STE2* deletion plasmid	25/26, 27/28	*Apa* I/*Sac* I
pRB95	*STE3* deletion plasmid	33/34, 35/36	*Apa* I/*Sac* I
pRB101	*STE2* complementation plasmid	25/42, 27/28	*Sma* I
pRB102	*STE3* complementation plasmid	33/43, 35/36	*Afl* II
pRB103	*WOR1* complementation plasmid	1/59, 3/4	*Apa* I/*Sac* I

Please refer to the following citation for the remaining supplemental tables:

(Porman *et al.*, 2013).

CHAPTER 5: DISCUSSION

RESULTS SUMMARY

Candida species inhabit nearly seven out of ten individuals, typically residing within the gastrointestinal tract as a component of the normal flora (Taylor *et al.*, 2003; Schulze and Sonnenborn, 2009). Despite being an ubiquitous commensal, *Candida* species also cause opportunistic disease such as invasive candidiasis, which kills approximately 4 out of every million Americans (Pfaller and Diekema, 2007). An essential component to their success in the human host is their ability to sense and respond to environmental signals. Signaling molecules, such as pheromones, allow *Candida* species to communicate between one another and to orchestrate complex multicellular responses. Therefore, it is imperative that we understand their contribution to the biology of this opportunistic pathogen.

Antagonism between pheromone and protease

This thesis began with an investigation of the role of the Bar1 protease and its ability to degrade α pheromone, as well as other potential targets including pheromones from related *Candida* species. Previous studies showed that Bar1 plays a critical role in regulating the pheromone response in *C. albicans* through degradation of α pheromone (Schaefer *et al.*, 2007). Not only does Bar1 act to restrict autocrine signaling, but it also enables cells to resume cell cycle progression and growth following pheromone exposure (Schaefer *et al.*, 2007; Alby *et al.*, 2009; Alby *et al.*, 2010). Additional studies have shown that *C. albicans* responds to a variety of peptides via the pheromone signaling cascade, including peptide pheromones from species that

share host niches with *C. albicans* (Alby and Bennett, 2011). This suggested that in its native environment, Bar1 likely encounters such peptides and, to act as an effective modulator of the signaling cascade, must also degrade them. We found strong evidence for this at the biochemical level, where mass-spectrometry data showed that Bar1 cleaves a variety of peptides including the α pheromones from several related *Candida* species (Chapter 2). Furthermore, cell-based assays showed that deletion of *BAR1* increased the sensitivity of *C. albicans* to other *Candida* pheromones, independent from the effects of the autocrine signaling mechanism (Alby et al., 2009; Yi, Sahni, Daniels, Lu, Huang, Srikantha, et al., 2011). The implications of these results are discussed later in the section "The role of Bar1 and pheromone in inter-species mating."

Biofilms, a pheromone response of multiple *Candida* species

Biofilm formation is one of several well-documented pheromone responses in *C. albicans*, and is known to contribute to the antibiotic resistance of the species. While *C. albicans* opaque cells respond to pheromones by forming conjugation tubes in preparation for mating, white cells respond by forming biofilms by adhering to and coordinating growth on abiotic substrates. It is proposed that biofilms formed in response to sexual pheromones function to facilitate mating among rare opaque cells in the host (Daniels *et al.*, 2006). Since *C. tropicalis* was recently found to undergo a white-opaque regulated sexual cycle similar to that of *C. albicans*, we reasoned that *C. tropicalis* white and opaque cells might also mount a dual response to pheromones. Early attempts at discovery of such biofilms in *C. tropicalis* were unsuccessful (SJ unpublished observations) for two important reasons: First, it is now apparent *C. tropicalis* opaque cells, and not white cells, undergo biofilm formation. That is, both mating *and* biofilm formation are opaque-specific responses to pheromone stimulation. Second, I

demonstrated that a single mating type alone (either **a** or α) will not form biofilms in response to exposure to the reciprocal pheromone. Rather, it appears that **a** and α cells must physically contact one another in order to form biofilms, which is supported by a number of experiments. These included the use of agglutinin deletion mutants, and differences in biofilm formation between exogenous pheromone addition and co-culturing of **a** and α cell mixtures. It is particularly interesting that although some of the parameters have changed, biofilm formation in response to pheromone stimulation is a conserved response among *C. albicans* and *C. tropicalis*.

The relationship between biofilm formation and cell phenotype

Work over the last decade has shown that the phenotypic state of a cell can be an important determinant of biofilm formation (Daniels *et al.*, 2006; Yi *et al.*, 2008; Jones *et al.*, 2014). Several stimuli are known to induce biofilm formation *in vitro* in *C. albicans*. Those commonly used include pheromones, blood serum, and RPMI and Spider media (Ramage *et al.*, 2001; Nobile and Mitchell, 2005; Daniels *et al.*, 2006; Daniels *et al.*, 2013). Many of these also induce filamentation (Taschdjian *et al.*, 1960; Liu *et al.*, 1994), which is an important component of biofilm development. However, biofilm formation typically occurs in cells of the white phenotypic state, with the exception of *C. tropicalis* sexual biofilms, as described in Chapter 3. Our curiosity about this relationship between phenotype and biofilm capability drove us to study phenotype dynamics within the sexual biofilm model. We showed that in *C. albicans,* the requirement for white and opaque cell participation in biofilm formation is strain dependent, and suggested compatibility between signaling partners is also important. In *C. tropicalis*, our work demonstrated that *WOR1*, which encodes the master regulator of the switch between white and opaque phenotypes, is a potent inducer of biofilm formation when highly expressed

(Chapter 4). *WOR1* was also demonstrated to regulate filamentation in *C. tropicalis*, providing a firm link between these two phenomena, as illustrated by our microscopy and gene regulation studies (Chapters 3 and 4).

THE PHEROMONE SIGNALING SYSTEM, AN EVOLUTIONARY ARMS RACE?

In a pheromone signaling system, the genes encoding both the pheromone and receptor are subject to evolutionary forces. Selection must act to maintain the integrity of the pheromone-receptor interaction or else the signaling system can fail. For example, in a receptor that recognizes a protein ligand, any mutation that modifies the ligand's sequence must usually be matched by a compensatory mutation in the receptor, or the signaling dynamics of the system may be altered. These evolutionary "arms races" have been occurring as long as life itself. Well-studied examples include egg-sperm interactions as in the abalone, where sperm lysin coevolves with VERL, an egg protein that is unraveled by lysin to allow sperm passage through the egg vitelline envelope (Evans and Sherman, 2013). This system is under positive selective pressure, where rapid evolution maintains the VERL-lysin interaction and isolates one species of abalone from another (Evans and Sherman, 2013). While the abalone egg and sperm benefit from this system, other coevolving systems are not necessarily beneficial to both components. For example, host-virus interactions often involve evolution by the virus to maintain recognition of its host receptor of choice, at the host's expense (Obbard and Dudas, 2014). As is the case for the transferrin receptor (TfR1) in mice, receptors may in turn evolve to reduce recognition. TfR1 is rare in that viruses do not recognize its transferrin binding pocket, which has allowed TfR1 to evolve lower detection by viruses with minimal effect of its interaction with transferrin (Demogines *et al.*, 2013). Typically, however, a shared signal and virus binding site limit receptor evolution.

Evolutionary relationships are further compounded in three-part systems, as is the case for *C. albicans*, where the α pheromone acts as a ligand for both the Ste2 receptor and Bar1 protease (Figure 1). Here, changes in pheromone sequence may affect recognition by Ste2, Bar1 or both. While comparing peptides that were initially designed to test Ste2 activation, we found that those showing the greatest activation are also degraded by Bar1 protease. Notably,

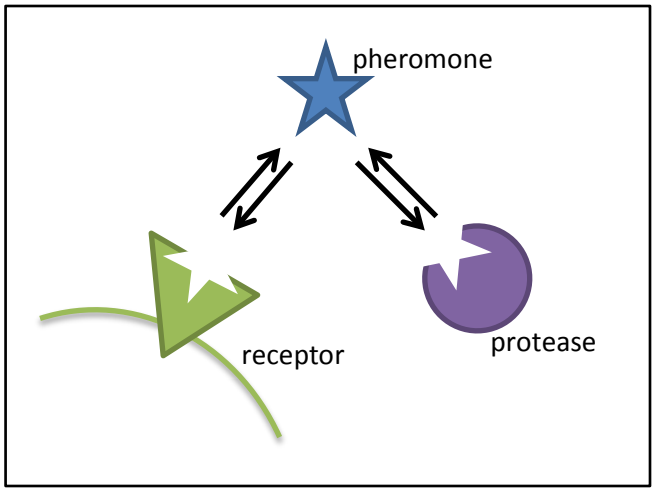

Figure 5-1: The three-part signaling system.

While no direct interaction occurs between receptor and protease, both are influenced by interactions with the pheromone.

peptides that are extremely divergent from *C. albicans* α pheromone (such as *S. cerevisiae* α-factor), very short, or modified at the C-terminus affected both of these interactions. This suggests that although Ste2 and Bar1 are very different types of proteins, they share similar ligand requirements; although, it may not be for the same reasons. For example, many proteases require a long substrate so that it can be 'held in position' during the subsequent cleavage event (Dunn and Hung, 2000). For Ste2, however, the length requirement may instead help differentiate the full length pheromone from the Bar1-degraded pheromone fragments. In comparison, both N- and C-terminus truncations of α-factor affect Ste2 binding in *S. cerevisiae*

(Eriotou-Bargiota *et al.*, 1992). Accordingly, we are currently determining the effects of shortening the C-terminus of α pheromone in *C. albicans*.

As detailed in the Introduction (Transducing the pheromone signal), *S. cerevisiae* provides much detail about the nature of the α pheromone – Ste2 interaction. It involves several regions of the receptor, including extracellular loops (EC) 2 and 3, and transmembrane regions (TM) 1, 5 and 6. Our group previously performed a multiple comparison among predicted Ste2 receptors of five *Candida* species, revealing that TM5 and TM6, which flank intracellular loop (IC) 3, are highly conserved among *Candida* species (Lin *et al.*, 2011). This region is needed for G-protein activation in *S. cerevisiae*, and the high sequence conservation between *S. cerevisiae* and *Candida* suggests this much is true for *Candida* as well, which is supported by experimental evidence in *C. albicans* (Lin *et al.*, 2011). On the other hand, TM1 is known to interact specifically with the C-terminus of α pheromone in *S. cerevisiae*, and it shows much greater divergence across *Candida* species than any other regions presumed to contact the pheromone. It is perhaps this interaction that determines the specificity of the pheromone – receptor interaction. Targeted mutation of this region could reveal if this is truly the case.

What is perhaps more interesting is that experiments in *C. albicans* have shown that the *C. albicans* Ste2 receptor can be activated by several *Candida* pheromones (Alby 2011), but when most other *Candida* Ste2 receptors are expressed in *C. albicans,* they can only be activated by the matching α pheromone (Lin 2013). The exception is a hybrid Ste2 made with a *C. albicans* C-terminal region connected to an otherwise-*C. tropicalis* Ste2 receptor, which responds to both *C. albicans* and *C. tropicalis* pheromones (Lin *et al.*, 2011). It is possible that the independence seen across the pheromone-receptor pairs relates to speciation events that

occurred in the *Candida* lineage, similarly to the VERL system described earlier, where compensatory mechanisms maintain specificity between the receptor and pheromone pair.

Alternatively, our studies have shown that a subset of peptides that activate Ste2 are not degraded by Bar1 (see Table 1, peptides 9, 12 and N-2). This may be due to differences in the sensitivity of assays used to detect interaction with Bar1 and Ste2, the nature of the activity (one may require higher specificity than the other) or perhaps, it highlights the evolutionary relationship between Bar1 and Ste2. That is, Bar1 activity on Ste2 ligands is selectable, since it can influence the frequency of signaling, but degradation of non-Ste2 ligands is not. Put simply, Bar1's utility disappears in the absence of Ste2. This inevitably shapes the arms race in *Candida albicans*. It is, of course, possible that there are peptides with the opposite characteristics – they are cleaved by Bar1 but do not activate Ste2. Our studies thus far have included only a few dozen peptides, so we are interested in exploring if Bar1-only interacting peptides exist. We have designed several peptides based on the iceLogo substrate motif for Bar1 (Chapter 2). Since the motif differs from α pheromone, it will be interesting to see how if and how the designed peptides interact with Bar1 and Ste2.

Future studies detailing the evolutionary history of α pheromone, Ste2 and Bar1 would be particularly insightful, showing how this evolutionary arms race has been manifested in different fungal species. One approach could include analysis of these three components across hemiascomycetes, as many species, including those without an identified mating cycle, are predicted to encode some of these components (see end of next section) (Butler *et al.*, 2009). It may also be illuminating to predict the pheromone sequence of *C. albicans* ancestors using the sequences of other *Candida* species as a guide, then testing how they perform in biological and biochemical experiments with *C. albicans*.

Table 5-1: Summary of peptides interacting with Bar1 protease and the Ste2 receptor.

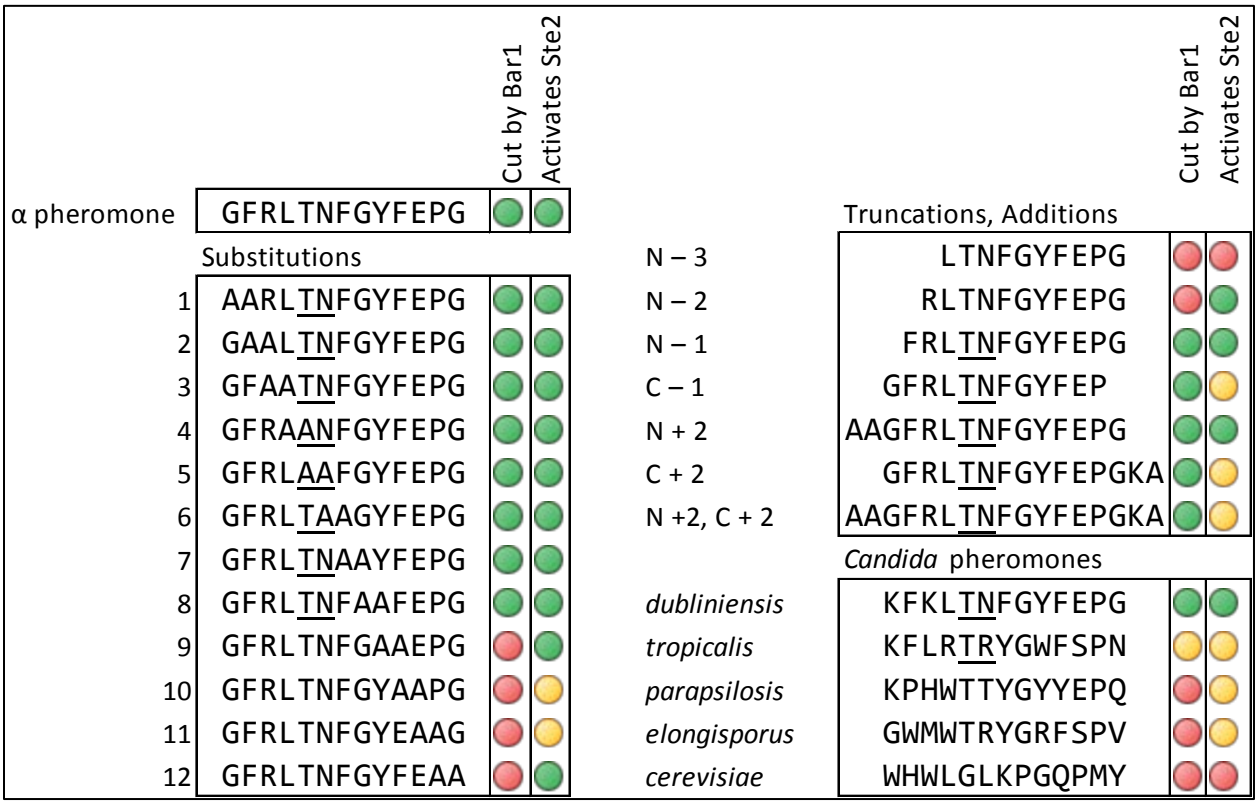

Bar1 degradation of peptide detected by mass spectrometry (Chapter 2); underlined residues denote cleavage site. Ste2 activation by peptide detected by mating response and biofilm production in *C. albicans* (Alby and Bennett, 2011).

Green: Cut by Bar1 in 1 hr incubation / Activates Ste2, showing response similar to α pheromone
Yellow: Cut by Bar1 in 24 hr incubation / Activates Ste2, showing a detectable response
Red: Not found to be cut by Bar1 / No detectable response

THE ROLE OF BAR1 AND PHEROMONES IN INTER-SPECIES SIGNALING

We have thus far detected inter-species signaling using synthetic pheromones to initiate communication and are currently extending these results to more physiologically relevant co-culture systems. The natural habitat of *Candida* species, however, is quite complex. Natural niches that *Candida* species occupy are also colonized by other microbes. For example, *Candida* share the human mouth with at least eighty-five fungal genera and at least ten thousand bacterial species (Ghannoum *et al.*, 2010; Liu *et al.*, 2012). Moreover, during infection, bacterial species such as *P. aeruginosa* are often co-isolated with *Candida* (Pierce, 2005; Huffnagle and Noverr, 2013). Accordingly, at least a dozen microbial signals involving *Candida* and its co-inhabitants have been described, though most are bacterial products that inhibit *Candida* growth and biofilm formation (Mallick and Bennett, 2013). Even among *Candida* species, production of farnesol and tyrosol are used to regulate filamentation and growth dynamics (Hogan, 2006; Lindsay *et al.*, 2012). Clearly, regulating growth patterns are an important goal of inter-species signaling.

Biofilm formation is an important growth strategy, and my work shows that it is controlled by pheromone signaling in *C. tropicalis* in addition to *C. albicans.* If pheromone signaling occurs among *Candida* species within the human host as it does *in vitro*, a logical assumption is that it can regulate biofilm formation in microbial communities containing multiple *Candida* species. This is then a plausible explanation for several aspects of *C. albicans* biology. First, the ability of *C. albicans* to respond to a variety of *Candida* pheromones (Alby and Bennett, 2011) may be a way for *C. albicans* to recognize biofilm formation cues (*i.e.* pheromones) that are secreted by a different *Candida* species. Autocrine signaling by biofilm-forming cells (Yi, Sahni, Daniels, Lu, Huang, Srikantha, *et al.*, 2011) would then be a method for

passing the signal to other *C. albicans* cells. Finally, Bar1 secretion removes the pheromone signal of multiple species when it is no longer favorable (Figure 2). This model suggests a positive role for Bar1 in a community containing multiple *Candida* species. Some aspects of this model will be tested in my future *C. albicans*/*C. tropicalis* co-culture biofilm experiments. I will begin by seeing if sexual biofilms of each species can form in the presence of the other, and if both species participate. If so, I can then use *MFα* and *BAR1* deletion mutants to investigate their roles in co-culture biofilms.

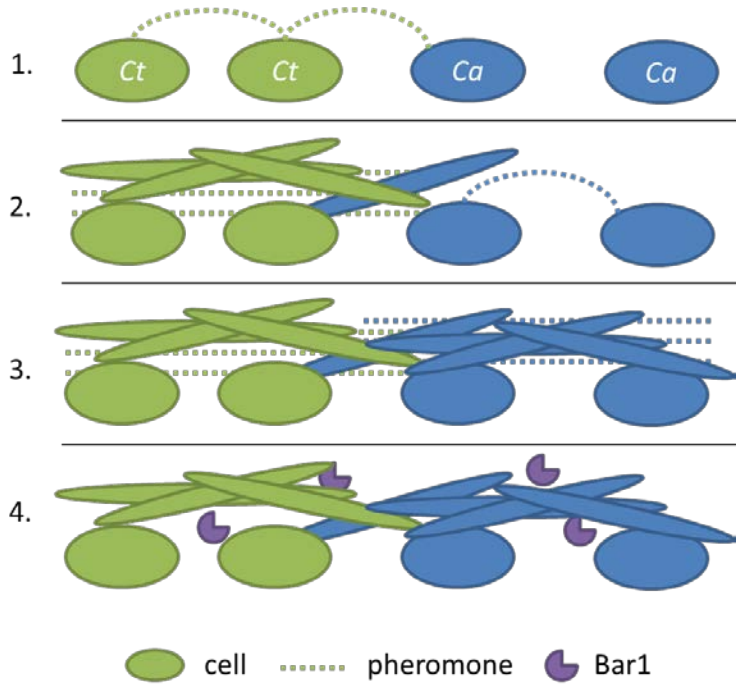

Figure 5-2: Model for pheromone signaling in a mixed species biofilm.

1. Conditions favor biofilm formation; *C. tropicalis* secretes pheromone.
2. *C. tropicalis* cells sense *C. tropicalis* pheromone and contribute to biofilm. *C. albicans* cells do too, but also secrete *C. albicans* pheromone via autocrine signaling.
3. Additional *C. albicans* cells sense *C. albicans* pheromone and contribute to biofilm.
4. After biofilm is formed, *C. albicans* produces bar1 to remove all pheromones from environment.

This model suggests a cooperative role for Bar1 in the mixed-species environment, however, it may instead provide a fitness advantage to *C. albicans* to the detriment of other *Candida* species. Bar1 activity could reduce other *Candida* species mating success by blocking or otherwise altering pheromone signaling in that species. This model is attractive if, first, mating is a positive attribute, and secondly, *Candida* species share an occupational niche. Bar1 activity would be one part of an overall strategy that *C. albicans* uses to compete against other *Candida* species.

The functional purpose of Bar1 probably lies somewhere between these roles and its roles in controlling same-sex mating and post-mating recovery (Schaefer *et al.*, 2007; Alby *et al.*, 2009). Data from similar proteins may be a useful way to cast an evolutionary perspective on this future area of research. Interestingly, *C. tropicalis* is predicted to encode its own pheromone protease (*CTRG_01112*), based on sequence similarity to *C. albicans BAR1*. Thus far, this gene and its product have not been studied, though the gene's transcript abundance was seen to increase in sexual biofilms (see Chapter 3). It would be worthwhile to investigate this gene product to examine its traits, how it compares to Bar1, and to see what role it plays within *C. tropicalis* and its greater microbial community. Mating and biofilm experiment using *CTRG_01112*-deleted cells would be a good initial strategy. It would be particularly interesting to see if white-phenotype deletion mutants approached the mating frequency of wildtype opaque cells, given that white cells mate only approximately one hundred times less frequently than opaque cells (Porman *et al.*, 2011), and that *CTRG_01112*-deleted cells may have increased pheromone sensitivity.

WHY SEPARATE MATING AND BIOFILM FORMATION?

C. albicans white cells form biofilms in response to pheromones while opaque cells mate, but in *C. tropicalis*, opaque cells mount both mating and biofilm responses. Thus, these closely related *Candida* species provide a unique opportunity to consider the effects of labor division within single-celled organisms. Biofilms are a communal structure, where the success of a cell is sacrificed for success of the community, much as in cells of a tissue of a plant or animal (Buss, 1987). Within the confines of a biofilm, cells of the white and opaque phenotypes, much like yeast and filaments, can fulfill distinct communal roles. In *C. albicans*, it is thought that opaque cells use pheromones to signal white cells to form biofilms, so that white cells can then provide a niche where signaling and mating are more efficient among opaque cells (Daniels *et al.*, 2006). While a seemingly sound strategy, *C. tropicalis* at least suggests that there are other methods.

Switching between phenotypic states can be costly. Overall, switching events are rare in *C. albicans*, happening approximately once per 10,000 generations (Rikkerink *et al.*, 1988; Bergen *et al.*, 1990) and depending strongly on growth rate, as switching requires buildup of the Wor1 transcription factor (Alby *et al.*, 2010). While switching may occur faster in some host conditions, its complex regulation (Hernday *et al.*, 2013) suggests that switching events will always burden the cell. Indeed, switching is a strategy employed by stressed cells, and desperation often induces expensive strategies. Therefore, the switching requirement would appear to be detrimental to speedy establishment of a biofilm.

It is important to realize, however, that using cell phenotypes to separate two responses (mating, biofilm formation) to the same stimulus (pheromone) can yield more specialization. Thus, this “division of labor” allows opaque cells to only express genes for mating and not

biofilms, and vise-versa. Each response is not burdened by the requirements of the other, and the differential transcriptomes of white and opaque cells upon pheromone exposure support this (Bennett *et al.*, 2003; Lin *et al.*, 2013). Exactly how this differential response is regulated is still unknown. Within the literature, it was suggested that either unique portions of the Ste2 receptor (Yi *et al.*, 2009) or the terminal transcription factor within the signaling cascade allowed for this differential response (Sahni *et al.*, 2010), but both were later proven false (Lin *et al.*, 2011). Some of the confusion may stem from the variety of conditions that can either support or discourage sexual biofilms in *C. albicans* (SJ unpublished results) (Daniels *et al.*, 2013). More likely though, it may be that these responses are not firmly bound to a single phenotypic state (Chapter 4), and that the use of cells in a single phenotypic state has biased our understanding of mating and biofilms in *C. albicans.*

What then of *C. tropicalis*, where opaque cells perform both biofilm and mating tasks? One important observation is that switching is more 'stubborn' in *C. tropicalis*. In our hands, switching events in *C. tropicalis* are rarer than in *C. albicans,* sustained longer, and less affected by environmental conditions (SJ unpublished data) (Porman *et al.*, 2011). Further, the transcriptional wiring of the white-opaque switch is quite different from *C. albicans*, with some transcription factors showing opposing roles in the two species, as well as stable, intermediate phenotypic states between white and opaque (Porman, 2015). This, along with recent work in *C. albicans* (Nobile *et al.*, 2012) and other evolutionary comparisons, indicate that the switch is quite young. As detailed in Chapter 4, *C. tropicalis* also has a clear overlap between the regulation of filamentation, which is necessary for biofilm formation, and the opaque phenotypic state, via Wor1. Like *C. tropicalis,* other fungal species contain Wor1 orthologs, and they are regulators of filamentation, too. Therefore, as is seen for filamentation and other biofilm models, the sexual biofilm response may precede a well-defined white-opaque switch

evolutionarily. Thus, the reasons as to why pheromone responses differ by phenotypic state are difficult to answer in the context of switching systems undergoing recent evolution.

How do *Candida* sexual biofilms relate to other microbial biofilms?

A variety of biofilm models have been designed and studied in *Candida* species. *In vitro* models are typically based on either a polystyrene substrate (as in the current study) or a silicone substrate (Hawser and Douglas, 1994; Daniels *et al.*, 2006), while popular *in vivo* models include rodent-implanted dentures and catheters (Andes *et al.*, 2004; Nett *et al.*, 2010). Despite the variety of conditions, there are common architectural traits found whenever *Candida* species form biofilms: a base layer of yeast-form cells is established directly on the substrate surface, and then a filamentous cell network develops on top, while extracellular matrix is produced throughout both layers (Chandra *et al.*, 2001). While thickness and orientation may be variable, the presence of both layers typically is not. Indeed, the sexual biofilms presented in this manuscript exhibit these structural hallmarks, and our results yield high-resolution details of this phenomenon (Chapter 3). We also provided analysis of *WOR1* overexpression biofilms, which were exceptional for their structural homogeneity in comparison to other *Candida* biofilms (Chapter 4).

Recently, colleagues in the Johnson laboratory at UCSF have described a core set of six transcriptional regulators that control the genes necessary for biofilm formation in *C. albicans* (Nobile *et al.*, 2012). Several *C. albicans* biofilm models, including pheromone-induced biofilms (Lin *et al.*, 2013) and poly-microbial biofilms (Fox and Nobile, 2012) support this assertion. Curiously, none of these core regulators were upregulated in the *C. tropicalis* biofilms we studied, though overall, the biofilms were transcriptionally similar to *C. albicans* pheromone-induced biofilms. Either sexual biofilms are one of several distinct biofilm types produced by *C.*

tropicalis and are unique in their difference from *C. albicans*, or the regulation of biofilms has undergone rapid evolution within the *Candida* clade. The latter is better supported: as stated earlier, 'younger' genes are overrepresented in the regulon of the core biofilm transcription factors (Nobile *et al.*, 2012). Furthermore, biofilms produced by the related species *Candida parapsilosis* are also divergent. In *C. parapsilosis,* the core factor Bcr1 is dispensable for biofilm formation, whereas it is a key player in *C. albicans* biofilms (Pannanusorn *et al.*, 2014).

While transcription factors may differ, like *C. albicans*, *C. tropicalis* biofilms have increased expression of adhesins and agglutinins that aid in the adhesion and cohesion necessary to establishing biofilms (Bonhomme and d' Enfert, 2013). Our work detailed how a particular agglutinin, Fgr23, is involved in biofilm formation. Interestingly, *FGR23* is upregulated in both *C. albicans* and *C.tropicalis* sexual biofilms (Lin *et al.*, 2013; Jones *et al.*, 2014), while most other biofilm models typically upregulate agglutinins of the *ALS* gene family (Nobile *et al.*, 2008). Unlike many *ALS* genes, *FGR23* is also induced upon pheromone receptor activation (Bennett *et al.*, 2003), and its deletion diminishes the mating response in *C. tropicalis* (Chapter 3), consistent with its role in sexual interactions. It may be interesting to move the sexual agglutinins of another species, such as *S. cerevisiae,* into *C. tropicalis* to see if they can function in place of Fgr23 in biofilm formation and mating. Additionally, we have begun investigating *FGR23* deletion mutants in *C. albicans*, to see how mating and biofilm formation are influenced. Between architecture, transcription and adhesion, there are clear similarities across *Candida* biofilms; though, studying their differences may tell us about how biofilms are specialized for each organism.

IS BIOFILM FORMATION A VALID TARGET FOR ANTIFUNGAL DRUGS?

Biofilms are medically relevant structures, known to form on a variety of medical devices, and are associated with mortal *Candida* infections (Febré *et al.*, 1999; Crump and Collignon, 2000; Tumbarello *et al.*, 2007; Mohammadi *et al.*, 2013). Once formed, biofilms are resistant to common antibiotic treatments (Melo *et al.*, 2011; Silva *et al.*, 2012). Recent research has shown that much of this resistance is due to carbohydrate components of the biofilm extracellular matrix (Nett *et al.*, 2010; Mitchell *et al.*, 2013). This suggests that rather than targeting existing biofilms, prevention of biofilm formation in the first place is a more tractable goal. One area of active development that is based in this strategy is the production of polymeric coatings that discourage microbial growth (Charnley *et al.*, 2011). These materials have already been successfully employed for spinal injury treatments (Difusiontech.com). While useful, unfortunately not all medically relevant biofilms grow on abiotic surfaces, and therefore require an alternative approach.

Administration of small molecules could be a method to block biofilm establishment. Clearly, as with *C. albicans* and *C. tropicalis* pheromones, they are enough to induce them. While a protease like Bar1 might appear to be an attractive method for blocking at least one biofilm-inducing signal (pheromone) in the host, its qualities make it a poor option: it is foreign, large and complex and would therefore almost certainly induce a strong immune response (Coico and Sunshine, 2009). Small molecules that could inhibit the signaling necessary for intercellular communication are more suitable. This approach has already seen some success in *C. albicans* (Grald *et al.*, 2012) and in *Pseudomonas aeruginosa* (O'Loughlin *et al.*, 2013). With proven efficacy against biofilms *in vitro*, hopefully, these advancements will find their way to medical use. Meanwhile, their development is a promising are of research.

CANDIDA SPECIES IN SYNTHETIC BIOLOGY

Synthetic biology is a growing area within the scientific community, promising to advance areas such as medicine, fuel production and industrial chemistry. Despite pharmacological successes such as Artemisinin and Sitagliptin (Ro *et al.*, 2006; Savile *et al.*, 2010), the field still faces many limitations. Currently, organisms used as chassis for synthetic biology are selected by their ease of manipulation rather than their overall suitability for the intended function, a weakness that has become more apparent in recent years. One of the greatest limitations due to this strategy is the lack of robustness in genetically modified organisms, where fast generation times and genomic instability often lead to short-lived synthetic biology constructs (Sleight *et al.*, 2010). When compared to the most commonly used organism in synthetic biology, *E. coli*, *Candida* exhibits longer generation times, lower mutational rates and does not undergo horizontal gene transfer (Dabrowa *et al.*, 1968; Drake, 1991; Fitzpatrick *et al.*, 2008; Butler *et al.*, 2009), which may make *Candida* species more stable, and therefore more suitable, than organisms currently used in synthetic biology. *E. coli*'s strength derives from its well-characterized genome and suite of available genetic tools, but work over recent decades has brought these strengths to *Candida* as well, especially *C. albicans*. In *C. albicans*, the genome is well-annotated and many tools for genetic engineering, such as auxotrophic markers, high-efficiency transformation protocols and protein tags are in regular use.

C. albicans has additional strengths when considering its use as a synthetic biology chassis. It properly expresses and glycosylates eukaryotic proteins, which is a sought out characteristic for systems engineered to produce human components. When considering organism robustness, it is worth noting that *C. albicans* maintains a diploid genome, which can

mask recessive mutant alleles that would otherwise lead to premature circuit failure. Furthermore, the extreme aneuploidy tolerance of *Candida* species suggests that it could stably propagate an additional synthetic chromosome if need be (Rustchenko, 2007). *C. albicans* has at least two unique features that may increase its suitability when compared to the current eukaryotic chassis of choice, *S. cerevisiae*. First, *C. albicans* pursues different metabolic pathways than *S. cerevisiae*; for example, in conditions where *S. cerevisiae* readily undergoes fermentation, *C. albicans* prefers the citric acid cycle. This may be useful in synthetic circuits that utilize TCA intermediaries, or where fermentation disrupts impedes correct circuit function. Second, *C. albicans* exhibits alternative codon usage, where CUG encodes serine rather than lysine (Sugita and Nakase, 1999). While this can impose a barrier during transfer of genes into *C. albicans*, it also works in the opposite way, limiting the activity of genomic contents upon transfer to organisms outside the *Candida* clade. In this way, alternative codon usage is a safety mechanism that prevents sharing of synthetic circuits among organisms once outside the lab; such traits are being actively pursued within the synthetic biology community and are an area of governmental concern (DARPA, n.d.). As synthetic biologists begin to select organisms for their overall suitability rather than just their ease of manipulation, a niche for *Candida* as chassis organisms will likely develop and progress the field.

Final Conclusions

The study of pheromone signals and responses in *Candida* species proposes challenging questions about the biology of these organisms. Their evolutionary success has been proven by their persistent threat to human health despite advances in our knowledge and anti-fungal therapies. Clearly, pheromone signaling contributes to this success, as we continue to find new ways in which these organisms use pheromones to coordinate their activities in and across

species boundaries. We discovered during our studies that *C. albicans* Bar1 exceeds the prescribed role for a pheromone protease by acting on a range of non-endogenous peptides including other *Candida* pheromones. This role 'extension' identifies an exciting method that *C. albicans* can use to control signal dynamics within the complex host environment. The discovery of sexual biofilms in *C. tropicalis* provides support for the utility of pheromone signaling and biofilm formation in pathogenesis, and when compared with *C. albicans,* affords an opportunity to study the evolutionary implications of the unique switching, signaling and biofilm forming abilities of these fungi. Finally, our results showing the shared role for Wor1 in biofilms, filamentation and switching indicate that these abilities overlap and are often integrated in unique ways befitting the organism. As a whole, these studies indicate the value of studying *Candida* species – while discovering the basic principles that guide the livelihood of these unusual microbes, we are also understanding the attributes that make them such tenacious pathogens.

REFERENCES

The references below pertain to Chapter 1 through Chapter 5.

Alberts, B., Johnson, A., Lewis, J., Raff, M., Roberts, K., and Walter, P. (2002) Meiosis. In *Molecular Biology of the Cell*. Garland Science, New York. http://www.ncbi.nlm.nih.gov/books/NBK26840/. Accessed December 24, 2014.

Alby, K., and Bennett, R.J. (2009) Stress-induced phenotypic switching in Candida albicans. *Mol Biol Cell* **20**: 3178–3191.

Alby, K., and Bennett, R.J. (2011) Interspecies pheromone signaling promotes biofilm formation and same-sex mating in Candida albicans. *Proc Natl Acad Sci U S A* **108**: 2510–2515.

Alby, K., Schaefer, D., and Bennett, R.J. (2009) Homothallic and heterothallic mating in the opportunistic pathogen Candida albicans. *Nature* **460**: 890–893.

Alby, K., Schaefer, D., Sherwood, R.K., Jones, S.K., and Bennett, R.J. (2010) Identification of a cell death pathway in Candida albicans during the response to pheromone. *Eukaryot Cell* **9**: 1690–1701.

Anderegg, R.J., Betz, R., Carr, S.A., Crabb, J.W., and Duntze, W. (1988) Structure of Saccharomyces cerevisiae mating hormone a-factor. Identification of S-farnesyl cysteine as a structural component. *J Biol Chem* **263**: 18236–18240.

Anderson, J., Cundiff, L., Schnars, B., Gao, M.X., Mackenzie, I., and Soll, D.R. (1989) Hypha formation in the white-opaque transition of Candida albicans. *Infect Immun* **57**: 458–467.

Anderson, J.M., and Soll, D.R. (1987) Unique phenotype of opaque cells in the white-opaque transition of Candida albicans. *J Bacteriol* **169**: 5579–5588.

Andes, D., Nett, J., Oschel, P., Albrecht, R., Marchillo, K., and Pitula, A. (2004) Development and characterization of an in vivo central venous catheter Candida albicans biofilm model. *Infect Immun* **72**: 6023–6031.

Bardwell, L. (2004) A walk-through of the yeast mating pheromone response pathway. *Peptides* **25**: 1465–1476.

Barkai, N., Rose, M.D., and Wingreen, N.S. (1998) Protease helps yeast find mating partners. *Nature* **396**: 422–423.

Bedell, G.W., and Soll, D.R. (1979) Effects of low concentrations of zinc on the growth and dimorphism of Candida albicans: evidence for zinc-resistant and -sensitive pathways for mycelium formation. *Infect Immun* **26**: 348–354.

Bennett, R.J., and Johnson, A.D. (2003) Completion of a parasexual cycle in Candida albicans by induced chromosome loss in tetraploid strains. *EMBO J* **22**: 2505–2515.

Bennett, R.J., and Johnson, A.D. (2005) Mating in Candida albicans and the search for a sexual cycle. *Annu Rev Microbiol* **59**: 233–255.

Bennett, R.J., Miller, M.G., Chua, P.R., Maxon, M.E., and Johnson, A.D. (2005) Nuclear fusion occurs during mating in Candida albicans and is dependent on the KAR3 gene. *Mol Microbiol* **55**: 1046–1059.

Bennett, R.J., Uhl, M.A., Miller, M.G., and Johnson, A.D. (2003) Identification and characterization of a Candida albicans mating pheromone. *Mol Cell Biol* **23**: 8189–8201.

Bergen, M.S., Voss, E., and Soll, D.R. (1990) Switching at the cellular level in the white-opaque transition of Candida albicans. *J Gen Microbiol* **136**: 1925–1936.

Bernhardt, J., Herman, D., Sheridan, M., and Calderone, R. (2001) Adherence and Invasion Studies of Candida albicans Strains, Using In Vitro Models of Esophageal Candidiasis. *J Infect Dis* **184**: 1170–1175.

Bobrowicz, P., Pawlak, R., Correa, A., Bell-Pedersen, D., and Ebbole, D.J. (2002) The Neurospora crassa pheromone precursor genes are regulated by the mating type locus and the circadian clock. *Mol Microbiol* **45**: 795–804.

Bonhomme, J., and Enfert, C. d' (2013) Candida albicans biofilms: building a heterogeneous, drug-tolerant environment. *Curr Opin Microbiol* **16**: 398–403.

Boyartchuk, V.L., Ashby, M.N., and Rine, J. (1997) Modulation of Ras and a-factor function by carboxyl-terminal proteolysis. *Science* **275**: 1796–1800.

Boyartchuk, V.L., and Rine, J. (1998) Roles of prenyl protein proteases in maturation of Saccharomyces cerevisiae a-factor. *Genetics* **150**: 95–101.

Breitkreutz, A., Boucher, L., and Tyers, M. (2001) MAPK specificity in the yeast pheromone response independent of transcriptional activation. *Curr Biol CB* **11**: 1266–1271.

Brown, G.D., Denning, D.W., and Levitz, S.M. (2012) Tackling human fungal infections. *Science* **336**: 647.

Buss, L.W. (1987) *The Evolution of Individuality*. Princeton University Press, .

Butler, G. (2010) Fungal sex and pathogenesis. *Clin Microbiol Rev* **23**: 140–159.

Butler, G., Rasmussen, M.D., Lin, M.F., Santos, M.A.S., Sakthikumar, S., Munro, C.A., *et al.* (2009) Evolution of pathogenicity and sexual reproduction in eight Candida genomes. *Nature* **459**: 657–662.

Butty, A.C., Pryciak, P.M., Huang, L.S., Herskowitz, I., and Peter, M. (1998) The role of Far1p in linking the heterotrimeric G protein to polarity establishment proteins during yeast mating. *Science* **282**: 1511–1516.

Cain, C.W., Lohse, M.B., Homann, O.R., Sil, A., and Johnson, A.D. (2012) A conserved transcriptional regulator governs fungal morphology in widely diverged species. *Genetics* **190**: 511–521.

Caplan, S., Green, R., Rocco, J., and Kurjan, J. (1991) Glycosylation and structure of the yeast MF alpha 1 alpha-factor precursor is important for efficient transport through the secretory pathway. *J Bacteriol* **173**: 627–635.

Chandra, J., Kuhn, D.M., Mukherjee, P.K., Hoyer, L.L., McCormick, T., and Ghannoum, M.A. (2001) Biofilm Formation by the Fungal PathogenCandida albicans: Development, Architecture, and Drug Resistance. *J Bacteriol* **183**: 5385–5394.

Chang, F., and Herskowitz, I. (1990) Identification of a gene necessary for cell cycle arrest by a negative growth factor of yeast: FAR1 is an inhibitor of a G1 cyclin, CLN2. *Cell* **63**: 999–1011.

Chan, R.K., and Otte, C.A. (1982) Isolation and genetic analysis of Saccharomyces cerevisiae mutants supersensitive to G1 arrest by a factor and alpha factor pheromones. *Mol Cell Biol* **2**: 11–20.

Charnley, M., Textor, M., and Acikgoz, C. (2011) Designed polymer structures with antifouling–antimicrobial properties. *React Funct Polym* **71**: 329–334.

Chen, H., Fujita, M., Feng, Q., Clardy, J., and Fink, G.R. (2004) Tyrosol is a quorum-sensing molecule in Candida albicans. *Proc Natl Acad Sci U S A* **101**: 5048–5052.

Chen, P., Choi, J.D., Wang, R., Cotter, R.J., and Michaelis, S. (1997) A novel a-factor-related peptide of Saccharomyces cerevisiae that exits the cell by a Ste6p-independent mechanism. *Mol Biol Cell* **8**: 1273–1291.

Chen, R.E., and Thorner, J. (2007) Function and regulation in MAPK signaling pathways: lessons learned from the yeast Saccharomyces cerevisiae. *Biochim Biophys Acta* **1773**: 1311–1340.

Choi, K.Y., Satterberg, B., Lyons, D.M., and Elion, E.A. (1994) Ste5 tethers multiple protein kinases in the MAP kinase cascade required for mating in S. cerevisiae. *Cell* **78**: 499–512.

Coico, R., and Sunshine, G. (2009) *Immunology: A Short Course*. Wiley, . http://books.google.com/books?id=Lxcj-PlALiIC.

Colaert, N., Helsens, K., Martens, L., Vandekerckhove, J., and Gevaert, K. (2009) Improved visualization of protein consensus sequences by iceLogo. *Nat Methods* **6**: 786–787.

Coppin, E., Renty, C. de, and Debuchy, R. (2005) The function of the coding sequences for the putative pheromone precursors in Podospora anserina is restricted to fertilization. *Eukaryot Cell* **4**: 407–420.

Coria, R., Kawasaki, L., Torres-Quiroz, F., Ongay-Larios, L., Sánchez-Paredes, E., Velázquez-Zavala, N., *et al.* (2006) The pheromone response pathway of Kluyveromyces lactis. *FEMS Yeast Res* **6**: 336–344.

Côte, P., Sulea, T., Dignard, D., Wu, C., and Whiteway, M. (2011) Evolutionary reshaping of fungal mating pathway scaffold proteins. *mBio* **2** http://www.ncbi.nlm.nih.gov/pubmed/21249169. Accessed February 18, 2011.

Côte, P., and Whiteway, M. (2008) The role of Candida albicans FAR1 in regulation of pheromone-mediated mating, gene expression and cell cycle arrest. *Mol Microbiol* **68**: 392–404.

Crump, J.A., and Collignon, P.J. (2000) Intravascular Catheter-Associated Infections. *Eur J Clin Microbiol Infect Dis* **19**: 1–8.

Dabrowa, N., Landau, J. w., and Newcomer, V. d. (1968) Generation time of Candida albicans in synchronized and nonsynchronized cultures. *Med Mycol* **6**: 51–56.

Daniels, K.J., Park, Y.-N., Srikantha, T., Pujol, C., and Soll, D.R. (2013) Impact of Environmental Conditions on the Form and Function of Candida albicans Biofilms. *Eukaryot Cell* **12**: 1389–1402.

Daniels, K.J., Srikantha, T., Lockhart, S.R., Pujol, C., and Soll, D.R. (2006) Opaque cells signal white cells to form biofilms in Candida albicans. *EMBO J* **25**: 2240–2252.

DARPA Biological Robustness in Complex Settings (BRICS) Proposers' Day - Federal Business Opportunities: Opportunities. https://www.fbo.gov/index?s=opportunity&mode=form&id=9754c98ba9410fcd7a3befe09c8d6b6f&tab=core&_cview=0. Accessed December 23, 2014.

Davidson, R.C., Moore, T.D., Odom, A.R., and Heitman, J. (2000) Characterization of the MFalpha pheromone of the human fungal pathogen cryptococcus neoformans. *Mol Microbiol* **38**: 1017–1026.

Demogines, A., Abraham, J., Choe, H., Farzan, M., and Sawyer, S.L. (2013) Dual host-virus arms races shape an essential housekeeping protein. *PLoS Biol* **11**: e1001571.

Dignard, D., André, D., and Whiteway, M. (2008) Heterotrimeric G-Protein Subunit Function in Candida albicans: both the α and β Subunits of the Pheromone Response G Protein Are Required for Mating. *Eukaryot Cell* **7**: 1591–1599.

Dignard, D., El-Naggar, A.L., Logue, M.E., Butler, G., and Whiteway, M. (2007) Identification and characterization of MFA1, the gene encoding Candida albicans a-factor pheromone. *Eukaryot Cell* **6**: 487–494.

Dmochowska, A., Dignard, D., Henning, D., Thomas, D.Y., and Bussey, H. (1987) Yeast KEX1 gene encodes a putative protease with a carboxypeptidase B-like function involved in killer toxin and alpha-factor precursor processing. *Cell* **50**: 573–584.

Dosil, M., Schandel, K.A., Gupta, E., Jenness, D.D., and Konopka, J.B. (2000) The C terminus of the Saccharomyces cerevisiae alpha-factor receptor contributes to the formation of preactivation complexes with its cognate G protein. *Mol Cell Biol* **20**: 5321–5329.

Drake, J.W. (1991) A constant rate of spontaneous mutation in DNA-based microbes. *Proc Natl Acad Sci* **88**: 7160–7164.

Dumitru, R., Navarathna, D.H.M.L.P., Semighini, C.P., Elowsky, C.G., Dumitru, R.V., Dignard, D., *et al.* (2007) In vivo and in vitro anaerobic mating in Candida albicans. *Eukaryot Cell* **6**: 465–472.

Dunn, B.M. (2001) Overview of pepsin-like aspartic peptidases. *Curr Protoc Protein Sci Editor Board John E Coligan Al* **Chapter 21**: Unit 21.3.

Dunn, B.M., and Hung, S.-H. (2000) The two sides of enzyme–substrate specificity: lessons from the aspartic proteinases. *Biochim Biophys Acta BBA - Protein Struct Mol Enzymol* **1477**: 231–240.

Eglen, R.M., and Reisine, T. (2009) New insights into GPCR function: implications for HTS. *Methods Mol Biol Clifton NJ* **552**: 1–13.

Eilers, M., Hornak, V., Smith, S.O., and Konopka, J.B. (2005) Comparison of class A and D G protein-coupled receptors: common features in structure and activation. *Biochemistry (Mosc)* **44**: 8959–8975.

Elion, E.A., Satterberg, B., and Kranz, J.E. (1993) FUS3 phosphorylates multiple components of the mating signal transduction cascade: evidence for STE12 and FAR1. *Mol Biol Cell* **4**: 495–510.

Eriotou-Bargiota, E., Xue, C.B., Naider, F., and Becker, J.M. (1992) Antagonistic and synergistic peptide analogues of the tridecapeptide mating pheromone of Saccharomyces cerevisiae. *Biochemistry (Mosc)* **31**: 551–557.

Ernst, J.F. (2000) Transcription factors in Candida albicans - environmental control of morphogenesis. *Microbiol Read Engl* **146 (Pt 8)**: 1763–1774.

Evans, J.P., and Sherman, C.D.H. (2013) Sexual Selection and the Evolution of Egg-Sperm Interactions in Broadcast-Spawning Invertebrates. *Biol Bull* **224**: 166–183.

Febré, N., Silva, V., Medeiros, E. a. S., Wey, S.B., Colombo, A.L., and Fischman, O. (1999) Microbiological Characteristics of Yeasts Isolated from Urinary Tracts of Intensive Care Unit Patients Undergoing Urinary Catheterization. *J Clin Microbiol* **37**: 1584–1586.

Filmore, D. (2004) It'sa GPCR world. *Mod Drug Discov* **7**: 24–28.

Finkel, J.S., and Mitchell, A.P. (2011) Genetic control of Candida albicans biofilm development. *Nat Rev Microbiol* **9**: 109–118.

Fitzpatrick, D.A., Logue, M.E., and Butler, G. (2008) Evidence of recent interkingdom horizontal gene transfer between bacteria and Candida parapsilosis. *BMC Evol Biol* **8**: 181.

Forche, A., Alby, K., Schaefer, D., Johnson, A.D., Berman, J., and Bennett, R.J. (2008) The parasexual cycle in Candida albicans provides an alternative pathway to meiosis for the formation of recombinant strains. *PLoS Biol* **6**: e110.

Fowler, T.J., Mitton, M.F., Rees, E.I., and Raper, C.A. (2004) Crossing the boundary between the B[alpha] and B[beta] mating-type loci in Schizophyllum commune. *Fungal Genet Biol* **41**: 89–101.

Fox, E.P., and Nobile, C.J. (2012) A sticky situation: untangling the transcriptional network controlling biofilm development in Candida albicans. *Transcription* **3**: 315–322.

Fujimura-Kamada, K., Nouvet, F.J., and Michaelis, S. (1997) A Novel Membrane-associated Metalloprotease, Ste24p, Is Required for the First Step of NH2-terminal Processing of the Yeast a-Factor Precursor. *J Cell Biol* **136**: 271 –285.

Fuller, R., Brake, A., Sterne, R., Kunisawa, R., Barnes, D., Flessel, M., and Thorner, J. (1985) Post-translational processing events in the maturation of yeast pheromone precursors. .

Fusek, M., Smith, E.A., Monod, M., Dunn, B.M., and Foundling, S.I. (1994) Extracellular Aspartic Proteinases from Candida albicans, Candida tropicalis, and Candida parapsilosis Yeasts Differ Substantially in Their Specificities. *Biochemistry (Mosc)* **33**: 9791–9799.

Geiger, J., Wessels, D., Lockhart, S.R., and Soll, D.R. (2004) Release of a Potent Polymorphonuclear Leukocyte Chemoattractant Is Regulated by White-Opaque Switching in Candida albicans. *Infect Immun* **72**: 667–677.

Ghannoum, M.A., Jurevic, R.J., Mukherjee, P.K., Cui, F., Sikaroodi, M., Naqvi, A., and Gillevet, P.M. (2010) Characterization of the Oral Fungal Microbiome (Mycobiome) in Healthy Individuals. *PLoS Pathog* **6**: e1000713.

Ghosh, A.K. (2011) *Aspartic Acid Proteases as Therapeutic Targets*. John Wiley & Sons, .

Glick, M., and Siegel, M.A. (1999) Viral and fungal infections of the oral cavity in immunocompetent patients. *Infect Dis Clin North Am* **13**: 817–831, vi.

Grald, A., Yargosz, P., Case, S., Shea, K., and Johnson, D.I. (2012) Small-molecule inhibitors of biofilm formation in laboratory and clinical isolates of Candida albicans. *J Med Microbiol* **61**: 109–114.

Guo, M., Aston, C., Burchett, S.A., Dyke, C., Fields, S., Rajarao, S.J.R., *et al.* (2003) The yeast G protein alpha subunit Gpa1 transmits a signal through an RNA binding effector protein Scp160. *Mol Cell* **12**: 517–524.

Guthrie, C., and Fink, G.R. (1991) *Guide to Yeast Genetics and Molecular Biology: Part A-C*. Academic Press, Incorporated, .

Hammer, Ø., Harper, D.A.T., and Ryan, P.D. (2001) PAST: Paleontogical statistical software for education and data analysis. *Palaeontol Electron* **4**.

Harriott, M.M., and Noverr, M.C. (2011) Importance of Candida–bacterial polymicrobial biofilms in disease. *Trends Microbiol* **19**: 557–563.

Hawser, S.P., and Douglas, L.J. (1994) Biofilm formation by Candida species on the surface of catheter materials in vitro. *Infect Immun* **62**: 915–921.

He, B., Chen, P., Chen, S.Y., Vancura, K.L., Michaelis, S., and Powers, S. (1991) RAM2, an essential gene of yeast, and RAM1 encode the two polypeptide components of the farnesyltransferase that prenylates a-factor and Ras proteins. *Proc Natl Acad Sci U S A* **88**: 11373–11377.

Hedges, S.B. (2002) The origin and evolution of model organisms. *Nat Rev Genet* **3**: 838–849.

Heitman, J. (2007) *Sex in fungi: molecular determination and evolutionary implications*. ASM Press, .

Hernday, A.D., Lohse, M.B., Fordyce, P.M., Nobile, C.J., DeRisi, J.L., and Johnson, A.D. (2013) Structure of the transcriptional network controlling white-opaque switching in Candida albicans. *Mol Microbiol* **90**: 22–35.

Herrera, M.L., Wiederhold, N.P., Kirkpatrick, W.R., Olivo, M., Westbrook, S.D., Berg, D.K., *et al.* (2012) Detection of Multiple Candida Species in Oropharyngeal Candidiasis (OPC) Patients Using Real Time PCR. ASM Press, Denver, CO. http://www.icaaconline.com/php/icaac2013abstracts/. Accessed December 22, 2014.

Hickman, M.A., Zeng, G., Forche, A., Hirakawa, M.P., Abbey, D., Harrison, B.D., *et al.* (2013) The "obligate diploid" Candida albicans forms mating-competent haploids. *Nature* **494**: 55–59.

Hicks, J.B., and Herskowitz, I. (1976) Evidence for a new diffusible element of mating pheromones in yeast. *Nature* **260**: 246–248.

Hirakawa, M.P., Martinez, D.A., Sakthikumar, S., Anderson, M., Berlin, A., Gujja, S., *et al.* (2014) Genetic and phenotypic intra-species variation in Candida albicans. *Genome Res* .

Hisatomi, T., Yanagishima, N., Sakurai, A., and Kobayashi, H. (1988) Interspecific actions of alpha mating pheromones on the a mating-type cells of three Saccharomyces yeasts. *Curr Genet* **13**: 25–27.

Hoffman, C.S. (2005) Except in every detail: comparing and contrasting G-protein signaling in Saccharomyces cerevisiae and Schizosaccharomyces pombe. *Eukaryot Cell* **4**: 495–503.

Hogan, D.A. (2006) Talking to Themselves: Autoregulation and Quorum Sensing in Fungi. *Eukaryot Cell* **5**: 613–619.

Hornby, J.M., Jensen, E.C., Lisec, A.D., Tasto, J.J., Jahnke, B., Shoemaker, R., *et al.* (2001) Quorum Sensing in the Dimorphic FungusCandida albicans Is Mediated by Farnesol. *Appl Environ Microbiol* **67**: 2982–2992.

Hrycyna, C.A., Sapperstein, S.K., Clarke, S., and Michaelis, S. (1991) The Saccharomyces cerevisiae STE14 gene encodes a methyltransferase that mediates C-terminal methylation of a-factor and RAS proteins. *EMBO J* **10**: 1699–1709.

Huang, G., Srikantha, T., Sahni, N., Yi, S., and Soll, D.R. (2009) CO(2) regulates white-to-opaque switching in Candida albicans. *Curr Biol CB* **19**: 330–334.

Huang, G., Wang, H., Chou, S., Nie, X., Chen, J., and Liu, H. (2006) Bistable expression of WOR1, a master regulator of white-opaque switching in Candida albicans. *Proc Natl Acad Sci U S A* **103**: 12813–12818.

Huang, G., Yi, S., Sahni, N., Daniels, K.J., Srikantha, T., and Soll, D.R. (2010) N-Acetylglucosamine Induces White to Opaque Switching, a Mating Prerequisite in Candida albicans. *PLoS Pathog* **6**: e1000806.

Huffnagle, G.B., and Noverr, M.C. (2013) The emerging world of the fungal microbiome. *Trends Microbiol* **21**: 334–341.

Hull, C.M., and Johnson, A.D. (1999) Identification of a mating type-like locus in the asexual pathogenic yeast Candida albicans. *Science* **285**: 1271–1275.

Hull, C.M., Raisner, R.M., and Johnson, A.D. (2000) Evidence for mating of the "asexual" yeast Candida albicans in a mammalian host. *Science* **289**: 307–310.

Huyer, G., Kistler, A., Nouvet, F.J., George, C.M., Boyle, M.L., and Michaelis, S. (2006) Saccharomyces cerevisiae a-factor mutants reveal residues critical for processing, activity, and export. *Eukaryot Cell* **5**: 1560–1570.

Hyland, L.J., Tomaszek, T.A., and Meek, T.D. (1991) Human immunodeficiency virus-1 protease. 2. Use of pH rate studies and solvent kinetic isotope effects to elucidate details of chemical mechanism. *Biochemistry (Mosc)* **30**: 8454–8463.

Ido, E., Han, H.P., Kezdy, F.J., and Tang, J. (1991) Kinetic studies of human immunodeficiency virus type 1 protease and its active-site hydrogen bond mutant A28S. *J Biol Chem* **266**: 24359–24366.

Janiak, A.M., Sargsyan, H., Russo, J., Naider, F., Hauser, M., and Becker, J.M. (2005) Functional expression of the Candida albicans alpha-factor receptor in Saccharomyces cerevisiae. *Fungal Genet Biol FG B* **42**: 328–338.

Ji, S., and Choi, Y. (2013) Innate immune response to oral bacteria and the immune evasive characteristics of periodontal pathogens. *J Periodontal Implant Sci* **43**: 3–11.

Jones, S.K., Hirakawa, M.P., and Bennett, R.J. (2014) Sexual biofilm formation in Candida tropicalis opaque cells. *Mol Microbiol* **92**: 383–398.

Julius, D., Brake, A., Blair, L., Kunisawa, R., and Thorner, J. (1984) Isolation of the putative structural gene for the lysine-arginine-cleaving endopeptidase required for processing of yeast prepro-alpha-factor. *Cell* **37**: 1075–1089.

Kim, H., Lee, B.-K., Naider, F., and Becker, J.M. (2009) Identification of specific transmembrane residues and ligand-induced interface changes involved in homo-dimer formation of a yeast G protein-coupled receptor. *Biochemistry (Mosc)* **48**: 10976–10987.

Kolotila, M.P., and Diamond, R.D. (1990) Effects of neutrophils and in vitro oxidants on survival and phenotypic switching of Candida albicans WO-1. *Infect Immun* **58**: 1174–1179.

Kothe, E. (2008) Sexual attraction: on the role of fungal pheromone/receptor systems (A review). *Acta Microbiol Immunol Hung* **55**: 125–143.

Krcmery, V., and Barnes, A.J. (2002) Non-albicans Candida spp. causing fungaemia: pathogenicity and antifungal resistance. *J Hosp Infect* **50**: 243–260.

Kurjan, J., and Herskowitz, I. (1982) Structure of a yeast pheromone gene (MF alpha): a putative alpha-factor precursor contains four tandem copies of mature alpha-factor. *Cell* **30**: 933–943.

Kvaal, C.A., Srikantha, T., and Soll, D.R. (1997) Misexpression of the white-phase-specific gene WH11 in the opaque phase of Candida albicans affects switching and virulence. *Infect Immun* **65**: 4468–4475.

Kvaal, C., Lachke, S.A., Srikantha, T., Daniels, K., McCoy, J., and Soll, D.R. (1999) Misexpression of the Opaque-Phase-Specific GenePEP1 (SAP1) in the White Phase of Candida albicans Confers Increased Virulence in a Mouse Model of Cutaneous Infection. *Infect Immun* **67**: 6652–6662.

Ladds, G., and Davey, J. (1996) Purification of Sxa2, a carboxypeptidase involved in pheromone recovery in fission yeast. *Biochem Soc Trans* **24**: 504S.

Ladds, G., and Davey, J. (2000) Sxa2 is a serine carboxypeptidase that degrades extracellular P-factor in the fission yeast Schizosaccharomyces pombe. *Mol Microbiol* **36**: 377–390.

Ladds, G., Davis, K., Das, A., and Davey, J. (2005) A constitutively active GPCR retains its G protein specificity and the ability to form dimers. *Mol Microbiol* **55**: 482–497.

Laffey, S.F., and Butler, G. (2005) Phenotype switching affects biofilm formation by Candida parapsilosis. *Microbiol Read Engl* **151**: 1073–1081.

Lan, C.-Y., Newport, G., Murillo, L.A., Jones, T., Scherer, S., Davis, R.W., and Agabian, N. (2002) Metabolic specialization associated with phenotypic switching in Candidaalbicans. *Proc Natl Acad Sci U S A* **99**: 14907–14912.

Lee, B.K., Khare, S., Naider, F., and Becker, J.M. (2001) Identification of residues of the Saccharomyces cerevisiae G protein-coupled receptor contributing to alpha-factor pheromone binding. *J Biol Chem* **276**: 37950–37961.

Lee, K.L., Buckley, H.R., and Campbell, C.C. (1975) An amino acid liquid synthetic medium for the development of mycellal and yeast forms of *Candida albicans*. *Med Mycol* **13**: 148–153.

Lee, S.C., Ni, M., Li, W., Shertz, C., and Heitman, J. (2010) The evolution of sex: a perspective from the fungal kingdom. *Microbiol Mol Biol Rev MMBR* **74**: 298–340.

Lengeler, K.B., Davidson, R.C., D'souza, C., Harashima, T., Shen, W.C., Wang, P., *et al.* (2000) Signal transduction cascades regulating fungal development and virulence. *Microbiol Mol Biol Rev MMBR* **64**: 746–785.

Lin, C.-H., Choi, A., and Bennett, R.J. (2011) Defining pheromone-receptor signaling in Candida albicans and related asexual Candida species. *Mol Biol Cell* **22**: 4918–4930.

Lin, C.-H., Kabrawala, S., Fox, E.P., Nobile, C.J., Johnson, A.D., and Bennett, R.J. (2013) Genetic Control of Conventional and Pheromone-Stimulated Biofilm Formation in Candida albicans. *PLoS Pathog* **9** http://www.ncbi.nlm.nih.gov/pmc/articles/PMC3630098/. Accessed May 29, 2013.

Lindsay, A.K., Deveau, A., Piispanen, A.E., and Hogan, D.A. (2012) Farnesol and Cyclic AMP Signaling Effects on the Hypha-to-Yeast Transition in Candida albicans. *Eukaryot Cell* **11**: 1219–1225.

Lin, J.C., Parrish, W., Eilers, M., Smith, S.O., and Konopka, J.B. (2003) Aromatic Residues at the Extracellular Ends of Transmembrane Domains 5 and 6 Promote Ligand Activation of the G Protein-Coupled α-Factor Receptor†. *Biochemistry (Mosc)* **42**: 293–301.

Liu, B., Faller, L.L., Klitgord, N., Mazumdar, V., Ghodsi, M., Sommer, D.D., *et al.* (2012) Deep Sequencing of the Oral Microbiome Reveals Signatures of Periodontal Disease. *PLoS ONE* **7**: e37919.

Liu, H., Kohler, J., and Fink, G.R. (1994) Suppression of hyphal formation in Candida albicans by mutation of a STE12 homolog. *Science* **266**: 1723–1726.

Lockhart, S.R., Daniels, K.J., Zhao, R., Wessels, D., and Soll, D.R. (2003) Cell biology of mating in Candida albicans. *Eukaryot Cell* **2**: 49–61.

Lockhart, S.R., Pujol, C., Daniels, K.J., Miller, M.G., Johnson, A.D., Pfaller, M.A., and Soll, D.R. (2002) In Candida albicans, white-opaque switchers are homozygous for mating type. *Genetics* **162**: 737–745.

Lockhart, S., Zhao, R., Daniels, K.J., and Soll, D.R. (2003) Alpha-pheromone-induced "shmooing" and gene regulation require white-opaque switching during Candida albicans mating. *Eukaryot Cell* **2**: 847–855.

Lohse, M.B., Hernday, A.D., Fordyce, P.M., Noiman, L., Sorrells, T.R., Hanson-Smith, V., *et al.* (2013) Identification and characterization of a previously undescribed family of sequence-specific DNA-binding domains. *Proc Natl Acad Sci U S A* **110**: 7660–7665.

Lohse, M.B., and Johnson, A.D. (2008) Differential Phagocytosis of White versus Opaque Candida albicans by Drosophila and Mouse Phagocytes. *PLoS ONE* **3**: e1473.

Lohse, M.B., and Johnson, A.D. (2010) Temporal anatomy of an epigenetic switch in cell programming: the white-opaque transition of C. albicans. *Mol Microbiol* **78**: 331–343.

Lu, H., Sun, Y., Jiang, Y.-Y., and Whiteway, M. (2014) Ste18p Is a Positive Control Element in the Mating Process of Candida albicans. *Eukaryot Cell* **13**: 461–469.

MacKay, V.L., Armstrong, J., Yip, C., Welch, S., Walker, K., Osborn, S., *et al.* (1991) Characterization of the Bar proteinase, an extracellular enzyme from the yeast Saccharomyces cerevisiae. *Adv Exp Med Biol* **306**: 161–172.

MacKay, V.L., Welch, S.K., Insley, M.Y., Manney, T.R., Holly, J., Saari, G.C., and Parker, M.L. (1988) The Saccharomyces cerevisiae BAR1 gene encodes an exported protein with homology to pepsin. *Proc Natl Acad Sci U S A* **85**: 55–59.

Magee, B.B., Legrand, M., Alarco, A.-M., Raymond, M., and Magee, P.T. (2002) Many of the genes required for mating in Saccharomyces cerevisiae are also required for mating in Candida albicans. *Mol Microbiol* **46**: 1345–1351.

Magee, B.B., and Magee, P.T. (1987) Electrophoretic karyotypes and chromosome numbers in Candida species. *J Gen Microbiol* **133**: 425–430.

Magee, B.B., and Magee, P.T. (2000) Induction of mating in Candida albicans by construction of MTLa and MTLalpha strains. *Science* **289**: 310–313.

Mallick, E.M., and Bennett, R.J. (2013) Sensing of the Microbial Neighborhood by Candida albicans. *PLoS Pathog* **9**: e1003661.

Manney, T.R. (1983) Expression of the BAR1 gene in Saccharomyces cerevisiae: induction by the alpha mating pheromone of an activity associated with a secreted protein. *J Bacteriol* **155**: 291–301.

McCreath, K.J., Specht, C.A., and Robbins, P.W. (1995) Molecular cloning and characterization of chitinase genes from Candida albicans. *Proc Natl Acad Sci U S A* **92**: 2544–2548.

Melo, A.S., Bizerra, F.C., Freymüller, E., Arthington-Skaggs, B.A., and Colombo, A.L. (2011) Biofilm production and evaluation of antifungal susceptibility amongst clinical Candida spp. isolates, including strains of the Candida parapsilosis complex. *Med Mycol* **49**: 253–262.

Michaelis, S., and Herskowitz, I. (1988) The a-factor pheromone of Saccharomyces cerevisiae is essential for mating. *Mol Cell Biol* **8**: 1309–1318.

Miller, M.G., and Johnson, A.D. (2002) White-opaque switching in Candida albicans is controlled by mating-type locus homeodomain proteins and allows efficient mating. *Cell* **110**: 293–302.

Mitchell, K.F., Taff, H.T., Cuevas, M.A., Reinicke, E.L., Sanchez, H., and Andes, D.R. (2013) Role of Matrix β-1,3 Glucan in Antifungal Resistance of Non-albicans Candida Biofilms. *Antimicrob Agents Chemother* **57**: 1918–1920.

Mochizuki, N., and Yamamoto, M. (1992) Reduction in the intracellular cAMP level triggers initiation of sexual development in fission yeast. *Mol Gen Genet MGG* **233**: 17–24.

Mohammadi, S., Mohammadi, J., and Forrest, G.N. (2013) Epidemiology of Candida Endocarditis. *Curr Fungal Infect Rep* 1–5.

Naider, F., and Becker, J.M. (2004) The alpha-factor mating pheromone of Saccharomyces cerevisiae: a model for studying the interaction of peptide hormones and G protein-coupled receptors. *Peptides* **25**: 1441–1463.

Nath, R. (1993) Properties of Barrier, a novel Saccharomyces cerevisiae acid protease. *Biochimie* **75**: 467–472.

Nett, J.E., Lepak, A.J., Marchillo, K., and Andes, D.R. (2009) Time course global gene expression analysis of an in vivo Candida biofilm. *J Infect Dis* **200**: 307–313.

Nett, J.E., Marchillo, K., Spiegel, C.A., and Andes, D.R. (2010) Development and Validation of an In Vivo Candida albicans Biofilm Denture Model. *Infect Immun* **78**: 3650–3659.

Nett, J.E., Sanchez, H., Cain, M.T., Ross, K.M., and Andes, D.R. (2011) Interface of Candida albicans Biofilm Matrix-Associated Drug Resistance and Cell Wall Integrity Regulation. *Eukaryot Cell* **10**: 1660–1669.

Nguyen, V.Q., and Sil, A. (2008) Temperature-induced switch to the pathogenic yeast form of Histoplasma capsulatum requires Ryp1, a conserved transcriptional regulator. *Proc Natl Acad Sci U S A* **105**: 4880–4885.

Nobile, C.J., Andes, D.R., Nett, J.E., Smith, F.J., Yue, F., Phan, Q.-T., *et al.* (2006) Critical role of Bcr1-dependent adhesins in C. albicans biofilm formation in vitro and in vivo. *PLoS Pathog* **2**: e63.

Nobile, C.J., Fox, E.P., Nett, J.E., Sorrells, T.R., Mitrovich, Q.M., Hernday, A.D., *et al.* (2012) A recently evolved transcriptional network controls biofilm development in Candida albicans. *Cell* **148**: 126–138.

Nobile, C.J., and Mitchell, A.P. (2005) Regulation of Cell-Surface Genes and Biofilm Formation by the C. albicans Transcription Factor Bcr1p. *Curr Biol* **15**: 1150–1155.

Nobile, C.J., Schneider, H.A., Nett, J.E., Sheppard, D.C., Filler, S.G., Andes, D.R., and Mitchell, A.P. (2008) Complementary adhesin function in C. albicans biofilm formation. *Curr Biol CB* **18**: 1017–1024.

Noble, S.M., and Johnson, A.D. (2005) Strains and Strategies for Large-Scale Gene Deletion Studies of the Diploid Human Fungal Pathogen Candida albicans. *Eukaryot Cell* **4**: 298–309.

Northrop, D.B. (2001) Follow the Protons: A Low-Barrier Hydrogen Bond Unifies the Mechanisms of the Aspartic Proteases. *Acc Chem Res* **34**: 790–797.

Nucci, M., and Anaissie, E. (2001) Revisiting the source of candidemia: skin or gut? *Clin Infect Dis Off Publ Infect Dis Soc Am* **33**: 1959–1967.

Obara, T., Nakafuku, M., Yamamoto, M., and Kaziro, Y. (1991) Isolation and characterization of a gene encoding a G-protein alpha subunit from Schizosaccharomyces pombe: involvement in mating and sporulation pathways. *Proc Natl Acad Sci U S A* **88**: 5877–5881.

Obbard, D.J., and Dudas, G. (2014) The genetics of host–virus coevolution in invertebrates. *Curr Opin Virol* **8**: 73–78.

O'Donoghue, A.J., Eroy-Reveles, A.A., Knudsen, G.M., Ingram, J., Zhou, M., Statnekov, J.B., *et al.* (2012) Global identification of peptidase specificity by multiplex substrate profiling. *Nat Methods* **9**: 1095–1100.

Olesnicky, N.S., Brown, A.J., Dowell, S.J., and Casselton, L.A. (1999) A constitutively active G-protein-coupled receptor causes mating self-compatibility in the mushroom Coprinus. *EMBO J* **18**: 2756–2763.

O'Loughlin, C.T., Miller, L.C., Siryaporn, A., Drescher, K., Semmelhack, M.F., and Bassler, B.L. (2013) A quorum-sensing inhibitor blocks Pseudomonas aeruginosa virulence and biofilm formation. *Proc Natl Acad Sci* **110**: 17981–17986.

Pannanusorn, S., Ramírez-Zavala, B., Lünsdorf, H., Agerberth, B., Morschhäuser, J., and Römling, U. (2014) Characterization of biofilm formation and the role of BCR1 in clinical isolates of Candida parapsilosis. *Eukaryot Cell* **13**: 438–451.

Panwar, S.L., Legrand, M., Dignard, D., Whiteway, M., and Magee, P.T. (2003) MFα1, the Gene Encoding the α Mating Pheromone of Candida albicans. *Eukaryot Cell* **2**: 1350–1360.

Paoletti, M., Seymour, F.A., Alcocer, M.J.C., Kaur, N., Calvo, A.M., Archer, D.B., and Dyer, P.S. (2007) Mating type and the genetic basis of self-fertility in the model fungus Aspergillus nidulans. *Curr Biol CB* **17**: 1384–1389.

Park, Y.-N., and Morschhäuser, J. (2005) Tetracycline-inducible gene expression and gene deletion in Candida albicans. *Eukaryot Cell* **4**: 1328–1342.

Pesole, G., Lotti, M., Alberghina, L., and Saccone, C. (1995) Evolutionary origin of nonuniversal CUGSer codon in some Candida species as inferred from a molecular phylogeny. *Genetics* **141**: 903–907.

Peter, M., Gartner, A., Horecka, J., Ammerer, G., and Herskowitz, I. (1993) FAR1 links the signal transduction pathway to the cell cycle machinery in yeast. *Cell* **73**: 747–760.

Peter, M., and Herskowitz, I. (1994) Direct inhibition of the yeast cyclin-dependent kinase Cdc28-Cln by Far1. *Science* **265**: 1228–1231.

Pfaller, M.A., and Diekema, D.J. (2007) Epidemiology of invasive candidiasis: a persistent public health problem. *Clin Microbiol Rev* **20**: 133–163.

Pierce, G.E. (2005) Pseudomonas aeruginosa, Candida albicans, and device-related nosocomial infections: implications, trends, and potential approaches for control. *J Ind Microbiol Biotechnol* **32**: 309–318.

Porman, A. (2015) Identification and Regulation of White-Opaque Phenotypic Switching in Candida tropicalis. .

Porman, A.M., Alby, K., Hirakawa, M.P., and Bennett, R.J. (2011) Discovery of a phenotypic switch regulating sexual mating in the opportunistic fungal pathogen Candida tropicalis. *Proc Natl Acad Sci U S A* **108**: 21158–21163.

Porman, A.M., Hirakawa, M.P., Jones, S.K., Wang, N., and Bennett, R.J. (2013) MTL–Independent Phenotypic Switching in Candida tropicalis and a Dual Role for Wor1 in Regulating Switching and Filamentation. *PLoS Genet* **9**: e1003369.

Powers, S., Michaelis, S., Broek, D., Santa Anna, S., Field, J., Herskowitz, I., and Wigler, M. (1986) RAM, a gene of yeast required for a functional modification of RAS proteins and for production of mating pheromone a-factor. *Cell* **47**: 413–422.

Prabu-Jeyabalan, M., Nalivaika, E., and Schiffer, C.A. (2002) Substrate Shape Determines Specificity of Recognition for HIV-1 Protease: Analysis of Crystal Structures of Six Substrate Complexes. *Structure* **10**: 369–381.

Pujol, C., Daniels, K.J., Lockhart, S.R., Srikantha, T., Radke, J.B., Geiger, J., and Soll, D.R. (2004) The Closely Related Species Candida albicans and Candida dubliniensis Can Mate. *Eukaryot Cell* **3**: 1015–1027.

Pujol, C., Pfaller, M.A., and Soll, D.R. (2004) Flucytosine Resistance Is Restricted to a Single Genetic Clade of Candida albicans. *Antimicrob Agents Chemother* **48**: 262–266.

Ramage, G., Vande Walle, K., Wickes, B.L., and López-Ribot, J.L. (2001) Standardized method for in vitro antifungal susceptibility testing of Candida albicans biofilms. *Antimicrob Agents Chemother* **45**: 2475–2479.

Ramírez-Zavala, B., Reuss, O., Park, Y.-N., Ohlsen, K., and Morschhäuser, J. (2008) Environmental induction of white-opaque switching in Candida albicans. *PLoS Pathog* **4**: e1000089.

Raths, S., Rohrer, J., Crausaz, F., and Riezman, H. (1993) end3 and end4: two mutants defective in receptor-mediated and fluid-phase endocytosis in Saccharomyces cerevisiae. *J Cell Biol* **120**: 55–65.

Reuss, O., Vik, A., Kolter, R., and Morschhäuser, J. (2004) The SAT1 flipper, an optimized tool for gene disruption in Candida albicans. *Gene* **341**: 119–127.

Rikkerink, E.H., Magee, B.B., and Magee, P.T. (1988) Opaque-white phenotype transition: a programmed morphological transition in Candida albicans. *J Bacteriol* **170**: 895–899.

Ro, D.-K., Paradise, E.M., Ouellet, M., Fisher, K.J., Newman, K.L., Ndungu, J.M., *et al.* (2006) Production of the antimalarial drug precursor artemisinic acid in engineered yeast. *Nature* **440**: 940–943.

Ruhnke, M., and Maschmeyer, G. (2002) Management of mycoses in patients with hematologic disease and cancer -- review of the literature. *Eur J Med Res* **7**: 227–235.

Rustchenko, E. (2007) Chromosome instability in Candida albicans. *FEMS Yeast Res* **7**: 2–11.

Sahni, N., Yi, S., Daniels, K.J., Huang, G., Srikantha, T., and Soll, D.R. (2010) Tec1 Mediates the Pheromone Response of the White Phenotype of Candida albicans: Insights into the Evolution of New Signal Transduction Pathways. *PLoS Biol* **8**.

Sahni, N., Yi, S., Pujol, C., and Soll, D.R. (2009) The White Cell Response to Pheromone Is a General Characteristic of Candida albicans Strains. *Eukaryot Cell* **8**: 251–256.

Sai, S., Holland, L.M., McGee, C.F., Lynch, D.B., and Butler, G. (2011) Evolution of Mating within the Candida parapsilosis Species Group. *Eukaryot Cell* **10**: 578–587.

Samaranayake, L.P., Fidel, P.L., Naglik, J.R., Sweet, S.P., Teanpaisan, R., Coogan, M.M., *et al.* (2002) Fungal infections associated with HIV infection. *Oral Dis* **8 Suppl 2**: 151–160.

Sapperstein, S., Berkower, C., and Michaelis, S. (1994) Nucleotide sequence of the yeast STE14 gene, which encodes farnesylcysteine carboxyl methyltransferase, and demonstration of its essential role in a-factor export. *Mol Cell Biol* **14**: 1438–1449.

Sasse, C., Hasenberg, M., Weyler, M., Gunzer, M., and Morschhäuser, J. (2013) White-opaque switching of Candida albicans allows immune evasion in an environment-dependent fashion. *Eukaryot Cell* **12**: 50–58.

Savile, C.K., Janey, J.M., Mundorff, E.C., Moore, J.C., Tam, S., Jarvis, W.R., *et al.* (2010) Biocatalytic Asymmetric Synthesis of Chiral Amines from Ketones Applied to Sitagliptin Manufacture. *Science* **329**: 305–309.

Schaefer, D., Cote, P., Whiteway, M., and Bennett, R.J. (2007) Barrier Activity in Candida albicans Mediates Pheromone Degradation and Promotes Mating. *Eukaryot Cell* **6**: 907–918.

Schandel, K.A., and Jenness, D.D. (1994) Direct evidence for ligand-induced internalization of the yeast alpha-factor pheromone receptor. *Mol Cell Biol* **14**: 7245–7255.

Schmoll, M., Seibel, C., Tisch, D., Dorrer, M., and Kubicek, C.P. (2010) A novel class of peptide pheromone precursors in ascomycetous fungi. *Mol Microbiol* **77**: 1483–1501.

Schulze, J., and Sonnenborn, U. (2009) Yeasts in the Gut: From Commensals to Infectious Agents. *Dtsch Ärztebl Int* **106**: 837–842.

Schweizer, A., Rupp, S., Taylor, B.N., Röllinghoff, M., and Schröppel, K. (2000) The TEA/ATTS transcription factor CaTec1p regulates hyphal development and virulence in Candida albicans. *Mol Microbiol* **38**: 435–445.

Shenbagamurthi, P., Baffi, R., Khan, S.A., Lipke, P., Pousman, C., Becker, J.M., and Naider, F. (1983) Structure-activity relationships in the dodecapeptide alpha factor of Saccharomyces cerevisiae. *Biochemistry (Mosc)* **22**: 1298–1304.

Shen, W.C., Bobrowicz, P., and Ebbole, D.J. (1999) Isolation of pheromone precursor genes of Magnaporthe grisea. *Fungal Genet Biol FG B* **27**: 253–263.

Sherwood, R.K., Scaduto, C.M., Torres, S.E., and Bennett, R.J. (2014) Convergent evolution of a fused sexual cycle promotes the haploid lifestyle. *Nature* **506**: 387–390.

Shimada, Y., Gulli, M.P., and Peter, M. (2000) Nuclear sequestration of the exchange factor Cdc24 by Far1 regulates cell polarity during yeast mating. *Nat Cell Biol* **2**: 117–124.

Si, H., Hernday, A.D., Hirakawa, M.P., Johnson, A.D., and Bennett, R.J. (2013) Candida albicans white and opaque cells undergo distinct programs of filamentous growth. *PLoS Pathog* **9**: e1003210.

Silva, S., Negri, M., Henriques, M., Oliveira, R., Williams, D.W., and Azeredo, J. (2012) Candida glabrata, Candida parapsilosis and Candida tropicalis: biology, epidemiology, pathogenicity and antifungal resistance. *FEMS Microbiol Rev* **36**: 288–305.

Singh, A., Chen, E.Y., Lugovoy, J.M., Chang, C.N., Hitzeman, R.A., and Seeburg, P.H. (1983) Saccharomyces cerevisiae contains two discrete genes coding for the alpha-factor pheromone. *Nucleic Acids Res* **11**: 4049–4063.

Sleight, S.C., Bartley, B.A., Lieviant, J.A., and Sauro, H.M. (2010) Designing and engineering evolutionary robust genetic circuits. *J Biol Eng* **4**: 12.

Slutsky, B., Staebell, M., Anderson, J., Risen, L., Pfaller, M., and Soll, D.R. (1987) "White-opaque transition": a second high-frequency switching system in Candida albicans. *J Bacteriol* **169**: 189–197.

Solano, C., Echeverz, M., and Lasa, I. (2014) Biofilm dispersion and quorum sensing. *Curr Opin Microbiol* **18**: 96–104.

Soll, D.R. (2014) The role of phenotypic switching in the basic biology and pathogenesis of Candida albicans. *J Oral Microbiol* **6** http://www.ncbi.nlm.nih.gov/pmc/articles/PMC3895265/. Accessed November 21, 2014.

Soll, D.R., and Pujol, C. (2003) Candida albicans clades. *FEMS Immunol Med Microbiol* **39**: 1–7.

Son, C.D., Sargsyan, H., Naider, F., and Becker, J.M. (2004) Identification of ligand binding regions of the Saccharomyces cerevisiae alpha-factor pheromone receptor by photoaffinity cross-linking. *Biochemistry (Mosc)* **43**: 13193–13203.

Sprague Jr, G.F., and Herskowitz, I. (1981) Control of yeast cell type by the mating type locus: I. Identification and control of expression of the a-specific gene BAR1. *J Mol Biol* **153**: 305–321.

Srikantha, T., Borneman, A.R., Daniels, K.J., Pujol, C., Wu, W., Seringhaus, M.R., *et al.* (2006) TOS9 regulates white-opaque switching in Candida albicans. *Eukaryot Cell* **5**: 1674–1687.

Stefan, C.J., and Blumer, K.J. (1994) The third cytoplasmic loop of a yeast G-protein-coupled receptor controls pathway activation, ligand discrimination, and receptor internalization. *Mol Cell Biol* **14**: 3339–3349.

Stokes, C., Moran, G.P., Spiering, M.J., Cole, G.T., Coleman, D.C., and Sullivan, D.J. (2007) Lower filamentation rates of Candida dubliniensis contribute to its lower virulence in comparison with Candida albicans. *Fungal Genet Biol FG B* **44**: 920–931.

Sudbery, P.E. (2011) Growth of Candida albicans hyphae. *Nat Rev Microbiol* **9**: 737–748.

Sugita, T., and Nakase, T. (1999) Non-universal Usage of the Leucine CUG Codon and the Molecular Phylogeny of the Genus Candida. *Syst Appl Microbiol* **22**: 79–86.

Tam, A., Nouvet, F.J., Fujimura-Kamada, K., Slunt, H., Sisodia, S.S., and Michaelis, S. (1998) Dual roles for Ste24p in yeast a-factor maturation: NH2-terminal proteolysis and COOH-terminal CAAX processing. *J Cell Biol* **142**: 635–649.

Tam, A., Schmidt, W.K., and Michaelis, S. (2001) The multispanning membrane protein Ste24p catalyzes CAAX proteolysis and NH2-terminal processing of the yeast a-factor precursor. *J Biol Chem* **276**: 46798–46806.

Tao, L., Cao, C., Liang, W., Guan, G., Zhang, Q., Nobile, C.J., and Huang, G. (2014) White Cells Facilitate Opposite- and Same-Sex Mating of Opaque Cells in Candida albicans. *PLoS Genet* **10**: e1004737.

Taschdjian, C.L., Burchall, J.J., and Kozinn, P.J. (1960) Rapid identification of Candida albicans by filamentation on serum and serum substitutes. *AMA J Dis Child* **99**: 212–215.

Taylor, B.N., Harrer, T., Pscheidl, E., Schweizer, A., Röllinghoff, M., and Schröppel, K. (2003) Surveillance of nosocomial transmission of Candida albicans in an intensive care unit by DNA fingerprinting. *J Hosp Infect* **55**: 283–289.

Tedford, K., Kim, S., Sa, D., Stevens, K., and Tyers, M. (1997) Regulation of the mating pheromone and invasive growth responses in yeast by two MAP kinase substrates. *Curr Biol CB* **7**: 228–238.

Torres, E.M., Sokolsky, T., Tucker, C.M., Chan, L.Y., Boselli, M., Dunham, M.J., and Amon, A. (2007) Effects of Aneuploidy on Cellular Physiology and Cell Division in Haploid Yeast. *Science* **317**: 916–924.

Tsong, A.E., Miller, M.G., Raisner, R.M., and Johnson, A.D. (2003) Evolution of a combinatorial transcriptional circuit: a case study in yeasts. *Cell* **115**: 389–399.

Tuch, B.B., Galgoczy, D.J., Hernday, A.D., Li, H., and Johnson, A.D. (2008) The evolution of combinatorial gene regulation in fungi. *PLoS Biol* **6**: e38.

Tuch, B.B., Mitrovich, Q.M., Homann, O.R., Hernday, A.D., Monighetti, C.K., La Vega, F.M. De, and Johnson, A.D. (2010) The transcriptomes of two heritable cell types illuminate the circuit governing their differentiation. *PLoS Genet* **6**: e1001070.

Tumbarello, M., Posteraro, B., Trecarichi, E.M., Fiori, B., Rossi, M., Porta, R., *et al.* (2007) Biofilm Production by Candida Species and Inadequate Antifungal Therapy as Predictors of Mortality for Patients with Candidemia. *J Clin Microbiol* **45**: 1843–1850.

Tzung, K.-W., Williams, R.M., Scherer, S., Federspiel, N., Jones, T., Hansen, N., *et al.* (2001) Genomic evidence for a complete sexual cycle in Candida albicans. *Proc Natl Acad Sci* **98**: 3249–3253.

Umanah, G.K.E., Huang, L., Ding, F.-X., Arshava, B., Farley, A.R., Link, A.J., *et al.* (2010) Identification of Residue-to-residue Contact between a Peptide Ligand and Its G Protein-coupled Receptor Using Periodate-mediated Dihydroxyphenylalanine Cross-linking and Mass Spectrometry. *J Biol Chem* **285**: 39425–39436.

Wagner, J.C., and Wolf, D.H. (1987) Hormone (pheromone) processing enzymes in yeast. The carboxy-terminal processing enzyme of the mating pheromone alpha-factor, carboxypeptidase ysc alpha, is absent in alpha-factor maturation-defective kex1 mutant cells. *FEBS Lett* **221**: 423–426.

Wang, H.X., and Konopka, J.B. (2009) Identification of Amino Acids at Two Dimer Interface Regions of the α-Factor Receptor (Ste2). *Biochemistry (Mosc)* **48**: 7132–7139.

Waters, M.G., Evans, E.A., and Blobel, G. (1988) Prepro-alpha-factor has a cleavable signal sequence. *J Biol Chem* **263**: 6209–6214.

Wiget, P., Shimada, Y., Butty, A.-C., Bi, E., and Peter, M. (2004) Site-specific regulation of the GEF Cdc24p by the scaffold protein Far1p during yeast mating. *EMBO J* **23**: 1063–1074.

Willger, S.D., Grim, S.L., Dolben, E.L., Shipunova, A., Hampton, T.H., Morrison, H.G., *et al.* (2014) Characterization and quantification of the fungal microbiome in serial samples from individuals with cystic fibrosis. *Microbiome* **2**: 40.

Wisplinghoff, H., Bischoff, T., Tallent, S.M., Seifert, H., Wenzel, R.P., and Edmond, M.B. (2004) Nosocomial bloodstream infections in US hospitals: analysis of 24,179 cases from a prospective nationwide surveillance study. *Clin Infect Dis Off Publ Infect Dis Soc Am* **39**: 309–317.

Wu, W., Lockhart, S.R., Pujol, C., Srikantha, T., and Soll, D.R. (2007) Heterozygosity of genes on the sex chromosome regulates Candida albicans virulence. *Mol Microbiol* **64**: 1587–1604.

Xie, J., Du, H., Guan, G., Tong, Y., Kourkoumpetis, T.K., Zhang, L., *et al.* (2012) N-Acetylglucosamine Induces White-to-Opaque Switching and Mating in Candida tropicalis, Providing New Insights into Adaptation and Fungal Sexual Evolution. *Eukaryot Cell* **11**: 773–782.

Xie, J., Tao, L., Nobile, C.J., Tong, Y., Guan, G., Sun, Y., *et al.* (2013) White-Opaque Switching in Natural MTLa/α Isolates of Candida albicans: Evolutionary Implications for Roles in Host Adaptation, Pathogenesis, and Sex. *PLoS Biol* **11**: e1001525.

Xue, C., Hsueh, Y.-P., and Heitman, J. (2008) Magnificent seven: roles of G protein-coupled receptors in extracellular sensing in fungi. *FEMS Microbiol Rev* **32**: 1010–1032.

Yi, S., Sahni, N., Daniels, K.J., Lu, K.L., Huang, G., Garnaas, A.M., *et al.* (2011) Utilization of the mating scaffold protein in the evolution of a new signal transduction pathway for biofilm development. *mBio* **2** http://www.ncbi.nlm.nih.gov/pubmed/21221248. Accessed February 18, 2011.

Yi, S., Sahni, N., Daniels, K.J., Lu, K.L., Huang, G., Srikantha, T., and Soll, D.R. (2011) Self-induction of a/a or alpha/alpha biofilms in Candida albicans is a pheromone-based paracrine system requiring switching. *Eukaryot Cell* **10**: 753–760.

Yi, S., Sahni, N., Daniels, K.J., Pujol, C., Srikantha, T., and Soll, D.R. (2008) The Same Receptor, G Protein, and Mitogen-activated Protein Kinase Pathway Activate Different Downstream Regulators in the Alternative White and Opaque Pheromone Responses of Candida albicans. *Mol Biol Cell* **19**: 957–970.

Yi, S., Sahni, N., Pujol, C., Daniels, K.J., Srikantha, T., Ma, N., and Soll, D.R. (2009) A Candida albicans-specific region of the alpha-pheromone receptor plays a selective role in the white cell pheromone response. *Mol Microbiol* **71**: 925–947.

Zhang, Y.L., Lu, H.F., Becker, J.M., and Naider, F. (1997) Position one analogs of the Saccharomyces cerevisiae tridecapeptide pheromone. *J Pept Res Off J Am Pept Soc* **50**: 319–328.

Zhang, Y.L., Marepalli, H.R., Lu, H.F., Becker, J.M., and Naider, F. (1998) Synthesis, biological activity, and conformational analysis of peptidomimetic analogues of the Saccharomyces cerevisiae alpha-factor tridecapeptide. *Biochemistry (Mosc)* **37**: 12465–12476.

Zhao, H., Shen, Z.-M., Kahn, P.C., and Lipke, P.N. (2001) Interaction of α-Agglutinin and a-Agglutinin,Saccharomyces cerevisiae Sexual Cell Adhesion Molecules. *J Bacteriol* **183**: 2874–2880.

Zhao, R., Daniels, K.J., Lockhart, S.R., Yeater, K.M., Hoyer, L.L., and Soll, D.R. (2005) Unique Aspects of Gene Expression during Candida albicans Mating and Possible G1 Dependency. *Eukaryot Cell* **4**: 1175–1190.

Zhou, Z., Gartner, A., Cade, R., Ammerer, G., and Errede, B. (1993) Pheromone-induced signal transduction in Saccharomyces cerevisiae requires the sequential function of three protein kinases. *Mol Cell Biol* **13**: 2069–2080.

Zordan, R.E., Galgoczy, D.J., and Johnson, A.D. (2006) Epigenetic properties of white-opaque switching in Candida albicans are based on a self-sustaining transcriptional feedback loop. *Proc Natl Acad Sci U S A* **103**: 12807–12812.

Zordan, R.E., Miller, M.G., Galgoczy, D.J., Tuch, B.B., and Johnson, A.D. (2007) Interlocking Transcriptional Feedback Loops Control White-Opaque Switching in Candida albicans. *PLoS Biol* **5**: e256.

APPENDIX 1: PARASEXUALITY AND PLOIDY CHANGE IN *CANDIDA TROPICALIS*

ABSTRACT

Candida species exhibit a variety of ploidies and modes of sexual reproduction. Most species possess the requisite genes for sexual reproduction, recombination, and meiosis, yet only a few have been reported to undergo a complete sexual cycle including mating and sporulation. *Candida albicans*, the most studied *Candida* species and a prevalent human fungal pathogen, completes its sexual cycle via a parasexual process of concerted chromosome loss rather than a conventional meiosis. In this study, we examine ploidy changes in *Candida tropicalis*, a closely related species to *C. albicans* that was recently revealed to undergo sexual mating. *C. tropicalis* diploid cells mate to form tetraploid cells, and we show that these can be induced to undergo chromosome loss to regenerate diploid forms by growth on sorbose medium. The diploid products are themselves mating-competent, thereby establishing a parasexual cycle in this species for the first time. Extended incubation (>120 generations) of *C. tropicalis* tetraploid cells in rich culture conditions also resulted in instability of the tetraploid form and a gradual reduction in ploidy back to the diploid state. The fitness of *C. tropicalis* diploid and tetraploid cells were compared and diploid cells exhibited increased fitness relative to tetraploid cells *in vitro,* despite diploid and tetraploid cells having similar doubling times. Collectively, these experiments demonstrate distinct pathways by which a parasexual cycle can occur in *C. tropicalis*, and indicate that non-meiotic mechanisms drive ploidy changes in this prevalent human pathogen.

INTRODUCTION

Many yeast species can reproduce by both sexual and asexual mechanisms. Asexual reproduction is generally utilized when conditions are favorable for growth, while sexual reproduction is favored when nutrients are limiting (1). Sexual reproduction can generate increased levels of genomic diversity that promote adaptation to a changing or hostile environment (2). However, sex is also associated with an increased cost relative to asexual reproduction (3, 4). The ability to switch between sexual and asexual modes of reproduction (facultative sex) allows for reallocation of resources to sexual reproduction during periods of low fitness and also provides a mechanism for coping with deleterious mutations (5, 6).

Saccharomyces cerevisiae, the most widely studied of the ascomycetes, has served as a model organism for the study of mating and meiosis in fungi. It exhibits a mating cycle in which yeast cells alternate between haploid and diploid phases. Mating between haploid *MATα* and *MATα* cells generates diploid a/α cells that subsequently can undergo meiosis to form haploid ascospores (7, 8). Similar to *S. cerevisiae*, several human fungal pathogens have been shown to exhibit extant sexual programs (4, 8, 9). *Cryptococcus neoformans*, a basidiomycete that is a causative agent of fungal meningoencephalitis, exhibits both homothallic (same-sex) and heterothallic (inter-sex) mating (10, 11). This has direct implications for pathogenesis, as sexual spores of *C. neoformans* are infectious propagules in animal models of infection (12). Furthermore, phylogenetic analysis of the sibling species *Cryptococcus gattii* has implicated α-α same-sex mating in the generation of a highly virulent isolate responsible for an ongoing outbreak that initiated on Vancouver Island (13-15). *Aspergillus fumigatus*, a prevalent airborne, ascomycetous pathogen, was also recently shown to undergo a complete sexual program complete with the formation of recombinant ascospores (16).

Candida species represent an important genus of human pathogens and these ascomycetes vary in their potential to undergo sexual reproduction. Several clinically relevant species reside within the so-called *Candida* clade, a group of species that translate the CUG codon as serine instead of leucine, as in the universal genetic code (17, 18). Within this clade, *Candida lusitaniae, Candida guillermondii*, *Debaromyces hansenii*, and *Lodderomyces elongisporus* have been reported to undergo full sexual cycles that include sporulation (19-23). In the case of *C. lusitaniae*, studies reveal that although this species lacks several conserved meiosis genes it completes its sexual cycle through Spo11-dependent recombination and sporulation (17, 20). The meiotic process leads to high levels of aneuploidy and resulting asci contain a dyad of ascospores rather than the conventional tetrads formed by *S. cerevisiae* (20).

The most prevalent human fungal pathogen is *Candida albicans,* a *Candida* clade member that undergoes both homothallic and heterothallic mating (24-26). Mating in this species is regulated by a phenotypic switch in which cells must transition from the conventional white state to the alternative opaque state to become mating-competent (27). *C. albicans* possesses a number of genes implicated in meiosis (17, 28), but has not been observed to undergo a conventional meiotic program. In its place, ploidy reduction occurs through a process of concerted chromosome loss that results in high levels of chromosomal aneuploidy (29, 30). This parasexual chromosome loss has been proposed to promote adaptation through the generation of a large pool of genetically diverse progeny (31). Recombination during the parasexual process is dependent on the conserved meiosis-specific protein Spo11, indicating parallels with a conventional meiosis (30). Furthermore, *C. albicans* has recently been shown to form viable haploid cells that can undergo either auto-diploidization or mating to return to the diploid state (32).

Candida tropicalis is also a clinically relevant *Candida* clade species and is rapidly emerging as a major cause of candidiasis on a global scale (33). Until recently, *C. tropicalis* strains were believed to be asexual, but it is now apparent that a and α diploid cells can undergo efficient mating to generate tetraploid a/α cells (34, 35). *C. tropicalis* mating is controlled by a white-opaque transition related to that in *C. albicans*. However, it is not known if *C. tropicalis* cells can complete a sexual or parasexual program to return to the diploid state.

In this study, we tested the ability of genetically marked tetraploid strains of *C. tropicalis* to undergo a conventional meiosis or a parasexual (non-meiotic) reduction in ploidy. We show that tetraploid cells can be induced to undergo a parasexual process when grown on sorbose medium. The resulting progeny are diploid, and a or α cells are capable of re-mating to form tetraploid cells, thus establishing a complete parasexual cycle for *C. tropicalis*. We also observed that *C. tropicalis* tetraploid cells are unstable during prolonged propagation in rich medium, eventually returning to the diploid state after ~240 generations. Furthermore, we show that *C. tropicalis* diploid cells out-compete tetraploid cells during prolonged co-culture *in vitro.* Taken together, our work compares the fitness of diploid and tetraploid states in *C. tropicalis*, and demonstrates that this species can complete a parasexual cycle via distinct ploidy-reduction pathways.

MATERIALS AND METHODS

Media

Standard media were prepared as previously described (36, 37). Yeast Extract Peptone Dextrose (YPD) contained 1% yeast extract, 2% peptone, and 2% glucose. YPD was supplemented with 200 μg/ml nourseothricin (YPD+NAT) to select for nourseothricin-resistant (NAT^R) strains (38). Sporulation medium #1 consisted of 1% potassium acetate, 0.05% dextrose, 0.1% yeast extract, and 0.01% complete amino acid mix. Sporulation medium #2 was Gorodkowa medium and consisted of 1% peptone, 0.5% NaCl, and 0.1% glucose. Potato dextrose agar (PDA) medium was 3.9% Difco Potato Dextrose Agar and 0.07% tartaric acid. Minimal medium was 0.7% yeast nitrogen base (YNB) and 2% glucose. Sorbitol medium contained 18.2% sorbitol, 0.7% YNB, 2% glucose, complete amino acids, and 25 μg/ml uridine. Malt extract medium was 3% malt extract and 0.5% peptone. Sheep's blood agar was Columbia agar with 5% sheep's blood (Beckton, Dickinson & Co). V8 medium contained 5% V8 juice and 0.05% KH_2PO_4 (pH 7.0). Serum medium was YPD medium supplemented with 10% fetal bovine serum. Low phosphate medium contained YNB w/o phosphate (#CYN6701, Formedium LTD, Hunstanton, England) and KH_2PO_4 (10 μM) and was adjusted to pH 4.7 with 3 M HCl. Synthetic SLAD was YNB (without amino acids or ammonium sulphate) supplemented with 50 μM ammonium sulphate and 2% glucose. Sorbose medium contained 0.7% yeast nitrogen base, 2% sorbose, and 25 μg/ml uridine (+/- amino acids). 2-Deoxygalactose (2-DOG) and pre-sporulation (pre-spo) media were prepared as described (29). Solid media contained 2% agar.

Strain and Plasmid Construction

All strains used in this study are listed in Table 1. Gene deletions in *C. tropicalis* strains were performed using the *SAT1* flipper strategy (38). Strains were transformed with ~1 μg of

DNA using a modified electroporation protocol, as described in (20, 34). In brief, cells were grown overnight at 30°C in 3 ml YPD and diluted into 50 ml YPD cultures, which were grown overnight at 30°C. Samples were centrifuged and resuspended in 0.1 M lithium acetate, 7.5 mM Tris-HCl (pH 8.0), 1 mM EDTA, 10 mM dithiothreitol for 1 hour at room temperature. After washing twice with water and once with 1M sorbitol, cells were resuspended in the liquid that remained after decantation. For each transformation, ~50 µl of cells was mixed with 10-15 µl DNA, and the mixture was electroporated at 1.8 kV using a MicroPulsor Electroporator (Bio-Rad). The cells were immediately re-suspended in 1 ml of cold 1M sorbitol, followed by a recovery period of 4 hours at 30°C in 1 ml YPD. Finally, cells were plated onto YPD medium containing 200 µg/ml nourseothricin (YPD+NAT) to select for cells that had incorporated the construct into the genome through homologous recombination. PCR was used to confirm proper integration into the correct locus. In order to flip out the *SAT1* marker from the genome, cells were grown in liquid YP + 2% maltose for 5 days at 30°C and plated on YPD medium containing 20 µg/ml nourseothricin. Small colonies were replica patched onto YPD and YPD+NAT plates to confirm loss of nourseothricin resistance. For double mutants, the transformation process was repeated and PCR used to confirm loss of the open reading frame (ORF).

In order to delete genes using the *SAT1*-flipper, the 5' and 3' regions of the gene of interest were PCR amplified and cloned into the plasmid pSFS2a (38). The 5' flank of the target gene was digested with *Apa*I/*Xho*I, and the 3' flank was digested with *Sac*I/*Sac*II and cloned into pSFS2a. The resulting plasmid was digested with *Apa*I/*Sac*I in order to liberate the deletion cassette. Correct integration of the cassette into the genome was confirmed by PCR. All oligonucleotides used in this study are listed in Table 2.

C. tropicalis Mating Assay

Mating in *C. tropicalis* was carried out using two methods. In the first, strains with deletions at the *HIS1* or *ARG4* loci were streaked onto YPD medium, and cells resuspended in liquid Spider medium and grown for 3-5 days at 30°C. Following incubation, equal amounts (0.5 OD_{600}, or ~10^7 cells) of each strain were mixed together in 100 µl YPD and pipetted onto 0.8-µm pore-sized nitrocellulose filters on the surface of Spider medium plates. Plates were incubated at 30°C for 5 days, after which cells were collected from the filters and streaked onto His-/Arg- plates in order to select for successful mating products. PCR using primers directed at *MTL*a1 and *MTL*α2 (see Table 2) was used to confirm the presence of both mating types in the mating products. Ploidy was checked using flow cytometry as described below. The second method used the same steps, except that cells from YPD were streaked directly onto plates containing Spider medium and grown at room temperature for 5 days.

Flow Cytometric Analysis

Cytometric analysis of cells was performed essentially as described (25). Cells were grown in 500 ml YPD to an OD_{600} of ~0.5 and fixed in 70% ethanol at 4°C overnight. Cells were then washed twice in water and resuspended in 0.5 mM Tris-HCl, pH 8.0, followed by sonication at low power. Following this, cells were resuspended in freshly prepared 2 mg/ml RNaseA solution in 0.5 mM Tris-HCl, pH 8.0 (heated to 98°C for 10 minutes and allowed to slowly cool to room temperature). Samples were incubated at 37°C for two hours, centrifuged, and resuspended in freshly prepared 5 mg/ml pepsin in 55 mM HCl at 37°C for 45 minutes. They were then washed with 0.5 mM Tris-HCl, pH 7.5, sonicated at low power, and resuspended in 200 µl 0.5 mM Tris-HCl, pH 7.5. 50 µl of each sample was stained with 500 µl Sytox Green dye (1

μM) at 4°C for 1-48 hours. 10,000 cells from each sample were run on a MACSQuant Analyzer 10 (Miltenyi Biotech), and data analyzed using FlowJo (Tree Star Inc.).

Chromosome Loss Assay

Chromosome loss in *C. tropicalis* was measured using a method similar to that described for *C. albicans* (29). Tetraploid strains CAY3373-5 were grown on YPD, streaked onto test media, and incubated at 30°C or 37°C for 8-10 days. Cells were then removed from the plates and resuspended in water. The OD_{600} was measured and used to plate ~10^3 cells on YPD and ~10^5 cells on 2-DOG plates. The percentage of chromosome loss was calculated as described previously (29).

Batch Culture Evolution Assay

C. tropicalis diploid and tetraploid strains were maintained in a manner similar to that performed in *S. cerevisiae* (39). Frozen stocks were streaked onto YPD and subsequently grown overnight in liquid YPD medium. 100 μl of the overnight culture was diluted into 10 ml YPD medium and grown at 30°C. Three replicates of each cell line were maintained. Cells were diluted 1:100 (100 μl culture into a fresh tube of 10 ml YPD) daily (24 hours $\pm$ 1 hour) for 42 days. Such dilution allows for approximately 6.64 ($\log_2 100$) mitotic divisions before the population returns to stationary phase (39). A 500 μl sample was taken from each line and frozen in 500 μl of 1:1 YPD:50% glycerol at -80°C every three days (72 hours $\pm$ 1 hour) for subsequent cytometric analysis. For analysis of ploidy change, control diploid and tetraploid cells were used to define gates for regions where diploid G1 and tetraploid G2 peaks were

present. The percentage of total cells present in the peaks was calculated by dividing the number of cells in the gated region by the total cell count.

***In vitro* Competition Assay**

Diploid and tetraploid strains were compared for fitness in co-culture experiments. The frozen stock of each strain was grown on YPD plates overnight at 30°C, and subsequently grown in 3-5 ml YPD cultures overnight at 30°C. A hemocytometer was used to determine the concentration of cells present. Competing strains were then mixed together in equal amounts of ~10^7 colony forming units (CFU) in 10 ml YPD. Two independent cultures were used for each assay in each independent experiment. Cells were diluted 1:100 (100 µl culture into a fresh tube of 10 ml YPD) daily (24 hours $\pm$ 1 hour) for 7 days. This allowed for a maximum of ~6.64 divisions each day. After one week, an equal number of cells were plated to YPD and YPD+NAT plates and the percentage of NAT^R cells calculated.

***In vivo* Competition Assay**

Female BALB/c mice (18-20g, Charles River Laboratories) were made neutropenic by intraperitoneal injection of 200 µg anti-Gr-1 monoclonal anitbody (clone: RB6-8C5, BioXCell) 24 hours prior to infection. *C. tropicalis* strains were grown overnight in liquid YPD medium at 30°C. On the day of infection, *C. tropicalis* cells were diluted to an OD_{600} of 0.2 into 10 ml of fresh YPD medium and grown at 30°C for 5 hours. Log phase cells were collected and washed three times in sterile phosphate-buffered saline (PBS). Cell concentrations were measured with a hemocytometer. Mice were infected with a mixture of two *C. tropicalis* strains in a ~50:50 ratio, with a total inoculum of ~1.0 x 10^6 colony forming units (CFUs) by injection into the lateral tail vein. Each *C. tropicalis* competition mixture included one isolate resistant to nourseothricin (NAT^R) and one isolate sensitive to nourseothricin (NAT^S). Each competition mixture was

injected into 4 neutropenic female BALB/c mice. Dilutions of the inoculum were plated onto YPD agar and YPD+NAT agar to confirm initial CFUs. Mice were euthanized 48 hours post-infection, and the liver, spleen, brain and kidneys were isolated from each mouse. The organs were homogenized using a gentleMACS Dissociator. Dilutions of each tissue homogenate was plated onto YPD and incubated at 30°C for 24 hours to calculate the total fungal burden from each organ. Colonies were then replica plated from YPD onto YPD+NAT to calculate the percentage of the recovered *C. tropicalis* population that included NAT resistance. Four to eight mice were used for each combination of *C. tropicalis* strains. Neutropenia was monitored by collecting blood daily through retro-orbital bleeding of mice. Blood samples were stained with FITC-labeled anti-GR1-antibody and neutrophil populations were identified by FITC-staining, cell size, and cell complexity using flow cytometry. Neutropenia in mice treated with the anti-Gr-1 antibody was confirmed 4 days following injection with the antibody (data not shown).

Measurement of Doubling Times

Strains used in the competition assay were streaked onto YPD plates and grown overnight at 30°C and subsequently resuspended in liquid YPD. Cells were diluted to an OD_{600} of 0.2 in 1 ml YPD, and 4 x 150 µl for each strain transferred into a 96-well plate. The plate was incubated at 30°C in a Synergy HT multi-mode plate reader (BioTek), and OD_{600} measured every 30 minutes. To calculate the doubling time of each strain, readings were averaged and plotted against time as a semi-logarithmic graph.

Statistical Analysis

Statistical analysis was completed using the PAST (Paleontological Statistics Software for Education and Data Analysis) Software Package. Overall, parametric tests were used whenever data sets were found to be normally distributed via the Anderson-Darling

method, otherwise non-parametric tests were used. A p-value of 0.05 was used throughout as a measure of significant difference. For the chromosome loss assay, a Bonferroni-corrected Mann-Whitney U-test was used. For the batch culture evolution experiments, Tukey's test was used to compare between diploid and tetraploid samples on the same given day. The *in vitro* competition data was compared using an independent-samples T-test. The *in vivo* competition data was compared using a one-way ANOVA.

Table A1-0-1: Figures used in this study

Strain	Genotype	*MTL* type	Ploidy
CAY2059	*arg4/arg4*	a/a	Diploid
CAY2060	*arg4/arg4*	a/a	Diploid
CAY2881	*his1/his1 GAL1/gal1::SAT1*	α/α	Diploid
CAY3031	*his1/his1 GAL1/gal1*	α/α	Diploid
CAY3371	*his1/his1 gal1/gal1::SAT1*	α/α	Diploid
CAY3372	*his1/his1 gal1/gal1::SAT1*	α/α	Diploid
CAY3373	*his1/his1/HIS1/HIS1 arg4/arg4/ARG4/ ARG4 gal1/gal1::SAT1/GAL1/GAL1*	a/a/α/α	Tetraploid
CAY3374	*his1/his1/HIS1/HIS1 arg4/arg4/ARG4/ ARG4 gal1/gal1::SAT1/GAL1/GAL1*	a/a/α/α	Tetraploid
CAY3375	*his1/his1/HIS1/HIS1 arg4/arg4/ARG4/ ARG4 gal1/gal1::SAT1/GAL1/GAL1*	a/a/α/α	Tetraploid
CAY4090	*his1/HIS1 arg4/ARG4 gal1::SAT1/GAL1*	a/α	Diploid
CAY4276	*his1/HIS1 arg4/ARG4 gal1/GAL1*	a/α	Diploid
CAY4277	*his1/HIS1 arg4/ARG4 gal1/GAL1*	a/α	Diploid
CAY4281	*his1/HIS1 arg4/ARG4 gal1::SAT1/GAL1*	a/α	Diploid
CAY4283	*his1/HIS1 arg4/ARG4 gal1::SAT1/GAL1*	a/α	Diploid
CAY4311	*his1/HIS1 arg4/ARG4 gal1/GAL1*	a/α	Diploid
CAY4539	*his1/HIS1 arg4/ARG4 gal1/GAL1 ura3::SAT1/URA3*	a/α	Diploid
CAY4888	*his1/his1/HIS1/HIS1 arg4/arg4/ARG4/ ARG4 gal1/gal1/GAL1/GAL1*	a/a/α/α	Tetraploid
CAY4890	*his1/his1/HIS1/HIS1 arg4/arg4/ARG4/ ARG4 gal1/gal1/GAL1/GAL1*	a/a/α/α	Tetraploid

Table A1-0-2: Oligonucleotides used in this study

Oligonucleotide no.	Oligonucleotide name	Sequence
562	CtMTLα2 Check 1	TAA AAC ATT AAG CAT AGA GGA CAA AGA A
563	CtMTLα2 Check 2	AAC TTC AAA TGC AAA ATG TAA AAC ATA C
564	CtMTLa1 Check 1	GGA TAA AGA GAG CTT AAG TTC AGA AGA G
565	CtMTLa1 Check 2	AAG TAT CAT CTG TCT TAT CTG ATT CCT TC
641	CtHIS1 (ApaI) −900	GGA GCG GGG CCC ACC TCA AGA GAT GAA TGA CA
642	CtHIS1 (XhoI) 0	GCC GGC TCG AGA ACT CTA AAC TAT GAT TGT ATT C
643	CtHIS1 (SacII) +900	GGA GCG CCG CGG AGT TCA TCT GTA TAA TAG TAC A
644	CtHIS1 (SacI) +1,800	GGC CGC GAG CTC TCC ACA CAT TCA TAA ATG TTC A
645	CtHIS1 5′ Check −950	CCA AGG ACA ACA CTC GTG CAG T
646	CtHIS1 3′ Check + 1,900	CAA ATT GAT CAC TTC TCT AGT CGA
647	CtHIS1 5′ ORF +200	AGG GTA ATT GTG ATT TGG GTA
648	CtHIS1 3′ ORF +600	CTT GGA AGA AAC CAA GTG AG
657	CtARG4 (ApaI) −900	GGA GCG GGG CCC TGA ATG TGT TGG TGG TGA TG
658	CtARG4 (XhoI) 0	GCC GGC CTC GAG GAC ATT GTT GTT AGA ATA AGT T
659	CtARG4 (NotI) +1,400	GGA GCG GCG GCC GCA CAT TCA TTC TCC TTC CCT CTC
660	CtARG4 (SacII) +2,300	GGC CGC CGC GGG AAT ATT GAT TGT TGA TTG TTG
661	CtARG4 5′ Check −950	GAC GTT GTT TAC CCT TGG TAT C
662	CtARG4 3′ Check + 2400	TTG TGG AAT GTA ATT TGC ACA C
663	CtARG4 5′ ORF +200	TCA GGA TTA GAA GAA ATT CGT G
664	CtARG4 3′ ORF +600	TGG ACT TTG ATT AAC TCT GGT T
1046	CtGAL1 (ApaI) −900	GGC GCC GGG CCC GAA ACG AAG ACC TAA TTC ACC C
1047	CtGAL1 (XhoI) +50	GCC GGC CTC GAG GGT TCA TTA GAA TGA GGA TCA G
1048	CtGAL1 (SacII) +1,200	GGA GCG CCG CGG GAA TCA CAG GGC TGA TTT AG
1049	CtGAL1 (SacI) +2,150	GGC CGC GAG CTC CGT TAA TTG TCA CCT ATC TAG AC
1050	CtGAL1 5′ Check −950	GGG ATC TAG TCA GGG AAG TTC
1051	CtGAL1 3′ Check + 2200	CTT CTA ATA CCC CAT AGT AC
1052	CtGAL1 5′ ORF +250	CAT CAT AAC CAA CAC AGA TAG C
1053	CtGAL1 3′ ORF +650	CGT AAA CTG CTT GTA CCA ATG
1054	CtADE2 (ApaI) −950	GGC GCC GGG CCC CCT GCG TAT TCT TAC GTA CA
1055	CtADE2 (XhoI) 0	GCC GGC CTC GAG TGA CCA CCT CCT AAA ATA CC
1056	CtADE2 (SacII) +1,500	GGA GCG CCG CGG GAG GTA TTC CAG TAG CTA CTG
1057	CtADE2 (SacI) +2,500	GGC CGC GAG CTC TCG CAC CAT GCG ATT CCT TG
1058	CtADE2 5′ check	CGA CCT GCG TAT TCT TAC GT
1059	CtADE2 3′ check	GAG ACA ATT GCT ACG CTG CG
2295	CtURA3 (ApaI) −450	GGC GCC GGG CCC GAA ATC TAT CAA GCT TCA TGT GAC
2296	CtURA3 (XhoI) 0	GCC GGC CTC GAG GGA TGT TTA GAT GCT CTT TC
2297	CtURA3 (SacII) +750	GGC GCC CCG CGG GAT ATA GAG AAG CCG GTT GG
2298	CtURA3 (SacI) +1300	CCG GCG AGC TCG GGA TGA TGA TCA AGT TGA TG
2299	CtURA3 5′ ORF −800	GGA GAC TAC TCC ATC ATC GT
2300	CtURA3 3′ ORF +1,500	GTG TAT TTG CAG GTT ATG GG

RESULTS

A Screen for Ploidy Reduction in C. tropicalis Tetraploids

Previous studies showed that *C. tropicalis* a and α diploid cells are able to mate to form stable a/α tetraploid cells (34, 35). In order to test for conditions that result in a reduction of ploidy in *C. tropicalis* tetraploid cells, we constructed a genetically marked tetraploid strain as outlined in Figure 1. Diploid α/α strains were constructed that were homozygous mutants for *HIS1* and *GAL1* genes (*MTL*α/α*; Δgal1/Δgal1*; *Δhis1*/*Δhis1*) and mated to diploid a/a cells in which both copies of the *ARG4* gene had been deleted (*MTL*a/a*; Δarg4*/*Δarg4*). The resulting tetraploids were therefore heterozygous at the *MTL, GAL1, HIS1,* and *ARG4* loci (Fig. 1). We note that the chromosomal locations of these loci have not been determined for *C. tropicalis*, although each locus resides on a different supercontig (17). Three tetraploid strains (CAY3373, CAY3374, and CAY3375) resulting from independent mating experiments (Supplemental Fig. 1) were used to screen for chromosome loss. *S. cerevisiae* and *C. albicans* strains expressing *GAL1* are unable to grow on medium containing 2-deoxygalactose (2-DOG) as the carbon source (40, 41), and we similarly used 2-DOG as a positive selection for *C. tropicalis* cells that had lost both copies of the wild type *GAL1* allele (Fig. 1).

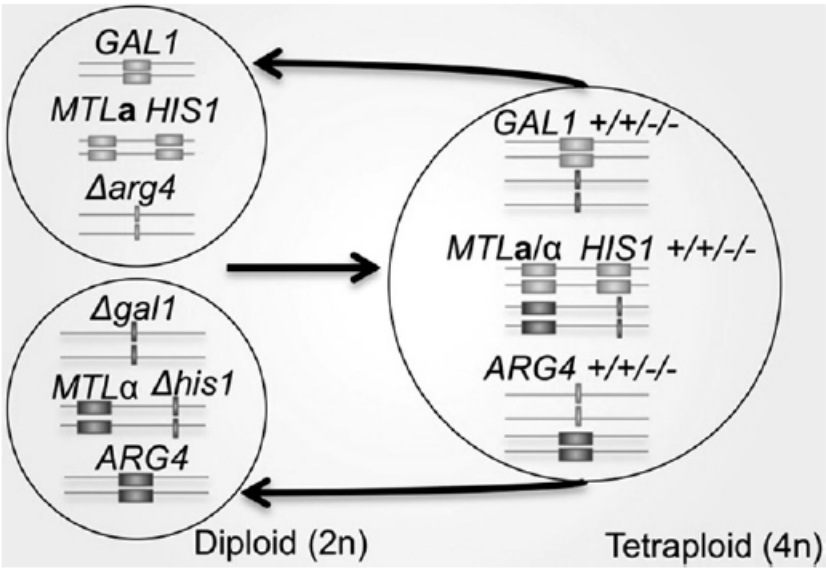

Figure A1-1: A genetic selection to monitor ploidy reduction in *C. tropicalis*.

Diploid a/a (CAY2059 and CAY2060) and α/FIG 1 A genetic selection to monitor ploidy reduction in C. tropicalis. Diploid a/a (CAY2059 and CAY2060) and α/ α (CAY3371 and CAY3372) C. tropicalis cells were mated to generate tetraploid strains (CAY3373, CAY3374, and CAY3375) that were heterozygous at the GAL1, MTL, HIS1, and ARG4 loci. Loss of GAL1 function was screened for by selection on 2-deoxygalactose (2- DOG) medium, which selects for Δgal1 cells. Chromosomal positions of genes are implicated based on chromosome positioning in the related species C. albicans. Linkage of MTL and HIS1 loci in C. tropicalis was also demonstrated in the present studies. (CAY3371 and CAY3372) C. tropicalis cells were mated to generate tetraploid strains (CAY3373, CAY3374, and CAY3375) that were heterozygous at the GAL1, MTL, HIS1, and ARG4 loci. Loss of GAL1 function was screened for by selection on 2-deoxygalactose (2- DOG) medium, which selects for Δgal1 cells. Chromosomal positions of genes are implicated based on chromosome positioning in the related species C. albicans. Linkage of MTL and HIS1 loci in C. tropicalis was also demonstrated in the present studies.

The genetically marked tetraploid strains were grown under a series of environmental conditions to identify those that could induce either parasexual chromosome loss or meiosis in *C. tropicalis*. As a proxy for ploidy reduction, we initially monitored loss of *GAL1* alleles via selection on 2-DOG medium. A total of 14 different laboratory media were tested, including rich (YPD), *S. cerevisiae* pre-sporulation (pre-spo), sorbose, potato dextrose agar (PDA), malt extract (malt), sorbitol, YPD+serum, low phosphate, low nitrogen (SLAD), and blood agar media. Cultures were grown at 30°C and 37°C for 8-10 days and subsequently plated onto YPD medium

to determine the total number of viable cells and onto 2-DOG medium to determine the number of cells that had lost *GAL1*.

Of all the media tested, sorbose medium induced the greatest formation of *Δgal1/Δgal1* cells from *C. tropicalis* tetraploid cells (Fig. 2C). For cells grown at 30°C on sorbose medium, 9.4% of viable cells were resistant to 2-DOG (DOG^R) compared to 0.0028% of those from YPD medium (p=2.3E-6). Similarly, at 37°C, 3.3% of viable cells taken from sorbose medium were found to be DOG^R, compared to 0.039% of cells from YPD (p=1.9E-4). Analysis of cells grown on other types of laboratory media generally revealed low rates of formation of DOG^R colonies, similar to those of cells grown on YPD medium. For example, testing on *S. cerevisiae* sporulation media at 30°C and 37°C resulted in 0.058% and 0.019% of cells becoming DOG^R, respectively. These data indicate that growth on sorbose medium leads to increased rates of *gal1*- colony formation in *C. tropicalis* tetraploid strains relative to other culture conditions. Interestingly, growth on pre-spo medium led to negligible loss of *GAL1*, which was not significantly different to growth on YPD when compared at 30°C (p=1.0) or 37°C (p=1.0). This finding contrasts with results in *C. albicans*, where incubation on pre-spo medium at 37°C led to high rates of *GAL1* loss from tetraploid cells (29, 30).

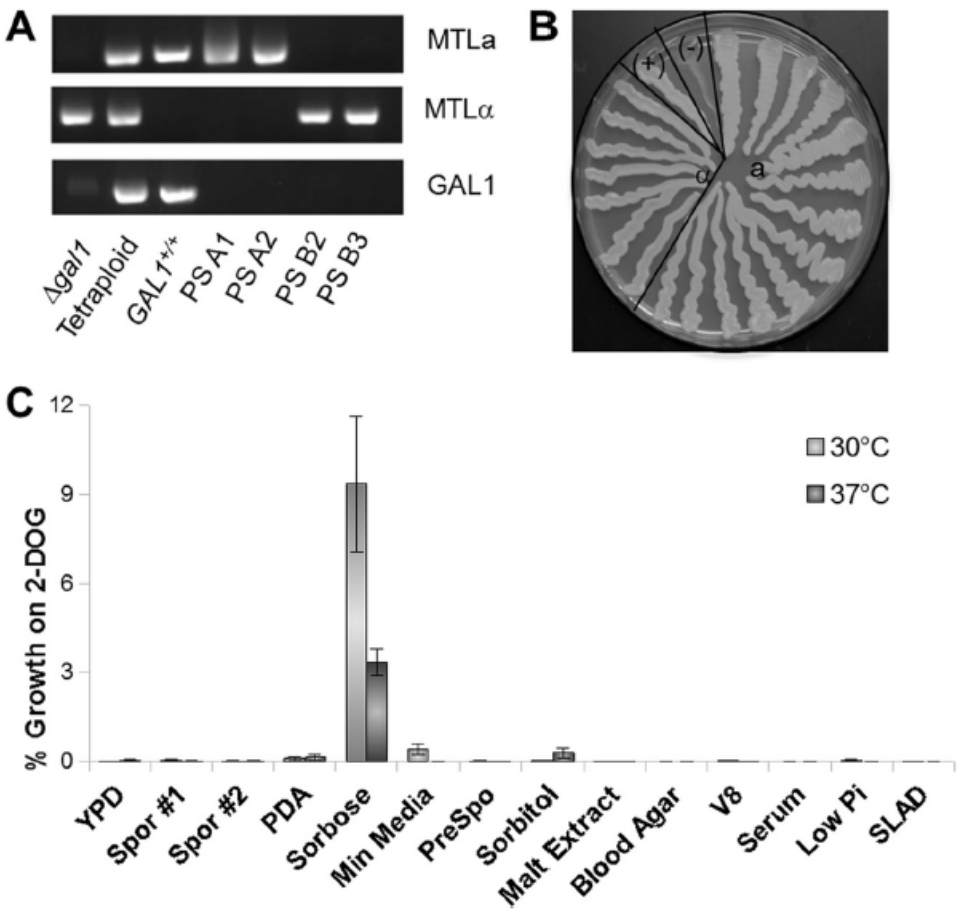

Figure A1-2: FIG 2 Chromosome loss in C. tropicalis tetraploid strains.

(A) A Δgal1 MTLα strain (CAY3371) was mated with a GAL1 +/+ MTLa strain (CAY2059) to generate the starting tetraploid strain (CAY3373) that was heterozygous at the GAL1 and MTL loci. Cells grown on sorbose medium for 8 to 10 days and selected on 2-DOG medium are shown as parasexual (PS) products. Parasexual colonies were screened for cells containing only MTLa (PS A1 and PS A2) or MTLα (PS B2 and PS B3) loci. (B) A 2-DOG plate showing selection of Δgal1 cells homozygous at the MTL locus after growth on sorbose for 8 to 10 days. CAY3371 (Δgal1 MTLα) and CAY3373 (the parental tetraploid) are shown as positive and negative controls, respectively. (C) Graph showing tetraploid stability under various medium conditions at 30°C and 37°C. The y axis represents a linear scale of percentage growth on 2-DOG medium. Bars represent means ± standard errors (n = 2 for minimal medium, sorbitol, malt extract, blood agar, V8, serum, low P i , and SLAD; n = 3 for sporulation medium 1; n = 4 for sporulation medium 2, PDA, and presporulation medium; n = 5 for YPD medium; n = 7 for sorbose).

Tetraploid Cells Recovered from Sorbose Medium have Reduced Ploidy

Growth on 2-DOG medium is indicative of loss of the wild-type *GAL1*, alleles but is not necessarily demonstrative of chromosome loss. In order to characterize the chromosome

content in progeny cells selected on 2-DOG medium, we first analyzed the genotype of 2-DOG^R cells at the *MTL* locus. PCR was used to identify cells that had lost both copies of *MTLα* (two such progeny are shown in Fig. 2A). Since we observed that *MTL* and *HIS1* loci are genetically linked (these loci are also linked in *C. albicans* where they both reside on chromosome 5), α progeny were identified by an inability to grow on medium lacking histidine. In total, we observed that 13 out of 198 DOG^R colonies (6.6%) were *MTL*a, while 7 out of 460 colonies (1.5%) were *MTLα,* with the rest of the colonies being heterozygous at the *MTL*. Cells were also directly picked from colonies on sorbose plates, restreaked on YPD medium, and 8 colonies out of 84 (9.52%) were *MTL*a by PCR screening. We identified a single *MTL*α isolate directly from sorbose plates out of 376 tested (0.27%). These experiments establish that *MTL* alleles were concomitantly lost during growth on sorbose medium, and that chromosome loss was not completely random as *MTL*a cells were generated at a higher frequency than *MTL*α cells. The reason for the bias in *MTL* loss is not known; however, it is possible that his- cells are selected against during growth on sorbose medium (even though this medium was supplemented with amino acids), thereby promoting the recovery of *MTL*a cells over *MTL*α cells.

We next used flow cytometry to determine the overall ploidy of selected parasexual progeny. Eight DOG^R progeny colonies that were homozygous at the *MTL* (four that were *MTL*a [Fig. 3B-E] and four that were *MTL*α [Fig. 3F-I]) were chosen for cytometric analysis. While small variations in ploidies were observed between the parasexual progeny, all of the progeny were similar in DNA content to control diploid strains. We also examined the ploidy of colonies selected directly from 2-DOG plates with unknown *MTL* status. Again, all samples analyzed showed peaks that were similar to those in the control diploid strain (Fig. 3J-O), which has a ploidy profile similar to that of other parental diploid strains (Supp. Fig. 1). Overall, this analysis

establishes that growth on sorbose medium leads to increased rates of ploidy reduction in *C. tropicalis*, resulting in progeny cells that are diploid, or close to diploid, in DNA content.

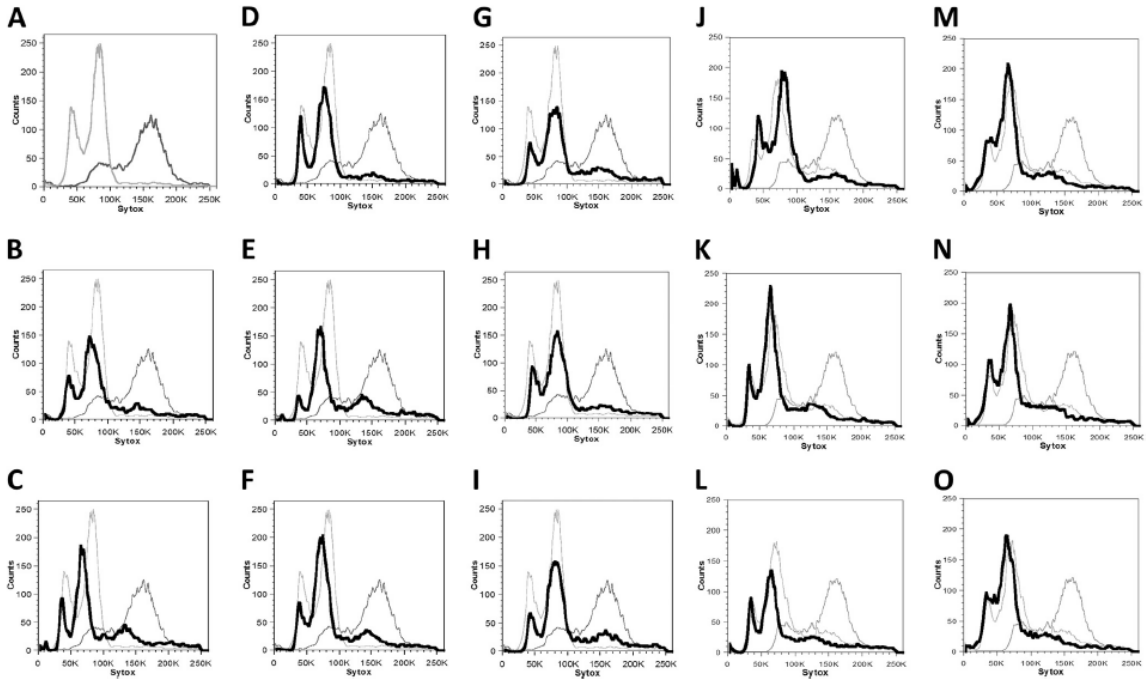

Figure A1-3: FIG 3 Cell cytometric analysis of parasexual cells.

The x axis (Sytox) represents a linear scale of fluorescence, and the y axis represents a linear scale of cell number. (A) Comparison of the initial Δgal1 diploid strain (CAY3371; light gray) with the starting tetraploid (CAY3373; dark gray). These strains are also included for reference in panels B to O. Eight independent colonies were isolated from 2-DOG selection after growth on sorbose for 8 to 10 days and identified as MTLa (B to E) or MTLα (F to I) isolates and catalogued as parasexual strains A1 to A4 and B2 to B5, respectively (Table 3). (J to O) Cell cytometric analysis of tetraploid cells exposed to sorbose and selected for loss of gal1 only, taken from plates grown at 30°C (parasexual strains F1, F2, and F7 in panels J to L, respectively) and 37°C (parasexual strains F9, F11, and G1 in panels M to O, respectively). Samples in panels A to I and J to O were analyzed on separate days, and thus, control diploid and tetraploid plots show minor differences.

Parasexual Progeny Cells are Mating-Competent

Given that the progeny cells arising from sorbose medium include a and α diploid cell types, we tested whether these cells could undergo additional rounds of mating to re-form tetraploid cells. *MTL*α progeny that were *Δhis1*/*Δhis1* were mated with a control *MTL*a strain

that is auxotrophic for arginine (CAY2060). Within 3-5 days, co-cultured cells began to exhibit a mating response (Fig. 4A) and formed zygotes (Fig. 4B), indicative of productive mating. Mating cells were also plated to -His/-Arg medium and the resulting colonies identified as *MTL*a/α cells (Fig. 4C). The ploidies of these mating products were examined using flow cytometry and showed peaks close to those of a tetraploid control (Fig. 4D-G). Re-mated tetraploids could also be induced to undergo chromosome loss when grown on sorbose medium at 30°C or 37°C, again as indicated by the generation of 2-DOG resistant colonies (data not shown). Together, these experiments demonstrate that a parasexual cycle can be established for *C. tropicalis* in which cells transition between diploid and tetraploid states.

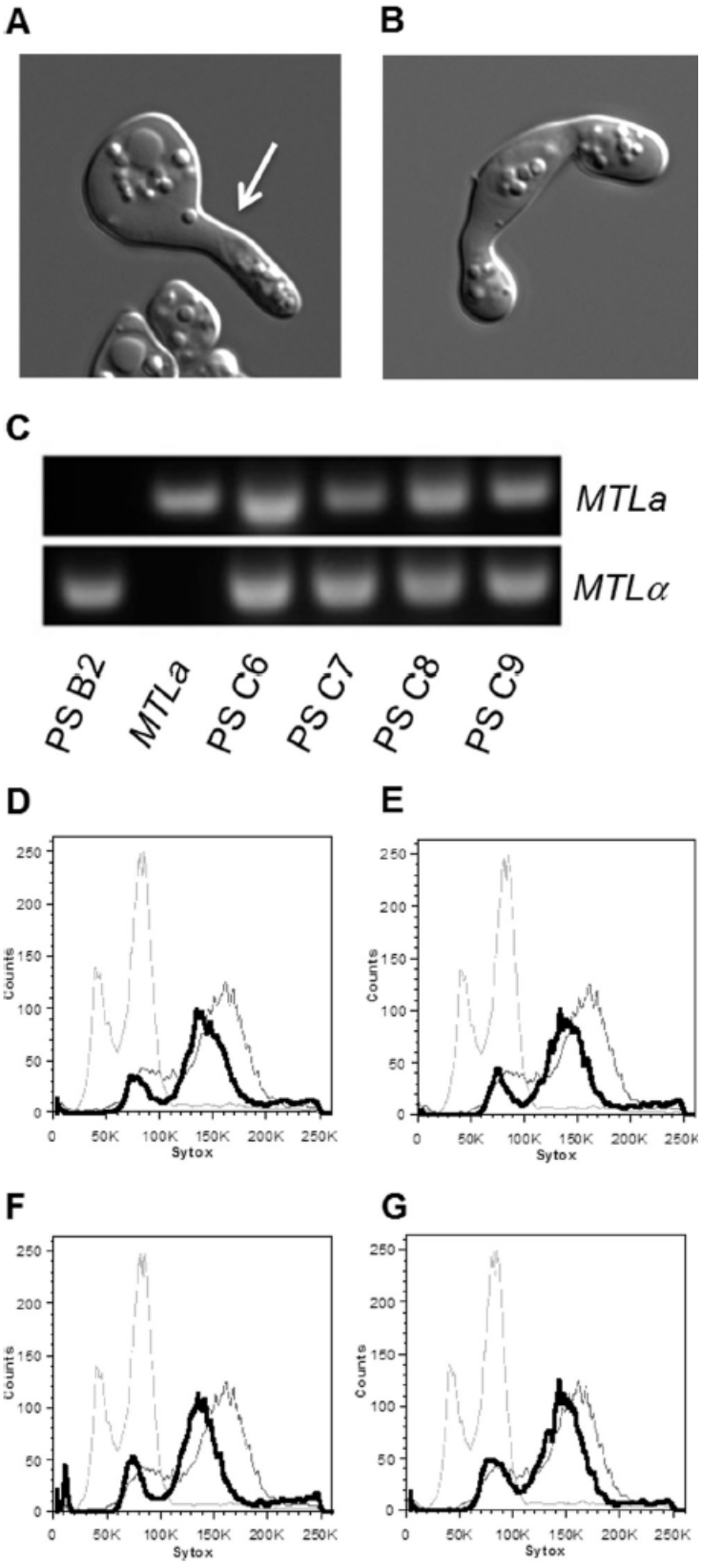

Figure A1-4: FIG 4 C. tropicalis parasexual progeny are mating competent.

(A and B) Representative images of mating projections (A) and zygotes (B) seen during mating of parasexual progeny with wild-type strains. (C) Characterization of MTL loci from four parasexual remating products (parasexual strains [PS] C6 to C9), compared with the parasexual parent (B2) and MTLa parental strain (CAY2060). (D to G) Cell cytometric data showing ploidy of parasexual remating products PS C6 (D), PS C7 (E), PS C8 (F), and PS C9 (G). The x axis (Sytox) represents a linear scale of fluorescence, and the y axis (counts) represents a linear scale of cell number. Diploid (light gray) and tetraploid (dark gray) controls are shown in the background as described in the legend of Fig. 3.

C. tropicalis Tetraploid Cells Become Diploid During Prolonged Culture in Rich Medium

As shown above, chromosome loss in *C. tropicalis* tetraploid cells is facilitated by growth on sorbose medium over a period of 8-10 days. Studies in *S. cerevisiae* have shown that tetraploid, triploid, and haploid strains trend toward the diploid state when cultured over multiple generations, and that the process of chromosome loss from tetraploid to diploid is concerted across the genome (39, 42). We therefore addressed whether ploidy reduction in *C. tropicalis* tetraploid cells might also occur during extended culture in YPD medium. A genetically marked tetraploid strain (CAY3373) and a control *MTL*a/α diploid (CAY4311) were grown separately in YPD medium in three replicate lines for 42 days at 30°C. Cells were diluted back 1:100 (100 µl into 10 ml YPD) every 24 hours allowing for ~6.6 generations each day, and samples were frozen down every 72 hours for subsequent analysis. Flow cytometry showed that all three *C. tropicalis* tetraploid cell cultures lost ploidy over the course of the experiment and returned to the diploid state (Fig. 5A-C). Interestingly, the temporal profiles of the independent tetraploid lineages showed a very similar pattern of ploidy reduction. G1 and G2 peaks were distinct up to day 18 (120 generations) then multiple peaks were observed between generations 120 and 140. Distinct peaks started to reappear around day 24 (160 generations) and eventually reached a defined diploid state by 36 days (240 generations). Three independent diploid cultures were also propagated in YPD for multiple generations and two of the three showed a steady diploid state across the period of the experiment (Fig. 5D). One diploid lineage unexpectedly showed a trend towards increased ploidy (data not shown).

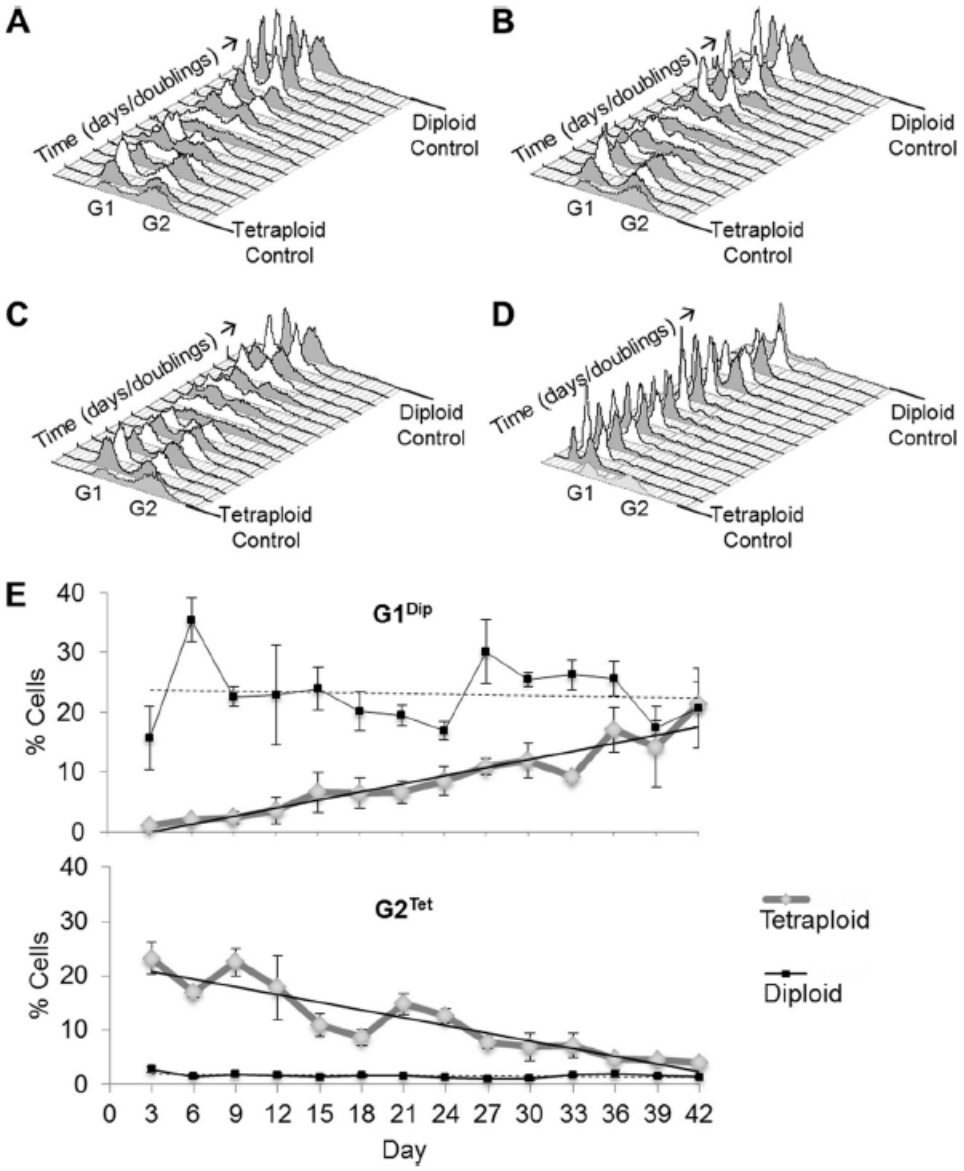

Figure A1-5: Ploidy reduction in C. tropicalis tetraploid strains.

(A to C) Cytometric data showing gradual ploidy change from the tetraploid (4n) state to the diploid (2n) state, as evidenced by the leftward shift of G 1 and G 2 peaks in three independent lines. (D) Cytometric data showing stability of a diploid strain under the same conditions. The x axes represent a linear scale of fluorescence, the y axes represent a linear scale of cell number, and the z axes represent a linear scale of time in days. Control tetraploid (front) and diploid (back) strains are shown on either end for reference. (E) Changes in the G 1 Dip peak and G 2 Tet peak during passage of tetraploid strains. Values for control diploid strains are shown in black. The y axis represents the proportion of total cells contained within the given peak with reference to a control strain. The solid and dashed black lines represent the best-fit lines for tetraploids and diploids, respectively. Values represent means ± standard deviations (n = 3 for tetraploids).

To quantify changes in ploidy, we measured the percentage of cells within the diploid G1 peak ($G1^{Dip}$) and tetraploid G2 peak ($G2^{Tet}$) relative to control strains. As predicted for tetraploid strains, $G1^{Dip}$ showed an increasing trend over time, while $G2^{Tet}$ decreased to a basal level by 36 days / 240 generations (Fig. 5E). Diploid strains showed static trends for both of these parameters, as expected for a stable diploid population, while tetraploid strains converged toward the diploid state by the 42 day time point, or 279 generations (Fig. 5E). The difference in $G1^{Dip}$ between the diploid and tetraploid lines was significant until approximately day 30 / 200 generations (average p= 0.012), and this significance was lost over the final twelve-day period. The $G2^{Tet}$ difference remained statistically significant until day 33 / 220 generations (average p= 0.0046). Our analysis shows that *C. tropicalis* tetraploid cells, while generally stable, begin to lose chromosomes during prolonged culture in rich medium, becoming aneuploid and eventually returning to the diploid state in a manner similar to that described in *S. cerevisiae*.

C. tropicalis Diploid Cells Outcompete Tetraploid Cells During Co-Culture In Vitro

To investigate the conversion of tetraploid populations to diploid populations, we determined if there was a fitness advantage to propagating in the diploid state. To compare the fitness of tetraploid and diploid cells, we maintained cultures containing cells of both ploidy states in YPD medium for 7 days at 30°C, diluting them 1:100 every 24 hours. A nourseothricin-resistant (NAT^{R}) diploid strain was grown in competition with a nourseothricin-sensitive (NAT^{S}) tetraploid strain, or conversely, a NAT^{R} tetraploid strain was grown in competition with a NAT^{S} diploid strain. Nourseothricin resistance served as a selectable marker for determining the fraction of the population that derived from the diploid or tetraploid strain (Fig. 6A). In both

cases, the diploid strain used was a prototrophic precursor to the *MTL*α strain used to construct the tetraploid strain.

Following culture for 7 days in YPD, cells were plated onto YPD plates with or without nourseothricin to distinguish NAT^R and NAT^S colonies. The proportion of tetraploid cells showed a statistically significant decrease from day 0 to day 7 ($p = 0.005$) comprising only 20 % of the population recovered on day 7 despite representing 50% of the initial inoculum (Fig. 6A). Furthermore, occasional NAT^R diploid cells were recovered despite entering the experiment as tetraploid, while the opposite was not true. We conclude that *C. tropicalis* diploid cells hold a significant fitness advantage over tetraploid cells *in vitro*, and that this is independent of the NAT marker used in these studies, given that tetraploid populations decreased in both NAT^R and NAT^S configurations.

To determine if these results were due to differential growth rates between diploid and tetraploid strains, we analyzed the doubling times for each of the strains used in the competition assay. However, no significant differences in growth rates were observed between diploid and tetraploid strains, as both doubled every 60 minutes during exponential growth. We also determined that diploid and tetraploid strains were able to grow to the same maximum optical density in saturated cultures (Fig. 6B and data not shown). These results indicate that the increased fitness of diploid strains is not simply the consequence of faster growth under these culture conditions.

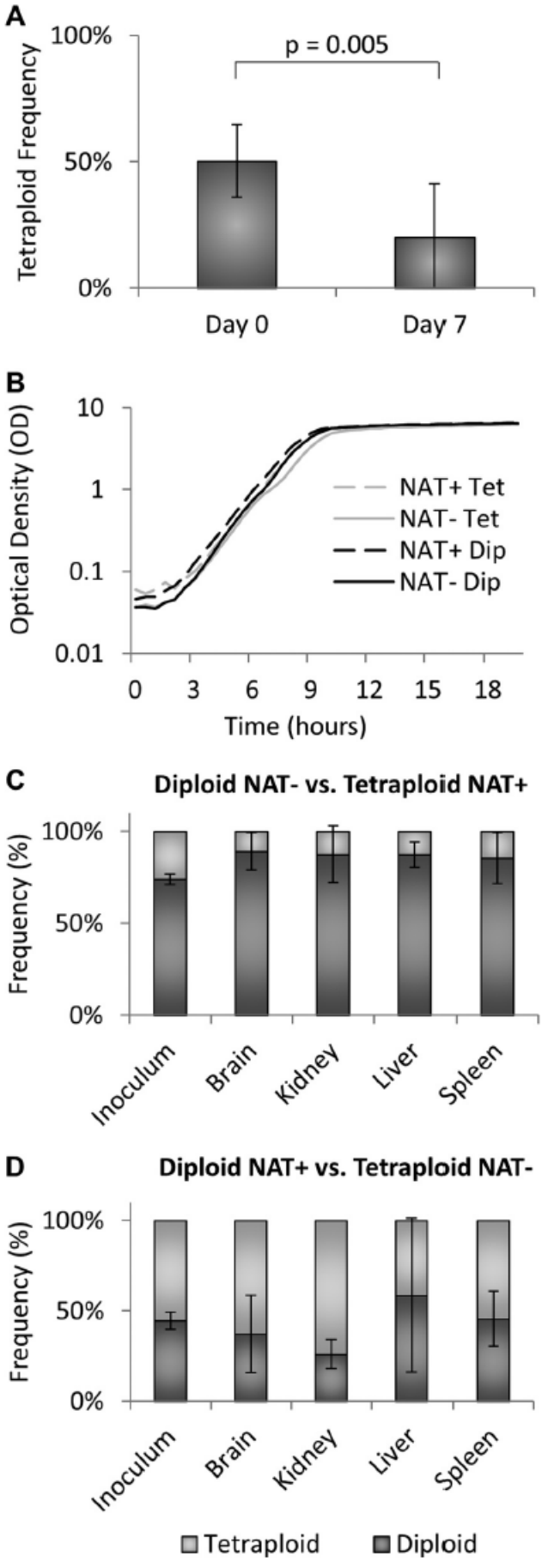

Figure A1-6: C. tropicalis ploidy competition assays.

(A) Coculture of NAT R diploid with NAT S tetraploid strains and NAT R tetraploid with NAT S diploid strains. The y axis represents the percentage of tetraploid cells present at the beginning (day 0) and end (day 7) of the experiment. Bars represent means ± standard deviations. NAT R diploid strains (CAY4090, CAY4281, and CAY4282) were competed with NAT S tetraploid strains (CAY4888 and CAY4890), while NAT R tetraploid strains (CAY3373 and CAY3374) were competed with NAT S diploid strains (CAY3031, CAY4276, and CAY4277) ($P = 0.005$; $n = 8$). (B) Growth curve for strains used in the assay. The x axis represents a linear scale of time in hours, and the y axis represents a logarithmic scale of optical density (OD) as a measure of cell concentration. The experiment was carried out twice, with one representative figure shown here. (C and D) In vivo competition assay showing population frequencies of NAT R diploids versus NAT S tetraploids (C) and NAT R tetraploids versus NAT S diploids (D) in murine brain, kidney, liver, and spleen tissue after 48 h, compared to the initial inoculum. Bars represent means ± standard deviations for 4 to 8 mice in independent experiments.

To determine if a fitness advantage of diploid cells was also observed *in vivo*, we performed a competition experiment using an established murine model for systemic infection (43). Mice were infected via the tail-vein with mixed populations of diploid and tetraploid cells, and cells subsequently recovered from the brain, kidney, liver, and spleen. After 2 days of infection, we saw no change in the relative proportions of diploid and tetraploid strains between the inoculum and the recovered cells (Fig. 6C and D). Thus, the initial NAT^R diploid inoculum (44.4%) showed similar frequencies in the brain (B; 37.0%), kidney (K; 25.9%), liver (L; 58.5%), and spleen (S; 45.5%) following infection. Similarly, the initial frequency of NAT^R tetraploids (26.2%) was not significantly different when recovered from any of the infected organs (B, 10.8%; K, 12.5%; L, 12.7%; S, 14.5%). Longer time points during *in vivo* infection were not possible as *C. tropicalis* strains led to murine morbidity and mice had to be euthanized, or strains were cleared from the infection.

DISCUSSION

C. tropicalis was recently discovered to have an extant mating program in which diploid cells fuse to form tetraploid products (34, 35). In this study, we used a genetic selection to identify conditions that induce *C. tropicalis* tetraploid cells to return to the diploid state. Populations of *C. tropicalis* tetraploid cells were stable for multiple generations when grown on diverse laboratory media, but exhibited chromosome instability when propagated for extended periods in rich (YPD) medium. In addition, tetraploid cells could also be induced to return to the diploid state by selective growth on sorbose medium. The diploid products of chromosome reduction were mating competent, thereby establishing that *C. tropicalis* can undergo a parasexual program.

The efficiency of chromosome loss in *C. tropicalis* tetraploid cells was highest when grown on sorbose medium; 3-9% of *C. tropicalis* tetraploid cells became DOG^R when incubated on this medium. Assuming a random segregation of chromosomes (and no loss of *GAL1* due to recombination) this indicates that 18-54% of sorbose-selected colonies became disomic for this chromosome. In contrast, only 0.003-0.04% of *C. tropicalis* cells grown on YPD medium lost *GAL1*, a difference of two to three orders of magnitude. Flow cytometric analysis of *Δgal1* progeny confirmed that most chromosomes had become disomic during growth on sorbose medium and thus parasexual progeny exhibited a ploidy similar to that of control diploid cells.

Sorbose medium has also been shown to induce concerted chromosome loss in tetraploid cells of the related species *C. albicans* (29, 30). In *C. albicans*, growth on sorbose medium is stressful as most cells in the population are unable to survive on this medium (29, 44). We saw a similar stress response in *C. tropicalis,* with reduced cell viability on sorbose medium. The survival rate was even lower when cells were grown on sorbose without amino

acids (1-6%), although there was no difference in loss of the *GAL1* marker between the two conditions. In both *Candida* species, colonies that survive stressful growth on sorbose medium have frequently undergone parasexual chromosome loss. *C. albicans* tetraploid cells were also previously shown to exhibit chromosome instability when incubated on *S. cerevisiae* 'pre-sporulation' medium at 37°C (29). In contrast, growth on pre-spo medium did not result in high rates of chromosome loss in *C. tropicalis*. Furthermore, whereas pre-spo induced high rates of cell death in both *C. albicans* and *C. tropicalis* tetraploid cells at 2 days, only *C. tropicalis* cells recovered viability after 4 days growth on this medium (data not shown). We surmise that chromosome instability is associated with cell stress, and induction of the parasexual program may be used to survive hostile environmental conditions, as further discussed below.

Notably, none of the conditions tested in this study was found to induce sporulation in *C. tropicalis* tetraploid cells, and we thus found no evidence for a meiotic program in this species. Identification of a conventional meiosis in *C. albicans* has been a long-standing goal, as it would allow the use of classical genetics in this important human pathogen (45, 46). Similarly, we now report that *C. tropicalis* appears to undergo a parasexual cycle rather than a true sexual cycle that culminates in meiosis. Growth of *C. tropicalis* tetraploid cells on sorbose medium induced an efficient reduction in ploidy, but the surviving colonies on this medium did not produce any spore-like cells. It therefore remains to be seen if a cryptic meiotic program exists for either *C. albicans* or *C. tropicalis*.

C. tropicalis tetraploid cells were also found to undergo a reduction in ploidy to the diploid state during prolonged culture in YPD medium. Strikingly, each of three independent tetraploid lines showed a similar trend towards diploidy via intermediate aneuploid states. This ploidy change began around day 18 in YPD culture following approximately 120 generations of

propagation. Since cells were cultured under rich growth conditions, it therefore appears that the parasexual process in *Candida* species does not take place exclusively under conditions of stress (30, 31), an important factor when considering where chromosome loss may occur in host environments.

Studies of genomic states in *S. cerevisiae* have established that this organism is also capable of undergoing asexual changes in ploidy. *S. cerevisiae* cells preferentially propagate as diploid cells, and prolonged culture of haploid, triploid, or tetraploid cells results in their convergence toward the diploid state (39, 42, 47). This genomic convergence is independent of mating or meiosis, and may occur by chromosome nondisjunction during mitosis (e.g. to drive a ploidy reduction) or by endoreduplication (e.g., to drive a ploidy increase). *Aspergillus nidulans*, a primarily haploid ascomycete, also undergoes a reduction in ploidy (from diploid to haploid) via a parasexual mechanism when grown continuously in standard medium (48). It is therefore apparent that extended culture can induce ploidy changes in diverse fungal species, although the precise molecular mechanisms driving parasexual ploidy changes remain to be elucidated.

The fitness of *C. tropicalis* diploid and tetraploid cells was also directly compared in this study. When co-cultured in YPD medium for 7 days, diploid cells showed enhanced fitness over tetraploid cells. This is in spite of the fact that diploid and tetraploid cells showed indistinguishable growth rates *in vitro*. However, co-culture in a murine model of infection failed to demonstrate an enhanced fitness of diploids, which may be due to the limited time period (2 days) used for *in vivo* experiments. It therefore appears that diploid cells exhibit increased fitness over tetraploid cells, but that tetraploid cells can stably survive and propagate in *in vivo* niches, at least for a defined period of time. In *S. cerevisiae*, haploid cell populations were also shown to be overtaken by diploid cells, even though the investigators failed to

pinpoint any overt fitness advantage of diploids over haploids (47). Other studies have also failed to identify specific fitness advantages of diploid strains over haploid strains of *S. cerevisiae* (49, 50). We conclude that *C. tropicalis* diploids hold a cryptic fitness advantage over tetraploids but that the nature of the fitness advantage is currently unknown.

Recent studies have revealed that *C. albicans* diploid cells can also undergo a ploidy reduction to the haploid state *in vitro* and *in vivo* (32). This discovery was surprising as *C. albicans* was thought to be an obligate diploid due to the presence of multiple recessive lethal alleles on different chromosome homologs (51, 52). The formation of *C. albicans* haploids presumably occurs via a non-meiotic mechanism as very few chromosomal crossovers were detected in haploid cells (32). To test if *C. tropicalis* can also exist in the haploid state, we screened for *C. tropicalis* haploid cells using a diploid strain heterozygous for *GAL1*, *HIS1*, *ARG4*, and *URA3*. We observed loss of several genetic markers in a subset of the population but have so far been unable to obtain *C. tropicalis* haploid cells under a variety of *in vitro* culture conditions (data not shown).

What are the consequences of parasex for the lifestyles of *Candida* species? Berman and Hadany (31) have proposed that diverse progeny resulting from parasex would have the potential to better survive and adapt to stressful environments. In support of this model, they note that many of the steps in the *C. albicans* parasexual cycle are induced by stress, and thus parasex can generate recombinant forms precisely when needed for adaptation to a hostile environment. Preliminary experiments in *C. albicans* support this hypothesis as they show that parasexual progeny can better resist stressful conditions *in vitro* than parental diploid cells (M.P.H and R.J.B, unpublished observations). We note that both stressful culture conditions (growth on sorbose) and non-stressful conditions (prolonged culture in YPD) induce parasexual

chromosome loss in *C. tropicalis* tetraploid cells. It therefore remains an intriguing question as to the precise conditions that induce the parasexual cycle in nature, and the role of this cycle in generating recombinant forms that can promote adaptation to environmental niches.

ACKNOWLEDGEMENTS

S.K.J. and A.M.P. were supported by pre-doctoral fellowships F31DE022701 and F31DE022703, respectively. M.P.H. was supported by a Graduate Assistance in Areas of National Need Training Grant P200A100100. This work was supported by National Institutes of Health grant AI081704 (to R.J.B.) and by National Science Foundation Grant MCB1021120 (to R.J.B). R.J.B. also holds an Investigator in the Pathogenesis of Infectious Disease Award from the Burroughs Wellcome Fund.

REFERENCES

1. **Nielsen K, Heitman J.** 2007. Sex and virulence of human pathogenic fungi. Adv Genet **57:**143-173.

2. **Goddard MR, Godfray HC, Burt A.** 2005. Sex increases the efficacy of natural selection in experimental yeast populations. Nature **434:**636-640.

3. **Heitman J.** 2006. Sexual reproduction and the evolution of microbial pathogens. Curr Biol **16:**R711-725.

4. **Heitman J.** 2010. Evolution of eukaryotic microbial pathogens via covert sexual reproduction. Cell Host Microbe **8:**86-99.

5. **Hadany L, Otto SP.** 2007. The evolution of condition-dependent sex in the face of high costs. Genetics **176:**1713-1727.

6. **Hadany L, Otto SP.** 2009. Condition-dependent sex and the rate of adaptation. The American naturalist **174 Suppl 1:**S71-78.

7. **Neiman AM.** 2005. Ascospore formation in the yeast *Saccharomyces cerevisiae*. Microbiol Mol Biol Rev **69:**565-584.

8. **Ni M, Feretzaki M, Sun S, Wang X, Heitman J.** 2011. Sex in fungi. Annu Rev Genet **45:**405-430.

9. **Butler G.** 2010. Fungal sex and pathogenesis. Clin Microbiol Rev **23:**140-159.

10. **Kwon-Chung KJ.** 1976. Morphogenesis of *Filobasidiella neoformans*, the sexual state of *Cryptococcus neoformans*. Mycologia **68:**821-833.

11. **Lin X, Hull CM, Heitman J.** 2005. Sexual reproduction between partners of the same mating type in *Cryptococcus neoformans*. Nature **434:**1017-1021.

12. **Giles SS, Dagenais TR, Botts MR, Keller NP, Hull CM.** 2009. Elucidating the pathogenesis of spores from the human fungal pathogen *Cryptococcus neoformans*. Infect Immun **77:**3491-3500.

13. **Fraser JA, Giles SS, Wenink EC, Geunes-Boyer SG, Wright JR, Diezmann S, Allen A, Stajich JE, Dietrich FS, Perfect JR, Heitman J.** 2005. Same-sex mating and the origin of the Vancouver Island *Cryptococcus gattii* outbreak. Nature **437:**1360-1364.

14. **Ma H, Hagen F, Stekel DJ, Johnston SA, Sionov E, Falk R, Polacheck I, Boekhout T, May RC.** 2009. The fatal fungal outbreak on Vancouver Island is characterized by enhanced intracellular parasitism driven by mitochondrial regulation. Proc Natl Acad Sci U S A **106:**12980-12985.

15. **Byrnes EJ, 3rd, Li W, Lewit Y, Ma H, Voelz K, Ren P, Carter DA, Chaturvedi V, Bildfell RJ, May RC, Heitman J.** 2010. Emergence and pathogenicity of highly virulent *Cryptococcus gattii* genotypes in the northwest United States. PLoS Pathog **6:**e1000850.

16. **O'Gorman CM, Fuller HT, Dyer PS.** 2009. Discovery of a sexual cycle in the opportunistic fungal pathogen *Aspergillus fumigatus*. Nature **457:**471-474.

17. **Butler G, Rasmussen MD, Lin MF, Santos MA, Sakthikumar S, Munro CA, Rheinbay E, Grabherr M, Forche A, Reedy JL, Agrafioti I, Arnaud MB, Bates S, Brown AJ, Brunke S, Costanzo MC, Fitzpatrick DA, de Groot PW, Harris D, Hoyer LL, Hube B, Klis FM, Kodira C, Lennard N, Logue ME, Martin R, Neiman AM, Nikolaou E, Quail MA, Quinn J, Santos MC, Schmitzberger FF, Sherlock G, Shah P, Silverstein KA, Skrzypek MS, Soll D, Staggs R, Stansfield I, Stumpf MP, Sudbery PE, Srikantha T, Zeng Q, Berman J, Berriman M, Heitman J, Gow NA, Lorenz MC, Birren BW, Kellis M, Cuomo CA.** 2009. Evolution of pathogenicity and sexual reproduction in eight *Candida* genomes. Nature **459:**657-662.

18. **Miranda I, Silva R, Santos MA.** 2006. Evolution of the genetic code in yeasts. Yeast **23:**203-213.

19. **van der Walt JP.** 1966. *Lodderomyces*, a new genus of the Saccharomycetaceae. Antonie Van Leewenhoek **32:**1-5.

20. **Reedy JL, Floyd AM, Heitman J.** 2009. Mechanistic plasticity of sexual reproduction and meiosis in the *Candida* pathogenic species complex. Curr Biol **19:**891-899.

21. **van der Walt JP, Taylor MB, Liebenberg NV.** 1977. Ploidy, ascus formation and recombination in *Torulaspora* (*Debaryomyces*) *hansenii*. Antonie Van Leeuwenhoek **43:**205-218.

22. **Wickerham LJ, Burton KA.** 1954. A clarification of the relationship of *Candida guilliermondii* to other yeasts by a study of their mating types. J Bacteriol **68:**594-597.

23. **Gargeya IB, Pruitt WR, Simmons RB, Meyer SA, Ahearn DG.** 1990. Occurrence of *Clavispora lusitaniae*, the teleomorph of *Candida lusitaniae*, among clinical isolates. J Clin Microbiol **28:**2224-2227.

24. **Alby K, Schaefer D, Bennett RJ.** 2009. Homothallic and heterothallic mating in the opportunistic pathogen *Candida albicans*. Nature **460:**890-893.

25. **Hull CM, Raisner RM, Johnson AD.** 2000. Evidence for mating of the "asexual" yeast *Candida albicans* in a mammalian host. Science **289:**307-310.

26. **Magee BB, Magee PT.** 2000. Induction of mating in *Candida albican*s by construction of *MTLa* and *MTLalpha* strains. Science **289:**310-313.

27. **Miller MG, Johnson AD.** 2002. White-opaque switching in *Candida albicans* is controlled by mating-type locus homeodomain proteins and allows efficient mating. Cell **110:**293-302.

28. **Tzung KW, Williams RM, Scherer S, Federspiel N, Jones T, Hansen N, Bivolarevic V, Huizar L, Komp C, Surzycki R, Tamse R, Davis RW, Agabian N.** 2001. Genomic evidence for a complete sexual cycle in *Candida albicans*. Proc Natl Acad Sci U S A **98:**3249-3253.

29. **Bennett RJ, Johnson AD.** 2003. Completion of a parasexual cycle in *Candida albicans* by induced chromosome loss in tetraploid strains. Embo J **22:**2505-2515.

30. **Forche A, Alby K, Schaefer D, Johnson AD, Berman J, Bennett RJ.** 2008. The parasexual cycle in *Candida albicans* provides an alternative pathway to meiosis for the formation of recombinant strains. PLoS Biol **6:**e110.

31. **Berman J, Hadany L.** 2012. Does stress induce (para)sex? Implications for *Candida albicans* evolution. Trends Genet **28:**197-203.

32. **Hickman MA, Zeng G, Forche A, Hirakawa MP, Abbey D, Harrison BD, Wang YM, Su CH, Bennett RJ, Wang Y, Berman J.** 2013. The 'obligate diploid' *Candida albicans* forms mating-competent haploids. Nature.

33. **Kothavade RJ, Kura MM, Valand AG, Panthaki MH.** 2010. *Candida tropicalis*: its prevalence, pathogenicity and increasing resistance to fluconazole. Journal of medical microbiology **59:**873-880.

34. **Porman AM, Alby K, Hirakawa MP, Bennett RJ.** 2011. Discovery of a phenotypic switch regulating sexual mating in the opportunistic fungal pathogen *Candida tropicalis*. Proc Natl Acad Sci U S A **108:**21158-21163.

35. **Xie J, Du H, Guan G, Tong Y, Kourkoumpetis TK, Zhang L, Bai FY, Huang G.** 2012. N-acetylglucosamine induces white-to-opaque switching and mating in *Candida tropicalis*, providing new insights into adaptation and fungal sexual evolution. Eukaryot Cell **11:**773-782.

36. **Guthrie C, Fink GR.** 1991. Guide to Yeast Genetics and Molecular Biology. Academic Press, San Diego.

37. **Liu H, Kohler J, Fink GR.** 1994. Suppression of hyphal formation in *Candida albicans* by mutation of a *STE12* homolog. Science **266:**1723-1726.

38. **Reuss O, Vik A, Kolter R, Morschhauser J.** 2004. The *SAT1* flipper, an optimized tool for gene disruption in *Candida albicans*. Gene **341:**119-127.

39. **Gerstein AC, Chun HJ, Grant A, Otto SP.** 2006. Genomic convergence toward diploidy in *Saccharomyces cerevisiae*. PLoS Genet **2:**e145.

40. **Platt T.** 1984. Toxicity of 2-deoxygalactose to *Saccharomyces cerevisiae* cells constitutively synthesizing galactose-metabolizing enzymes. Mol Cell Biol **4:**994-996.

41. **Gorman JA, Gorman JW, Koltin Y.** 1992. Direct selection of galactokinase-negative mutants of *Candida albicans* using 2-deoxy-galactose. Curr Genet **21:**203-206.

42. **Gerstein AC, McBride RM, Otto SP.** 2008. Ploidy reduction in *Saccharomyces cerevisiae*. Biology letters **4:**91-94.

43. **Noble SM, French S, Kohn LA, Chen V, Johnson AD.** 2010. Systematic screens of a *Candida albicans* homozygous deletion library decouple morphogenetic switching and pathogenicity. Nat Genet **42:**590-598.

44. **Janbon G, Sherman F, Rustchenko E.** 1998. Monosomy of a specific chromosome determines L-sorbose utilization: a novel regulatory mechanism in *Candida albicans*. Proc Natl Acad Sci U S A **95:**5150-5155.

45. **Alby K, Bennett RJ.** 2010. Sexual reproduction in the *Candida* clade: cryptic cycles, diverse mechanisms, and alternative functions. Cell Mol Life Sci.

46. **Bennett RJ, Johnson AD.** 2005. Mating in *Candida albicans* and the Search for a Sexual Cycle. Annu Rev Microbiol **59:**233-255.

47. **Gerstein AC, Otto SP.** 2011. Cryptic fitness advantage: diploids invade haploid populations despite lacking any apparent advantage as measured by standard fitness assays. PLoS One **6:**e26599.

48. **Schoustra SE, Debets AJ, Slakhorst M, Hoekstra RF.** 2007. Mitotic recombination accelerates adaptation in the fungus *Aspergillus nidulans*. PLoS Genet **3:**e68.

49. **Mable BK.** 2001. Ploidy evolution in the yeast *Saccharomyces cerevisiae*:

a test of the nutrient limitation hypothesis. J. Evol. Biol. **14:**157-170.

50. **Dickinson WJ.** 2008. Synergistic fitness interactions and a high frequency of beneficial changes among mutations accumulated under relaxed selection in *Saccharomyces cerevisiae*. Genetics **178:**1571-1578.

51. **Sarachek A, Weber DA.** 1986. Segregant-defective heterokaryons of *Candida albicans*. Curr Genet **10:**685-693.

52. **Whelan WL, Soll DR.** 1982. Mitotic recombination in *Candida albicans*: recessive lethal alleles linked to a gene required for methionine biosynthesis. Mol Gen Genet **187**.

Table A2-3: Parasexual strains in this study

PS group and strain no.[a]	Cell type or genotype	Isolate no.	Original strain(s) (growth condition
Selected progeny tested for *MTL* type			
*MTL***a**/**a**			
A1	*MTL***a**/**a** Δ*gal1*/Δ*gal1*::*SAT1*	1	CA3373 (sorbose at 30°C)
A2	*MTL***a**/**a** Δ*gal1*/Δ*gal1*::*SAT1*	2	CA3373 (sorbose at 30°C)
A3	*MTL***a**/**a** Δ*gal1*/Δ*gal1*::*SAT1*	3	CA3373 (sorbose at 30°C)
A4	*MTL***a**/**a** Δ*gal1*/Δ*gal1*::*SAT1*	4	CA3373 (sorbose at 30°C)
A5	*MTL***a**/**a** Δ*gal1*/Δ*gal1*::*SAT1*	5	CA3373 (sorbose at 30°C)
A6	*MTL***a**/**a** Δ*gal1*/Δ*gal1*::*SAT1*	6	CA3373 (sorbose at 30°C)
A7	*MTL***a**/**a** Δ*gal1*/Δ*gal1*::*SAT1*	7	CA3373 (sorbose at 37°C)
A8	*MTL***a**/**a** Δ*gal1*/Δ*gal1*::*SAT1*	8	CA3373 (sorbose at 37°C)
A9	*MTL***a**/**a** Δ*gal1*/Δ*gal1*::*SAT1*	9	CA3373 (sorbose at 37°C)
A10	*MTL***a**/**a** Δ*gal1*/Δ*gal1*::*SAT1*	10	CA3373 (sorbose at 37°C)
A11	*MTL***a**/**a** Δ*gal1*/Δ*gal1*::*SAT1*	11	CA3374 (sorbose at 30°C)
A12	*MTL***a**/**a** Δ*gal1*/Δ*gal1*::*SAT1*	12	CA3374 (sorbose at 37°C)
B1	*MTL***a**/**a** Δ*gal1*/Δ*gal1*::*SAT1*	13	CA3375 (sorbose at 30°C)
*MTL*α/α			
B2	*MTL*α/α Δ*gal1*/Δ*gal1*::*SAT1* Δ*his1*/Δ*his1*	23	CA3373 (sorbose at 30°C)
B3	*MTL*α/α Δ*gal1*/Δ*gal1*::*SAT1* Δ*his1*/Δ*his1*	25	CA3373 (sorbose at 30°C)
B4	*MTL*α/α Δ*gal1*/Δ*gal1*::*SAT1* Δ*his1*/Δ*his1*	242	CA3373 (sorbose at 30°C)
B5	*MTL*α/α Δ*gal1*/Δ*gal1*::*SAT1* Δ*his1*/Δ*his1*	283	CA3373 (sorbose at 30°C)
B6	*MTL*α/α Δ*gal1*/Δ*gal1*::*SAT1* Δ*his1*/Δ*his1*	302	CA3374 (sorbose at 30°C)
B7	*MTL*α/α Δ*gal1*/Δ*gal1*::*SAT1* Δ*his1*/Δ*his1*	320	CA3374 (sorbose at 30°C)
B8	*MTL*α/α Δ*gal1*/Δ*gal1*::*SAT1* Δ*his1*/Δ*his1*	336	CA3374 (sorbose at 30°C)
Progeny from sorbose tested for *MTL* type			
B9	*MTL***a**/**a** Δ*gal1*/Δ*gal1*::*SAT1*	1	
B10	*MTL***a**/**a**	2	CA3373 (sorbose at 37°C)
B11	*MTL***a**/**a**	3	CA3373 (sorbose at 37°C)
B12	*MTL***a**/**a**	4	CA3373 (sorbose at 37°C)
C1	*MTL***a**/**a**	7	CA3373 (sorbose at 37°C)
C2	*MTL***a**/**a**	9	CA3374 (sorbose at 37°C)
C3	*MTL***a**/**a**	10	CA3375 (sorbose at 37°C)
C4	*MTL***a**/**a**	11	CA3375 (sorbose at 37°C)
Randomly selected progeny from 2-DOG			
F1	Δ*gal1*/Δ*gal1*::*SAT1*	1	CA3373 (sorbose at 30°C)
F2	Δ*gal1*/Δ*gal1*::*SAT1*	2	CA3373 (sorbose at 30°C)
F3	Δ*gal1*/Δ*gal1*::*SAT1*	3	CA3373 (sorbose at 30°C)
F4	Δ*gal1*/Δ*gal1*::*SAT1*	4	CA3373 (sorbose at 30°C)
F5	Δ*gal1*/Δ*gal1*::*SAT1*	5	CA3373 (sorbose at 30°C)
F6	Δ*gal1*/Δ*gal1*::*SAT1*	6	CA3373 (sorbose at 30°C)
F7	Δ*gal1*/Δ*gal1*::*SAT1*	7	CA3373 (sorbose at 30°C)
F8	Δ*gal1*/Δ*gal1*::*SAT1*	8	CA3373 (sorbose at 30°C)
F9	Δ*gal1*/Δ*gal1*::*SAT1*	1	CA3373 (sorbose at 37°C)
F10	Δ*gal1*/Δ*gal1*::*SAT1*	2	CA3373 (sorbose at 37°C)
F11	Δ*gal1*/Δ*gal1*::*SAT1*	3	CA3373 (sorbose at 37°C)
F12	Δ*gal1*/Δ*gal1*::*SAT1*	4	CA3373 (sorbose at 37°C)
G1	Δ*gal1*/Δ*gal1*::*SAT1*	5	CA3373 (sorbose at 37°C)
G2	Δ*gal1*/Δ*gal1*::*SAT1*	7	CA3373 (sorbose at 37°C)
G3	Δ*gal1*/Δ*gal1*::*SAT1*	8	CA3373 (sorbose at 37°C)
G4	Δ*gal1*/Δ*gal1*::*SAT1*	9	CA3373 (sorbose at 37°C)
Mating products			
C5	*MTL***a**/**a**/α/α *his1*/*his1*/*HIS1*/*HIS1 arg4*/*arg4*/*ARG4*/*ARG4 gal1*/*gal1*::*SAT1*/*GAL1*/*GAL1*	5	B2 × CAY2060; mating product G
C6	*MTL***a**/**a**/α/α *his1*/*his1*/*HIS1*/*HIS1 arg4*/*arg4*/*ARG4*/*ARG4 gal1*/*gal1*::*SAT1*/*GAL1*/*GAL1*	6	B2 × CAY2060; mating product G
C7	*MTL***a**/**a**/α/α *his1*/*his1*/*HIS1*/*HIS1 arg4*/*arg4*/*ARG4*/*ARG4 gal1*/*gal1*::*SAT1*/*GAL1*/*GAL1*	7	B2 × CAY2060; mating product G
C8	*MTL***a**/**a**/α/α *his1*/*his1*/*HIS1*/*HIS1 arg4*/*arg4*/*ARG4*/*ARG4 gal1*/*gal1*::*SAT1*/*GAL1*/*GAL1*	19	B3 × CAY2060; mating product H
C9	*MTL***a**/**a**/α/α *his1*/*his1*/*HIS1*/*HIS1 arg4*/*arg4*/*ARG4*/*ARG4 gal1*/*gal1*::*SAT1*/*GAL1*/*GAL1*	20	B3 × CAY2060; mating product H
C10	*MTL***a**/**a**/α/α *his1*/*his1*/*HIS1*/*HIS1 arg4*/*arg4*/*ARG4*/*ARG4 gal1*/*gal1*::*SAT1*/*GAL1*/*GAL1*	21	B3 × CAY2060; mating product H
Haploid screen			
D1	*Gal1*$^-$	1	CAY4539 (2μM H_2O_2)
D2	*Gal1*$^-$ *Ura3*$^-$	2	CAY4539 (H_2O_2)
D3	*Gal1*$^-$	3	CAY4539 (H_2O_2)
D4	*Gal1*$^-$	4	CAY4539 (H_2O_2)
D5	*Gal1*$^-$ *Arg4*$^-$	5	CAY4539 (H_2O_2)
D6	*Gal1*$^-$ *Ura3*$^-$	6	CAY4539 (H_2O_2)
D7	*Gal1*$^-$	7	CAY4539 (H_2O_2)
D8	*Gal1*$^-$	8	CAY4539 (H_2O_2)
D9	*Gal1*$^-$	9	CAY4539 (H_2O_2)
D10	*Gal1*$^-$	11	CAY4539 (H_2O_2)
D11	*Gal1*$^-$ *Ura3*$^-$ *Arg4*$^-$	12	CAY4539 (H_2O_2)
D12	*Gal1*$^-$ *Arg4*$^-$	13	CAY4539 (H_2O_2)
E1	*Gal1*$^-$ *Ura3*$^-$	15	CAY4539 (42°C)
E2	*Gal1*$^-$	16	CAY4539 (42°C)
E3	*Gal1*$^-$ *Arg4*$^-$	17	CAY4539 (42°C)
E4	*Gal1*$^-$	19	CAY4539 (42°C)
E5	*Gal1*$^-$ *Ura3*$^-$	20	CAY4539 (42°C)
E6	*Gal1*$^-$	21	CAY4539 (42°C)
E7	*Gal1*$^-$	22	CAY4539 (42°C)

[a] PS, parasexual.

APPENDIX 2: IDENTIFICATION OF A CELL DEATH PATHWAY IN CANDIDA ALBICANS DURING THE RESPONSE TO PHEROMONE

ABSTRACT

Mating in hemiascomycete yeasts involves the secretion of pheromones that induce sexual differentiation in cells of the opposite mating type. Studies in *Saccharomyces cerevisiae* have revealed that a sub-population of cells experience cell death during exposure to pheromone. In this work, we tested whether the phenomenon of pheromone-induced death (PID) also occurs in the opportunistic pathogen *Candida albicans*. Mating in *C. albicans* is uniquely regulated by white-opaque phenotypic switching; both cell types respond to pheromone but only opaque cells undergo the morphological transition and cell conjugation. We show that approximately 20% of opaque cells, but not white cells, of laboratory strain SC5314 experience pheromone-induced death. Furthermore, analysis of mutant strains revealed that PID was significantly reduced in strains lacking Fig1 or Fus1 transmembrane proteins that are induced during the mating process and, we now show, are necessary for efficient mating in *C. albicans*. The level of PID was also Ca^{2+}-dependent, as chelation of Ca^{2+} ions increased cell death to almost 50% of the population. However, in contrast to *S. cerevisiae* PID, pheromone-induced killing of *C. albicans* cells was largely independent of signaling via the Ca^{2+}-dependent protein phosphatase, calcineurin, even when combined with the loss of Cmk1 and Cmk2 proteins. Finally, we demonstrate that levels of PID vary widely between clinical isolates of *C. albicans*, with some strains experiencing close to 70% cell death. We discuss these

findings in light of the role of pro-death and pro-survival pathways operating in yeast cells undergoing the morphological response to pheromone.

INTRODUCTION

Mating in the model yeast *Saccharomyces cerevisiae,* as well as in the related hemiascomycete *Candida albicans,* involves communication between **a** and α cells via sexual pheromones. The program of sexual differentiation has been particularly well defined in *S. cerevisiae*, where pheromone signaling activates a conserved MAP kinase cascade culminating in the transcriptional response of almost 500 genes (44). During mating, yeast cells increase the expression of genes required for conjugation, undergo arrest in G_1 of the cell cycle, and produce polarized mating projections in preparation for cell fusion (52). Mating also requires partial degradation of the cell wall to allow direct membrane fusion between **a** and α cells, followed by nuclear karyogamy and formation of a diploid cell. Previous studies have established that a sub-population of *S. cerevisiae* **a** cells responding to high levels of α pheromone undergo cell death (23, 48, 58). In these studies, pheromone treatment resulted in 25-30% cell death. However, prevention of a Ca^{2+} ion influx resulted in cell death in up to 95% of the population (23, 58). High levels of pheromone-induced death were also observed in mutants lacking components required for calcium signaling, including the high-affinity Ca^{2+} influx channel (Cch1/Mid1), calmodulin (Cmd1) and calcineurin (Cnb1). Calcineurin is a highly conserved protein phosphatase whose activity is regulated by Ca^{2+}/calmodulin, and is known to play a general role in the cellular response of yeast cells to environmental stresses (13). In general, it is thought that a rise in cytosolic Ca^{2+} levels activates calcineurin, leading to dephosphorylation of key target proteins including the transcription factor, Crz1p (54). The calcineurin-signaling pathway also plays a central role in protecting yeast cells from the toxic effects of multiple anti-fungal drugs (9, 55).

In addition to Ca^{2+} signaling, several other pathways influence the sensitivity of *S. cerevisiae* cells to pheromone toxicity, including multiple factors upregulated during the morphological response to pheromone. These include Fus1 and Fig1, two cell membrane proteins required for efficient cell fusion (16, 35, 58). Fus1 localizes to the cell tip of mating projections and coordinates the process of cell fusion, including the secretion of cell wall hydrolases that degradate the cell wall (36, 56). Fig1 forms part of a low-affinity Ca^{2+} influx system, although its role in PID appears independent of its function in Ca^{2+} transport (58). Mutants lacking either Fig1 or Fus1 exhibit significantly reduced levels of PID, indicating that although these factors are necessary for efficient mating their expression can also compromise cell viability.

To combat the potentially lethal effects of pheromone treatment *S. cerevisiae* cells activate repair pathways that help maintain cell viability. Cell wall degradation induces the cell wall integrity (CWI) signaling pathway, which involves a protein kinase cascade culminating in the activation of the MAP kinase, Slt2 (8, 27). Activation of the CWI pathway enhances chitin and glucan synthesis to compensate for cell wall damage induced by the mating program. Loss of CWI signaling therefore leads to greater death in the presence of pheromone, whereas hyperactivation of the CWI pathway limits pheromone-induced death (8, 58).

Candida albicans is a related hemiascomycete yeast that last shared a common ancestor with *S. cerevisiae* around 700 million years ago (19). *C. albicans* is a prevalent human fungal pathogen and was originally categorized as an asexual species. Work during the past decade has uncovered an elaborate mating cycle that, while similar to that of *S. cerevisiae*, also shows fundamental differences. For example, *C. albicans* mating takes place between **a** and α cells but requires that cells switch from the regular 'white' state to the alternative 'opaque' state (33). The regulation of mating by a phenotypic switch is unique to *C. albicans* (and the sister species

Candida dubliniensis) and may have evolved due to the close association of this yeast with its mammalian host (26, 42). Though only opaque cells secrete sex-specific pheromones, both white and opaque cells can respond to pheromone. Opaque cells form polarized mating projections and subsequently undergo cell fusion, while white cells exhibit increased adhesion and biofilm formation (3, 4, 14, 29, 59). It is speculated that the matrix formed by responding white cells helps maintain pheromone gradients and thereby promotes cell fusion between mating opaque cells *in vivo* (14, 50).

In this work, we examine the response of *C. albicans* cells to pheromone and demonstrate that cell death occurs in a subpopulation of cells similar to that shown in *S. cerevisiae*. *C. albicans* opaque cells, but not white cells, experience cell death, consistent with opaque cells undergoing the morphological response to pheromone leading to the formation of polarized mating projections. We also tested whether the same genetic pathways acting in *S. cerevisiae* contribute to *C. albicans* cell death, including the cell integrity pathway, the calcineurin-signaling pathway, and the mating factors, Fus1 and Fig1. Notable differences were found between the two yeast species to pheromone treatment, including a limited role for calcineurin signaling in protecting *C. albicans* cells compared to that in *S. cerevisiae*. These results demonstrate that the phenomenon of pheromone-induced death is shared by two diverse hemiascomycete yeasts, but that the mechanisms protecting yeast cells from pheromone toxicity differ. We further demonstrate that clinical isolates exhibit a remarkable range in their susceptibility to pheromone killing (from 2% to almost 70%), indicating that some *C. albicans* strains are highly susceptible to pheromone-induced cell death, while others are resistant to pheromone killing.

MATERIALS AND METHODS

Media and Reagents

Standard laboratory media were prepared as described previously (18). Spider medium contained 1.35% agar, 1% nutrient broth, 0.4% potassium phosphate (pH 7.2) supplemented with 2% mannitol (28). SCD medium refers to synthetic complete medium supplemented with 2% glucose. Alpha pheromone MF13 (GFRLTNFGYFEPG) was synthesized by Genemed Synthesis. Propidium iodide (BD Biosciences), BAPTA (Invitrogen) and geldanamycin (InvivoGen) were added at the indicated concentrations.

Strains

The *C. albicans* strains used in this study are listed in Table 1. Unless stated otherwise, strains are derived from SC5314, the laboratory strain of *C. albicans*. Newly constructed strains were generated in SNY152 (37). First, **a** and α derivatives of SNY152 were generated by growth on sorbose medium, as previously described (25), to create RBY1132 (**a**/**a**) and RBY1133 (α/α). Gene knockouts of *FUS1, FIG1, CNB1, MKC1, CMK1*, and *CMK2* were generated either using the fusion PCR (37) or *SAT1*-flipper (43) methods described previously. For each gene targeted using the fusion PCR method, oligonucleotides were used to PCR amplify approximately 500 bp of the 5' and 3' flanking sequence of the gene (see Tables 1 and 2). In addition, the *Candida dubliniensis HIS1*, *C. dubliniensis ARG4*, and *Candida maltosa LEU2* markers were PCR amplified from plasmids pSN52, pSN69, or pSN40, respectively, using universal primers 2 and 5 (37). Gene disruption cassettes were then generated by fusion PCR, combining the flanking PCR products with a selectable marker PCR product (37). RBY1132 and RBY1133 were transformed with the

gene disruption cassettes and correct integration confirmed by PCR using check oligonucleotides (Table 1) that flank the disruption cassette in combination with primers internal to the marker gene, as previously described (37). Subsequent transformation with a second marker fusion construct was similarly used for deletion of the remaining copy of the gene, and loss of the ORF confirmed by PCR with primers internal to the ORF (see Table 1). To delete *CMK1* and *CMK2* genes using the *SAT1*-flipper method, oligonucleotides were used to amplify approximately 500 bp of the 5' and 3' homologous flanks of each gene. The resulting PCR products were digested with *Apa*I/*Xho*I and *Sac*I/*Sac*II, respectively, and cloned into the plasmid pSFS2a (43). The resulting plasmids were digested with *Apa*I/*Sac*I to liberate cassettes containing the 5' and 3' gene flanks as well as the *SAT1* selectable marker, and used for transformation. Correct genomic integration was confirmed by PCR of the 5' and 3' disruption junctions. The *SAT1* marker was then counter-selected via outgrowth in YPD media followed by selection on plates containing low concentrations of nourseothricin (43). The transformation process was repeated to delete the remaining copy of the gene and loss of the ORF confirmed by PCR. Multiple gene knockouts were generated for each mutant strain to confirm that the observed phenotype was due to the targeted gene deletion.

Plasmid pWor1-Stim, which provides constitutive expression of Wor1p, was constructed as follows. First, a region of the *C. albicans LEU2* ORF sequence was PCR amplified using primers *LEU2* 5' (*Sac*II) and *LEU2* 3' (*Sac*I) (see Table 1). The PCR product was then digested with *Sac*II and *Sac*I and ligated into pSFS2a between these restriction enzyme sites creating plasmid pRS1. Next, the *ADH1* terminator sequence was PCR amplified and *Xho*I/*Bam*HI and *Bgl*II sites introduced at the 5' and 3' ends, respectively. The *ADH1* terminator sequence was digested with *Xho*I and *Bgl*II and ligated into plasmid pRS1 digested with *Xho*I and *Bam*HI creating plasmid pRS2. The *ACT1* promoter sequence was PCR amplified and restriction enzyme digested with

*Kpn*I and *Xho*I, and the *WOR1* ORF was PCR amplified and digested with *Xho*I and *Bgl*II restriction enzymes. Plasmid pRS2 was digested with *Kpn*I and *Bam*HI, and both *ACT1* and *WOR1* PCR fragments inserted into this plasmid creating pWor1-Stim. The vector was linearized by cutting within the *LEU2* ORF sequence with *Bsg*I, or within the *ACT1* promoter sequence with *Bgl*II, in preparation for transformation.

Pheromone Response and Mating Assays

Overnight cultures of *C. albicans* cells were grown in SCD medium at room temperature (22-25°C) following inoculation from single colonies. Cells were washed in water and resuspended in Spider medium at a concentration of 2 x 10^7 cells per ml. Alpha pheromone was added to 10 µM and cultures incubated for 5 h at room temperature prior to analysis by microscopy. Pictures were taken using a Zeiss Axioplan 2 microscope equipped with a Hamamatsu ORCA camera.

Quantitative mating experiments were performed by crossing strains with different auxotrophic markers as previously described (47). For evaluating the effect of geldanamycin on mating, matings were performed in liquid Spider medium containing the indicated concentrations of geldanamycin and incubated at room temperature for 24 h. Cells were then plated on selective media and analyzed for the formation of mating products.

Cell Death Assays

Overnight cultures of *C. albicans* cells were grown in SCD medium at room temperature, cells washed in water and resuspended in Spider medium at a concentration of 2 x 10^7 cells/ml. Alpha pheromone was added to a final concentration of 10 µM, unless stated otherwise, and

cultures were incubated at room temperature for 1-6 h. At different time points, 0.5 ml of the culture was removed, washed and resuspended in Spider medium, and treated with 1 μg/ml propidium iodide for 15 min. Cells were then washed with water and resuspended in SCD media for analysis by flow cytometry. At least 10,000 cells were counted in the FL3 channel on a FACSCalibur, where PI-positive cells represent dead yeast cells (15).

TABLE 1. Strains used in this study

Strain	Genotype or description	*MTL*	Reference or source
RBY1118	*leu2/leu2 his1/his1*	a/a	47
RBY1132	*leu2/leu2 his1/his1 arg4/arg4*	a/a	47
RBY1133	*leu2/leu2 his1/his1 arg4/arg4*	α/α	47
RBY1180	*arg4::hisG/arg4::hisG his1::hisG/HIS1*	α/α	47
RBY1220	*leu2::hisG/leu2::hisG his1::hisG/his1::hisG arg4::hisG/arg4::hisG bar1::LEU2/bar1::HIS1*	a/a	47
DSY162	Sorbose-selected AM2003/0191 clinical isolate	a/a	1
DSY164	Sorbose-selected L1086 clinical isolate	a/a	1
DSY168	Sorbose-selected IHEM16614 clinical isolate	a/a	1
DSY194	Sorbose-selected J981315 clinical isolate	a/a	1
DSY810/839	*fig1::HIS1/fig1::LEU2 arg4/arg4*	a/a	This study
DSY812/814	*mkc1::HIS1/mkc1::LEU2 arg4/arg4*	a/a	This study
DSY817/819	*cnb1::HIS1/cnb1::ARG4 leu2/leu2*	α/α	This study
DSY834/837	*cnb1::HIS1/cnb1::LEU2 arg4/arg4*	a/a	This study
DSY835/838	*fus1::HIS1/fus1::ARG4 leu2/leu2*	α/α	This study
DSY840/866	*fus1::HIS1/fus1::LEU2 arg4/arg4*	a/a	This study
DSY855/869	*fig1::HIS1/fig1::ARG4 leu2/leu2*	α/α	This study
DSY861/871	*mkc1::HIS1/mkc1::ARG4 leu2/leu2*	α/α	This study
DSY872/873	*leu2/leu2 his1/his1 pACT1-WOR1:SAT*	a/a	This study
DSY874/875	*fig1::HIS1/fig1::LEU2 pACT1-WOR1:SAT1 arg4/arg4*	a/a	This study
DSY876	*mkc1::HIS1/mkc1::LEU2 pACT1-WOR1:SAT1 arg4/arg4*	a/a	This study
DSY877	*cnb1::HIS1/cnb1::LEU2 pACT1-WOR1:SAT1 arg4/arg4*	a/a	This study
DSY878/879	*fus1::HIS1/fus1::LEU2 pACT1-WOR1:SAT1 arg4/arg4*	a/a	This study
DSY886/887	*leu2::hisG/leu2::hisG his1::hisG/his1::hisG arg4::hisG/arg4::hisG bar1::LEU2/bar1::HIS1 pACT1-WOR1:SAT1*	a/a	This study
KAY485/486	*cmk1/cmk1::SAT1 pACT1-WOR1:SAT1 his1/his1 leu2/leu2*	a/a	This study
KAY487/488	*cnb1::HIS1/cnb1::LEU2 cmk1/cmk1::SAT1 pACT1-WOR1:SAT1 arg4/arg4*	a/a	This study
KAY489/490	*cmk2/cmk2::SAT1 pACT1-WOR1:SAT1 his1/his1 leu2/leu2*	a/a	This study
KAY491/492	*cnb1::HIS1/cnb1::LEU2 cmk2/cmk2::SAT1 pACT1-WOR1:SAT1 arg4/arg4*	a/a	This study
KAY502/504	T101 clinical isolate *pACT1-WOR1:SAT1*	a/a	This study
CAY320	*leu2::hisG/leu2::hisG his1::hisG/his1::hisG arg4::hisG/arg4::hisG bar1::LEU2/bar1::ARG4*	a/a	1
CAY829/832	*cnb1::HIS1/cnb1::LEU2 cmk1/cmk1::SAT1 cmk2/cmk2::SAT1 arg4/arg4*	a/a	This study
CAY831/833	*cmk1/cmk1::SAT1 cmk2/cmk2::SAT1 his1/his1 leu2/leu2*	a/a	This study
CAY1078	AM2003/0191 *bar1/bar1::SAT1*	a/a	This study
AM2005/0377	Clinical isolate	a/a	1
L26	Clinical isolate	a/a	1
P37005	Clinical isolate	a/a	1

Table A2-2: Oligonucleotides used in this study.

TABLE 2. Oligonucleotides used in this study

Name	Sequence (5′ to 3′)*
Universal primer 2	CCGCTGCTAGGCGCGCCGTGACCAGTGTGATGGATATCTGC
Universal primer 5	GCAGGGATGCGGCCGCTGACAGCTCGGATCCACTAGTAACG
FIG1 5′ flank for	CCATTTTTAGCTACCATTGC
FIG1 5′ flank rev	CACGGCGCGCCTAGCAGCGGGAATACAATGGTGAATTTCAATGG
FIG1 3′ flank for	GTCAGCGGCCGCATCCCTGCCAACAACCACTGGTGGATAC
FIG1 3′ flank rev	AATGTCTCAATTCGCCCTCG
FIG1 5′ check	GGTGAAGATGTTGATGATATTG
FIG1 3′ check	CTTGGTATAATCACTGCCAC
FIG1 5′ ORF	CATAACTGCTGCGTTATTAAG
FIG1 3′ ORF	CATTGATCCTAATCCCCAAAG
FUS1 5′ flank for	AGAGGGAAATATGCAGTGCC
FUS1 5′ flank rev	CACGGCGCGCCTAGCAGCGGGGTAGTATCACCGTCATCTC
FUS1 3′ flank for	GTCAGCGGCCGCATCCCTGCATCTCTGGATATCGGCTTGG
FUS1 3′ flank rev	TCCATTCGTGGCATATACAG
FUS1 5′ check	GGAGGAGCAATAGGTATCAG
FUS1 3′ check	GTTAGTAGTTGTGTTCACTGC
FUS1 5′ ORF	AAAGCTCTCCAAATGCGAGC
FUS1 3′ ORF	TTGCATCACTTTCTCTGGGC
CNB1 5′ flank for	CAGGTTGTAATGGGTTGTTG
CNB1 5′ flank rev	CACGGCGCGCCTAGCAGCGGGTCAGTAGTTGTTGAAGTCG
CNB1 3′ flank for	GTCAGCGGCCGCATCCCTGCACCGATACAATTGCCAACAC
CNB1 3′ flank rev	GGTACGTGTATGTGCAGATC
CNB1 5′ check	GACTGAAAGCGCAACCTTTG
CNB1 3′ check	GATGAGAGTTCTAGAATCTC
CNB1 5′ ORF	GAGATTGATAGATTGCGCAAG
CNB1 3′ ORF	CTTGCCATCACCGTCCAAAT
MKC1 5′ flank for	CAGAAAGCCGTTCAAACGTTC
MKC1 5′ flank rev	CACGGCGCGCCTAGCAGCGGTGGGTGCTTCTTGTTGATCC
MKC1 3′ flank for	GTCAGCGGCCGCATCCCTGCCGACCACCAGTAGTTGAAAC
MKC1 3′ flank rev	AGCTCCACACAACTAGCATG
MKC1 5′ check	TGATAACGACCTGGTTGCA
MKC1 3′ check	CCCAAGAGAGAGTCGTTCTA
MKC1 5′ ORF	GCATCGTTTGTGGCAATCAA
MKC1 3′ ORF	CAACCAACAGACCAGATGTC
CMK1 5′ for (ApaI)	GGAGCGGGGCCCAATGTCGTTACAGTGTTCGC
CMK1 5′ rev (XhoI)	GGCCGCCTCGAGACTTGCCTGTCTTGGTCATC
CMK1 3′ for (SacII)	GGAGCGCCGCGGGCATTACCGTTGAATACCTTG
CMK1 3′ rev (SacI)	GGCCGCGAGCTCTGCTGAATCGTAGGTTTGTG
CMK1 5′ check	CCAGAACTCATGACTGACAC
CMK1 3′ check	CCCTAAGTGATGCATTGAGC
CMK1 5′ ORF	CACATCTACTGGAAGACACT
CMK1 3′ ORF	CTTCTGAAGAAACATCGACCC
CMK2 5′ for (ApaI)	GGAGCGGGGCCCCAGCTACATACACTTGTGTG
CMK2 5′ rev (XhoI)	GGCCGCCTCGAGGGGAATGATGATCAGTTGAC
CMK2 3′ for (SacII)	GGACCGCCGCGGGTGAATTCTGGTGGTTGGAG
CMK2 3′ rev (SacI)	GGCCGCGAGCTCCGTTTAGAAGGCAGGCTAGT
CMK2 5′ check	GACATGATTCGTGTAATTGTACG
CMK2 3′ check	GACGTTGGCCGATCCAACAT
CMK2 5′ ORF	GGTAAGACTTTAGGAGCAGG
CMK2 3′ ORF	CATGACCAGTACCTAATATGAC
LEU2 5′ (SacII)	GGCGCCCCGCGGGTGCTAAATCATCCGATGCAG
LEU2 3′ (SacI)	GCCGGCGAGCTCGAGAAATCTGTAGACTTTGGAG
ADH1 Term 5′ (XhoI/BamHI)	GCGGCGCTCGAGGCGGGGGATCCGGCAAATAGCTAAATTATATACGAATTAATA
ADH1 Term 3′ (BglII)	GGGCGCAGATCTACGCCTTCCAGCAATTGTCTCAAA
ACT1 Prom 5′ (KpnI)	GGCGCCGGTACCGGGGTTCCTATACTTTCTAGAGAATAGGAACTTCGGAGATAGAGC TATTAAGATCACCAG
ACT1 Prom 3′ (XhoI)	GCCGGCCTCGAGTTTGAARGATTATATTTTTTTAATATTAAT
WOR1 5′ ORF (XhoI)	GGCGCCCTCGAGTAAAATGTCTAATTCAAGTATAGTCCCTAC
WOR1 3′ ORF (BglII)	GCCGGCAGATCTCGAATTCACACACAGACCCAC

* Underlined sequences indicate the introduced restriction sites.

RESULTS

Pheromone-induced cell death in C. albicans

In *S. cerevisiae*, treatment of **a** cells with α pheromone leads to cell death in approximately 25% of cells in the population (58). To test whether *C. albicans* cells also experience pheromone-induced death (PID), *MTL***a** cells derived from the laboratory strain SC5314 were treated with synthetic α pheromone (10 μM) and cell death determined by staining cells with propidium iodide and analysis by flow cytometry (see Materials and Methods). A subset of cells in the opaque (mating-competent) form began to lose viability between 2-3 h and by 4-6 h approximately 20% of the cells were dead (PI-positive cells, see Figure 1A and 1B). Similar levels of inviable cells were detected when staining with an alternative vital dye, eosin Y (see Supplementary Figure S1). Cell death in opaque cells occurred after they began to exhibit polarized mating projections, which are first observed at 2 h and more clearly evident by 4 h (6). At time points later than 6 h, levels of cell death began to decline, possibly due to continued growth of non-responding cells. Cell killing was also dependent on Ste2, the receptor for α pheromone (see Supplementary Figure S1), suggesting that death required activation of the canonical pheromone-signaling MAPK cascade. In addition, no cell death was observed when white-phase **a** cells were treated with the synthetic α pheromone (Supplementary Figure S1). *C. albicans* white-phase cells upregulate a limited set of genes in response to pheromone, but do not form polarized mating projections or undergo efficient cell-cell conjugation (6, 14, 29).

The observation that cell death only occurs in opaque-phase cells led us to design a construct that locks cells into this phenotypic state. The central regulator of the white-opaque switch is the Wor1 protein, a putative transcription factor that is expressed only in opaque cells

and not in white cells (20, 53, 60, 61). Constitutive expression of Wor1 protein can maintain cells in the opaque state, and we therefore designed a vector in which *WOR1* was expressed under control of the *ACT1* promoter (see Materials and Methods). Insertion of this construct into **a** cells ensured that >99% of cells were maintained in the opaque state. A time course of pheromone-induced death showed that wildtype opaque strains with or without the constitutive Wor1 expression vector showed very similar levels of cell death (Figure 1B). These results allowed us to utilize the Wor1 expression vector as a tool to ensure we were examining >99% pure opaque populations in further analyses.

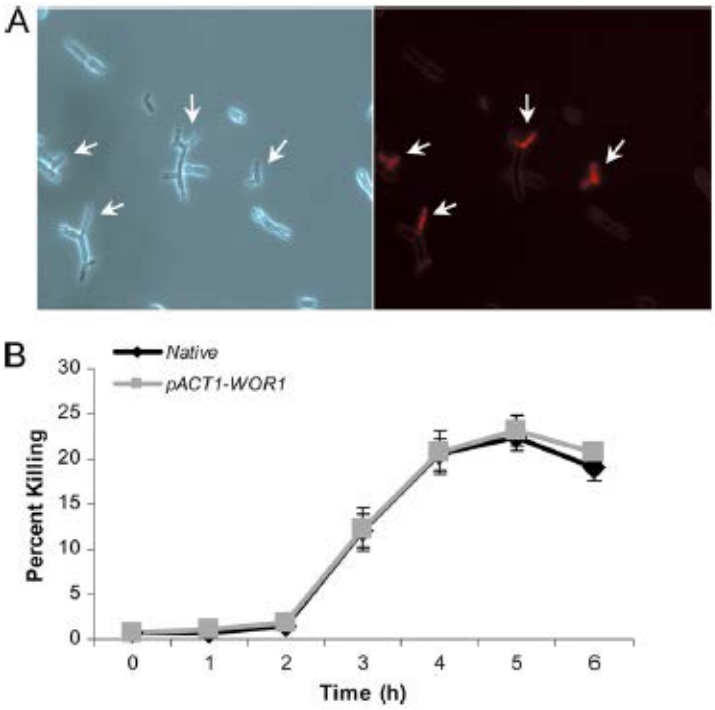

Figure A2-1:

Pheromone-induced cell death in *C. albicans*. (A) Picture of responding opaque cells and those that are dead (staining with propidium iodide, right panel). (B) Time course of cell death in *C. albicans MTLa* cells in the presence of α pheromone. Opaque **a** cells (derived from strain SC5314) were treated with 10 μM α pheromone, aliquots were removed, and cells were tested for viability by staining with propidium iodide. Both native opaque cells and cells locked in the opaque form by constitutive expression of Wor1 (*pACT1-WOR1*) were quantitated for cell death.

Factors Affecting Mating Efficiency and Cell Conjugation in C. albicans

In *S. cerevisiae*, multiple genetic pathways have been shown to influence the sensitivity of cells to pheromone-induced death. These include the calcineurin-signaling pathway, the cell wall integrity (CWI) pathway, and mating-specific factors upregulated during the morphological response to pheromone (8, 35, 58). We tested mutants in each of these pathways by examining *C. albicans* strains lacking *CNB1* (encoding the regulatory subunit of calcineurin), *MKC1* (encoding the CWI protein kinase), as well as *FUS1* and *FIG1* (encoding mating–specific cell membrane proteins). These mutants were constructed in *MTL***a** and *MTL*α strains of SC5314, and were first tested for their ability to undergo polarized growth in response to pheromone, and subsequently for their ability to undergo efficient cell-cell conjugation with a mating partner.

Each of the mutants was able to efficiently respond to pheromone and form polarized mating projections (approximately 70% of cells formed characteristic projections similar to wildtype cells, Figure 2A). Analysis of the shape of the mating projections (average width and length) revealed only subtle differences between the mutants, although $\sim$ *fus1* strains consistently exhibited projections that were longer (9.3 µm) than those in other strains (average 6-7 µm, Figure 2B). Quantitative mating experiments were also performed with each of the mutant strains. These were performed using bilateral crosses, as described in Materials and Methods. *C. albicans* wildtype strains mated at 77% efficiency when co-incubated on solid Spider medium for 2 days, and at 58% efficiency when grown in liquid medium (Figure 2C). Mutant *cnb1* strains lacking calmodulin mated with a similar mating efficiency to wildtype strains. In contrast, mutants lacking *FIG1*, *FUS1,* or *MKC1,* all showed a significant decrease in mating efficiency. The *fig1* mutant mated with the lowest efficiency, undergoing only 16% or 5% mating on solid or liquid medium, respectively. The *fus1* and *mkc1* mutants also showed a

reduced mating efficiency, with *fus1* strains undergoing 14%/31% mating and *mkc1* strains undergoing 30%/22% mating on solid or liquid medium, respectively (Figure 2C). These results indicate that *FIG1*, *FUS1*, and *MKC1* genes play important, but non-essential, roles in promoting mating and tetraploid formation in *C. albicans*. In *S. cerevisiae*, defects in the homologous genes similarly reduced mating efficiency; loss of *ScFIG1* reduced mating 2.5 fold (16), while loss of *ScFUS1* or *ScMPK1* resulted in moderate decreases in mating efficiency (17, 56).

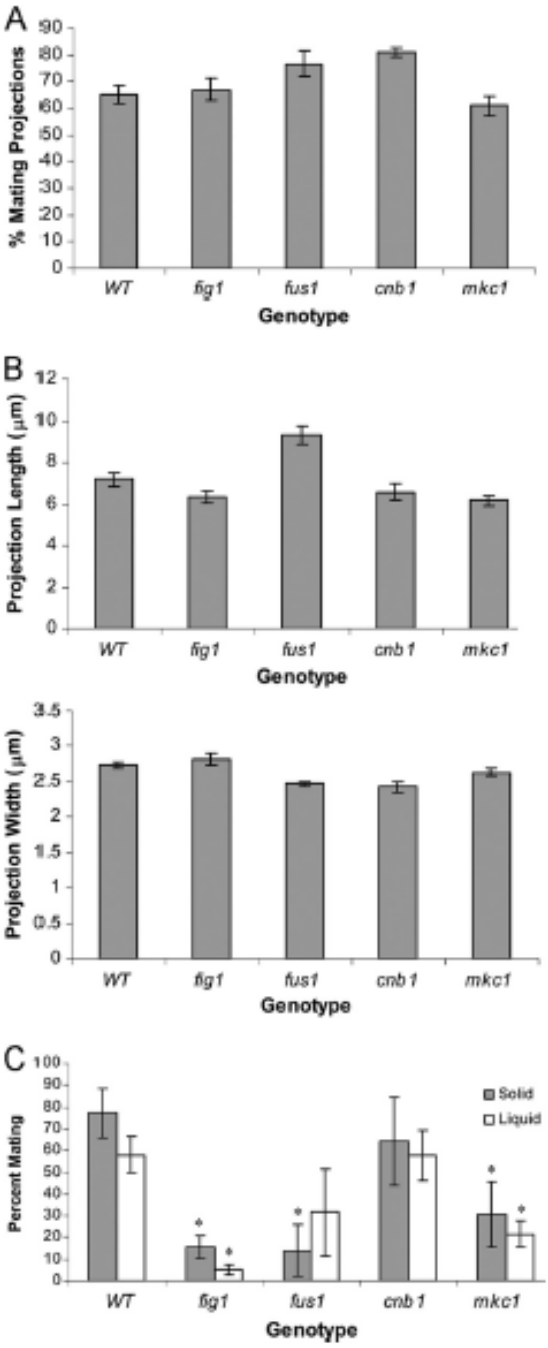

Figure A2-2:

Formation of mating projections and mating efficiency in mutant strains of *C. albicans*. (A) *C. albicans* **a** strains lacking the *FIG1*, *FUS1*, *CNB1*, or *MKC1* gene were tested for their ability to form mating projections in response to 10 μM α pheromone. Strains were treated with pheromone in Spider medium, and the percentage of responding cells was determined after 5 h of incubation at room temperature. (B) The length and width of mating projections formed by the mutant strains in response to 10 μM α pheromone were analyzed. (C) Quantitative mating efficiency of mutant strains. Bilateral mating experiments were performed (mutant x mutant) by coincubation of **a** and α mutant strains on Spider medium plates (Solid) or in liquid Spider medium (Liquid). Opaque cells were coincubated for 2 days, and the frequency of formation of mating products was determined as previously described (47). Asterisks indicate a significant difference between mutant and wild-type strains ($P<0.05$) using a two-tailed t test (two-sample test assuming equal variances). WT, wild type.

Genetic Pathways Influencing Pheromone Killing in *C. albicans*

Each of the four mutant strains, *fig1*, *fus1*, *cnb1*, and *mkc1*, were tested for their sensitivity to killing during exposure to pheromone. To ensure that pure populations of opaque cells were used in these experiments, each strain was transformed with the Wor1-constitutive

expression vector to lock cells into the opaque state. However, we note that the mutant strains showed no obvious defects in white-opaque switching. A time-course of pheromone treatment was performed and cell death determined by staining cells with propidium iodide and analysis by flow cytometry, as described above.

The temporal profile of cell death in response to pheromone was similar in each of the strains, with cell inviability first observed between 2 h and 3 h, and maximal levels of death at 5-6 h. Very little cell death, however, was observed in the *fus1* mutant, which showed only 2% cell death at the 5 h time point (Figure 3A). The *fig1* mutant also showed decreased cell death compared to wildtype strains, with only 11% of cells becoming inviable (Figure 3B). In contrast, the *cnb1* strain showed a very modest, but statistically significant, increase in the frequency of cell death with 25-27% of cells inviable at 5-6 h (Figure 3C). The *mkc1* strain was the only mutant strain that did not exhibit a significant difference in pheromone-induced death compared with the wildtype strain (Figure 3D).

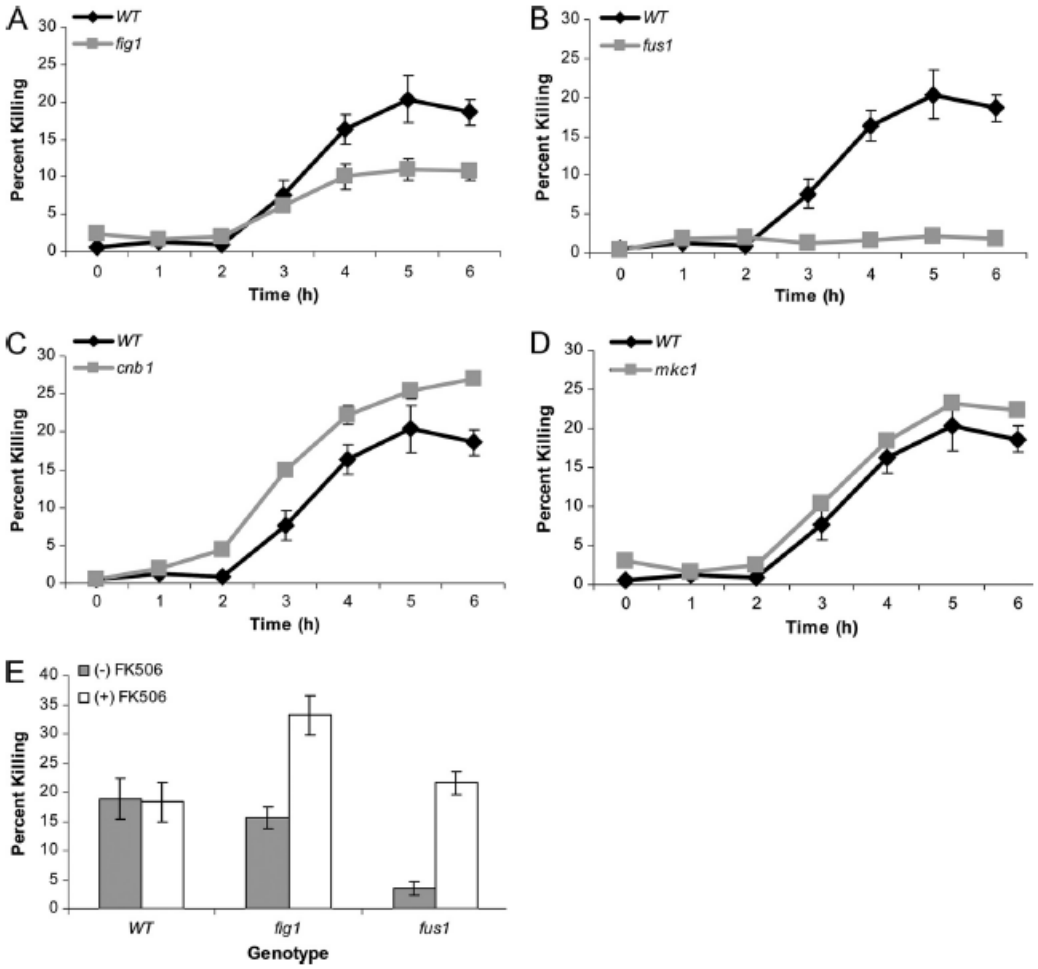

Figure A2-3:

Time course of pheromone-induced cell death in different C. albicans mutants. (A to D) Opaque MTLa strains lacking the FIG1, FUS1, CNB1, orMKC1 gene were treated with 10 µM α pheromone, and the percentage of dead cells was determined by staining with propidium iodide and analysis by flow cytometry. (E) Evaluation of PID in the presence or absence of 2.5 µM FK506. Wild-type, *fus1*, and *fig1* cells were treated with 10 µM α pheromone in the presence or absence of FK506 for 5 h and then stained with propidium iodide and analyzed by flow cytometry.

These results show both parallels and notable differences with the program of pheromone-induced cell death in *S. cerevisiae*. In both *C. albicans* and *S. cerevisiae*, loss of Fus1 or Fig1 activity results in a considerable decrease in the level of pheromone killing. In contrast, deletion of *CNB1* led to almost complete killing (80-95%) of *S. cerevisiae* cells (22, 58), but only a subtle increase in cell death in *C. albicans*. Furthermore, compromising the CWI pathway in *S.*

cerevisiae by deletion of *MPK1/SLT2* resulted in decreased viability in the presence of pheromone (17, 58) while deletion of the homolog, *MKC1*, in *C. albicans* had no discernable effect on cell viability. The lack of a significant role for calcineurin signaling in *C. albicans* cell survival was also confirmed by addition of FK506, a chemical inhibitor of calcineurin in fungal species (9, 55). The presence of FK506 did not significantly affect the level of pheromone-induced cell death in wildtype cells of *C. albicans* (Figure 3E), while this compound led to high levels of pheromone-killing in *S. cerevisiae* (58). Interestingly, the addition of FK506 did lead to a significant increase in the frequency of cell death in the *fus1* (3.5% to 21.5%) and *fig1* (15.6% to 33.1%) mutants (Figure 3E). No other strain showed a significant increase in cell death in the presence of FK506. These results indicate that calcineurin signaling can play a role in protecting against pheromone-induced cell death in *C. albicans*, and this is particularly evident in *fig1* and *fus1* backgrounds.

The Role of Ca^{2+}-Signaling in Pheromone-Induced Cell Death in C. albicans

Several reports have demonstrated that Ca^{2+}-signaling is critical for maintaining the viability of *S. cerevisiae* cells in the presence of pheromone, including a central role for the calcineurin pathway (22, 23, 35, 58). These studies showed that depletion of extracellular Ca^{2+} causes *S. cerevisiae* cells to die during prolonged exposure to pheromone. To test if Ca^{2+} ions are similarly required for *C. albicans* cells to survive pheromone exposure, a cell-impermeant Ca^{2+}chelator (BAPTA) was added to the culture medium. We found that relatively high concentrations of BAPTA (10 mM) were necessary to see any significant effect on the survival of *C. albicans* cells (cell death increased from 16% to 31%, see Figure 4). BAPTA had little or no effect on cell viability when present in the absence of pheromone regardless of the strain genotype (10 mM BAPTA increased basal levels of cell death, on average, from 0.5% to 1.52%).

BAPTA also showed a strong effect on mating efficiency, reducing mating of wildtype strains from 15.9% after 24 hours to 0.2%. These results indicate that the loss of Ca^{2+} ions from the medium causes a major defect in mating in *C. albicans*, but only partially compromises cell survival during the response to pheromone.

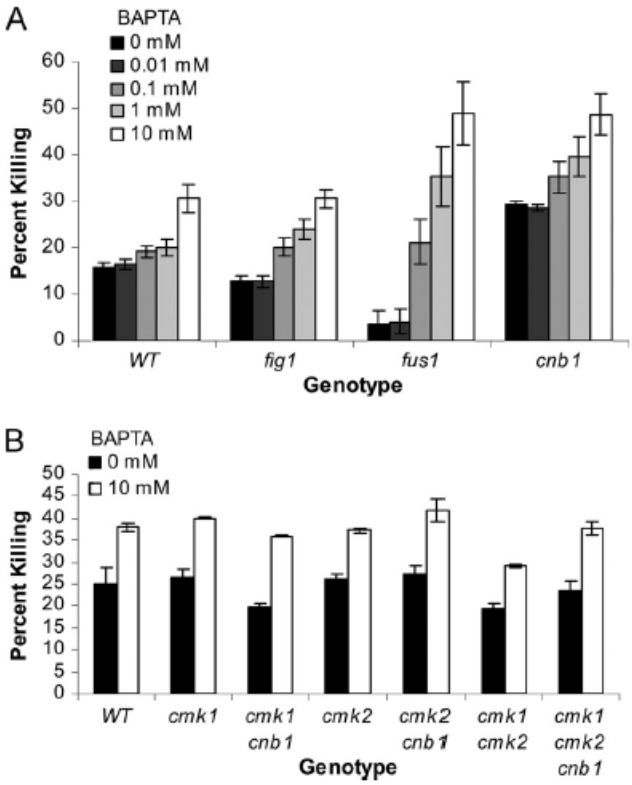

Figure A2-4:

Increased pheromone-induced cell death following chelation of extracellular Ca 2+ ions with BAPTA. (A) C. albicans strains were incubated with 10 µM α pheromone in the presence of increasing concentrations of the Ca 2+ chelator BAPTA. Cells were treated with pheromone for 5 h and analyzed by staining with propidium iodide and flow cytometry to determine the percentage of dead cells. (B) Additional C. albicans strains were incubated with 10 µM α pheromone in the presence or absence of 10 mM BAPTA.

BAPTA similarly increased the level of pheromone killing in the *cnb1* and *fig1* mutant strains (Figure 4A). The *cnb1* mutant result is notable, as it suggests that Ca^{2+}-signaling provides protection against pheromone-induced death, but does so via a largely calcineurin-independent mechanism. The most striking result, however, was observed with the *fus1* strain, as this

mutant usually exhibits very low amounts of cell death (3.6% in this experiment) but was hypersensitive to pheromone killing in the presence of BAPTA (21% death at 0.1 mM BAPTA and 49% death at 10 mM BAPTA, see Figure 4A). In fact, *fus1* cell death in the absence of Ca^{2+} ions was equivalent to the highest level of cell death observed in any mutant SC5314 strain, and represents an increase of 14-fold over medium containing Ca^{2+}.

To further pursue the role of Ca^{2+} signaling in cell death, we constructed mutants lacking the *CMK1* and *CMK2* genes that encode Ca^{2+}/calmodulin-dependent protein kinases (41). Loss of *CMK1* and *CMK2* in *S. cerevisiae* can lead to increased sensitivity to pheromone killing, and can also further potentiate cell death in strains lacking the *CNB1* calcineurin gene (34). Due to the limited levels of PID observed in $\sim$ *cnb1* mutants of *C. albicans*, we speculated that *CMK1* or *CMK2* may play a more important role in the pheromone response in *C. albicans* than in *S. cerevisiae*. However, strains lacking both *CMK1* and *CMK2* genes showed no significant increase in the rates of pheromone-induced death. Additionally, a triple mutant lacking *CMK1, CMK2*, and *CNB1* genes showed levels of cell death that were not significantly increased (Figure 4B). Each of these mutants (*cmk1, cmk2*, and the related double and triple mutants) also responded similarly to 10 mM BAPTA treatment (Figure 4B), supporting the hypothesis that Ca^{2+} provides protection against cell death in a calcineurin-independent manner. These results demonstrate that although PID in *C. albicans* is sensitive to changes in extracellular Ca^{2+} levels, the signaling pathways regulated by *CMK1, CMK2,* and *CNB1* play relatively minor roles in this process, or that additional (yet to be identified) Ca^{2+}-signaling pathways can compensate for the loss of these factors.

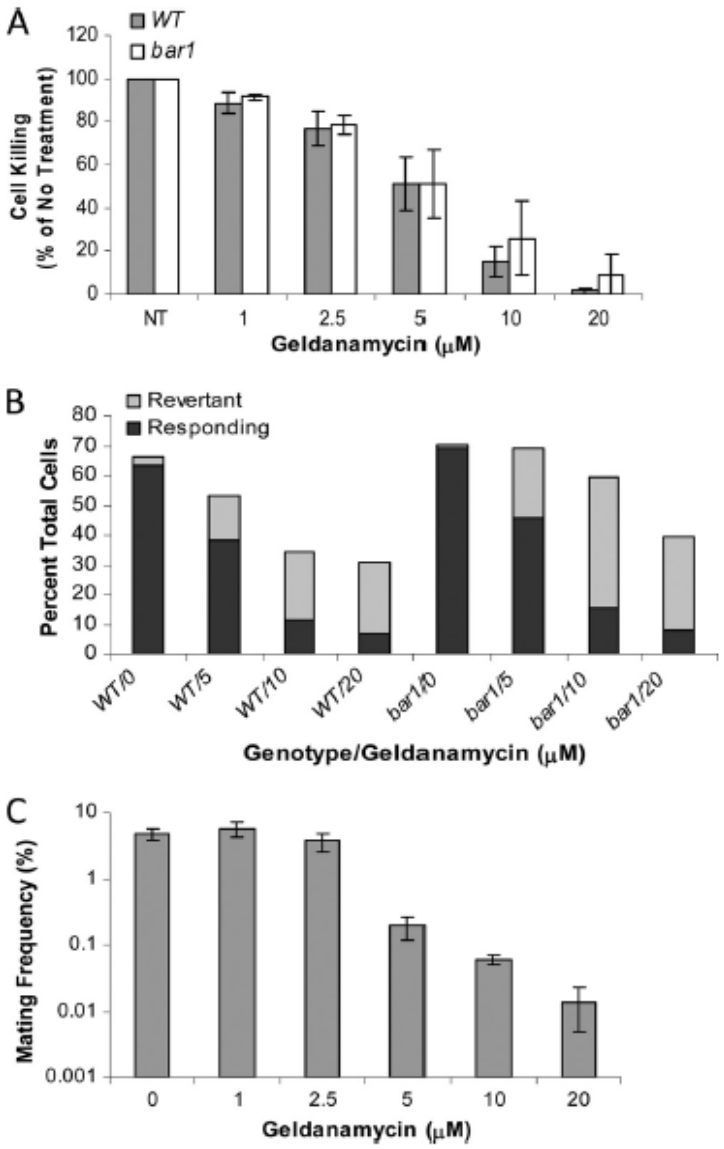

Figure A2-5:

Inhibition of pheromone-induced death and the morphological response to pheromone by the Hsp90 inhibitor geldanamycin. (A) Geldanamycin inhibits cell killing by pheromone in MTLa cells of wild-type and *bar1 C. albicans* strains. Opaque cells were incubated with 10 μM α pheromone for 5 h in the presence of the indicated concentrations of geldanamycin, and cell death was determined by staining with propidium iodide and flow cytometry. NT, no treatment. (B) Fractions of cells responding to α pheromone in the presence of geldanamycin. Opaque cells were treated with pheromone for 5 h and then analyzed microscopically to determine the percentage of cells with mating projections (responding cells) or those cells that had initiated mating projections but then had reverted to budding (revertant cells). (C) Geldanamycin inhibits mating of wild-type *C. albicans* **a** and α cells. *MTLa* and *MTLα* opaque cells were coincubated for 2 days in the presence of various concentrations of geldanamycin, and the mating frequency was determined by the fraction of prototrophic mating products formed, as previously described (47).

Role of Hsp90 in Mediating the Response to Pheromone and Cell Death

There is now a substantial body of evidence indicating a connection between calcineurin signaling and the heat shock protein, Hsp90, in multiple fungal species. In particular, it appears that the Hsp90-calcineurin interaction is necessary for calcineurin activation and subsequent signaling to downstream effectors (24). Thus, inhibition of either Hsp90 activity (e.g. using the chemical inhibitor geldanamycin) or calcineurin activity (e.g. using FK506) can abrogate a subset of the same signaling pathways (9). The Hsp90-calcineurin pathway is particularly relevant for cellular responses to stress, and has been shown to promote the accumulation of drug-resistant isolates (9-12, 49, 55).

To test the role of *C. albicans* Hsp90 during pheromone signaling, wildtype or *bar1* cells were treated with increasing concentrations of the Hsp90 inhibitor, geldanamycin. Bar1 protease is a secreted protein that acts to degrade α pheromone in both *S. cerevisiae* and *C. albicans* (32, 47, 51). Loss of Bar1 sensitizes *S. cerevisiae* and *C. albicans* cells to respond to lower concentrations of α pheromone (discussed below). As shown in Figure 5, as the concentration of the inhibitor increased the frequency of pheromone-induced cell death decreased in both wildtype and *bar1* cells. Thus, at 5 μM geldanamycin, cell death was approximately 50% that of assays lacking the drug, while at 20 μM geldanamycin cell death in both wildtype and *bar1* cells was virtually abolished (Figure 5A). Geldanamycin alone had very little or no effect on *C. albicans* cell viability when used at these concentrations (data not shown).

To examine the effect of geldanamycin on the morphological response to pheromone, microscopic analysis of cells was performed. These experiments revealed that geldanamycin also inhibited the morphological response of cells to pheromone. Thus, whereas close to 70% of cells formed polarized mating projections in the absence of geldanamycin, as the concentration

of the drug increased fewer cells exhibited polarized growth (Figure 5B). In addition, a significant number of cells initiated a mating response but then reverted to dividing as budding yeast in the presence of geldanamcin (Figure 5B). Consistent with a role for geldanamycin in blocking pheromone signaling, we also observed a decrease in mating frequencies in the presence of high concentrations of the drug. Mating frequencies were unaltered in assays using 1 - 2.5 μM geldanamycin, while higher concentrations of the drug significantly inhibited the formation of conjugation products by nearly 100-fold (Figure 5C).

These results establish that loss of Hsp90 activity results in inhibition of the morphological response to pheromone. We observed a correlation between inhibition of the pheromone response and decreased cell death, indicating that loss of viability is dependent on processes accompanying the morphological transition. In *S. cerevisiae*, Hsp90 inhibitors have also been shown to block polarized growth in response to pheromones, possibly due to defective signaling via Ste11, a component of the pheromone MAP kinase cascade (31). Our findings now indicate that Hsp90 plays an important role in mediating pheromone signaling in a distantly related hemiascomycete. In addition, we demonstrate that Hsp90 and calcineurin play distinct roles in the mating program. Inhibition of Hsp90 activity prevents activation of the pheromone-signaling response, while calcineurin is not required for the pheromone response, but does play a role (albeit a minor one in wildtype strains) in protecting cells from pheromone toxicity.

Pheromone-induced cell death in clinical isolates of C. albicans

The experiments described above utilized derivatives of the standard laboratory strain of *C. albicans*, SC5314. Mating has also been observed in multiple clinical isolates of *C. albicans*, including those from alternative clades (5, 21, 40). In total, 17 distinct clades of *C. albicans*

strains have been described, although 68% of strains belong to the four most populous clades, numbered 1 through 4 (38). To compare the frequency of cell death between natural *C. albicans* strains, we initially treated six clinical opaque **a** strains with α pheromone and determined the efficiency of the mating response as well as the susceptibility to cell death. These six strains were chosen at random as representatives of the four major clades of *C. albicans*.

Each of the clinical strains showed a robust morphological response to pheromone, with the majority of cells forming polarized mating projections (see Figure 6B). Despite the similar frequencies of responding cells, there was a marked difference in the susceptibility of clinical strains to pheromone-induced death. As shown in Figure 6A, only 2% of J981315 cells became inviable during pheromone treatment, while 40-50% of L26 and P37005 cells were killed, and ~70% of AM2003/0191 cells died. These experiments reveal that cell death varies by more than an order of magnitude between strains with different genetic backgrounds. The strain that showed the highest survival rate, J981315, belongs to clade 3, while the strain with the lowest survival rate, AM2003/0191, belongs to clade 2 (38). To test if other isolates from these clades showed similar susceptibilities to cell death, we examined the frequency of killing in several additional strains belonging to clades 1-4. The additional strains revealed that high (~70%) levels of cell death are observed in isolates from each of the four clades. However, low (<7%) levels of cell death, in the presence of an otherwise robust mating response, only occurred in a subset of clade 3 strains (K.A. and R.J.B. unpublished observations). These data suggest that clade-specific differences may exist in the susceptibility of strains to pheromone-induced cell death.

Due to the differential response of SC5314 mutants to FK506 treatment (Figure 3B), we tested if clinical isolates of *C. albicans* showed increased susceptibility to PID in the presence of FK506. None of the isolates showed a significant difference in PID when treated with FK506,

although AM2005/0377 was slightly more sensitive to killing in the presence of the drug (Figure 6C). This indicates that FK506-mediated inhibition of calcineurin does not significantly affect the level of PID in *C. albicans*, regardless of the genetic background of the strain.

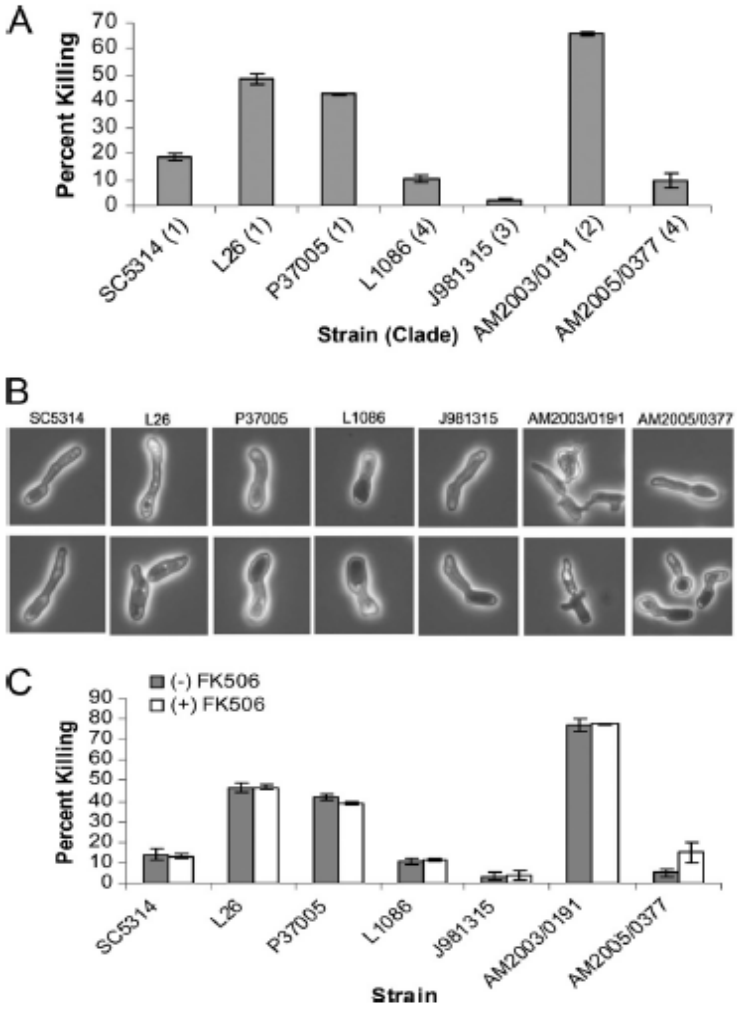

Figure 2A-6:

Pheromone-induced death in clinical isolates of C. albicans. Six clinical strains were analyzed to determine their susceptibilities to killing by pheromone. (A) MTLa/a isolates were switched to the opaque phase and treated with 10 µM α pheromone for 5 h, prior to staining with propidium iodide and analysis by flow cytometry. Clade designations for each strain are in parentheses. (B) Formation of mating projections by the clinical isolates. Opaque cells were treated with α pheromone for 5 h and analyzed by microscopy. All isolates were able to efficiently undergo the morphological response to pheromone, despite significant differences in their susceptibilities to killing by pheromone. (C) Evaluation of the presence or absence of FK506 on PID in clinical isolates. Cells were treated with 10 µM α pheromone in the presence or absence of 2.5 µM FK506 for 5 h and then stained with propidium iodide and analyzed by flow cytometry.

We also compared the role of the Bar1 protease during PID in both the SC5314 background and in the hypersensitive clinical strain, AM2003/0191. In *S. cerevisiae*, loss of Bar1 activity results in strains exhibiting PID at lower concentrations of α pheromone due to reduced degradation of the peptide (58). In *C. albicans*, we similarly found that *bar1* mutants experienced cell death at lower concentrations of pheromone than wildtype cells. Thus, whereas 10 μM pheromone was required to cause maximal levels of cell killing in SC5314 cells (~23%, Figure 1B), 10-fold less pheromone (1 μM) was sufficient to cause the same frequency of killing in *bar1* cells (Figure 7A). Even with 100-fold less pheromone (0.1 μM) there was still appreciable death in *bar1* cells but not in wildtype cells. Similarly, maximal killing in AM2003/0191 (~70% cells inviable, Figure 6A) required 3 μM α pheromone in the wildtype strain but only 0.03 μM pheromone in the *bar1* mutant (Figure 7B). It is notable that the maximal levels of cell death in SC5314 and AM2003/0191 strains were the same in both wildtype and *bar1* cells. These results indicate that while Bar1 plays an important role in determining the amount of pheromone necessary to induce cell death, Bar1 activity does not influence the maximal level of death in a given strain. Thus, at least in the case of AM2003/0191, the high susceptibility of this strain to PID is not due to defective production of Bar1 protein.

Finally, we examined the subset of clinical strains to determine if susceptibility to killing by pheromone correlated with sensitivity to other fungal stresses. Strains were incubated on plates containing the cell wall stressors Congo Red, SDS (sodium dodecyl sulfate), or Calcofluor White. Strains were also tested for susceptibility to killing with the antifungal drug fluconazole, which targets the cell membrane. The subset of clinical strains exhibited a wide range of susceptibilities to these agents (see Supplemental Figure S2). However strain AM2003/0191, which was the most sensitive to killing by pheromone, was as resistant to each of these types of

cell stress as isolates from the other clades. This demonstrates that the susceptibility to pheromone killing by this strain is not due to its general sensitivity to stress.

Taken together, these results demonstrate an unexpected variability in the response of natural isolates of *C. albicans* to pheromone. Each of the clinical strains underwent the morphological response to pheromone, but levels of cell death varied from 2% to 70%, far more than that observed even between mutant derivatives of SC5314. Cell killing by pheromone did not correlate with sensitivity to other cell stresses, indicating that pheromone toxicity is not related to that of other antifungal agents. We note that we have not, however, observed any obvious synergy between killing by pheromone treatment and cell death induced by azole or echinocandin classes of drugs (K.A. and R.J.B, unpublished observations).

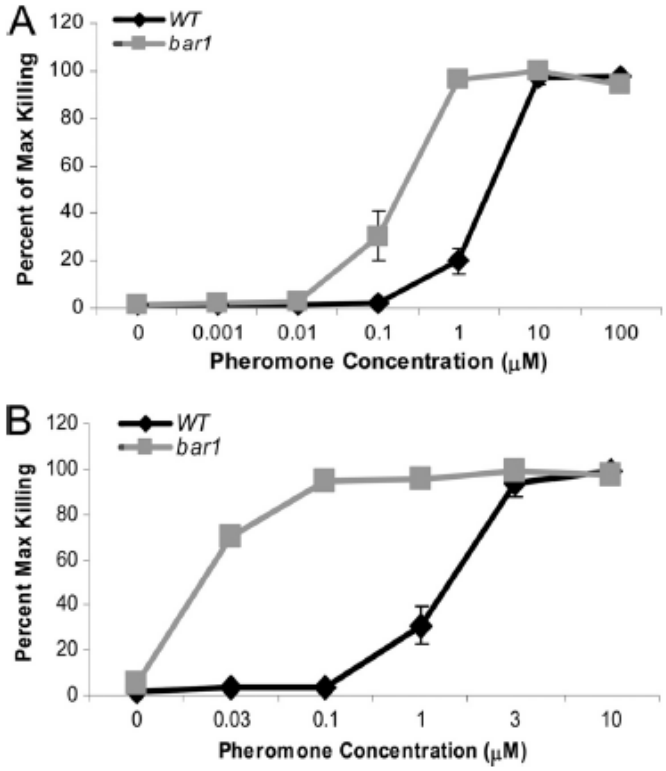

Figure A2-7:

Effect of BAR1 on pheromone-induced death. (A) Titration of α pheromone with wild-type and *bar1* SC5314 a strains. Strains were analyzed by PI staining at 5 h after the addition of pheromone. (B) Titration of α pheromone with wild-type and *bar1* AM2003/0191 a strains. Strains were analyzed by PI staining at 5 h after the addition of pheromone.

DISCUSSION

This work is the first to report the phenomenon of pheromone-induced cell death in *C. albicans*, a hemiascomycete yeast that diverged from *S. cerevisiae* approximately 700 million years ago (19). Using homozygous **a**/**a** derivatives of SC5314, the standard laboratory strain of *C. albicans,* cell death was first observed 2-3 h after pheromone treatment, coincident with the initial formation of polarized mating projections. Cell death gradually increased and was maximal at 5-6 h, where it was observed in approximately 20% of cells in a population. Cell death was also dependent on Ste2, the receptor for α pheromone (6), confirming that it required the canonical pheromone-signaling pathway.

Unlike *S. cerevisiae*, **a** and α cells of *C. albicans* can exist in two alternative physical states, 'white' and 'opaque', and cells undergo heritable and reversible switching between these states (30, 33, 50). Both white and opaque forms can respond to pheromone via the MAP kinase cascade, but signaling results in the upregulation of phase-specific genes. White cells treated with pheromone exhibit increased adhesion and biofilm formation, whereas opaque cells undergo the more conventional program of mating including polarized growth, cell-cell conjugation, and zygote formation (14, 46, 57). Consistent with cell death being dependent on the morphological response to pheromone, only opaque cells showed a loss of viability in these studies, while white cells were resistant to pheromone-induced death. As predicted by experiments in *S. cerevisiae*, mutants lacking the *BAR1* gene were hypersensitive to killing by low concentrations of pheromone. *BAR1* encodes a conserved aspartyl protease that degrades α pheromone in both *S. cerevisiae* and *C. albicans* (1, 47).

In *S. cerevisiae*, multiple genes have been implicated both in mediating the toxic effects of pheromone and in protecting cells against killing. It was recently proposed that three signaling pathways, with distinct kinetics and genetic requirements, modulate the response to pheromone. Loss of calcineurin signaling promotes 'slow cell death' and requires mitochondrial respiration, loss of the cell wall integrity (CWI) pathway leads to 'intermediate cell death' due to increased cell wall degradation, while a wave of 'fast cell death' is dependent on the Fig1 protein (58). In all three waves of death, reactive oxygen species (ROS) were at least transiently observed, although only slow cell death required mitochondrial function (58).

In comparison, our studies in *C. albicans* demonstrate that genes functioning in calcineurin signaling (*CNB1*) and the cell wall integrity pathway (*MKC1*) play only minor roles in providing overall protection against pheromone-induced death, at least in wildtype cells. Thus, *mkc1* and *cnb1* mutants exhibited similar levels of cell death to wildtype strains. In *S. cerevisiae*, the calcineurin-signaling pathway is particularly important in counteracting pheromone toxicity, but the level of protection can vary depending on the strain background. For example, in some strains deletion of the Ca^{2+}/calmodulin-dependent kinase Cmk2 is required in addition to Cnb1 in order to see high levels of pheromone-induced killing (Kyle Cunningham, personal communication). In *C. albicans* loss of *CNB1* did not result in high levels of cell death even when combined with deletion of the *CMK2* gene. Furthermore, a triple mutant lacking *CNB1, CMK1*, and *CMK2* genes was also tested and did not exhibit increased sensitivity to pheromone killing. Thus, in contrast to *S. cerevisiae*, the calcineurin-signaling pathway does not appear to play a central role in protecting *C. albicans* cells from pheromone-induced death, even when combined with loss of Ca^{2+}/calmodulin-dependent kinases. It remains to be seen, however, if other pathways can compensate for the loss of these signaling pathways. The latter is a strong possibility given that chelation of Ca^{2+} ions by BAPTA significantly increased cell death (even in

$\sim$ *cnb1* strains), suggesting that Ca^{2+}-signaling can activate protective pathways that are independent of calcineurin and Cmk1/2 function.

Two genes that did show similar effects on PID in both *S. cerevisiae* and *C. albicans* were *FIG1* and *FUS1*. These genes are highly induced as part of the transcriptional response to pheromone in both yeasts (6, 16, 56). In addition, in both species loss of these cell membrane proteins results in a reduction in pheromone-induced death, as well as a reduction in mating efficiency. *S. cerevisiae* Fig1 has been shown to be part of a low affinity Ca^{2+}-influx system (35), although recent studies indicate that its role in cell death is independent of Ca^{2+} uptake (58). Fus1 promotes cell death by mediating the local secretion of hydrolases necessary for cell wall degradation (7, 58). The roles of Fig1 and Fus1 are closely related, as Fus1 activity is required for Fig1-dependent cell death in *S. cerevisiae* (58). The current work shows that Fus1 and Fig1 also act as prodeath factors during the pheromone response in *C. albicans*. The result with the *C. albicans* $\sim$ *fus1* strain was particularly striking, as cell death occurred in only 2-4% of cells. Despite the low frequency of killing, chelation of Ca^{2+} ions in the medium increased $\sim$ *fus1* cell death to ~50% of the population. The high frequency of cell death (even higher than that of wildtype SC5314 cells) indicates that although death is rare in the absence of Fus1, these cells are highly susceptible to loss of calcium-signaling pathway(s). In support of this model, treatment of $\sim$ *fus1* strains with the calcineurin inhibitor FK506 also resulted in a significant increase in cell death (from 3.5% to 21.5%). Thus, although wildtype strains are not markedly affected by the loss of calcineurin, $\sim$ *fus1* strains are exquisitely sensitive to the loss of this activity. Furthermore, the very high levels of cell death observed in the absence of both Fus1 and Ca^{2+} ions indicate that this protein can perform a prosurvival role, in addition to its prodeath function, during the response to pheromone.

We report that the strain background of *C. albicans* can also have a dramatic effect on the level of PID. In total, we have analyzed cell death in over 20 clinical strains and found that levels varied from ~2% in J981315 to ~70% in AM2003/0191. This difference was not due to differences in the ability of these strains to respond to pheromone, as each of these clinical strains efficiently formed mating projections. In addition, while AM2003/0191 was the most susceptible strain to pheromone-induced death, it was not hypersensitive to other types of cell stress, including the presence of antifungal drugs (azoles) and cell wall stressors (SDS, Congo Red, or Calcofluor White). Thus, the high levels of cell death seen in the presence of pheromone are not due to a general susceptibility to different forms of cell stress.

Natural isolates of *C. albicans* strains have been classified into 17 distinct clades, with almost 70% of the isolates belonging to the four largest clades (clades 1-4) (38). Clade-specific associations are relatively rare, although one example is the number of tandem repeats in alleles of *ALS* and *HYR* family members, genes involved in adhesion to host surfaces (38, 39). Our results suggest that pheromone-induced death may also exhibit clade specific differences. Multiple strains from Clade 3 experience very low levels of PID (2-6%), while still exhibiting a robust mating response. Given the limited number of natural *MTL***a**/**a** strains from Clade 3, confirmation of a clade-specific phenotype will require construction of additional *MTL* homozygous strains from **a**/α parental strains and testing for their survival in the presence of pheromone.

The role of pheromone-induced death in yeast biology continues to be more of an enigma than the signaling pathways influencing it. Based on studies in *S. cerevisiae,* it is thought that PID may act to selectively discard older or weaker cells, allowing only the healthiest cells to survive and propagate (48). In this model, such programmed cell death can potentially benefit the species by increasing overall fitness in the population. An alternative hypothesis suggests

that PID is a direct consequence of cells failing to undergo cell-cell conjugation, with decreased viability due to pheromone-induced degradation of cell wall material and subsequent loss of cell integrity (58). A third possibility is that PID is a result of phenotypic variation within a population, and that only a subpopulation of cells are actually 'programmed' to mate. The remaining cells in the population experience only the stressful consequences of pheromone exposure that can result in cell death. This phenomenon is commonly seen in bacteria in response to external stresses such as antibiotic treatment (2, 45). While these three models are not mutually exclusive, our studies in *C. albicans* indicate that a simple relationship does not exist between a cell's susceptibility to undergo pheromone-induced death and its ability to undergo mating. This is most apparent in comparing natural isolates of *C. albicans*; the J981315 isolate is resistant to PID (~2% death) whereas the AM2003/191 isolate exhibits the highest level of PID (~70% death), yet both strains undergo efficient conjugation in quantitative mating assays (1). Clearly, it will be revealing to determine which pathways (either prodeath or prosurvival) contribute to the marked differences in cell death between *C. albicans* isolates, and if these differences affect the fitness of mating products produced by the parasexual mating cycle.

In summary, our results demonstrate that the phenomenon of pheromone-induced death has been conserved between two diverse species of hemiascomycete yeast. However, the signaling pathways that influence the susceptibility to killing by pheromone have diverged, and natural isolates can exhibit dramatically different levels of cell death in response to pheromone. It is therefore evident that the study of mechanisms of pheromone-induced killing in *C. albicans* will help further elucidate the genetic factors that contribute to this phenomenon in hemiascomycetes, as well as the role of PID in yeast biology.

ACKNOWLEDGEMENTS

The authors would like to specially thank Kyle Cunningham (John Hopkins University) for discussions and the communication of unpublished data, and Donna MacCullum (University of Aberdeen) for providing clinical isolates of *C. albicans*. Work in the authors' laboratory was supported by the NIH (R21AI081560AI081560 and AI081704 to RJB, F31DE019752 to KA, and F31AI075607 to RS). RJB also holds an investigator in the Pathogenesis of Infectious Disease Award from the Burroughs Wellcome Fund.

REFERENCES

1. Alby, K., D. Schaefer, and R. J. Bennett. 2009. Homothallic and heterothallic mating in the opportunistic pathogen *Candida albicans*. Nature 460:890-893.

2. Beaumont, H. J., J. Gallie, C. Kost, G. C. Ferguson, and P. B. Rainey. 2009. Experimental evolution of bet hedging. Nature 462:90-93.

3. Bennett, R. J., and A. D. Johnson. 2003. Completion of a parasexual cycle in *Candida albicans* by induced chromosome loss in tetraploid strains. Embo J 22:2505-2515.

4. Bennett, R. J., and A. D. Johnson. 2006. The role of nutrient regulation and the Gpa2 protein in the mating pheromone response of *C. albicans*. Mol Microbiol 62:100-119.

5. Bennett, R. J., M. G. Miller, P. R. Chua, M. E. Maxon, and A. D. Johnson. 2005. Nuclear fusion occurs during mating in *Candida albicans* and is dependent on the *KAR3* gene. Mol Microbiol 55:1046-1059.

6. Bennett, R. J., M. A. Uhl, M. G. Miller, and A. D. Johnson. 2003. Identification and characterization of a *Candida albicans* mating pheromone. Mol Cell Biol 23:8189-8201.

7. Brizzio, V., A. E. Gammie, and M. D. Rose. 1998. Rvs161p interacts with Fus2p to promote cell fusion in *Saccharomyces cerevisiae*. J Cell Biol 141:567-584.

8. Buehrer, B. M., and B. Errede. 1997. Coordination of the mating and cell integrity mitogen-activated protein kinase pathways in *Saccharomyces cerevisiae*. Mol Cell Biol 17:6517-6525.

9. Cowen, L. E. 2008. The evolution of fungal drug resistance: modulating the trajectory from genotype to phenotype. Nat Rev Microbiol 6:187-198.

10. Cowen, L. E. 2009. Hsp90 orchestrates stress response signaling governing fungal drug resistance. PLoS Pathog 5:e1000471.

11. Cowen, L. E., and S. Lindquist. 2005. Hsp90 potentiates the rapid evolution of new traits: drug resistance in diverse fungi. Science 309:2185-2189.

12. Cowen, L. E., S. D. Singh, J. R. Kohler, C. Collins, A. K. Zaas, W. A. Schell, H. Aziz, E. Mylonakis, J. R. Perfect, L. Whitesell, and S. Lindquist. 2009. Harnessing Hsp90 function as a powerful, broadly effective therapeutic strategy for fungal infectious disease. Proc Natl Acad Sci U S A 106:2818-2823.

13. Cyert, M. S. 2003. Calcineurin signaling in *Saccharomyces cerevisiae*: how yeast go crazy in response to stress. Biochem Biophys Res Commun 311:1143-1150.

14. Daniels, K. J., T. Srikantha, S. R. Lockhart, C. Pujol, and D. R. Soll. 2006. Opaque cells signal white cells to form biofilms in *Candida albicans*. Embo J 25:2240-2252.

15. Dudgeon, D. D., N. Zhang, O. O. Ositelu, H. Kim, and K. W. Cunningham. 2008. Nonapoptotic death of *Saccharomyces cerevisiae* cells that is stimulated by Hsp90 and inhibited

by calcineurin and Cmk2 in response to endoplasmic reticulum stresses. Eukaryot Cell 7:2037-2051.

16. Erdman, S., L. Lin, M. Malczynski, and M. Snyder. 1998. Pheromone-regulated genes required for yeast mating differentiation. J Cell Biol 140:461-483.

17. Errede, B., R. M. Cade, B. M. Yashar, Y. Kamada, D. E. Levin, K. Irie, and K. Matsumoto. 1995. Dynamics and organization of MAP kinase signal pathways. Mol Reprod Dev 42:477-485.

18. Guthrie, C., and G. R. Fink. 1991. Guide to Yeast Genetics and Molecular Biology. Academic Press, San Diego.

19. Hedges, S. B., J. E. Blair, M. L. Venturi, and J. L. Shoe. 2004. A molecular timescale of eukaryote evolution and the rise of complex multicellular life. BMC Evol Biol 4:2.

20. Huang, G., H. Wang, S. Chou, X. Nie, J. Chen, and H. Liu. 2006. Bistable expression of *WOR1*, a master regulator of white-opaque switching in *Candida albicans*. Proc Natl Acad Sci U S A 103:12813-12818.

21. Ibrahim, A. S., B. B. Magee, D. C. Sheppard, M. Yang, S. Kauffman, J. Becker, J. E. Edwards, Jr., and P. T. Magee. 2005. Effects of ploidy and mating type on virulence of *Candida albicans*. Infect Immun 73:7366-7374.

22. Iida, H., H. Nakamura, T. Ono, M. S. Okumura, and Y. Anraku. 1994. *MID1*, a novel *Saccharomyces cerevisiae* gene encoding a plasma membrane protein, is required for Ca2+ influx and mating. Mol Cell Biol 14:8259-8271.

23. Iida, H., Y. Yagawa, and Y. Anraku. 1990. Essential role for induced Ca2+ influx followed by [Ca2+]i rise in maintaining viability of yeast cells late in the mating pheromone response pathway. A study of [Ca2+]i in single *Saccharomyces cerevisiae* cells with imaging of fura-2. J Biol Chem 265:13391-13399.

24. Imai, J., and I. Yahara. 2000. Role of *HSP90* in salt stress tolerance via stabilization and regulation of calcineurin. Mol Cell Biol 20:9262-9270.

25. Janbon, G., F. Sherman, and E. Rustchenko. 1998. Monosomy of a specific chromosome determines L-sorbose utilization: a novel regulatory mechanism in *Candida albicans*. Proc Natl Acad Sci U S A 95:5150-5155.

26. Johnson, A. 2003. The biology of mating in *Candida albicans*. Nat Rev Microbiol 1:106-116.

27. Levin, D. E. 2005. Cell wall integrity signaling in *Saccharomyces cerevisiae*. Microbiol Mol Biol Rev 69:262-291.

28. Liu, H., J. Kohler, and G. R. Fink. 1994. Suppression of hyphal formation in *Candida albicans* by mutation of a *STE12* homolog. Science 266:1723-1726.

29. Lockhart, S. R., R. Zhao, K. J. Daniels, and D. R. Soll. 2003. Alpha-pheromone-induced "shmooing" and gene regulation require white-opaque switching during *Candida albicans* mating. Eukaryot Cell 2:847-855.

30. Lohse, M. B., and A. D. Johnson. 2009. White-opaque switching in *Candida albicans*. Curr Opin Microbiol 12:650-654.

31. Louvion, J. F., T. Abbas-Terki, and D. Picard. 1998. Hsp90 is required for pheromone signaling in yeast. Mol Biol Cell 9:3071-3083.

32. MacKay, V. L., S. K. Welch, M. Y. Insley, T. R. Manney, J. Holly, G. C. Saari, and M. L. Parker. 1988. The *Saccharomyces cerevisiae BAR1* gene encodes an exported protein with homology to pepsin. Proc Natl Acad Sci U S A 85:55-59.

33. Miller, M. G., and A. D. Johnson. 2002. White-opaque switching in *Candida albicans* is controlled by mating-type locus homeodomain proteins and allows efficient mating. Cell 110:293-302.

34. Moser, M. J., J. R. Geiser, and T. N. Davis. 1996. Ca2+-calmodulin promotes survival of pheromone-induced growth arrest by activation of calcineurin and Ca2+-calmodulin-dependent protein kinase. Mol Cell Biol 16:4824-4831.

35. Muller, E. M., N. A. Mackin, S. E. Erdman, and K. W. Cunningham. 2003. Fig1p facilitates Ca2+ influx and cell fusion during mating of *Saccharomyces cerevisiae*. J Biol Chem 278:38461-38469.

36. Nelson, B., A. B. Parsons, M. Evangelista, K. Schaefer, K. Kennedy, S. Ritchie, T. L. Petryshen, and C. Boone. 2004. Fus1p interacts with components of the Hog1p mitogen-activated protein kinase and Cdc42p morphogenesis signaling pathways to control cell fusion during yeast mating. Genetics 166:67-77.

37. Noble, S. M., and A. D. Johnson. 2005. Strains and strategies for large-scale gene deletion studies of the diploid human fungal pathogen *Candida albicans*. Eukaryot Cell 4:298-309.

38. Odds, F. C., M. E. Bougnoux, D. J. Shaw, J. M. Bain, A. D. Davidson, D. Diogo, M. D. Jacobsen, M. Lecomte, S. Y. Li, A. Tavanti, M. C. Maiden, N. A. Gow, and C. d'Enfert. 2007. Molecular phylogenetics of *Candida albicans*. Eukaryot Cell 6:1041-1052.

39. Oh, S. H., G. Cheng, J. A. Nuessen, R. Jajko, K. M. Yeater, X. Zhao, C. Pujol, D. R. Soll, and L. L. Hoyer. 2005. Functional specificity of *Candida albicans* Als3p proteins and clade specificity of *ALS3* alleles discriminated by the number of copies of the tandem repeat sequence in the central domain. Microbiology 151:673-681.

40. Panwar, S. L., M. Legrand, D. Dignard, M. Whiteway, and P. T. Magee. 2003. MFalpha1, the gene encoding the alpha mating pheromone of *Candida albicans.* Eukaryot Cell 2:1350-1360.

41. Pausch, M. H., D. Kaim, R. Kunisawa, A. Admon, and J. Thorner. 1991. Multiple Ca2+/calmodulin-dependent protein kinase genes in a unicellular eukaryote. EMBO J 10:1511-1522.

42. Pujol, C., K. J. Daniels, S. R. Lockhart, T. Srikantha, J. B. Radke, J. Geiger, and D. R. Soll. 2004. The closely related species *Candida albicans* and *Candida dubliniensis* can mate. Eukaryot Cell 3:1015-1027.

43. Reuss, O., A. Vik, R. Kolter, and J. Morschhauser. 2004. The *SAT1* flipper, an optimized tool for gene disruption in *Candida albicans*. Gene 341:119-127.

44. Roberts, C. J., B. Nelson, M. J. Marton, R. Stoughton, M. R. Meyer, H. A. Bennett, Y. D. He, H. Dai, W. L. Walker, T. R. Hughes, M. Tyers, C. Boone, and S. H. Friend. 2000. Signaling and Circuitry of Multiple MAPK Pathways Revealed by a Matrix of Global Gene Expression Profiles. Science 287:873-880.

45. Rotem, E., A. Loinger, I. Ronin, I. Levin-Reisman, C. Gabay, N. Shoresh, O. Biham, and N. Q. Balaban. 2010. Regulation of phenotypic variability by a threshold-based mechanism underlies bacterial persistence. Proc Natl Acad Sci U S A 107:12541-12546.

46. Sahni, N., S. Yi, K. J. Daniels, T. Srikantha, C. Pujol, and D. R. Soll. 2009. Genes selectively up-regulated by pheromone in white cells are involved in biofilm formation in *Candida albicans*. PLoS Pathog 5:e1000601.

47. Schaefer, D., P. Cote, M. Whiteway, and R. J. Bennett. 2007. Barrier Activity in *Candida albicans* Mediates Pheromone Degradation and Promotes Mating. Eukaryot Cell. 6:907-918

48. Severin, F. F., and A. A. Hyman. 2002. Pheromone induces programmed cell death in *S. cerevisiae*. Curr Biol 12:R233-235.

49. Slutsky, B., J. Buffo, and D. R. Soll. 1985. High-frequency switching of colony morphology in *Candida albicans.* Science 230:666-669.

50. Soll, D. R. 2009. Why does *Candida albicans* switch? FEMS Yeast Res 9:973-989.

51. Sprague, G. F., Jr., and I. Herskowitz. 1981. Control of yeast cell type by the mating type locus. I. Identification and control of expression of the a-specific gene *BAR1*. J Mol Biol 153:305-321.

52. Sprague, G. F. J., and J. T. Thorner. 1992. Pheromone Response and Signal Transduction during the Mating Process of *S. cerevisiae*, p. 657-744. *In* J. R. Pringle, J. R. Broach, and E. W. Jones (eds.), Molecular and Cellular Biology of the Yeast Saccharomyces. CSH Laboratory Press, Cold Spring Harbor.

53. Srikantha, T., A. R. Borneman, K. J. Daniels, C. Pujol, W. Wu, M. R. Seringhaus, M. Gerstein, S. Yi, M. Snyder, and D. R. Soll. 2006. *TOS9* regulates white-opaque switching in *Candida albicans*. Eukaryot Cell 5:1674-1687.

54. Stathopoulos, A. M., and M. S. Cyert. 1997. Calcineurin acts through the *CRZ1/TCN1*-encoded transcription factor to regulate gene expression in yeast. Genes Dev 11:3432-3444.

55. Steinbach, W. J., J. L. Reedy, R. A. Cramer, Jr., J. R. Perfect, and J. Heitman. 2007. Harnessing calcineurin as a novel anti-infective agent against invasive fungal infections. Nat Rev Microbiol 5:418-430.

56. Trueheart, J., J. D. Boeke, and G. R. Fink. 1987. Two genes required for cell fusion during yeast conjugation: evidence for a pheromone-induced surface protein. Mol Cell Biol 7:2316-2328.

57. Yi, S., N. Sahni, C. Pujol, K. J. Daniels, T. Srikantha, N. Ma, and D. R. Soll. 2009. A *Candida albicans*-specific region of the alpha-pheromone receptor plays a selective role in the white cell pheromone response. Mol Microbiol 71:925-947.

58. Zhang, N. N., D. D. Dudgeon, S. Paliwal, A. Levchenko, E. Grote, and K. W. Cunningham. 2006. Multiple signaling pathways regulate yeast cell death during the response to mating pheromones. Mol Biol Cell 17:3409-3422.

59. Zhao, R., K. J. Daniels, S. R. Lockhart, K. M. Yeater, L. L. Hoyer, and D. R. Soll. 2005. Unique aspects of gene expression during *Candida albicans* mating and possible G(1) dependency. Eukaryot Cell 4:1175-1190.

60. Zordan, R. E., D. J. Galgoczy, and A. D. Johnson. 2006. Epigenetic properties of white-opaque switching in *Candida albicans* are based on a self-sustaining transcriptional feedback loop. Proc Natl Acad Sci U S A 103:12807-12812.

61. Zordan, R. E., M. G. Miller, D. J. Galgoczy, B. B. Tuch, and A. D. Johnson. 2007. Interlocking Transcriptional Feedback Loops Control White-Opaque Switching in *Candida albicans*. PLoS Biol 5:e256.

SUPPLEMENTAL TABLES AND FIGURES

Please refer to the following reference for access to supplemental tables and figures:

(Alby *et al.*, 2010).